Electric taxiing: an optimisation study on the future of airport operations

Master of Science Thesis

Jurjen Kroese

TU Delft

Electric taxiing: an optimisation study on the future of airport operations

Master of Science Thesis

by

Jurjen Kroese

to obtain the degree of Master of Science
at Delft University of Technology,
to be defended publicly on Monday January 18th, 2021.

Student number:	4371305	
Project duration:	March 2020 – January 2021	
Thesis committee:	Prof. Dr. M. Snellen	TU Delft, Chair
	Dr. M.A. Mitici	TU Delft, Supervisor
	Dr. F. Yin	TU Delft, External committee member

An electronic version of this thesis is available at http://repository.tudelft.nl/.

TU Delft

Acknowledgements

This thesis report is the work that concludes my master's degree in Aerospace Engineering at Delft University of Technology. I have been given the opportunity to work on a novel concept in aviation: electric taxiing. I hope my work can contribute to making aviation more sustainable and that, in the future, everyone will be able to enjoy the benefits and opportunities of flying without leaving a (large) carbon footprint.

This research focuses on one of my main professional interests, which is optimisation of processes, and I can honestly say that working on my thesis has been the most interesting part of my studies. I thoroughly enjoyed finding ways to approach the challenge of finding an optimal solution for the problem at hand as efficiently as possible. It was a lot of fun to write code, test and debug until it works and then improve it to reduce computational effort. Furthermore, I enjoyed applying these models to Amsterdam Airport Schiphol, thereby getting to know more about the main airport in our country.

This research would not have been possible without my supervisor, Mihaela Mitici. I would like to thank her for giving me lots of responsibility for my own research, but also stepping in when I needed a bit more guidance. I am grateful that Mihaela always freed up time to provide me with feedback on my work, especially since I know how busy her schedule is. I would also like to thank Juseong Lee for offering a new view on this research during the milestone presentations of this thesis.

Furthermore, I would like to thank my friends from Stud, my housemates, my study friends from ATO and all other friends I made in Delft and earlier in my life. Last but not least, I would like to thank my parents and sister, who have supported me during my entire life. I am very grateful to them for always being there for me.

J.W.D. Kroese
Delft, December 2020

Contents

List of Figures

List of Tables

List of Abbreviations

A	Arrival
AAS	Amsterdam Airport Schiphol
A/C	Aircraft
AGAP	Airport Gate Assignment Problem
AGV	Automated Guided Vehicle
API	Application Programming Interface
APU	Auxiliary Power Unit
ATC	Air Traffic Control
CDM	Collaborative Decision Making
CRR	Coefficient of Rolling Resistance
D	Departure
DLR	German Aerospace Centre (German: Deutsches Zentrum für Luft- und Raumfahrt)
ECDT	Engine Cool-Down Time
EOBT	Earliest Off-Block Time
EP	Electric push-back
ESUT	Engine Spool-Up Time
ET	Electric taxiing
ETS	Electric taxiing systems
FOD	Foreign Object Damage
GA	Genetic Algorithm
IAI	Israeli Aerospace Industries
IATA	International Air Transport Association
LINOS	Linear Optimised Sequencing
LVNL	Air Traffic Control the Netherlands (Dutch: Luchtverkeersleiding Nederland)
MILP	Mixed-Integer Linear Programming
MLG	Main Landing Gear
MTOW	Maximum Take-Off Weight
NLG	Nose Landing Gear
OBT	Off-Block Time
OEM	Original Equipment Manufacturer
Pax	Passengers
PSA	Path Search Algorithm
RH	Receding Horizon
SARDA	Spot and Runway Departure Advisor
SET	Single-Engine Taxiing

SM	Safety Margin
SOBT	Scheduled Off-Block Time
SOSS	Surface Operations Simulator and Scheduler
TET	Twin-Engine Taxiing
TMAT	Target Movement Area entry Time
TMET	Target Movement area Exit Time
TRACC_PB	Taxi Routing for Aircraft: Creation and Controlling for Pushback optimisation
TSAT	Target Startup Approval Time

List of Symbols

ΔT	Minimum charge time to charge batteries, used to balance battery charging in assignment model [s]
Δ_i^0	Time it takes an ET vehicle to drive from start location of ET vehicles at start of the day to task i's start node [s]
Δ_1	Time margin for any aircraft to leave start node [s]
Δ_{ij}^1	Time it takes an ET vehicle to drive from task i's end node to task j's start node [s]
Δ_{ij}^2	Time it takes an ET vehicle to drive from task i's end node to charging station j [s]
Δ_{ij}^3	Time it takes an ET vehicle to drive from charging station i to task j's start node [s]
Δ_i^l	Separation time of aircraft l for node i [s]
Δ_{ij}^l	Taxi time of aircraft l to taxi from node i to node j [s]
μ_0	Constant to calculate μ_g [-]
μ_g	Coefficient of Rolling Resistance [-]
ω_t^k	Weight of a towing vehicle of type k, with $k = \{1, 2, 3\}$ [N]
ω_{ac}^l	Weight of aircraft l [N]
A	Set of aircraft that arrive or depart from the airport at a certain day [-]
a	Total number of aircraft on a day [-]
c	Time penalty for using active runway [s]
c_{ij}^k	Variable that tells if the relevant ET vehicle is charged at charging station k in between tasks i and j [-]
C_{MAX}	Maximum rate at which a battery is being charged or discharged [h^{-1}]
C_{NOM}	Nominal rate at which a battery is being charged or discharged [h^{-1}]
$\overline{D}$	Average delay [s]
D^l	Delay of electrically taxiing aircraft l compared to conventionally taxiing aircraft l [s]
$d_S(e)$	Distance to travel edge e $\in E_S$ [m]
d^{sep}	Minimum separation distance [m]
$d_T(e)$	Distance to travel edge e $\in E_T$ [m]
E_1	Energy before charging batteries [kJ]
e_i'	End node of task i [-]
e_l	End node of aircraft l [-]
E_S	Set of edges in the service road network [-]
E_T	Set of edges in the taxiway network [-]
f_{ij}^l	Variables that tells if ET vehicle l performs tasks i and j consecutively and has a low enough battery to level to allow for ΔT seconds of charging [-]
g_{ij}	Optimal choice of charging station to charge an ET vehicle's batteries if it is driving from task i to task j
G_S	Set of charging station in service road network [-]

H	Set of ET vehicles that can be used [-]
h	Total number of ET vehicles that can be used [-]
h_0	Start number of ET vehicles for assignment model algorithm [-]
h_k	Total number of ET vehicles of type k, with k = {1, 2, 3} [-]
M_1	Big M used for one of the constraints of vehicle routing model [-]
M_2	Big M used for objective function of assignment model [-]
M_3	Big M used for two constraints in section on balancing battery charging [-]
M_4	Big M used for one constraint in section on balancing battery charging [-]
m_k	Mass of ET vehicle type k, with k = {1, 2, 3} [kg]
N	Narrow-body
N_i^+	Set of adjacent nodes from node i
N_i^-	Set of preceding nodes to node i
N_S	Set of nodes in the service road network [-]
N_T	Set of nodes in the taxiway network [-]
P	Set of time steps in a day [-]
p	Total number of time steps in one day [-]
P_k^C	Maximum charging power of ET vehicle battery [kW]
P_{ij}^l	Power for ET vehicle to tow aircraft l from node i to node j [kW]
P_k^{MAX}	Maximum discharge power of ET vehicle of type k, with k = {1, 2, 3} [kW]
Q	Maximum state of charge of ET vehicle [kWh]
q_i^0	Energy it takes an ET vehicle to drive from start location of ET vehicles at start of the day to task i's start node [kJ]
q_{ij}^1	Energy it takes an ET vehicle to drive from task i's end node to task j's start node [kJ]
q_{ij}^2	Energy it takes an ET vehicle to drive from task i's end node to charging station j [kJ]
q_{ij}^3	Energy it takes an ET vehicle to drive from charging station i to task j's start node [kJ]
q_i^E	Energy level at the end of task i [kJ]
Q_k	Maximum state of charge of ET vehicle of type k, with k = {1, 2, 3} [kWh]
q_{ij}^l	Energy required to tow aircraft aircraft l from node i to node j [kJ]
q_i^{req}	Energy level required to perform task i [kJ]
q_i^S	Energy level at the start of task i [kJ]
$taxi^l$	Taxi time of aircraft l [s]
$\overline{taxi}^l$	Average taxi time up to aircraft l [s]
R	Set of tasks that need to be executed by ET vehicles [-]
R_k^i	Subset of tasks for window i and ET vehicle type k [-]
R_k	Set of tasks that need to be executed by ET vehicles of type k, with k = {1, 2, 3} [-]
r_i^t	Set that defines if node i is located at an active runway at time t [-]
s_i'	Start node of task i [-]
s_l	Start node of aircraft l [-]
$taxi_C^l$	Taxi time of conventionally taxiing aircraft l [s]
$taxi_E^l$	Taxi time of electrically taxiing aircraft l [s]

t_{charge}	Charging time [s]
t_i^E	End time of task i [s]
t_{early}^l	Earliest push-back time for aircraft l [s]
t_{late}^l	Latest arrival time for aircraft l at its last node [s]
t_i^S	Start time of task i [s]
v_0	Constant to calculate μ_g [-]
v_k	Velocity of ET vehicles of type k, with $k = \{1, 2, 3\}$ [m/s]
v_{ij}	Velocity at which an aircraft is towed from node i to node j [m/s]
v_{ij}^l	Velocity of aircraft l from node i to node j [-]
v_S	Velocity limit on all edges $\in E_S$ [m/s]
$v_T(e)$	Velocity limit on edge e $\in E_T$ [m/s]
W	Wide-body standard
W^H	Wide-body heavy
w_k	Number of windows used in rolling window strategy for ET vehicles of type k, with $k = \{1, 2, 3\}$ [-]
w_{ij}^k	Placeholder variable to linearise constraints in assignment model [-]
x_i^l	Variables that tells which task i is performed by which ET vehicle l [-]
y_{ij}^{lt}	Variable that tells if aircraft l departs from node i to j at time t [-]
y_l^{lt}	Variables that tells if ET vehicle l performs tasks i and j consecutively [-]
z_{ij}^l	Placeholder variable to linearise constraints in assignment model [-]

Introduction

Nowadays, it is hard to imagine a world without air travel. In the past decades air travel has grown at an immense pace and has become a standard means of transport for people with different backgrounds from all over the world. This has resulted in economic and social prosperity and is therefore definitely something to cherish. On the other hand, one of the biggest challenges of our time is climate change. We need to aim for a more sustainable way of treating our planet in order to preserve it for generations to come. Aviation is no exception to this. Aviation is responsible for about 2.5% of global carbon emissions [28] and is therefore well-positioned to have serious impact on our carbon footprint.

The main challenge for aviation lies in the fact that large-scale air travel is inherently polluting due to the need to burn fuel. Furthermore, air travel is projected to double in size in the next 20 years [1] [21]. Although the Covid-19 pandemic is likely to seriously delay this growth, it does not solve the problem of finding a sustainable alternative to burning kerosene. One way to approach this challenge is by focusing on research on alternative power sources suitable for aviation, while in the meantime keeping aviation organised the way it is. However, a more sensible approach is to simultaneously focus on minimising our impact on the environment as much as possible with the current means available. One way to contribute to less impact of aviation on climate change is the adoption of electric taxiing procedures.

Currently, aircraft drive from the gate to the runway and vice versa using their engines in idle mode. This is highly inefficient due to the fact that aircraft engines are designed for thrust levels high enough to fly [22]. Furthermore, taxi procedures take up more and more of the block time of a flight. This is due to the fact that airports' ground networks are crowded by the high number of flights they need to handle on a daily basis. Major US airlines are reported to have an average taxi-out time of 16.7 minutes and average taxi-in time of 6.9 minutes [13]. These numbers are based on research performed over 10 years ago, which means that taxi-out and taxi-in times are likely to have increased even more. This shows that, especially on short-haul flights, a substantial amount of fuel can be saved and consequently emissions prevented.

Electric taxiing procedures replace engine taxiing by taxiing using an electric power source. The two main kinds of electric taxiing systems are external and on-board electric taxiing systems. The external electric taxiing systems are separate vehicles that tow an aircraft from the gate to the runway or vice versa, whereas on-board electrical taxiing systems are an integral part of the aircraft. Both of these systems are currently being developed by commercial parties and the aviation industry reacts to them with enthusiasm. However, they are not (widely) in operation yet due to the need for certification and small-scale testing of the new electric taxiing procedures. However, the European Commission has published the ambition to have all taxi operations performed electrically in Europe by the year 2050 [35]. This is an ambition that underlines the importance of a continuous effort to make electric taxiing a reality today rather than tomorrow.

This research focuses on the operational aspects of using external electric taxiing systems to perform taxi operations at a hub airport. The final goal of this research is to provide airports with a method to use historical flight data to estimate the required fleet size of external electric taxiing systems to perform all taxi operations at a specific airport electrically. This research has been conducted for the Aerospace Engineering faculty of Delft University of Technology and the hub airport chosen to investigate is Amsterdam Airport Schiphol. This research has not been executed in direct collaboration with Amsterdam Airport Schiphol, but the flight data used has been provided by this party. This research has been conducted from March 2020 to January 2021.

The structure of this report is as follows. First of all, the scientific paper is presented in Part I. This paper describes the problem definition, the models used to tackle the problem at hand and the most important results and conclusions. After that, the literature study performed prior to the work presented in the scientific paper is presented in Part II. This literature study has already been graded as one of the Aerospace Engineering master's degree courses. Lastly, Party III presents the work done that supports the scientific paper.

I

Scientific Paper

Electric taxiing: an optimisation study on the future of airport operations

Author: Jurjen Kroese
Supervisor: Mihaela Mitici

Faculty of Aerospace Engineering, Delft University of Technology, HS 2926 Delft, The Netherlands

Abstract

Electric taxiing (ET) is a novel concept that focuses on replacing engine-powered aircraft taxiing by taxiing using electrically powered towing vehicles, called ET vehicles. The main purpose of ET is reducing the impact of aviation on climate change while at the same time saving fuel costs. In this paper, we propose two models that can be used consecutively to analyse the operational implications of ET. Our goal is to determine the minimum number of ET vehicles required to perform all taxi procedures on a single day at a hub airport. First, we determine the optimal taxi routes for a set of aircraft towed by ET vehicles using a vehicle routing model. Then we find an optimal assignment of ET vehicles to these towing operations, taking into account time and energy constraints and scheduling the moments ET vehicles charge their batteries. We illustrate our models for a quiet and a busy day at Amsterdam Airport Schiphol. The models successfully give concrete guidelines on the required ET vehicle fleet size and infrastructure needed for the implementation of ET. The number of required ET vehicles can be decreased by tactically distributing battery charging over the entire day. Improved battery capacity and power can also effectively decrease ET vehicle fleet size.

Keywords: electric taxiing, airport operations, linear optimisation, towing vehicles

1. Introduction

Aviation is responsible for approximately 2.5% of global carbon dioxide emissions [1]. The number of global air travelers is forecast to nearly double in size in 2037 compared to the 2018 level according to the International Air Transport Association (IATA) [2]. Airbus projects 4.3% air traffic growth per year over the next 20 years in their Global Market Forecast 2019-2039 [3], which means air traffic will more than double before 2040.[1] Ideally, the environmental impact of aviation can be decreased in absolute numbers (e.g. in tonnes of carbon dioxide emissions); however, this is extremely difficult for an industry that grows at such a rapid rate and is, at least for now, inherently polluting due to the need to burn fuel. A lot of resources are invested in research into alternative ways of flying, e.g. electrically-powered flying [4] and burning bio fuels instead of kerosene [5]. However, in the meantime it is of utmost importance for the aviation industry to do everything in its power to minimise environmental impact with the current means available.

One of the possible ways to contribute to less environmental impact is the adoption of electric taxiing (ET). Most aircraft operations at the airport's surface are currently performed using aircraft's main engines in idle mode, which is highly inefficient [6]. Considerable amounts of fuel can be saved and consequently emissions prevented by replacing these engine-powered taxi operations by electrically powered taxi operations [7]. ET also saves airlines costs due to increased carbon brake lifetime [8] and lower chance of Foreign Object Damage (FOD) [9]. Furthermore, the European Commission published their vision on the future of aviation in 2011, which states that all taxi operations at airports need to be electrically powered by 2050 [10]. ET can be performed by external or on-board electric taxiing systems (ETS). External ETS, called ET vehicles, are separate electrically powered vehicles which tow an aircraft from the gate to the runway and vice versa. On-board ETS are installed on the aircraft and therefore require a lengthy certification process and add on-board weight, which increases in-flight fuel consumption. ET vehicles are currently the most technologically mature of the two options [9] and Israeli Aerospace Industries' (IAI) TaxiBot is used as a benchmark for ET vehicle characteristics in this research.

ET poses several operational challenges. First of all, aircraft engines need to warm-up before take-off and cool-down before turning them off after landing. This happens automatically while taxiing conventionally with the engines in idle mode. During ET, however, the engines are turned off and turning them on while taxiing electrically leads to safety issues due to the absence of ground staff and fire protection [11]. Therefore, the Engine Spool-Up Time (ESUT) needs to be added after the taxi-out procedure and the Engine Cool-Down Time (ECDT) before the taxi-in procedure. ET vehicles also need to attach to and detach from the aircraft before and after each taxi operation. These additional

[1] The estimates in this section have been made before the COVID-19 pandemic, which will inevitably slow down air traffic growth

operations inevitably incur delays at a busy hub airport. Furthermore, taxi schedules become much more complicated when using ET vehicles, since Air Traffic Control (ATC) has to make sure an ET vehicle is always present at the right place and time to perform an aircraft's taxi operation. Lastly, airports also need to determine the ET vehicle fleet size to be able to perform all taxi operations electrically on each day of the year.

In this paper, we address these challenges by analysing the implementation of ET vehicles at a hub airport. We develop two optimisation models: one that defines the optimal taxi schedule on one day when taxiing electrically and one that finds the optimal assignment of ET vehicles to all taxi operations in this schedule in order to minimise the ET vehicle fleet size. The first model is a vehicle routing model and takes into account the abovementioned additional operations specific to ET. This model is also used to generate the optimal taxi schedule of conventionally taxiing aircraft; these results are compared to the ET results in order to quantify the impact of electric taxiing on taxi operations. The second model is an assignment model and determines which ET vehicle performs which taxi operations in the ET taxi schedule generated by the vehicle routing model. We take into account the battery levels of all ET vehicles and optimally schedule battery charging in between taxi operations. We apply our optimisation models to two one-day flight schedules at Amsterdam Airport Schiphol (AAS). This use case is especially interesting due to the 'Draft agreement sustainable aviation' [12], which states the ambition to make ET the standard taxi procedure at all Dutch airports by the year 2030.

We propose novel research that focuses on fully incorporating ET at a hub airport. We are able to analyse this by means of separating a very large problem into two smaller problems. The vehicle routing model first finds the optimal taxi schedule without taking into account individual ET vehicle assignment. This substantially decreases computational effort and also accomplishes the goal of implementing ET with as little negative impact on on-time performance at the airport as possible. In the assignment model, we use a rolling window strategy that helps to significantly decrease computational time at the cost of slightly compromising solution quality. From a practical point of view, we provide airports with a method to use recent flight data to accurately estimate the number of ET vehicles required to perform all their taxi operations electrically. The models can be easily adapted to anticipate changes in ET vehicle characteristics, charging station locations and airport regulations. In this way, policy makers can use statistical results to define the roadmap towards fully electric taxiing in the near future.

This paper is structured as follows. We give an overview of relevant prior work in section 2. Then, we give a description of the problem in section 3 and an overview of the energy model in section 4. In section 5, we present the mathematical vehicle routing and assignment model. A description of the data used and the results are given in section 6. In section 7, we present the results of the sensitivity analysis to test the robustness of our models. Section 8 describes an addition to the assignment model and, lastly, section 9 presents our conclusions and recommendations for future work.

2. Prior Work

In this section, we give a description of optimisation techniques used to solve optimisation problems similar to the problem solved in this research. We use these insights to develop our vehicle routing and assignment model. The focus of this research lies on the operational aspects of ET and, therefore, this section also discusses three papers that specifically focus on ET operations. This information serves as a guideline to identify the knowledge gap this research aims to fill.

2.1. Optimisation Strategies

Smeltink and Soomer [13] have developed a MILP model that optimises taxi operations at AAS by defining a node-edge network of the airport and sequencing aircraft at each node in the network with enough separation time to ensure safe operations. The route of each individual aircraft is fixed beforehand, only the optimal times at which the nodes are reached are determined by the model. Holding points are modelled by nodes with a connecting edge with a length of zero. Smeltink and Soomer [13] use three different rolling window strategies in order to limit computational time. The first one fixes aircraft routes after they have been scheduled, the second allows for rescheduling in the next window and the third uses a sliding window technique. Clare and Richards [14] use a similar approach to the second rolling window strategy of Smeltink and Soomer [13], but use virtual nodes to define the last position of an overlapping aircraft in the previous execution window. Furthermore, Clare and Richards [14] do not define constraints to avoid conflicts between aircraft beforehand, but identify conflicts after having solved the optimisation problem and add constraints to resolve each conflict in the next run, in order to avoid using redundant constraints. In Roling's [15] optimisation model, all possible routes for each aircraft are defined beforehand and a subset of these routes is used as possible options for that aircraft when solving the optimisation problem. The subset always consists of the aircraft's shortest route and the other routes are chosen based on their length and on how much they differ from the shortest route in terms of nodes used. The more different a route is from the shortest route, the more likely it is to be chosen

for the subset of routes used in the optimisation problem. In this way, the model has a choice between substantially different routes for each aircraft.

In our research, we limit computational time by using, among others, the 'relevant nodes' strategy explained in section 5.1.4, which has similarities to the strategies used by Smeltink and Soomer [13] and Roling [15], but leaves the model more options to choose from since our strategy does not define the available routes beforehand. Furthermore, we use a rolling window strategy, explained in section 5.2.1, similar to the first strategy used by Smeltink and Soomer [13]. Contrary to Clare and Richards [14], we define all constraints before solving our models.

Pereira [16] has devised a MILP model that assigns electric aircraft to missions (i.e. flights) with a start/end time, duration and energy requirement. The number of aircraft required is determined by iteratively increasing the number of aircraft available until the model is able to fulfill all missions. Ding et al. [17] solve an over-constrained Airport Gate Assignment Problem (AGAP) by using "a hybrid simulated annealing with tabu search approach" [17], while minimising ungated flights and passenger walking time. A greedy method is used to get an initial flight-to-gate assignments solution. Wen et al. [18] present a MILP and a neighbourhood search model to schedule electric vehicles with charging options. They use a linearly varying charging time based on the amount of energy charged by the vehicle.

We have decided to employ an approach similar to the aircraft-to-mission assignment used by Pereira [16]. We also start with an initial number of ET vehicles and increase this number until we can perform all taxi operations electrically. This optimisation strategy will be further elaborated upon in subsection 5.2.2. Similar to Wen et al. [18], we determine ET vehicle charging time based on battery levels before and after charging.

2.2. Electric taxiing

Roling et al. [19] analyse the effect of on-board ETS on operations at AAS. Electrically taxiing aircraft are assumed to have a lower velocity than conventionally taxiing aircraft and the minimum ET velocity that does not cause (too much) delay is determined. Guillaume [20] investigates automated guided vehicle (AGV) operations at AAS, which is similar to ET vehicle operations. The AGVs only perform taxi-out procedures and the vehicles do not have to be charged. The objective is to incorporate AGVs in normal ground operations in a way that reduces costs and not to perform all taxi operations by AGVs. Van Baaren [21] researches the potential of ET operations at AAS by optimally assigning a fixed number of ET vehicles to aircraft taxi operations. Van Baaren [21] designs conceptual ET vehicles, determines costs, emissions and duration for each segment of the taxiway network and then solves a vehicle routing problem. The paper does not take into account conflicts between aircraft or delay caused by ET operations.

The main difference between our approach and the three abovementioned models, is the fact that we have split the problem into a vehicle routing model and an assignment model. Roling et al. [19] use on-board ETS and therefore do not need to assign ET vehicles to taxi operations. Compared to Guillaume [20] and Van Baaren [21], we are able to limit computational time of the vehicle routing model by performing ET vehicle assignment separately. This enables us to perform all taxi operations electrically, take into account conflicts between taxiing aircraft and incorporate ET vehicle charging within a practical computational time span.

3. Problem Description

We consider a set of non-homogeneous aircraft A, with $|A| = a$, that taxi at an airport during one day. We divide the aircraft into three groups based on each aircraft's weight: narrow-body (N), standard wide-body (W) and heavy wide-body (W^H). We also consider a set of ET vehicles H, with $|H| = h$, which have a battery capacity Q and are used to perform the taxi operations of all aircraft in A. A taxi operation is defined as a procedure in which an ET vehicle tows an aircraft from the gate to the runway or vice versa. This includes the additional actions that need to be executed before and after the actual towing of the aircraft. Figure 1 gives a schematic overview of the entire taxi operation for departing and arriving aircraft. A departing aircraft is first connected to an ET vehicle, which pushes the aircraft back towards the taxiway. We assume deterministic durations for these actions. After that, the ET vehicle tows the aircraft to the runway, of which the duration depends on how the taxiing aircraft will be scheduled. Once the runway is reached, post-processing is carried out, which has a deterministic duration and includes detaching the ET vehicle. Lastly, the engines need to warm up for a duration equal to the ESUT; the ET vehicle is not required for this. For arriving aircraft, the engines first need to cool down after landing for a duration equal to the ECDT. Then, the ET vehicle connects to the aircraft and tows it to the gate, of which the duration depends on how the taxiing aircraft will be scheduled. Lastly, post-processing is carried out. We use three types of ET vehicles: 1 (for N aircraft), 2 (for W aircraft) and 3 (for W^H aircraft). Each ET vehicle type can only tow aircraft of its corresponding group. The set of ET vehicles H is, therefore, split into subsets H_1, H_2 and H_3, with $|H_1| = h_1$, $|H_2| = h_2$ and $|H_3| = h_3$ and fixed battery capacities Q_1, Q_2 and Q_3. The maximum velocities at which each ET vehicle type can tow an aircraft are defined as v_1, v_2 and v_3. The values of h_1, h_2 and h_3 are not know a priori and are the final results we want to obtain.

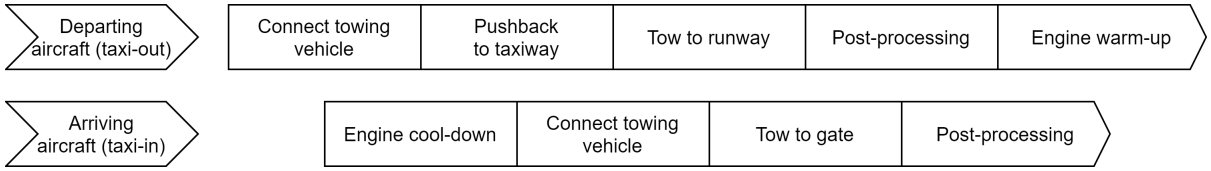

Figure 1: Taxi operation of a departing (taxi-out) and arriving (taxi-in) aircraft

We consider two graphs that describe an airport: directed taxiway network graph $T(N_T, E_T, d_T(e), v_T(e))$ and undirected service road network graph $S(N_S, E_S, G_S, d_S(e), v_S)$. Set N_T defines the nodes and set E_T the edges in $T(N_T, E_T, d_T(e), v_T(e))$. $d_T(e)$ defines the distance to travel edge $e \in E_T$. $v_T(e)$ defines the velocity limit of edge $e \in E_T$. The velocity v_{ij}^l at which aircraft l is towed along edge (i, j) in E_T is defined by $v_{ij}^l = \min(v_T(i, j), v_k)$, where k equals the type number of the ET vehicle that tows aircraft l. Set N_S defines the nodes and set E_S the edges in $S(N_S, E_S, G_S, d_S(e), v_S)$. Set G_S defines the nodes at which we have located charging stations, with $G_S \subset N_S$. $d_S(e)$ defines the distance to travel edge $e \in E_S$. We assume v_S to be a constant velocity limit for all edges in E_S. Part of the nodes in N_T are located at a runway entrance/exit or gate, which are the start and end points of each taxi operation. Each runway or gate node in N_T has a node in N_S located right next to it, so the start and end point of each taxi operation can be reached both through $T(N_T, E_T, d_T(e), v_T(e))$ and $S(N_S, E_S, G_S, d_S(e), v_S)$. $T(N_T, E_T, d_T(e), v_T(e))$ is only used by ET vehicles attached to an aircraft in order to perform taxi operations. After an ET vehicle detaches from an aircraft, it individually drives to the start node of another taxi operation using $S(N_S, E_S, G_S, d_S(e), v_S)$. We assume that ET vehicles do not have to be deconflicted while driving individually, since the edges in E_S do not overlap with the edges in E_T and ground personnel driving the ET vehicles can avoid other ET vehicles similarly to driving a normal car. Consequently, we can assume that ET vehicles can always drive the shortest route between all nodes in $S(N_S, E_S, G_S, d_S(e), v_S)$. Furthermore, we assume that each ET vehicle can always drive at the maximum allowed velocity specified by v_S while driving individually.

Each aircraft l in A starts its taxi operation at start node $s_l \in N_T$, ends its taxi operation at end node $e_l \in N_T$ and has an earliest time t_{early}^l at which it can start taxiing from s_l through $T(N_T, E_T, d_T(e), v_T(e))$. We define the taxi path of aircraft l as the sequence of nodes in N_T the aircraft follows to get from s_l to e_l during a specific time period. This taxi path defines the 'tow to runway' or 'tow to gate' actions in figure 1. We are interested in finding the optimal taxi paths of all aircraft in A in order to minimise total taxi time while avoiding any conflicts between taxiing aircraft. A conflict is defined as a violation of the minimum separation distance d^{sep}, which is the minimum distance an aircraft needs to keep from another aircraft. A conflict could occur when two aircraft are towed along an edge in E_T in the same direction and the trailing aircraft catches up with the leading aircraft. This can only occur if the trailing aircraft is towed by a faster type of ET vehicle than the leading aircraft. Secondly, two aircraft could violate d^{sep} by crossing the same node in N_T too shortly after one another. Lastly, a conflict situation occurs when two aircraft are towed along the same edge in E_T in opposite directions at the same time, which results in a head-on conflict.

Having obtained all taxi paths, we first note that gate/runway nodes s_l and e_l have a corresponding node in N_S located next to it, which we define as s_l' and e_l'. Then, we define a towing task as follows. Towing task i is a tow operation of aircraft l that starts at node s_l' at time t_i^S and ends at node e_l' at time t_i^E and requires a certain amount of energy q_i^{req}. The energy model in section 4 describes how to calculate the energy requirement, which is a function of aircraft and ET vehicle weight, taxi velocity and taxi time. We define a set of towing tasks R, with $|R| = a$. We are interested in finding an optimal assignment of ET vehicles to all towing tasks in R in order to minimise the total number of ET vehicles required. Since ET vehicles can only tow aircraft of their corresponding group of aircraft, we can split the towing tasks in R into subsets of tasks R_1 (for N aircraft), R_2 (for W aircraft) and R_3 (for W^H aircraft), where $|R_1| + |R_2| + |R_3| = |R|$, and find the minimum number of ET vehicles h_1, h_2 and h_3 for each subset separately.

The assignment of ET vehicles to towing tasks is constrained by both time and energy. An ET vehicle must be able to arrive at the start node of task i before t_i^S. An ET vehicle also needs to have an energy level higher than or equal to q_i^{req} plus a safety margin SM at the start of task i. For an ET vehicle of type k, with $k = \{1, 2, 3\}$, we assume $SM = 0.2 \cdot Q_k$. Lastly, ET vehicles can drive from the end node of a task to the start node of another task either directly or via a charging station to charge their batteries. We assume that, if an ET vehicle of type k decides to charge, it always needs to charge to Q_k.

As an example, we consider a set of aircraft $A = \{1, 2, 3\}$. We assume that all aircraft in this example are of type N, all ET vehicles are of type 1 and that Q_1 equals 12000 kJ. We consider graphs $T(N_T, E_T, d_T(e), v_T(e))$, with $N_T = \{1, 2, 3, 4\}$ and $E_T = \{(1,3), (2,1), (2,3), (3,2), (3,4), (4,2)\}$, and $S(N_S, E_S, G_S, d_S(e), v_S)$, with $N_S = \{1, 2, 3\}$, $E_S = \{(1,2), (1,3), (2,1), (2,3), (3,1), (3,2)\}$ and $G_S = 1$, as shown in figure 2. $(d_T(e), v_T(e))$ and $(d_S(e), v_S)$ are displayed next to their corresponding edges, in meters and meters per second respectively.

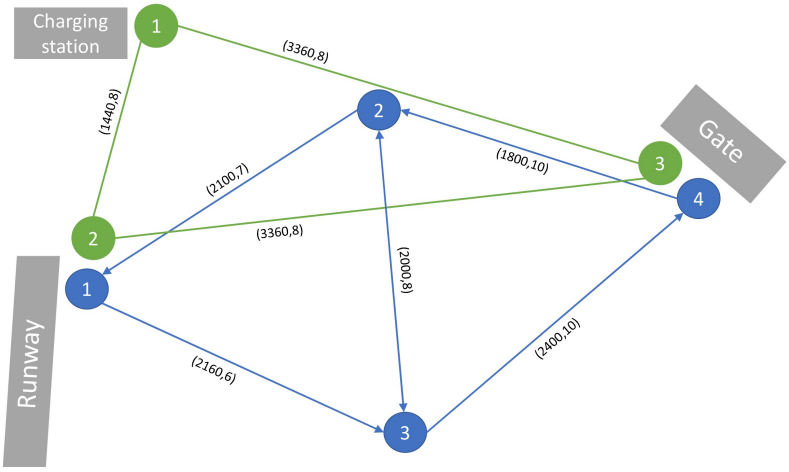

Figure 2: Mock networks $T(N_T, E_T, d_T(e), v_T(e))$ and $S(N_S, E_S, G_S, d_S(e), v_S)$

We determine the optimal taxi paths for all aircraft in A; the results are shown in table 1. In this example, we assume that the aircraft can be towed at the velocity limits defined by $v_T(e)$. Table 1 shows the sequence of nodes each aircraft follows, where the first node in the sequence is s_l and the last node in the sequence is e_l for $l = \{1, 2, 3\}$. The last column of table 1 shows the time stamps at which each node in the sequence is reached; the first time stamp equals t^l_{early} for $l = \{1, 2, 3\}$.

Aircraft l	**Nodes**	**Times [HH:mm]**
1	1 - 3 - 4	09:00 - 09:06 - 09:10
2	1 - 3 - 4	09:13 - 09:19 - 09:23
3	4 - 2 - 1	10:40 - 10:43 - 10:48

Table 1: Mock taxi paths for aircraft in A

The taxi paths are converted to set of towing tasks $R = \{1, 2, 3\}$; these tasks are shown in figure 2. The durations of the additional actions from figure 1 are added before and after the taxi paths' start and end time. Also, s_l and e_l are converted to s'_i and e'_i, where aircraft l corresponds to task i.

Task i	**q_i^{req} [kJ]**	**s'_i**	**t_i^S [HH:mm]**	**e'_i**	**t_i^E [HH:mm]**	**ET vehicle type**
1	3500	2	08:59	3	09:11	1
2	5000	2	09:12	3	09:24	1
3	6500	3	10:37	2	10:49	1

Table 2: Mock table with towing task

In order to find an optimal assignment of ET vehicles to the towing tasks, we also need to know how much time and energy it takes to drive between nodes in $S(N_S, E_S, G_S, d_S(e), v_S)$. This is shown in table 3.

Node 1	**Node 2**	**Duration [s]**	**Energy [kJ]**
1	2	180	276
1	3	420	643
2	3	420	643

Table 3: Mock table with shortest ET vehicle routes in $S(N_S, E_S, G_S, d_S(e), v_S)$

We intuitively explain the way an optimal assignment can be determined, taking into account time and energy constraints, as follows. If an ET vehicle performs task 1 and drives to task 2, it arrives at the start node of task 2 at 09:18, which is later than t_2^S. This means that we need a second ET vehicle to perform task 2. ET vehicle one can easily perform task 3 in time but will have a battery level of 2000 kJ (12000 - 3500 - 6500) after performing task 3, which is less than the SM of 20% of Q_1. Therefore, ET vehicle one first drives to the charging station node defined by

G_S and charges its batteries to Q_1, which we assume to take 20 minutes. After that, ET vehicle one is able to perform task 3 and, consequently, the minimum number of ET vehicles h_1 required to perform all towing tasks in R is equal to two.

4. Energy Model

We use a simple energy model to define the energy required to perform each towing task. The model is described by equations (1), (2), (3) and (4) [21] [22] and is used to calculate the energy consumption to tow aircraft l from node $i \in N_T$ to node $j \in N_T$. It is assumed that the slope of the taxiway is always equal to 0°.

$$q_{ij}^l = P_{ij}^l \cdot \Delta_{ij}^l \tag{1}$$

$$\Delta_{ij}^l = \frac{d_T(i,j)}{v_{ij}^l} \tag{2}$$

$$P_{ij}^l = \mu_g \cdot (\omega_{ac}^l + \omega_t^k) \cdot v_{ij}^l \tag{3}$$

$$\mu_g = \mu_0 \left(1 + \frac{v_{ij}^l}{v_0}\right) \tag{4}$$

where q_{ij}^l denotes the energy required to tow aircraft l for Δ_{ij}^l seconds at a power level of P_{ij}^l. Δ_{ij}^l defines the time it takes to tow aircraft l along edge $(i,j) \in E_T$. P_{ij}^l denotes the required power to tow aircraft l with weight ω_{ac}^l at velocity v_{ij}^l using an ET vehicle of type k with weight ω_t^k. The type k of the ET vehicle depends on the weight group of aircraft l, as defined in section 3. μ_g denotes the Coefficient of Rolling Resistance (CRR) of an aircraft towed at velocity v_{ij}^l; μ_0 and v_0 are constants to calculate the CRR [22].

To calculate the required energy per towing task, we use the sequence of nodes which is defined by each aircraft's taxi path, as shown in table 1. In this explanation, we assume an arbitrary taxi path with sequence of nodes {1,2,...,n} for aircraft l and corresponding ET vehicle type k. We determine the energy consumption for this taxi path as follows. First, we use equations (2), (3) and (4) to calculate $P_{i,i+1}^l$ and $\Delta_{i,i+1}^l$, for $1 \leq i \leq n-1$. This gives us the required power level and the time this power needs to be supplied on each edge of the taxi path. Then, we use equation (1) to calculate $q_{i,i+1}^l$, for $1 \leq i \leq n-1$, which gives us the energy required for each edge. Finally, we calculate the total energy required to tow aircraft l along its entire taxi path by means of $\sum_{i=1}^{n-1} q_{i,i+1}^l$.

Equations (5) and (6) are used to calculate the time, t_{charge}, to charge an ET vehicle of type k from initial energy level E_1 to capacity Q_k [23]. These equations are used to define time-related constraint (23).

$$t_{charge} = \frac{Q_k - E_1}{P_k^C} \tag{5}$$

$$P_k^C = \frac{P_k^{MAX}}{\frac{C_{MAX}}{C_{NOM}}} \tag{6}$$

where P_k^C denotes the charging power of ET vehicle type k and is calculated using its maximum discharge power P_k^{MAX} and the nominal and maximum C-rates C_{NOM} and C_{MAX} which are "a measure of the rate at which a battery charges/discharges relative to its maximum capacity" [16].

5. Taxi Schedule Generation and ET Vehicle Assignment

The assignment of ET vehicles to the optimal electric taxi routes for an entire day of operations at a hub airport has been split into two stages: the vehicle routing model described in subsection 5.1 and the assignment model described in subsection 5.2.

In the first stage, the vehicle routing model defines the optimal taxi routes of all aircraft in a one-day flight schedule of an airport by minimising total taxi time. The aircraft are towed by ET vehicles and therefore need to take into account additional operations and performance characteristics specific to ET. The vehicle routing model assumes that there is always an ET vehicle available to perform an aircraft's taxi operation. In this way, we truly find the taxi schedule which minimises negative impact of ET on on-time performance at the airport. The vehicle routing model also ensures there are no conflicts between taxiing aircraft. After the optimal taxi schedule has been defined for ET, we also run the model for conventional taxiing in order to compare ET performance to the current situation.

The results of the vehicle routing model provide us with the timing, locations and ET vehicle type for each taxi operation. We want to find out how many ET vehicles we require to perform all these taxi operations. Therefore, in the second stage, we take the taxi schedule from the first stage and convert each taxi operation to a towing task. We use the energy model described in section 4 to calculate the ET vehicle energy consumption for each towing task. Next, we determine the duration and energy consumption of the ET vehicle movements in $S(N_S, E_S, G_S, d_S(e), v_S)$ by means of a shortest path algorithm and the energy model from section 4. These movements can be divided into two groups. First, we determine the time and energy it takes an ET vehicle to drive from the end node of a certain towing task to the start node of all towing tasks that are planned later during the day. Secondly, ET vehicles have the option to charge their batteries at a charging station between two tasks they perform. Therefore, we determine the time and energy it takes to drive from the end node of each task to all charging station nodes and from all charging station nodes to the begin node of each task. Furthermore, we assume that all ET vehicles start their day of operations from the same charging station node. Having defined the towing tasks and the possible ET vehicle movements between these towing tasks, we use the rolling window strategy described in subsection 5.2.1 and the algorithm described in subsection 5.2.2 to find the minimum number of ET vehicles required to perform all towing tasks.

5.1. Vehicle Routing Model

In section 3, we have introduced set of aircraft A, set of nodes N_T and set of edges E_T. Each aircraft $l \in A$ has an earliest time it can start taxiing t^l_{early} from start node $s_l \in N_T$ and a latest time it is allowed to arrive t^l_{late} at its end node $e_l \in N_T$.

In this subsection, we define set of time steps P, with $|P| = p$, which is used to discretise our model. We also introduce $N_i^+ = \{ j \mid (i,j) \in E_T \} \ \forall\, i,j \in N_T$ and $N_i^- = \{ j \mid (j,i) \in E_T \} \ \forall\, i,j \in N_T$. N_i^+ is a nested list that holds the nodes which can be reached directly from node i. N_i^- is a nested list that holds the nodes from which node i can be reached directly. We use the mock network of $T(N_T, E_T, d_T(e), v_T(e))$ displayed in figure 2 to illustrate the meaning of sets N_i^+ and N_i^- as follows. In the mock network, N_1^+ is equal to {3}, since node 3 is the only node an aircraft can travel to from node 1. N_1^-, on the other hand, is equal to {2} since node 1 can only be reached from node 2. N_3^+ is equal to {2, 4} and N_3^- is equal to {1, 2}, since the edge between nodes 2 and 3 is a two-way edge and the other edges are one-way edges.

5.1.1. Variables

We define the following decision variables:

$$y_{ij}^{lt} = \begin{cases} 1, & \text{if aircraft } l \text{ departs from node } i \text{ to } j \text{ at time } t \ \ \forall\, l \in A,\ i \in N_T,\ j \in N_i^+,\ t \in P \\ 0, & \text{otherwise} \end{cases}$$

We define the following additional variables:

Δ_{ij}^l : taxi time of aircraft l from node i to j $\forall\ l \in A, i \in N_T, j \in N_i^+$

$$r_i^t = \begin{cases} 1, & \text{if node } i \text{ is located at an active runway at time } t \ \ \forall\, i \in N_T,\ t \in P \\ 0, & \text{otherwise} \end{cases}$$

Δ_i^l *:* separation time for aircraft l and node i $\forall\ l \in A, i \in N_T$

Δ_{ij}^l is calculated by means of equation (2) using $d_T(e)$ and v_{ij}^l as inputs, which are defined in section 3. Regarding r_i^t, we note that an active runway is defined as a runway that is being used for landing and take-off at time t. The separation time Δ_i^l is defined as the travel time required for aircraft l to reach a distance from node i that equals d^{sep} and is calculated using: $\Delta_i^l = \max_{j \in N_i^+}(\frac{d^{sep}}{v_{ij}^l})$. The reason why we define Δ_i^l by taking the maximum travel time for the edges going from node i to nodes $j \in N_i^+$ will be explained in subsection 5.1.3.

5.1.2. Objective Function

The objective function minimises the total taxi time of all aircraft in A. The first term considers the time between t^l_{early} and the moment node $e^l \in N_T$ is reached for all $l \in A$. $y_{ie_l}^{lt}$ equals 1 if aircraft l starts taxiing its last edge to its end node e_l at time t. $\Delta_{ie_l}^l$ is added to t to take into account the time it takes aircraft l to travel its last edge and t^l_{early} is subtracted to get the total taxi time of aircraft l measured from its earliest possible start time. We want to minimise the negative impact of ET on on-time performance at the airport and therefore measure taxi time from t^l_{early}, also if aircraft l decides to start taxiing later than its earliest possible start time.

$$min \left(\sum_{l \in A} \sum_{t^l_{early} \le t \le t^l_{late}} \sum_{i \in N_{e_l}^-} (t - t^l_{early} + \Delta_{ie_l}^l) \cdot y_{ie_l}^{lt} + c \cdot \sum_{l \in A} \sum_{t^l_{early} \le t \le t^l_{late}} \sum_{i \in N_T} \sum_{j \in N_i^+} r_i^t \cdot y_{ij}^{lt} \right) \tag{7}$$

The second term adds a time penalty c to the objective function each time a towed aircraft uses a node located at a runway crossing if that runway is used for departures or arrivals at time t, since crossing an active runway realistically induces some waiting time for the towed aircraft in order to get clearance from ATC to cross the runway.

5.1.3. Constraints

We define the following constraints:

$$y_{ij}^{lt} - \sum_{\substack{k \in N_j^+ \\ k \neq i}} y_{jk}^{l\, t+\Delta_{ij}^l} \leq 0 \qquad \forall\, l \in A,\ \ i \in N_T,\ \ j \in N_i^+,\ \ t_{early}^l \leq t \leq t_{late}^l,\ \ \substack{i \neq e_l \\ j \neq e_l} \tag{8}$$

$$\sum_{j \in N_{s_l}^+} \sum_{t_{early}^l \leq t \leq t_{early}^l + \Delta_1} y_{s_l j}^{lt} - \sum_{i \in N_{s_l}^-} \sum_{t_{early}^l \leq t \leq t_{early}^l + \Delta_1 + \Delta_{s_l i}^l} y_{i s_l}^{lt} = 1 \qquad \forall\, l \in A \tag{9}$$

$$\sum_{i \in N_{e_l}^-} \sum_{t_{early}^l \leq t \leq t_{late}^l} y_{i e_l}^{lt} - \sum_{j \in N_{e_l}^+} \sum_{t_{early}^l \leq t \leq t_{late}^l} y_{e_l j}^{lt} = 1 \qquad \forall\, l \in A \tag{10}$$

$$\sum_{l \in A} \sum_{j \in N_i^+} \sum_{t \leq t_1 < t + \Delta_i^{W^H}} y_{ij}^{lt_1} \leq 1 \qquad \forall\, i \in N_T,\ \ t \in P \tag{11}$$

$$\sum_{l \in A} y_{ij}^{lt} \cdot \sum_{l \in A} \sum_{t \leq t_1 < t + \Delta_{ij}^{W^H}} y_{ji}^{lt_1} = 0 \qquad \forall\, i \in N_T,\ \ j \in N_i^+,\ \ t \in P \tag{12}$$

Constraint (8) ensures that each aircraft that reaches a certain node j, also has to leave that node right after it has arrived. The moment in time at which aircraft l has to leave node j is determined by adding Δ_{ij}^l, the taxi time between nodes i and j, to the time t aircraft l has left node i. This makes sure that aircraft are towed along a continuous path between nodes and cannot hold at any of the nodes or start being towed from a node if it has not arrived there first. A few exceptions are required to be able to define a route from aircraft l's start node s_l to its end node e_l. First of all, e_l is excluded from this constraint for all $l \in A$, since an end node should not be left after it has been reached. Secondly, node k cannot be equal to node i since that would give the aircraft the option to travel back the same way it came. Lastly, the left-hand side needs to be smaller than or equal to 0 since the second term can also be equal to 1 when the first term equals 0.

Constraint (9) ensures each aircraft l leaves s_l within the first Δ_1 time steps from t_{early}^l. s_l can be a gate node, in case of departures, or a runway node, in case of arrivals. Constraint (10) ensures each aircraft l finishes its path at e_l, which can be a gate node, in case of arrivals, or a runway node, in case of departures.

Constraint (11) ensures a minimum separation, equal to d^{sep}, between all aircraft. If aircraft l leaves node i at time t, no other aircraft are allowed to reach node i for the next $\Delta_i^{W^H}$ time steps. Since aircraft can only be towed along an edge with a constant velocity, ensuring separation at the nodes also ensures separation on the edges. $\Delta_i^{W^H}$ is defined as the separation time for an aircraft of type W^H and node i; its use will be further explained below by remarks 1 and 2.

Constraint (12) ensures aircraft can never be taxiing the same edge in opposite directions during the same time period, which would result in a head-on conflict. If aircraft l starts being towed from node i to node j at time t, no other aircraft are allowed to be towed from node j to node i for the next $\Delta_{ij}^{W^H}$ time steps. $\Delta_{ij}^{W^H}$ is defined as the taxi time of an aircraft of type W^H from node i to node j; its use will be further explained below by remark 3. Since it is not known beforehand how many aircraft are towed in one of the two directions, constraint (12) has been written as a multiplication of decision variables. However, we have rewritten constraint (12) as a linear constraint in equation (13) using the Big M method. Constraint (13) is only generated for two-way edges; for one-way edges it is impossible to get head-on conflicts.

$$(1 - \sum_{l \in A} y_{ij}^{lt}) \cdot M_1 - \sum_{l \in A} \sum_{t \leq t_1 \leq t + \Delta_{ij}^{W^H}} y_{ji}^{lt_1} \geq 0 \qquad \forall\, i \in N_T,\ \ j \in N_i^+,\ \ t \in P \tag{13}$$

Remark 1. In constraint (11), we use $\Delta_i^{W^H}$ instead of Δ_i^l since it is not known beforehand which kind of aircraft will be towed from node i and therefore a worst-case (slowest) scenario needs to be assumed. The following example illustrates why using Δ_i^l would not result in the correct constraint. We consider two aircraft that can taxi from node i to i's only adjacent node j at time step $t = 1$: an N aircraft, $l = 1$, with Δ_i^1 equal to two time steps and a W^H aircraft, $l = 2$, with Δ_i^2 equal to four time steps. If Δ_i^l were used, we would get the following constraint: $y_{ij}^{1,1} + y_{ij}^{1,2} + y_{ij}^{2,1} + y_{ij}^{2,2} + y_{ij}^{2,3} + y_{ij}^{2,4} \leq 1$. If aircraft 2 starts travelling edge *(i,j)* at $t = 1$, no other aircraft should be allowed to start being towed from node i to any adjacent nodes, in this example only node j, for four time steps (since that is how long it takes aircraft 2 to travel d^{sep} meters from node i). However, according to this constraint, aircraft 1 can start taxiing from node i at $t = 3$ again, since the constraint only includes decision variables for aircraft 1 at $t = \{1, 2\}$. Therefore, the constraint should be $y_{ij}^{1,1} + y_{ij}^{1,2} + y_{ij}^{1,3} + y_{ij}^{1,4} + y_{ij}^{2,1} + y_{ij}^{2,2} + y_{ij}^{2,3} + y_{ij}^{2,4} \leq 1$.

Remark 2. Similarly, the separation time is defined per node and not for the individual edges: $\Delta_i^{W^H}$ instead of $\Delta_{ij}^{W^H}$. As an example, we consider node i at time step t and two W^H aircraft, $l = \{1, 2\}$. Node i has two adjacent nodes: $j = \{1, 2\}$. Therefore, the aircraft can choose between two edges: *(i,1)* and *(i,2)*. Due to a different maximum allowed velocity per edge, it takes one time step to get to the separation distance via *(i,1)* and two time steps via *(i,2)*. This results in the following constraint if $\Delta_{ij}^{W^H}$ were used: $y_{i1}^{1,1}+y_{i2}^{1,1}+y_{i2}^{1,2}+y_{i1}^{2,1}+y_{i2}^{2,1}+y_{i2}^{2,2} \leq 1$. If aircraft 1 starts being towed along edge *(i,2)* at $t = 1$, node i should be unavailable for aircraft 2 for two time steps. However, this constraint would allow $y_{i1}^{2,2}$ to be equal to 1. Therefore the constraint should be: $y_{i1}^{1,1}+y_{i1}^{1,2}+y_{i2}^{1,1}+y_{i2}^{1,2}+y_{i1}^{2,1}+y_{i1}^{2,2}+y_{i2}^{2,1}+y_{i2}^{2,2} \leq 1$.

Remark 3. In constraint (13), the parameter $\Delta_{ij}^{W^H}$ is used instead of Δ_{ij}^{l} since both terms have a separate summation of l over A. The time, Δ_{ij}^{l}, edge *(j,i)* is unavailable for towed aircraft, depends on the type of aircraft l that taxis edge *(i,j)*. However, l in the first and second term of constraint (13) are defined separately; therefore, Δ_{ij}^{l} cannot be adjusted for the type of aircraft l that taxis edge *(i,j)* but depends on the aircraft taxiing the opposite edge *(j,i)*. For this reason, we always assume a longest separation time equal to $\Delta_{ij}^{W^H}$, since this makes sure no head-on conflicts occur for all types of aircraft.

5.1.4. Computational Time

One of the most important characteristics of the model is the time it takes to solve a full-day flight schedule at AAS. This subsection gives an overview of the strategies used and choices made in order to reduce computational time.

Time Variables

The most straightforward way to reduce computational time is limiting the number of decision variables and constraints by using discrete time steps. In this model, time steps of 10 seconds are used and all taxi times between nodes in N_T are rounded up to their closest ten. Secondly, we only define decision variables for each aircraft l within the time window between their earliest and latest taxi time, t_{early}^{l} and t_{late}^{l}, as can be seen in the constraints.

Shortest Path

We have run a shortest path algorithm, Dijkstra's algorithm [24], from each runway and gate node to any other node in N_T. This leads to a list that holds the minimum time a towed aircraft requires to reach each node in the network starting from a specific runway or gate node if no other traffic were to be taken into account. Since we know t_{early}^{l} and s_l for each aircraft l, we can use this minimum taxi time list to only define decision variable y_{ij}^{lt} if node i could have potentially been reached by aircraft l at time t.

Relevant Nodes

The abovementioned shortest path strategy already eliminates a lot of irrelevant nodes based on the variable t. However, it still includes nodes that will never be used in a realistic taxi path. Therefore, the following strategy aims to define a set of 'relevant nodes' for each gate-runway and runway-gate pair. We have run a k-shortest path algorithm that determines the k shortest paths for all gate-runway/runway-gate pairs in $T(N_T, E_T, d_T(e), v_T(e))$ and have stored the nodes used in these paths. Since we know from which runway or gate node an aircraft l starts taxiing, s_l, and at which runway or gate node it ends its taxi path, e_l, we can use this list of 'relevant nodes' to only generate decision variables y_{ij}^{lt} for nodes i and j in the relevant nodes list of pair s_l - e_l.

5.1.5. Comparison to Conventional Taxiing

We also run the model for conventionally taxiing aircraft in order to compare ET performance to conventional taxiing performance. The differences between electric and conventional taxiing are as follows. First of all, ET requires additional operations for each taxi procedure, as can be seen in figure 1. The ESUT needs to be added after each taxi-out operation and the ECDT needs to be added before each taxi-in operation, which is not needed for conventional taxiing. During taxi-out, post-processing occurs near the runway entrance for ET, whereas for conventional taxiing this happens after push-back. During taxi-in, connecting the ET vehicle to the aircraft and post-processing are only required for ET, since conventionally taxiing aircraft simply use their engines to taxi. Secondly, we allow the electrically taxiing aircraft to taxi closer to each other, since the engines are turned off while taxiing and do not pose any safety risks due to jet blast. Thirdly, we define different taxi velocities for electrically taxiing aircraft types than for conventionally taxiing aircraft based on values found in literature. The input parameters for both types of taxiing and their corresponding references can be found in table 7.

5.2. Assignment Model

In this subsection, we first explain the rolling window strategy used to solve the assignment problem. Then, we present the algorithm used to find the number of ET vehicles required to perform all towing tasks. Lastly, we define the variables, objective function and constraints of the assignment model.

5.2.1. Rolling Window

A full-day flight schedule consists of a large number of towing tasks that need to be performed by the ET vehicles, which leads to a very large problem size if we wanted to solve the model in one optimisation effort. Therefore, the rolling window strategy cuts the entire set of towing tasks R into smaller sets of tasks and solves these sets consecutively. All tasks in R are ordered from earliest to latest t_i^S, for $1 \leq i \leq a$, and each window consists of a fixed number of consecutive tasks. This means that the windows are not equal in terms of time span: a lot of tasks need to be performed in a short time period during peak hours whereas tasks in off-peak hours are distributed over a longer period of time. We illustrate the rolling window strategy by means of figures 3 and 4, which show a set of six tasks, $R = \{1, 2, .., 6\}$, divided into two windows. We define the two sets of tasks as $R^1 = \{1, 2, 3\}$ and $R^2 = \{4, 5, 6\}$.

In figure 3, the tasks in R^1 are displayed in bold and the tasks outside R^1 are displayed in grey. The assignment model uses two ET vehicles to perform the tasks in R^1, as can be seen in the table and timeline showing the results.

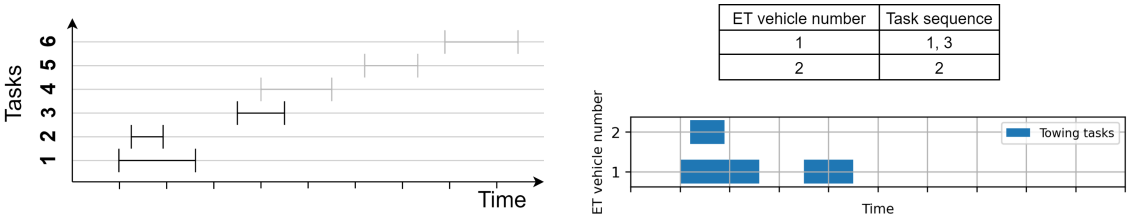

ET vehicle number	Task sequence
1	1, 3
2	2

Figure 3: First window in rolling window strategy

After we have solved the first window, all tasks in R^1 are frozen and the last task performed by each ET vehicle is used as input to the constraints in the next window. In this way, tasks in different windows are still regarded as consecutive tasks and ET vehicle batteries can be charged in between two tasks in different time windows as well as within one time window. In figure 4, we see that the tasks in R^2 as well as the end points of tasks 2 and 3 are displayed in bold. The information from the first window we use for each ET vehicle is: t_i^E and e_i' of its last task i and battery level q_i^E after performing its last task i. The results in the table and timeline show that this information is taken into account when assigning the ET vehicles to the tasks in R^2. Furthermore, ET vehicle one decides to charge in between tasks 3 and 6.

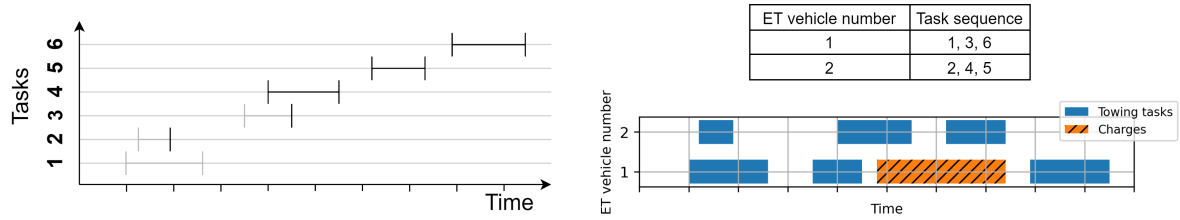

ET vehicle number	Task sequence
1	1, 3, 6
2	2, 4, 5

Figure 4: Second window in rolling window strategy

5.2.2. Optimisation Strategy

As mentioned before, we solve the assignment model separately for the three types of aircraft, since each type of aircraft can only be towed by a corresponding ET vehicle. Therefore, we split the set of towing tasks R into three subsets of tasks based on the type of ET vehicle which can perform the tasks: R_1, R_2 and R_3. The total number of ET vehicles h is split into three variables based on ET vehicle type as well: h_1, h_2 and h_3. These variables are the final results we want to obtain. We employ an optimisation strategy that does not include h_1, h_2 and h_3 as decision variables, in order to minimise computational time. Algorithm 1 shows the pseudo code of our strategy. As explained in subsection 5.2.1, we use a rolling window strategy that divides each set of towing tasks R_1, R_2 and R_3 into smaller sets. These subsets are denoted R_k^i for $1 \leq i \leq w_k$ and $k = \{1, 2, 3\}$, where w_k equals the number of windows used for ET vehicle type k. h_0 is the number of ET vehicles the algorithm starts with for each ET vehicle type and can be set to one, since we always need at least one vehicle to perform any tasks.

Algorithm 1 Optimisation algorithm assignment model

1: **for** $k \leftarrow 1, 2, 3$ **do**
2: $h_k \leftarrow h_0$
3: *Boolean* $\leftarrow$ True
4: **while** *Boolean* **do**
5: *Boolean* $\leftarrow$ False
6: **for** $i \leftarrow 1 \ldots w_k$ **do**
7: Solve assignment model with R_k^i and h_k
8: **if** h_k ET vehicles can not perform all tasks in R_k^i **then**
9: $h_k \leftarrow h_k + 1$
10: *Boolean* $\leftarrow$ True
11: **break** *for loop*

The outer for loop used in the algorithm makes sure we separately find the minimum number of ET vehicles h_1, h_2 and h_3. Within this for loop, we set the start value of h_k equal to h_0 and try to fulfill all tasks in R_k^1 using h_k ET vehicles. If this succeeds, we move on and try to fulfill all tasks in R_k^2 using h_k ET vehicles. This continues until all windows w_k have been solved. However, if we come across a window i for which h_k ET vehicles cannot perform all tasks in R_k^i, we automatically increase h_k by one and reset i to one by breaking the for loop. This process repeats itself until a value for h_k has been found such that the tasks in all windows R_k^i, $1 \leq i \leq w_k$, are performed. *Boolean* makes sure that the while loop is terminated for each ET vehicle type k once this value for h_k has been found. Since we start with a value of h_0 equal to one and increase it step by step, we are sure to find the lowest number of ET vehicles required to perform all tasks.

It is important to note that every time we reach line 7 of algorithm 1, we define a new assignment model for R_k^i and h_k. We present the mathematical formulation of this model in the following subsections. In the mathematical model we use a general formulation for the set of towing task R and the number of ET vehicles h, instead of specifying a specific ET vehicle type k and window i.

5.2.3. Variables

In section 3, we have introduced the set of towing tasks R, the set of ET vehicles H and the set of charging stations G_S. We have also introduced q_i^{req}, t_i^s and t_i^E, which represent the required energy, start time and end time of each task i respectively.

We define the following decision variables:

$$x_i^l = \begin{cases} 1, & \text{if task } i \text{ is performed by ET vehicle } l \ \ \forall\, l \in H,\ i \in R \\ 0, & \text{otherwise} \end{cases}$$

$$y_{ij}^l = \begin{cases} 1, & \text{if ET vehicle } l \text{ performs task } j \text{ directly after task } i \ \ \forall\, l \in H,\ i,j \in R,\ j > i \\ 0, & \text{otherwise} \end{cases}$$

$$c_{ij}^k = \begin{cases} 1, & \text{if batteries are charged between consecutive tasks } i \text{ and } j \text{ at charging station } k \\ & \quad \forall\, k \in G_S,\ i,j \in R,\ j > i \\ 0, & \text{otherwise} \end{cases}$$

q_i^S *:* energy level at the start of task $i \ \forall\, i \in R$

q_i^E *:* energy level at the end of task $i \ \forall\, i \in R$

We define the following additional variables:

q_i^0 *:* energy to drive from start location of ET vehicles at start of the day to task i's start node $\forall\, i \in R$

q_{ij}^1 *:* energy to drive from task i's end node to task j's start node $\forall\, i,j \in R,\ \ j > i$

q_{ij}^2 *:* energy to drive from task i's end node to charging station $j \ \forall\, j \in G_S,\ \ i \in R$

q_{ij}^3 *:* energy to drive from charging station i to task j's start node $\forall\, i \in G_S,\ \ j \in R$

Δ_i^0 : time to drive from start location of ET vehicles at start of the day to task i's start node $\forall\ i \in R$

Δ_{ij}^1 : time to drive from task i's end node to task j's start node $\forall\ i,j \in R,\ \ j > i$

Δ_{ij}^2 : time to drive from task i's end node to charging station j $\forall\ j \in G_S,\ \ i \in R$

Δ_{ij}^3 : time to drive from charging station i to task j's start node $\forall\ i \in G_S,\ \ j \in R$

The values of the additional variables are found by running a shortest path algorithm between all runway, gate and charging nodes in $S(N_S, E_S, G_S, d_S(e), v_S)$. The energy model from section 4 is used to calculate the energy consumption for all shortest paths.

5.2.4. Objective Function

Equation (14) gives the objective function of the assignment model. The first term of the objective function subtracts the number of tasks performed by the ET vehicles from the total number of tasks in R. In this way, the model aims to perform as many tasks as possible. The large coefficient M_2 is used for the first term to make sure performing all tasks is always prioritised over the second term in the objective function.

$$min\left(M_2 \cdot (a - \sum_{l \in H} \sum_{i \in R} x_i^l) + \sum_{k \in G_S} \sum_{i \in R} \sum_{\substack{j \in R \\ j > i}} c_{ij}^k \right) \tag{14}$$

The main drawback of the rolling window strategy is that the assignment model tries to fulfill all tasks in each time window without considering the objective values of later time windows. Therefore, ET vehicles are often able to charge in between two tasks but the model is indifferent to whether or not they will, since it does not affect the objective value of the current time window. These ambiguous cases lead to situations in which the model arbitrarily sets the relevant c_{ij}^k variable either to 0 or 1 based on the way the optimisation software breaks these ties. For this reason, the second term in equation (14) adds the number of times ET vehicle batteries are charged to the objective function. In this way, the model will try to perform all tasks while also trying to minimise battery charging. It is important to note that, although the objective function tries to minimise the number of times ET vehicles charge their batteries, ET vehicles are allowed to charge. Therefore, the number of times charging takes place is not part of the condition to increase h by one, as can be seen in algorithm 1.

In section 8, we present an extended model which suggests an alternative to this situation.

5.2.5. Constraints

We define the following constraints:

$$\sum_{l \in H} x_i^l \leq 1 \qquad \forall\ i \in R \tag{15}$$

$$x_i^l \geq \sum_{\substack{j \in R \\ j > i}} y_{ij}^l \qquad \forall\ l \in H,\ \ i \in R \tag{16}$$

$$x_j^l \geq \sum_{\substack{i \in R \\ i < j}} y_{ij}^l \qquad \forall\ l \in H,\ \ j \in R \tag{17}$$

$$y_{ij}^l \geq x_i^l + x_j^l - 1 - \sum_{i < k < j} y_{ik}^l \qquad \forall\ l \in H,\ \ i,j \in R,\ \ j > i \tag{18}$$

$$q_i^S = (1 - \sum_{l \in H} \sum_{\substack{j \in R \\ j < i}} y_{ji}^l) \cdot (Q - q_i^0) + \sum_{l \in H} \sum_{\substack{j \in R \\ j < i}} y_{ji}^l \cdot (q_j^E - q_{ji}^1) + \sum_{k \in G_S} \sum_{\substack{j \in R \\ j < i}} c_{ji}^k \cdot (Q - q_{ki}^3 - q_j^E + q_{ji}^1) \qquad \forall\ i \in R \tag{19}$$

$$q_i^S \geq q_i^R + S\,M \qquad \forall\ i \in R \tag{20}$$

$$q_i^E = q_i^S - q_i^R \qquad \forall\ i \in R \tag{21}$$

$$\sum_{k \in G_S} c_{ij}^k \leq \sum_{l \in H} y_{ij}^l \qquad \forall\ i,j \in R,\ j > i \tag{22}$$

$$t_i^S \geq (1 - \sum_{\substack{j \in R \\ j < i}} y_{ji}^l) \cdot \Delta_i^0 + \sum_{l \in H} \sum_{\substack{j \in R \\ j < i}} y_{ji}^l \cdot (t_j^E + \Delta_{ji}^1) + \sum_{k \in G_S} \sum_{\substack{j \in R \\ j < i}} c_{ji}^k \cdot (\Delta_{jk}^2 + \Delta_{ki}^3 + \frac{Q - q_j^E + q_{jk}^2}{P^{MAX} \cdot \frac{C_{NOM}}{C_{MAX}}} - \Delta_{ji}^1) \qquad \forall\ i \in R \tag{23}$$

Constraint (15) makes sure each task can only be performed by one ET vehicle. It is also allowed not to perform a certain task, but this will increase the objective value and is therefore tried to be avoided while solving the model. Constraints (16) and (17) make sure each task can only be followed or preceded by one task. Constraint (18) ensures decision variable y^l_{ij} can only be equal to 1 if ET vehicle l performs both tasks i and j without performing any tasks in between. Constraint (19) tracks the battery level of the ET vehicle that performs task i and is defined as follows. The first term on the right-hand side of the equation sets the battery level equal to Q minus the energy required to drive to task i from the start location of the ET vehicles if task i is the first task of the day for ET vehicle l performing task i. If task i is not ET vehicle l's first task, the battery level q^s_i is set equal to the battery level at the end of ET vehicle l's last task j minus the energy it takes ET vehicle l to drive from task j to task i. Lastly, the third term takes into account the option to charge the ET vehicle's batteries in between two tasks. If this is the case, q^s_i is set equal to the maximum state of charge Q minus the energy to drive from charging station k to task i.

Constraint (20) makes sure the energy level at the beginning of task i is enough to perform task i and meet the safety requirement. Constraint (21) sets the energy level at the end of task i equal to the energy level at the start of task i minus the energy required to perform task i. Constraint (22) ensures that batteries can only be charged between two consecutive tasks. The equation is an inequality since charging between two tasks is optional. Constraint (23) makes sure t^s_i is higher than the earliest time relevant ET vehicle l can reach the start location of task i, taking into account previous tasks and battery charging ET vehicle l has performed and the time it takes to drive to task i. Similar to constraint (19), the first term takes into account the option that task i is the first task in ET vehicle l's day schedule. The second term takes into account the time ET vehicle l's last task j has ended and the time it takes to drive from this task to task i. Lastly, the third term takes into account the option to charge between two consecutive tasks. It includes the time to drive to and from the charging station and the time it takes to fully charge the batteries.

Constraint (19) is non-linear, since decision variables y^l_{ji} and c^k_{ji} are both multiplied by decision variable q^E_j. Therefore, placeholder variable $z^l_{ij} = y^l_{ij} \cdot q^E_i$ is defined and equations (24) are used to linearise the second term of equation (19). Similarly, placeholder variable $w^k_{ij} = c^k_{ij} \cdot q^E_i$ is defined and used to linearise the third term of equation (19).

$$\begin{aligned} & z^l_{ij} \geq 0 \\ & z^l_{ij} \leq q^E_i \\ & z^l_{ij} \leq y^l_{ij} \cdot Q \\ & z^l_{ij} \geq q^E_i - (1 - y^l_{ij}) \cdot Q \end{aligned} \tag{24}$$

The resulting linearised constraint is given in equation (25).

$$q^s_i = (1 - \sum_{l \in H} \sum_{\substack{j \in R \\ j<i}} y^l_{ji}) \cdot (Q - q^0_i) + \sum_{l \in H} \sum_{\substack{j \in R \\ j<i}} z^l_{ji} - y^l_{ji} \cdot q^1_{ji} + \sum_{k \in G_S} \sum_{\substack{j \in R \\ j<i}} c^k_{ji} \cdot (Q - q^3_{ki} + q^1_{ji}) - w^k_{ji} \qquad \forall\, i \in R \tag{25}$$

Constraint (23) is also non-linear, since c^k_{ji} is multiplied by q^E_j. Placeholder variable w^k_{ij} is used again to linearise constraint (23), resulting in constraint (26).

$$t^s_i \geq (1 - \sum_{l \in H} \sum_{\substack{j \in R \\ j<i}} y^l_{ji}) \cdot t^0_i + \sum_{l \in H} \sum_{\substack{j \in R \\ j<i}} y^l_{ji} \cdot (t^E_j + \Delta^1_{ji}) + \sum_{k \in G_S} \sum_{\substack{j \in R \\ j<i}} c^k_{ji} \cdot (\Delta^2_{jk} + \Delta^3_{ki} + \frac{Q + q^2_{jk}}{P^{MAX} \cdot \frac{C_{NOM}}{C_{MAX}}} - \Delta^1_{ji}) - \frac{w^k_{ji}}{P^{MAX} \cdot \frac{C_{NOM}}{C_{MAX}}} \qquad \forall\, i \in R \tag{26}$$

6. Results

In this section we present the results of the models described in section 5. First of all, we give a description of the data used to generate the results. After that, we present the most important results of the vehicle routing model. Finally, we give an overview of the results of the assignment model. We have solved both the vehicle routing and assignment model with the Gurobi Optimiser version 9.0 on an Intel Core i7-4700MQ @ 2.40GHz.

6.1. Data Description

The use case of this research focuses on AAS. In this subsection, we first give an overview of the flight schedule data used as input to both models described in section 5. Then, we give an overview of the node-edge networks used to model the taxiway and service road networks of AAS. Lastly, we present the input parameter values for both the vehicle routing and assignment model.

6.1.1. Flight Schedule

We have analysed two flight schedules, which have been provided by AAS and both describe a full day of operations. The first day, the 14th of December, is picked from the top ten quietest days at AAS in 2019 in terms of aircraft movements and the second day, the 13th of September, is picked from the top ten busiest days at AAS in 2019. These two days are picked specifically since they cover all runways and a high number of runway modes. We analyse a quiet day since it is likely that ET will first be implemented on a day with a relatively small number of flights. We analyse a busy day since this gives an estimate of the ET vehicle fleet size eventually needed to perform all taxi operations electrically on each day of the year. An overview of the data on both days is given in table 4. The difference in number of flights is clear and both days largely cover different runway modes. Another clear difference is the average taxi time, which is partly caused by the higher traffic numbers on the busy day and partly by the runways used.

	#Flights	**#N flights**	**#W flights**	**#W^H flights**	**Average taxi time (min)**	**#Pax**	**Runways used**
14th of December	914	750	148	16	9.5	135294	18R, 22, 27, 18C, 24, 18L
13th of September	1487	1254	213	20	12.5	229242	18R, 18L, 18C, 36R, 36L, 36C

Table 4: Key figures quiet (14th of December) and busy (13th of September) day

We have processed the flight schedules and selected the relevant data for our models; a sample of the processed data is presented in table 5. This data, from left to right, holds day of the year, whether an aircraft arrives or departs, taxi time, actual in-block time, gate, runway and aircraft type.

Day of the year	**A/D**	**Taxi time [min]**	**Actual in-block time [yyyy-MM-dd HH:mm:ss]**	**Gate**	**Runway**	**A/C type**
256	A	4.0	2019-09-13 07:47:00	B17	36R	E190
256	A	9.0	2019-09-13 08:26:00	D14	36C	B737
256	A	5.0	2019-09-13 11:38:00	B24	36R	E190
256	A	4.0	2019-09-13 15:36:00	A04	36R	E190
256	A	4.0	2019-09-13 20:18:00	B23	36R	E190

Table 5: Sample of flight schedule on the 13th of September

We have divided the aircraft types into groups N, W and W^H based on their Maximum Take-off Weight (MTOW) according to the guidelines presented by Van Baaren [21]. The heaviest aircraft in the N, W and W^H categories are the Boeing 737-800, Airbus A340-500 and Airbus A380-800 respectively.

6.1.2. Airport Model

We have used AAS aerodrome charts [25] and relevant literature [20] [19] to define $T(N_T, E_T, d_T(e), v_T(e))$ and $S(N_S, E_S, G_S, d_S(e), v_S)$ for our case study. Figure 5 shows $T(N_T, E_T, d_T(e), v_T(e))$ and figure 6 zooms in on a section with various nodes close to each other. $d_T(e)$ and $v_T(e)$ are not displayed for the sake of readability. The arrowheads located on the edges in figure 5 denote one-way edges.

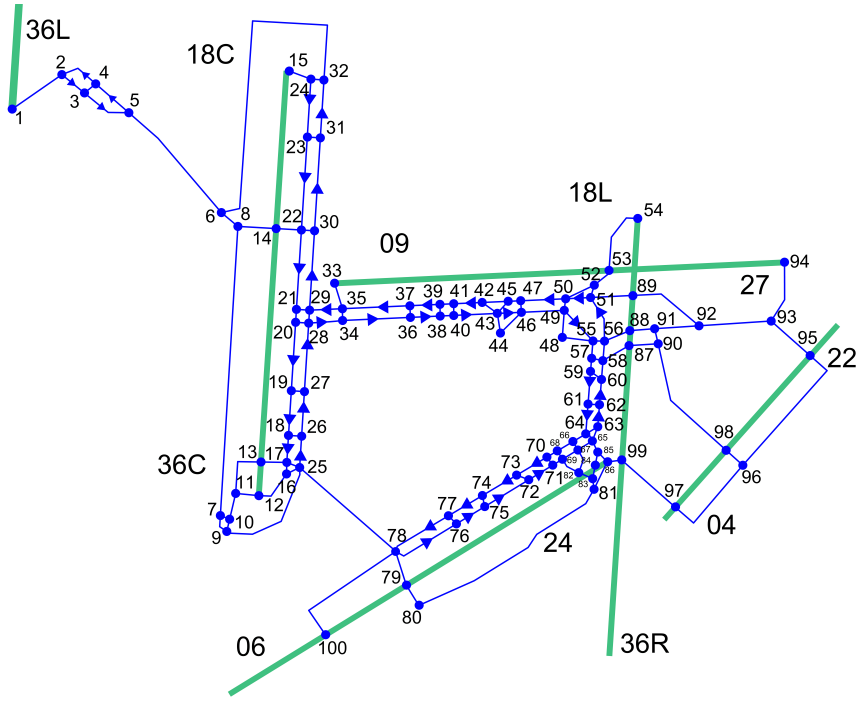

Figure 5: Taxiway network $T(N_T, E_T, d_T(e), v_T(e))$ of AAS

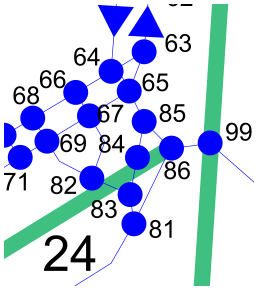

Figure 6: Section of $T(N_T, E_T, d_T(e), v_T(e))$

Figure 7 shows $S(N_S, E_S, G_S, d_S(e), v_S)$. We define charging stations 1 - 5, which are located at nodes 2, 19, 24, 36 and 42 respectively and are denoted by the grey rectangles in figure 7. We assume that all ET vehicles start their day of operations at the most centrally located charging station, which is charging station 3 (i.e. node 24).

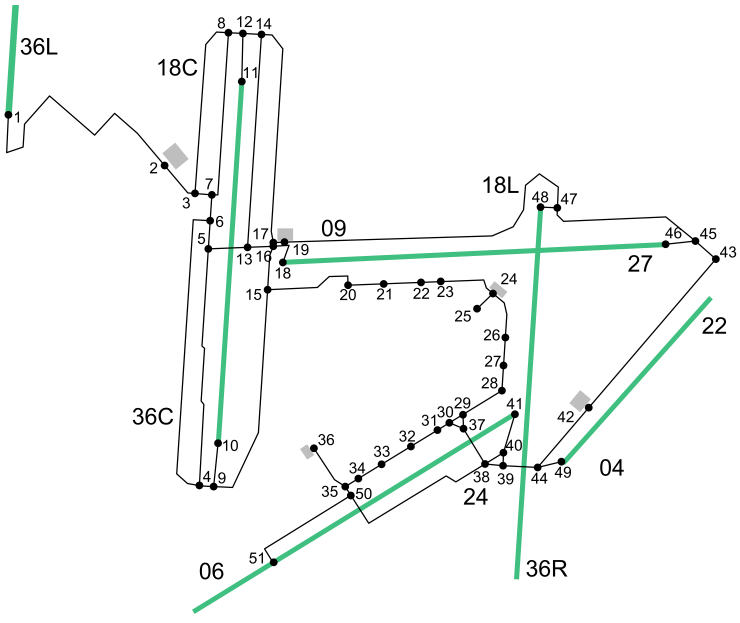

Figure 7: Service road network $S(N_S, E_S, G_S, d_S(e), v_S)$ of AAS

Figure 8: Mapping of AAS gates to node numbers in N_T

We have located one node in N_T and one node in N_S at each relevant runway exit/entrance. We have also allocated one node in N_T and one node in N_S to specific areas near the terminal that each cover a set of gates. Therefore, one gate node covers multiple gates. The mapping of the gate numbers to the gate nodes in N_T is displayed in figure 8. All gate numbers that are not displayed in the figure are allocated to a node number based on their location with respect to the zones indicated in figure 8. Furthermore, table 6 shows which nodes in N_S are connected to the gate and runway

nodes in N_T. This information is used to convert the taxi paths determined by the vehicle routing model to the set of towing tasks R used as input to the assignment model.

Runway nodes		**Gate nodes**	
Taxiway	**Service road**	**Taxiway**	**Service road**
1	1	36	20
12	10	40	21
15	11	44	22
33	18	48	25
54	48	59	26
86	41	61	27
94	46	64	28
97	49	70	29
100	51	73	32
		74	33

Table 6: Node connections between taxiway and service road network

6.1.3. Input Parameters

Table 7 gives an overview of the constants used in the vehicle routing model. The table is split into two main columns, holding values for ET and conventional taxiing. This gives an overview of the differences in input values between the two types of taxiing and can be used to explain the differences between the optimal taxi routes for ET and conventional taxiing. The k value is part of the k-shortest path algorithm explained in subsection 5.1.4.

	Electric taxiing		**Conventional taxiing**	
Constant	**Value**	**Reference**	**Value**	**Reference**
d^{sep} [m]	60	[26]	200	[27], [28], [13]
v_1 [m/s]	11.83	[9]	10	[29], [27]
v_2 [m/s]	10.29	[30]	10	[29], [27]
v_3 [m/s]	10.29	[30]	10	[29], [27]
ESUT [s]	300	[31], [8], [9], [21]	0	[32]
ECDT [s]	180	[31], [33]	0	[32]
Push-back time [s]	120	[34]	120	[34]
Post-processing time [s]	60	[34]	60	[34]
Connect (ET) vehicle time [s]	60	-	60	-
Time step [s]	10	-	10	-
k [-]	4	-	4	-
M_1 [-]	100	-	100	-
Penalty c [s]	30	-	30	-

Table 7: Overview of constants used in vehicle routing model

Table 8 gives an overview of the constants used in the assignment model.

Constant	**Value**	**Reference**	**Constant**	**Value**	**Reference**
μ_0 [-]	0.1	[22]	m_1 [kg]	15000	[21]
v_0 [m/s]	41.16	[22]	m_2 [kg]	35000	[21]
C_{MAX}	6	[16]	m_3 [kg]	50000	[21]
C_{NOM}	1	[16]	Q_1 [kWh]	390	[21]
P_1^{MAX} [kW]	650	[21]	Q_2 [kWh]	1260	[21]
P_2^{MAX} [kW]	2100	[21]	Q_3 [kWh]	3200	[21]
P_3^{MAX} [kW]	3200	[21]	v_S [m/s]	8.33	[35]

Table 8: Overview of constants used in assignment model

6.2. Vehicle Routing Model

The outcome of the vehicle routing model describes the optimal taxi routes of all aircraft in the schedule. The main purpose of these routes is to generate the towing tasks that need to be performed by the ET vehicles, but we have also used them to compare electric to conventional taxi performance. The first subsection gives an overview of the results of the quiet day, the 14th of December 2019, and the second subsection gives an overview of the results of the busy day, the 13th of September 2019.

6.2.1. 14th of December 2019

We have solved the vehicle routing model for ET on the quiet day in **196 seconds**, which, considering the size of this problem, is much shorter than comparable models found in literature [14] [20] [15] [13]. We have visualised the optimal taxi routes found by the model by splitting the aircraft into groups based on their arrival or departure runway. Furthermore, we have created an animation of the aircraft taxi movements during the entire day, which has been used to check if the taxiing aircraft behave unexpectedly. The main conclusion from the visualisations and animation is that the vehicle routing model performs as expected and its results can be used as a solid foundation for our assignment model.

As explained in subsection 5.1.5, the model is run for the electric *and* conventional taxiing scenarios in order to fairly compare their performance. Analysis of the taxi routes for both scenarios shows that the electrically and conventionally taxiing aircraft predominantly use the same routes from gate to runway and vice versa, since these routes simply lead to the shortest taxi times. However, in a few occasions, the conventionally taxiing aircraft are scheduled to take a detour, which is likely to be caused by the larger d^{sep} assumed for conventionally taxiing aircraft.

We have also calculated the total taxi time for each aircraft l by taking the difference between t^l_{early} and the time aircraft l arrived at e_l. $taxi^l_E$ is the total taxi time of aircraft l when taxiing electrically and $taxi^l_C$ is the total taxi time of aircraft l when taxiing conventionally. We define delay as $D^l = taxi^l_E$ - $taxi^l_C$; therefore, a positive value means ET induces a delay, whereas a negative value stands for a time gain due to ET.

Runway	**Oost**	**Aalsmeer**	**Kaag**		**Buitenveldert**		**Zwanenburg**	**Polder**	**Total [s]**
Mode	22A	18D	24A	24D	27A	27D	18A	18A	-
#Flights	70	65	5	314	214	75	5	166	914
$\overline{\textbf{taxi}}_{\textbf{E}}$ **[s]**	538	725	602	537	604	752	650	931	656
$\overline{\textbf{taxi}}_{\textbf{C}}$ **[s]**	363	428	430	241	434	459	472	793	429
$\overline{\textbf{D}}$ **[s]**	175	297	172	296	170	294	178	138	227

Table 9: Overview of results per runway on the 14th of December

In table 9, we give an overview of the results per runway mode, followed by the results for all flights. We use this information to assess the influence of ET on taxi time for different runway modes at AAS. The table shows the number of arrivals and departures on the quiet day, the average total taxi time per runway mode for electric and conventional taxiing and the average delay $\overline{D}$. Runway modes that are not used on the 14th of December are not included in the table to improve readability. We can see that the average delays are relatively close to the ESUT and ECDT, except for the arrivals at the 'Polderbaan'. This runway is located furthest from the gates and is reached via edges with relatively high velocity limits. Therefore, the electrically taxiing aircraft have more time to make up part of their delay by using their higher maximum velocity.

6.2.2. 13th of September 2019

We have solved the vehicle routing model for ET on the busy day in **558 seconds**. Like for the quiet day, the optimal ET routes have been visualised and used in an animation of the aircraft taxi movements during the entire day. They show that the vehicle model works as we expect it to and the results can be used in our assignment model. We have also compared the optimal taxi routes for conventional taxiing to the optimal ET routes and, like for the quiet day, conclude that they are largely the same.

Table 10 shows the taxi times and delay per runway mode. All of the delays are slightly below the ESUT and ECDT, except for runway mode 27A on the 'Buitenveldert' runway, which is only one aircraft. It can be seen that runway mode 36A on the 'Zwanenburg' runway has an average delay similar to the 'Polder' runway. This is caused by the higher velocity limit on the edges parallel to the 'Zwanenburg' runway and a relatively large number of aircraft taxiing from this runway to gate nodes 70, 73 and 74 (see figure 7 for reference), thereby using the entire parallel taxiway.

Runway	**Aalsmeer**	**Buitenveldert**		**Zwanenburg**			**Polder**		**Total**
Mode	36A	27A	09D	36A	18D	36D	18A	36D	-
#Flights	486	1	7	229	2	262	27	473	1487
$\overline{\textbf{taxi}}_{\textbf{E}}$ **[s]**	550	660	791	779	695	702	911	1069	785
$\overline{\textbf{taxi}}_{\textbf{C}}$ **[s]**	376	470	506	639	425	407	768	817	570
$\overline{\textbf{D}}$ **[s]**	174	190	286	140	270	296	143	253	215

Table 10: Overview of results per runway on the 13th of September

6.3. Assignment Model

We use the assignment model to find our final result: the ET vehicle fleet size. In this subsection, we present the results for the three types of towing vehicles on both analysed days at AAS. Furthermore, we present the energy requirements for each day of operations based on the results of the assignment model. The computational times given in this subsection represent the time to solve the assignment model for the final values of h_1, h_2 and h_3, not the entire iterative process explained in section 5.2.2.

6.3.1. 14th of December 2019

We have generated the results for the 14th of December with a rolling window strategy that holds 50 tasks per window for R_1, 50 for R_2 and 16 for R_3. The window sizes for R_1 and R_2 have been determined by means of trial and error, keeping window size as big as possible while keeping computational time within practical limits, and by making sure the last window is (almost) the same size as the other windows. The window size for R_3 is equal to the total number of tasks in R_3 on the 14th of December and therefore spans the entire day. For R_1 and R_2, the windows differ in terms of time periods they cover; the window that covers the smallest time period in R_1 has a length of 47 minutes and the window that covers the smallest time period in R_2 has a length of 179 minutes.

Figure 9 shows the results of the assignment model: an overview of the towing tasks and charges performed by each ET vehicle. ET vehicles 1 - 45 are used for the tasks in R_1, ET vehicles 46 - 58 for the tasks in R_2 and ET vehicles 59 - 60 for the tasks in R_3; a dashed lined has been added to the figure to separate these ET vehicle types. All tasks are performed and the number of type 1 ET vehicles required is equal to **45**, the number of type 2 ET vehicles is equal to **13** and the number of type 3 ET vehicles equals **2**. The computational times of the type 1, 2 and 3 models are 1075, 499 and 1 seconds respectively. This adds up to a total computational time of **1575** seconds.

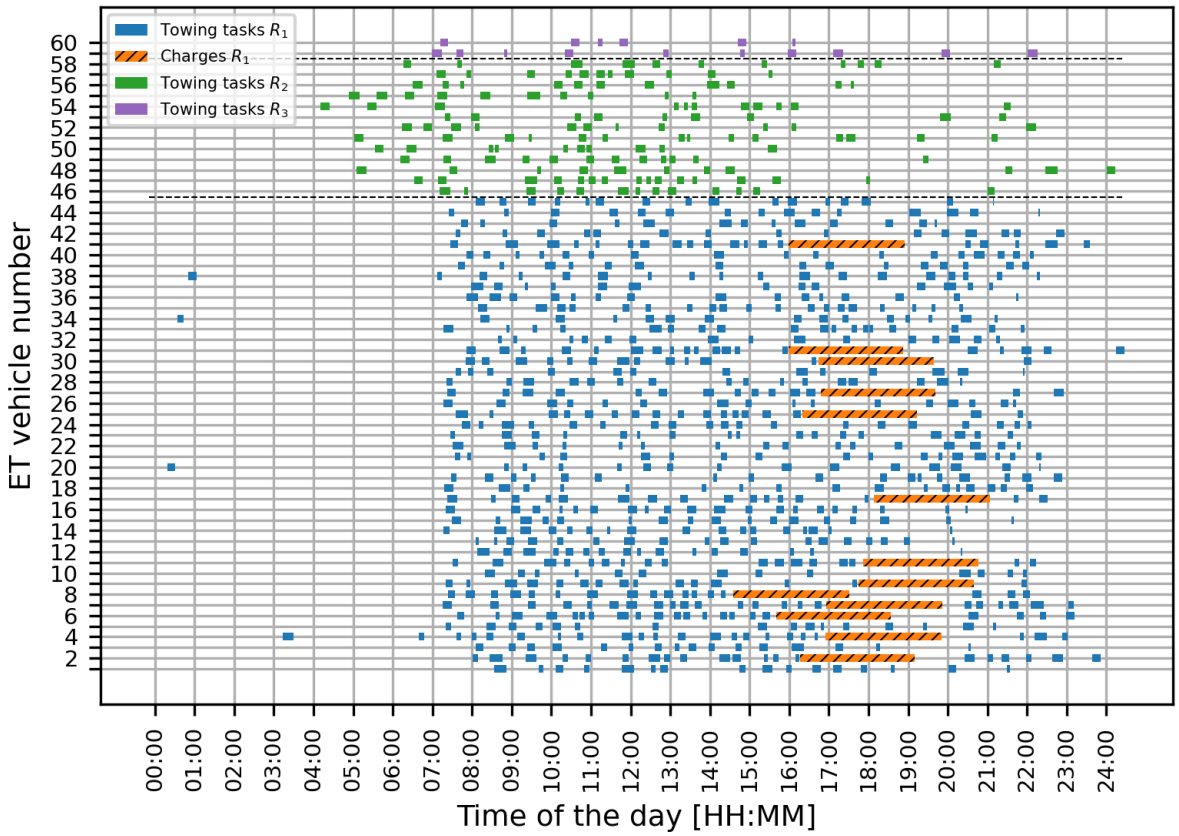

Figure 9: Results assignment model on the 14th of December

We can see that the ET vehicles are charged only during the second half of the day. This is due to the fact that the rolling window strategy focuses on minimising the number of unperformed tasks per window. Therefore, the model does not take into account long-term consequences of depleting the batteries without charging. As a result, ET vehicles are only scheduled to charge their batteries if this is required to fulfil their next task. In real-life, the ET vehicles are likely to charge their batteries earlier in the day during relatively quiet periods in order to avoid having to charge their batteries during a peak period or at the same time other ET vehicles also have to charge their batteries. This is a drawback of the rolling window strategy required to deal with the large problem size.

Furthermore, only type 1 ET vehicles are charged. This can be explained by the fact that the numbers of type 2 and 3 ET vehicles are relatively high compared to the number of tasks they need to perform. For the type 2 ET vehicles, this is largely due to a peak just before 11 a.m. This peak is the main factor that leads to a minimum of 13 ET vehicles to perform all tasks in R_2, which are not used extensively during the rest of the day and therefore none of them requires charging. Similarly, we frequently need to perform two tasks in R_3 at the same time and therefore require at least 2 type 3 ET vehicles.

Table 11 gives an overview of the energy and infrastructure requirements on the quiet day. The column 'Day [%]' shows the percentage of the total energy used on the 14th of December that is recharged during the day itself, i.e. during the 'charges' displayed in figure 9. It can be seen that most recharging is performed overnight. Furthermore, we show how intensively each charging station is used during the day. These percentages only take into account the charging performed during the day, since all overnight charging is assumed to take place at the start location of the ET vehicles, which is charging station 3. It can be seen that charging stations 1, 2, 4 and 5 are used with similar intensity, whereas charge station 3 is not used during the day. Lastly, the peak power requirement for the entire airport is equal to 7800 kW and is required from 18:08:25 to 18:33:57.

Total power used [kWh]	**Day [%]**	**Overnight [%]**	**Station 1 [%]**	**Station 2 [%]**	**Station 3 [%]**	**Station 4 [%]**	**Station 5 [%]**	**Peak power [kW]**
28411	14	86	31	23	0	23	23	7800

Table 11: Energy and infrastructure results on the 14th of December

6.3.2. *13th of September 2019*

The rolling window sizes for R_1, R_2 and R_3 on the 13th of September are equal to 57, 43 and 20 (equal to the total number of tasks in R_3) respectively. The minimum window size in terms of time is equal to 32 minutes for R_1 and equal to 132 minutes for R_2. the The computational times of the type 1, 2 and 3 models are 3384, 1398 and 1 seconds respectively. This adds up to a total computational time of **4782** seconds.

Figure 10 shows the results of the assignment model: an overview of the towing tasks and charges performed by each ET vehicle. ET vehicles 1 - 77 are used for the tasks in R_1, ET vehicles 78 - 94 for the tasks in R_2 and ET vehicles 95 - 97 for the tasks in R_3. All tasks are performed and the total number of type 1 ET vehicles required is equal to **77**, the number of type 2 ET vehicles is equal to **17** and the number of type 3 ET vehicles equals **3**. Especially the number of type 1 ET vehicles is considerably higher than on the quiet day. This is due to the large difference in number of tasks in R_1, which is 749 for the quiet day and 1254 for the busy day.

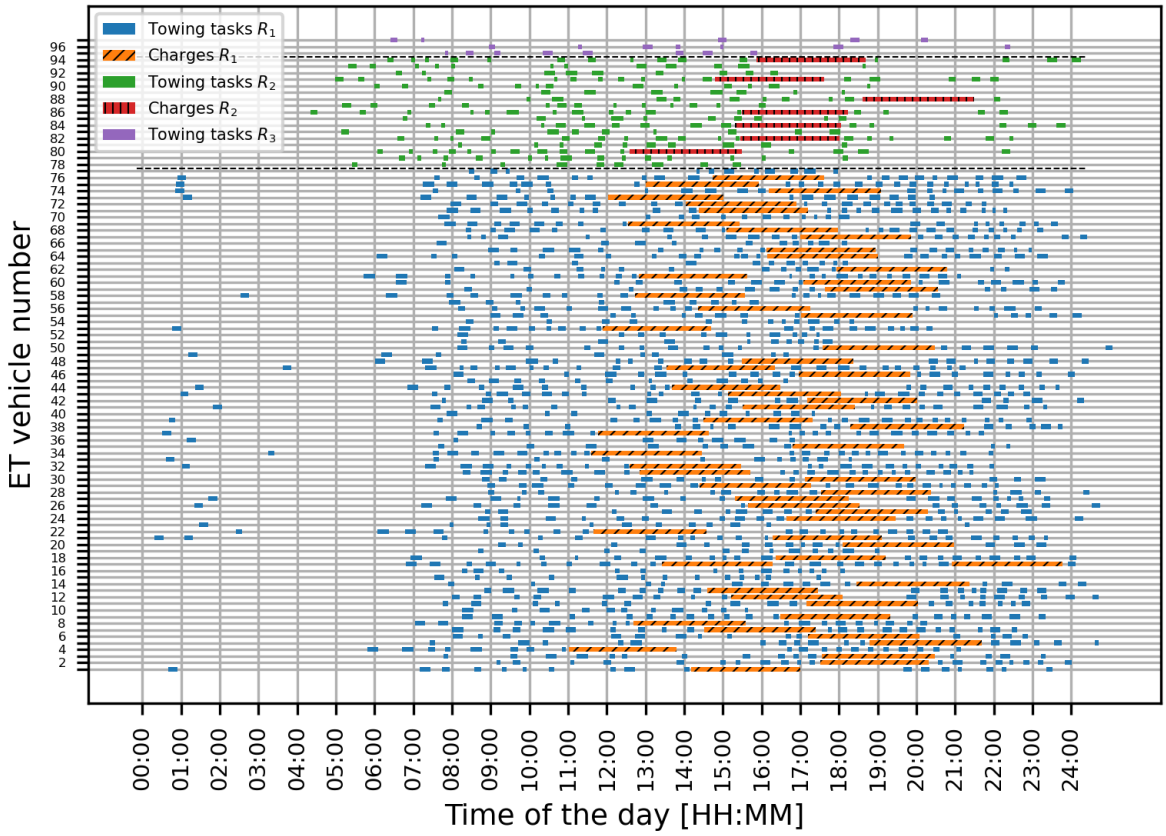

Figure 10: Results assignment model on the 13th of September

Table 12 gives an overview of the energy and infrastructure requirements for the busy day. We see that the ET vehicles are charged considerably more often during the day on the busy than on the quiet day. Furthermore, contrary to the quiet day, charging station 3 is used most intensively of all charging stations. Lastly, peak power is significantly higher and is required from 17:11:44 to 17:12:01 and from 17:56:36 to 17:58:24.

Total power used [kWh]	**Day [%]**	**Overnight [%]**	**Station 1 [%]**	**Station 2 [%]**	**Station 3 [%]**	**Station 4 [%]**	**Station 5 [%]**	**Peak power [kW]**
60843	42	58	23	11	35	16	15	19500

Table 12: Energy and infrastructure results on the 13th of September

7. Sensitivity Analysis

The results presented in section 6 are based on the input parameters specified in tables 7 and 8. These values are mostly derived from literature, but are likely to be (slightly) different in real-life due to a higher level of maturity of

technology or different airport regulations at the time of implementation. Therefore, a sensitivity analysis is performed in order to analyse the results of the models defined in section 5 with different input parameters. First, we analyse the effect of different input parameters for the vehicle routing model. Then we focus on different input parameters for the assignment model and, lastly, we analyse the influence of using less charging stations.

7.1. Taxi Velocity

The vehicle routing model cases we investigate are shown in table 13. We analyse one case with a lower and one with a higher velocity at which the aircraft are towed by the ET vehicles. These parameter values are varied because of the relatively high uncertainty in their assumed values for the base case, due to improvements in ET vehicle technology and possible alterations in airport regulations. Furthermore, changes in ET velocity have a less predictable influence on airport operations than parameters like the ESUT and ECDT: velocity alters the way aircraft move across the airport's surface whereas the ESUT and ECDT only add constant values at the start or end of a taxi operation.

	Slow case	**Base case**	**Fast case**
v_1 [m/s]	10	11.83	14
v_2 & v_3 [m/s]	8	10.29	12

Table 13: Slow, base and fast case for taxi velocity in vehicle routing model

The results of the quiet day are shown in table 14. We only discuss the quiet day in this subsection, since the results for both days show the same pattern. Table 14 shows a lower average taxi time for the fast case for all runway modes, which is the expected result. However, for some runway modes this decrease is more significant than for others. This is due to the prevailing maximum allowed velocities at parts of the taxiway network, which override the higher maximum velocity of the towed aircraft. Furthermore, a larger distance between gate and runway also increases the time an aircraft can be towed at its higher velocity, which increases the average taxi time difference between the slow and fast case for some modes.

	Runway	**Oost**	**Aalsmeer**	**Kaag**		**Buitenveldert**		**Zwanenburg**	**Polder**	**Total**
	Mode	22A	18D	24A	24D	27A	27D	18A	18A	-
	#Flights	70	65	5	314	214	75	5	166	1487
Slow	$\overline{\textbf{taxi}}_{\textbf{E}}$ **[s]**	541	726	638	540	616	773	674	1005	676
	$\overline{\textbf{taxi}}_{\textbf{C}}$ **[s]**	363	428	430	241	434	459	472	793	429
	$\overline{\textbf{D}}$ **[s]**	178	298	208	299	182	314	202	212	247
Fast	$\overline{\textbf{taxi}}_{\textbf{E}}$ **[s]**	537	725	600	537	604	752	646	930	656
	$\overline{\textbf{taxi}}_{\textbf{C}}$ **[s]**	363	428	430	241	434	459	472	793	429
	$\overline{\textbf{D}}$ **[s]**	174	297	170	296	170	293	174	137	227

Table 14: Overview of results for the slow and fast case per runway on the 14$^{\text{th}}$ of December 2019

We also use the routes generated for the slow and fast cases to define set of towing tasks R and solve the assignment problem. This gives insight into the consequences of a different v_1, v_2 and v_3 for the total number of required ET vehicles. It needs to be noted though, that v_S is still equal to 8.33 m/s. The results of the assignment model for the quiet day are shown in table 15.

	Slow case			**Base case**			**Fast case**		
ET vehicle type	**1**	**2**	**3**	**1**	**2**	**3**	**1**	**2**	**3**
#ET vehicles 14$^{\text{th}}$ of December	46	14	2	45	13	2	44	13	2

Table 15: Number of ET vehicles for all vehicle routing model cases

The total computational times are **1748** and **2886** seconds for the slow and fast case respectively. It can be seen that the change in velocity of the towed aircraft does not have a big impact on the total number of ET vehicles required. This is due to the fact that the same number of tasks still needs to be performed. Furthermore, the higher velocity

does decrease time required to perform each task, but also increases the energy required to perform a task. Equations (3) and (4) show that an increase in velocity increases power required directly in the former equation and indirectly through the latter, whereas the relation between velocity and taxi time is only linear. Therefore, the influence of a higher taxi velocity on the number of ET vehicles largely depends on whether the decrease in taxi time outweighs the increase in required energy.

7.2. Battery Capacity

For the assignment model, we have defined two cases in which we vary the battery capacity and maximum power. The low case assumes values 50% lower than the base case and the high case assumes values 50% higher than the base case. An overview of these cases is given in table 16. All other variables, e.g. vehicle weight, are kept constant, since we want to isolate the effect of increasing battery capacity and maximum power. We use the set of towing tasks R generated with the base case vehicle routing model.

	Low case	**Base case**	**High case**		**Low case**	**Base case**	**High case**
$\mathbf{Q_1}$	195	390	585	$\mathbf{P_1^{MAX}}$	325	650	975
$\mathbf{Q_2}$	630	1260	1890	$\mathbf{P_2^{MAX}}$	1050	2100	3150
$\mathbf{Q_3}$	960	1920	2880	$\mathbf{P_3^{MAX}}$	1600	3200	4800

Table 16: Low, base and high case for battery capacity and maximum power in assignment model

Table 17 shows the results for both days and all cases. It can be seen that for both the quiet and busy day, the low case results in significantly more type 1 and 2 ET vehicles. The number of type 3 ET vehicles stays the same, which can be explained by the fact that for the base case, time was the limiting factor. The low case computational times for the quiet and busy day are **3924** and **7235** seconds respectively.

For the high case, it can be seen that on the quiet day, the numbers of type 1 and 2 ET vehicles are decreased significantly, whereas the number of type 3 ET vehicles stays the same. This indicates that in the base case, decreasing the numbers of type 1 and 2 ET vehicles was (to some extent) limited by battery capacity, whereas the type 3 ET vehicles were limited by time. For the busy day, the high case results in a decrease in type 2 ET vehicles, whereas the numbers of type 1 and 3 ET vehicles stay the same. The high case computational times for the quiet and busy day are **1205** and **3673** seconds respectively.

It is interesting to see that for both the quiet and busy day, the low case leads to significantly higher computational times. A possible reason for this is the size of the problem which is significantly larger due to the higher number of available ET vehicles.

	Low case			**Base case**			**High case**		
ET vehicle type	**1**	**2**	**3**	**1**	**2**	**3**	**1**	**2**	**3**
#ET vehicles 14th of December	60	24	2	45	13	2	36	11	2
#ET vehicles 13th of September	100	26	3	77	17	3	77	13	3

Table 17: Number of ET vehicles for all assignment model cases

7.3. Charging Stations

The charging station locations are shown in figure 7 and are tactically chosen based on information about the aerodrome AAS [25]. In this subsection, we want to find out to what extent our assignment model depends on our choice of charging station locations. Furthermore, we want to know if decreasing the number of charging station locations significantly influences the number of required ET vehicles, since a lower number of charging stations is likely to decrease overall costs.

We have analysed three different charging station scenarios for the busy day. Table 18 shows these scenarios and their results. The scenarios each consider a different subset of the five available charging stations from the base case. The stations mentioned in the first column are the node numbers from figure 7 related to a specific charging station. The node number in bold is set as the start location of the ET vehicles at the beginning of the day. The computational times for the scenarios from top to bottom are **4306**, **4521** and **4592** seconds.

Scenario	#Type 1 vehicles	#Type 2 vehicles	#Type 3 vehicles	Computational time [s]
Stations 2, **24**, 42	77	17	3	4306
Stations 19, **24**, 36	77	17	3	4521
Stations **19**, 36, 42	78	18	3	4592

Table 18: Number of ET vehicles for a varying charging station infrastructure on the 13th of September

Table 18 indicates that the first two scenarios give the same results as the original situation with five charging stations. This shows that the results are barely dependent on our choice of charging station locations and the results are likely to remain a good estimate of ET vehicle fleet size even if the charging stations are placed at different locations. It also shows that we can cut costs by using three charging stations instead of five. Furthermore, the third scenario shows that the ET vehicle start location can have a small influence on ET vehicle fleet size and that it is best to pick a central ET vehicle start location.

8. Balancing of Battery Charging

In this section, we propose an adaptation to the model from subsection 5.2.4 which makes sure ET vehicles do not postpone charging until their batteries are depleted. In this way, the limitations due to the rolling window strategy are largely overcome and charging does not need to be penalised in the objective function. This leads to an even more realistic estimate of the required number of ET vehicles.

In order to achieve this, we alter the objective function from the original assignment model and add new decision variables and constraints. These adaptations make sure each ET vehicle charges its batteries in between two consecutive tasks if the available time in between those tasks allows it and the battery level is sufficiently low. The input parameter ΔT defines the minimum time an ET vehicle needs to charge its batteries and is used to avoid very short charging in between tasks, which might be impractical or speed up degradation of battery health. We also introduce the new variable g_{ij}, which defines the optimal choice of charging station to charge an ET vehicle's batteries if it is driving from task i to task j. g_{ij} is defined by computing the time an ET vehicle needs to drive from task i's end node to any of the charging stations in G_S plus the time it takes to drive from these charging stations to task j's start node. The charging station which leads to the shortest travel time is saved as g_{ij} for the combination of tasks i and j. Ties between two charging stations are broken arbitrarily.

We add the following decision variables:

$$f_{ij}^{l} = \begin{cases} 1, & \text{ET vehicle } l \text{ performs task } j \text{ directly after task } i \text{ and } l \text{ can charge} \\ & \text{for at least } \Delta T \text{ seconds in between tasks } i \text{ and } j \quad \forall\, l \in H,\ i,j \in R,\ j > i \\ 0, & \text{otherwise} \end{cases}$$

We adjust the objective function as follows:

$$min\left(a - \sum_{l \in H} \sum_{i \in R} x_i^l\right) \tag{27}$$

We add the following constraints:

$$f_{ij}^{l} \cdot M_3 + \Delta T - (y_{ij}^{l} \cdot \frac{Q + q_{jg_{ij}}^2}{P^{MAX} \cdot \frac{C_{NOM}}{C_{MAX}}} - \frac{z_{ij}^{l}}{P^{MAX} \cdot \frac{C_{NOM}}{C_{MAX}}}) \geq 0 \qquad \forall\, l \in H,\ \ i,j \in R,\ \ j > i \tag{28}$$

$$(1 - f_{ij}^{l}) \cdot M_3 - \Delta T + (y_{ij}^{l} \cdot \frac{Q + q_{jg_{ij}}^2}{P^{MAX} \cdot \frac{C_{NOM}}{C_{MAX}}} - \frac{z_{ij}^{l}}{P^{MAX} \cdot \frac{C_{NOM}}{C_{MAX}}}) \geq 0 \qquad \forall\, l \in H,\ \ i,j \in R,\ \ j > i \tag{29}$$

$$\sum_{k \in G_S} c_{ij}^{k} \leq \sum_{l \in H} f_{ij}^{l} \qquad \forall\, i,j \in R,\ j > i \tag{30}$$

$$t_i^s \leq M_4 \cdot (1 - \sum_{l \in H} \sum_{\substack{j \in R \\ j<i}} y_{ji}^{l}) \cdot + \sum_{l \in H} \sum_{\substack{j \in R \\ j<i}} y_{ji}^{l} \cdot (t_j^E + \Delta_{jg_{ji}}^2 + \Delta_{g_{ji}i}^3 + \frac{Q + q_{jg_{ji}}^2}{P^{MAX} \cdot \frac{C_{NOM}}{C_{MAX}}}) - \frac{z_{ji}^{l}}{P^{MAX} \cdot \frac{C_{NOM}}{C_{MAX}}}$$
$$+ M_4 \cdot \sum_{k \in G_S} \sum_{\substack{j \in R \\ j<i}} c_{ji}^{k} + (1 - \sum_{l \in H} \sum_{\substack{j \in R \\ j<i}} f_{ji}^{l}) \cdot M_4 \qquad \forall\, i \in R \tag{31}$$

Constraints (28) and (29) are used to set the value of decision variable f_{ij}^{l} to 1 if y_{ij}^{l} equals 1 *and* the battery level of ET vehicle l is low enough to allow for at least ΔT seconds of charging when reaching the optimal charging station after finishing task i and driving to task j. Constraint (30) replaces constraint (22) and says that decision variable c_{ij}^{k} can only be equal to 1 if tasks i and j are performed consecutively by the same ET vehicle l *and* the battery level of l is low enough to allow for ΔT seconds of charging. Constraint (31) is an adaptation of constraint (26); if ET vehicle l has enough time to charge between consecutive missions j and i and f_{ji}^{l} is equal to 1, c_{ji}^{k} has to equal 1 as well. It needs to be noted that constraint (31) does not replace constraint (26), the latter is still used too. Furthermore, like in the original model from subsection 5.2, the ET vehicles have to charge to their full capacity Q if they decide to charge their batteries.

We use three input parameters for the newly defined constraints. M_3 is set to 13000, since this is slightly higher than the number of seconds in a day. M_4 is set to 90000, since this is slightly higher than the time in seconds to charge the batteries of an ET vehicle from 0 to Q. Lastly, the minimum charge time ΔT is set to 1800 seconds, which equals half an hour. Figures 11 and 12 show the results for the quiet and busy day, using the input parameters from the base case specified in subsection 6.1.3. The computational times to solve the problem are **3845** and **4536** seconds for the quiet and busy day respectively and the rolling window sizes are the same as for the original assignment model. It can be seen that for both days, the ET vehicles are charged more often than without the additions proposed in this section. On the quiet day, a total of **38** type 1 ET vehicles, **13** type 2 ET vehicles and **2** type 3 ET vehicles are required to perform all tasks.

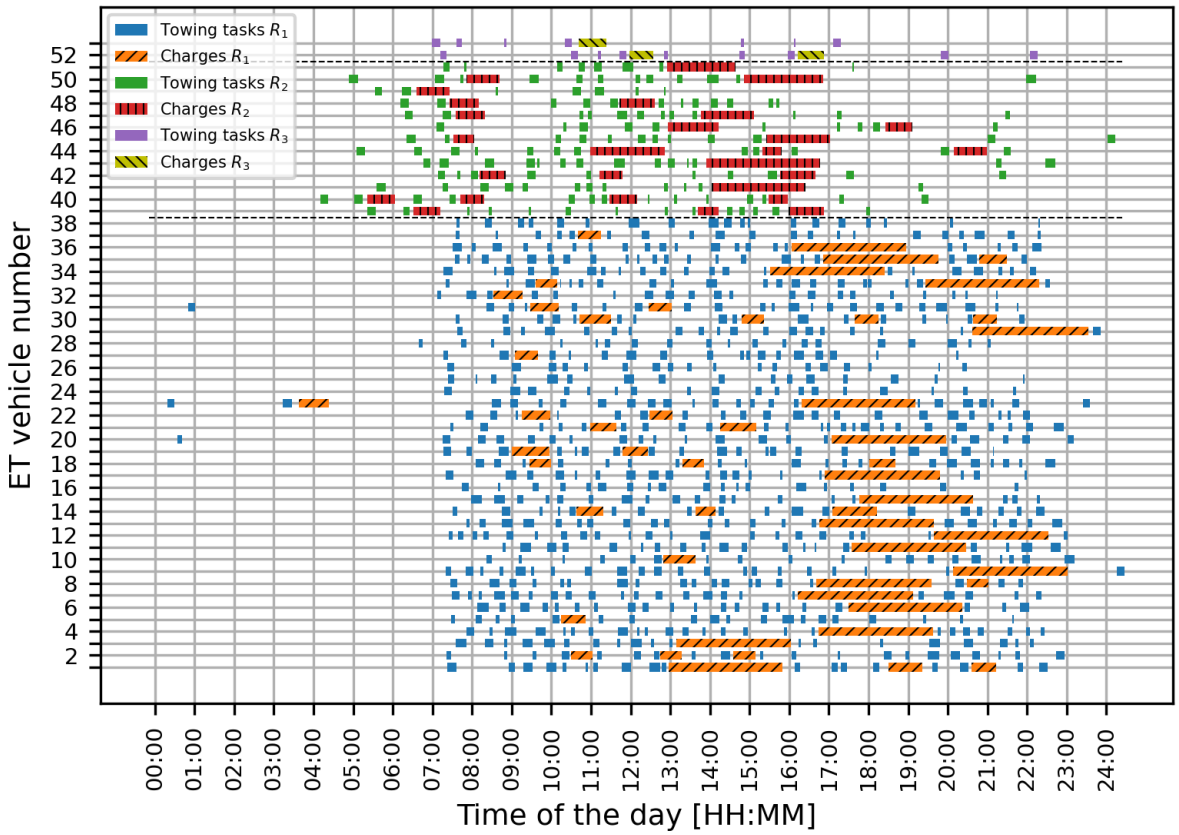

Figure 11: Results assignment model on the 14th of December when balancing charges

On the busy day, a total of **69** type 1 ET vehicles, **17** type 2 ET vehicles and **3** type 3 ET vehicles are required to perform all tasks. These numbers are equal to or lower than the results in subsections 6.3.1 and 6.3.2. It is expected that the number of required ET vehicles will decrease further if ΔT is decreased. A decrease in ΔT will especially lead to more charging during the beginning of the day, as ET vehicles have enough time to charge but have not reached a battery level that allows for 1800 seconds of charging yet. However, this is a matter of airport policy and optimal battery health management.

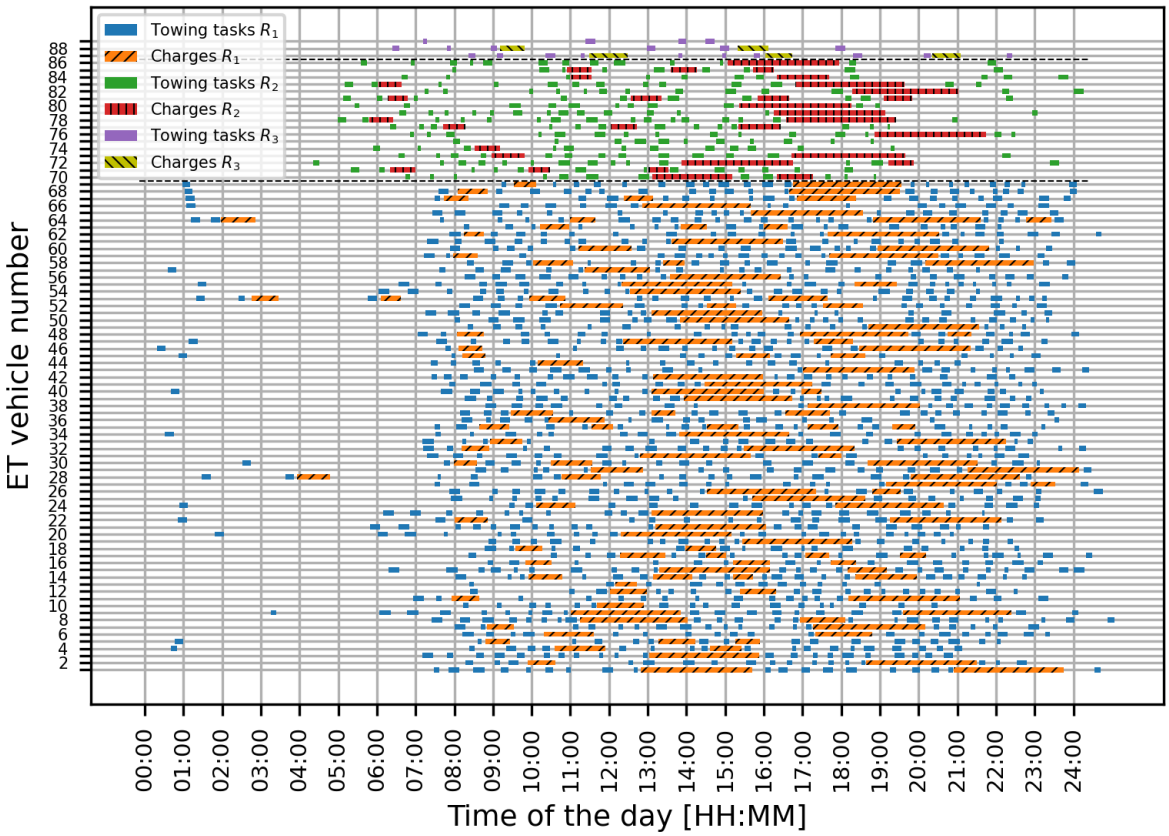

Figure 12: Results assignment model on the 13th of September when balancing charges

Table 19 shows the energy requirements per day, the ratio day and overnight charging, the distribution of charging energy over the charging stations and the peak power. The percentage day charging is much higher for the results in table 19 than in tables 11 and 12: a logical result of charging more frequently in between tasks. Peak power on the quiet day when balancing battery charging is higher than in table 11, which is due to the fact that batteries are charged very infrequently on the quiet day in the original model. For the busy day, the peak power is lower when balancing battery charging. This can be explained by the fact that the moments ET vehicles charge their batteries are distributed more evenly over the day. Peak power is required from 18:00:37 to 18:12:54 on the quiet day and from 14:36:20 to 14:45:35 on the busy day.

	Total energy used [kWh]	**Day [%]**	**Overnight [%]**	**Station 1 [%]**	**Station 2 [%]**	**Station 3 [%]**	**Station 4 [%]**	**Station 5 [%]**	**Peak power [kW]**
Quiet	28951	66	34	27	9	29	21	14	10400
Busy	61392	67	33	18	23	28	16	15	16900

Table 19: Energy and infrastructure results

9. Conclusions and Recommendations

In this research, we have successfully developed two optimisation models that can be used consecutively to give strategic insight into the ET vehicle fleet size required to perform all taxi operations at a hub airport electrically. The first model is a vehicle routing model and finds the optimal taxi routes for a set of aircraft towed by ET vehicles. This information is processed and converted to a set of towing tasks. The second model is an assignment model and determines the minimum number of ET vehicles required to perform all towing tasks, taking into account time and energy constraints. Our case study focuses on one of the quietest (14th of December) and one of the busiest (13th of September) days at AAS in 2019. On the quiet day, 914 aircraft need to be towed; whereas on the busy day, 1487 aircraft need to be towed. We have split these aircraft into three groups: N, W and W^H. We have also considered three types of ET vehicles that can only tow aircraft from their own group: 1 (for N), 2 (for W) and 3 (for W^H).

The models show that on the quiet day, we require **45** type 1, **13** type 2 and **2** type 3 ET vehicles to perform all towing tasks. On the busy day, we require **77** type 1, **17** type 2 and **3** type 3 ET vehicles to perform all towing tasks. We have obtained these results by using a rolling window strategy to solve the assignment model. This impairs the quality of the results and leads to a higher estimate of the required ET vehicle fleet size. Therefore, we have developed an alternative model that forces ET vehicles to charge in between towing tasks if possible. Besides, the battery level of an ET vehicle needs to be low enough to allow for at least 30 minutes of charging, in order to avoid very short battery charging. This results in **38** type 1, **13** type 2 and **2** type 3 ET vehicles on the quiet day and **69** type 1, **17** type 2 and **3** type 3 ET vehicles on the busy day. These numbers are more realistic, since ET vehicles are likely to be charged tactically during the day in a real-life situation.

Further analysis shows that, under the current assumptions, increasing the velocity at which aircraft can be towed by ET vehicles does not have much influence on the total number of ET vehicles required. This is due to the fact that an increase in velocity leads to a higher energy consumption, which largely negates the benefits of shorter taxi times. On the other hand, increasing battery capacity of the ET vehicles can have a large impact on the minimum number of ET vehicles required. However, this research shows that the effect differs per case: increasing battery capacity has more impact on the quiet day than on the busy day. The effect depends on to what extent battery capacity is the limiting factor to decrease the number of ET vehicles. Lastly, we show that the quality of the results is not impaired by the choice of charging station locations. The assignment model provides realistic results even if the charging stations are placed at different locations at the airport.

Due to the novelty of ET, future research could focus on analysing the assumptions made and input parameter values used to generate the results in this paper. The assumptions regarding the three types of ET vehicles are likely to be challenged in the near future once more companies develop new ET vehicles. This could lead to more flexible usage of ET vehicle types for different types of aircraft, higher taxi velocities and increased ET vehicle battery capacity. A safety study could focus on performing engine warm-up and cool-down while the aircraft is towed, minimising the effect of the ESUT and ECDT. The models developed and methods used in this research can then be used to estimate ET vehicle fleet size for these new conditions.

Another assumption that could be re-evaluated is the type of ETS used in this research. We have chosen to tow aircraft from the gate to the runway and vice versa using ET vehicles instead of using on-board ETS. On-board ETS are currently less technologically mature than ET vehicles, but might be a serious alternative in the near future. Wheeltug is currently developing an on-board ETS that is installed at the nose landing gear (NLG) and is powered by the auxiliary power unit (APU) [36]. German Aerospace Centre (DLR) develops an on-board ETS that is also installed at the NLG but is powered by on-board hydrogen or electric fuel cells, ensuring zero emissions [37] [38]. Lastly, Safran designs a main landing gear (MLG) on-board ETS [8]. In terms of modelling, the adoption of on-board ETS would render the assignment model redundant, since each aircraft is equipped with its own on-board ETS.

Another interesting area for future research, would be to implement battery swapping in the assignment model. It largely depends on ET vehicle design whether or not battery swapping is possible, but the assignment model used in this research can relatively easily be adapted to allow for this. Furthermore, future research could focus on decreasing computational time of the assignment model to enable solving an entire day of operations without a rolling window strategy. This will further decrease the estimated ET vehicle fleet size. A next step could even be to combine the vehicle routing model and assignment model in order to schedule the taxi routes in a way that minimises ET vehicle fleet size. This does mean that a trade-off has to be made between the importance of minimising delay at the airport and decreasing ET vehicle fleet size. If minimising delay is found to be the most important factor to consider, the results will not differ significantly from the results presented in this paper.

References

[1] D. S. Lee, G. Pitari, V. Grewe, K. Gierens, J. E. Penner, A. Petzold, M. Prather, U. Schumann, A. Bais, T. Berntsen, et al., Transport impacts on atmosphere and climate: Aviation, Atmospheric environment 44 (2010) 4678–4734.

[2] IATA, IATA Forecast Predicts 8.2 billion Air Travelers in 2037, published: 24-10-2018. URL: `https://www.iata.org/en/pressroom/pr/2018-10-24-02/`.

[3] Airbus, Airbus Global Market Forecast - Cities, Airports & Aircraft, published: 12-09-2019. URL: `file:///C:/Users/Jurjen/Downloads/GMF-2019-2038-Airbus-Commercial-Aircraft-book.pdf`.

[4] J. Rosero, J. Ortega, E. Aldabas, L. Romeral, Moving towards a more electric aircraft, IEEE Aerospace and Electronic Systems Magazine 22 (2007) 3–9.

[5] T. K. Hari, Z. Yaakob, N. N. Binitha, Aviation biofuel from renewable resources: Routes, opportunities and challenges, Renewable and Sustainable Energy Reviews 42 (2015) 1234–1244.

[6] M. Ithnan, T. Selderbeek, W. B. van Blokland, G. Lodewijks, Aircraft taxiing strategy optimization, 2013.

[7] N. Dzikus, J. Fuchte, A. Lau, V. Gollnick, Potential for fuel reduction through electric taxiing, in: 11th AIAA Aviation Technology, Integration, and Operations (ATIO) Conference, including the AIAA Balloon Systems Conference and 19th AIAA Lighter-Than, 2011, p. 6931.

[8] M. Lukic, A. Hebala, P. Giangrande, C. Klumpner, S. Nuzzo, G. Chen, C. Gerada, C. Eastwick, M. Galea, State of the art of electric taxiing systems, in: 2018 IEEE International Conference on Electrical Systems for Aircraft, Railway, Ship Propulsion and Road Vehicles & International Transportation Electrification Conference (ESARS-ITEC), IEEE, 2018, pp. 1–6.
[9] M. Lukic, P. Giangrande, A. Hebala, S. Nuzzo, M. Galea, Review, challenges and future developments of electric taxiing systems, IEEE Transactions on Transportation Electrification (2019).
[10] European Commission - High Level Group on Aviation Research, Airbus Global Market Forecast - Cities, Airports & Aircraft, published: 2011. URL: https://ec.europa.eu/transport/sites/transport/files/modes/air/doc/flightpath2050.pdf.
[11] F. Re, Model-based Optimization, Control and Assessment of Electric Aircraft Taxi Systems, Ph.D. thesis, Technical University of Darmstadt, 2017.
[12] Ministry of Infrastructure and Water Management (Dutch: Ministerie van Infrastructuur en Waterstaat), Draft agreement sustainable aviation (Dutch: Ontwerpakkoord Duurzame Luchtvaart), version: 21-02-2019. URL: file:///C:/Users/Jurjen/Downloads/bijlage-2-ontwerpakkoord-duurzame-luchtvaart.pdf.
[13] J. Smeltink, M. Soomer, An optimisation model for airport taxi scheduling*, 2004.
[14] G. Clare, A. G. Richards, Optimization of taxiway routing and runway scheduling, IEEE Transactions on Intelligent Transportation Systems 12 (2011) 1000–1013.
[15] P. Roling, Airport surface traffic planning optimization: a case study of amsterdam airport schiphol, in: 9th AIAA Aviation Technology, Integration, and Operations Conference (ATIO) and Aircraft Noise and Emissions Reduction Symposium (ANERS), 2009, p. 7079.
[16] M. Pereira, Short-range route scheduling for e-ac with battery-charging and battery-swapping constraints, Delft University of Technology (2019).
[17] H. Ding, A. Lim, B. Rodrigues, Y. Zhu, The over-constrained airport gate assignment problem, Computers & Operations Research 32 (2005) 1867–1880.
[18] M. Wen, E. Linde, S. Ropke, P. Mirchandani, A. Larsen, An adaptive large neighborhood search heuristic for the electric vehicle scheduling problem, Computers & Operations Research 76 (2016) 73–83.
[19] P. C. Roling, P. Sillekens, R. Curran, W. D. Wilder, The effects of electric taxi systems on airport surface congestion, in: 15th AIAA Aviation Technology, Integration, and Operations Conference, 2015, p. 2592.
[20] N. Guillaume, Finding the viability of using an automated guided vehicle taxiing system for aircraft, Master's thesis, Delft University of Technology, 2018.
[21] E. van Baaren, The feasibility of a fully electric aircraft towing system, Master's thesis, Delft University of Technology, 2019.
[22] N. E. Daidzic, Determination of taxiing resistances for transport category airplane tractive propulsion, Advances in aircraft and spacecraft science 4 (2017) 651.
[23] J. Domínguez-Navarro, R. Dufo-López, J. Yusta-Loyo, J. Artal-Sevil, J. Bernal-Agustín, Design of an electric vehicle fast-charging station with integration of renewable energy and storage systems, International Journal of Electrical Power & Energy Systems 105 (2019) 46–58.
[24] T. H. Cormen, C. E. Leiserson, R. L. Rivest, C. Stein, Introduction to algorithms, MIT press, 2009.
[25] LVNL, EHAM — AMSTERDAM/SCHIPHOL, accessed: April 2020. URL: https://www.lvnl.nl/eaip/2019-08-01-AIRAC/html/eAIP/EH-AD-2.EHAM-en-GB.html.
[26] J.-B. Gotteland, N. Durand, J.-M. Alliot, E. Page, Aircraft ground traffic optimization, 2001.
[27] Y. Jiang, X. Xu, H. Zhang, Y. Luo, Taxiing route scheduling between taxiway and runway in hub airport, Mathematical Problems in Engineering 2015 (2015).
[28] P. C. Roling, H. G. Visser, Optimal airport surface traffic planning using mixed-integer linear programming, International Journal of Aerospace Engineering 2008 (2008).
[29] Y. Jiang, Z. Liao, H. Zhang, A collaborative optimization model for ground taxi based on aircraft priority, Mathematical Problems in Engineering 2013 (2013).
[30] J. Hospodka, Electric taxiing–taxibot system, MAD-Magazine of Aviation Development 2 (2014) 17–20.
[31] N. M. Dzikus, R. Wollenheit, M. Schaefer, V. Gollnick, The benefit of innovative taxi concepts: the impact of airport size, fleet mix and traffic growth, in: 2013 Aviation Technology, Integration, and Operations Conference, 2013, p. 4212.
[32] F. Re, Viability and state of the art of environmentally friendly aircraft taxiing systems, in: 2012 Electrical Systems for Aircraft, Railway and Ship Propulsion, IEEE, 2012, pp. 1–6.
[33] J. Stockford, C. Lawson, Z. Liu, Benefit and performance impact analysis of using hydrogen fuel cell powered e-taxi system on a320 class airliner, The Aeronautical Journal 123 (2019) 378–397.
[34] F. Dieke-Meier, H. Fricke, Expectations from a steering control transfer to cockpit crews for aircraft pushback, in: Proceedings of the 2nd International Conference on Application and Theory of Automation in Command and Control Systems, 2012, pp. 62–70.
[35] Health, Safety and Environment office Schiphol - Schiphol Group, Schiphol Regulations, version: January 2020.
[36] W. Pan, Y. Ye, X. Li, Z. Li, Q. Zhang, The impact of green taxiing systems using on airport, DEStech Transactions on Computer Science and Engineering (2017).
[37] M. Schier, F. Rinderknecht, A. Brinner, H. Hellstern, High integrated electric machine for aircraft autonomous taxiing, in: International Conference on Electric Vehicles and Renewable Energies EVER, volume 11, 2011, p. 31.
[38] T. Raminosoa, T. Hamiti, M. Galea, C. Gerada, Feasibility and electromagnetic design of direct drive wheel actuator for green taxiing, in: 2011 IEEE Energy Conversion Congress and Exposition, IEEE, 2011, pp. 2798–2804.

II

Literature Study
previously graded under AE4020

1

Introduction

The number of global air travelers is forecast to nearly double in size in 2037 compared to the 2018 level according to the International Air Transport Association (IATA). This growth can partly be attributed to fast-growing economies like China, India and Indonesia, but it can also be seen that the aviation industry in most western countries, e.g. in Europe and the USA, is expected to steadily keep on growing in the next 20 years as well[1]. Furthermore, Airbus even projects a 4.3% air traffic growth per year over the next 20 years in their Global Market Forecast 2019-2039[2], which means air traffic will more than double before 2040.[3] On the one hand, this is a good sign for the aviation industry and, arguably, world economics. On the other hand, today's world does not only ask for economic growth, but also for a sustainable mind-set towards economics. Aviation is certainly no exception to this new mind-set and has a huge challenge ahead in terms of sustainable growth. Ideally, the environmental impact of aviation can be decreased in absolute numbers (e.g. in tonnes of CO2 emissions); however, this is extremely difficult for an industry that grows at such a rapid rate and is, at least for now, inherently polluting due to the need to burn fuel. A lot of resources are invested in research into alternative ways of flying, e.g. electrically-powered flying [43] and burning bio fuels instead of kerosene [19]. However, in the meantime it is of utmost importance for the aviation industry to do everything in its power to minimise environmental impact with the current means available.

One of the possible ways to contribute to less environmental impact is the adoption of electric taxiing (ET). Most aircraft operations at the airport's surface are currently performed using the main engines of aircraft. Considerable amounts of fuel can be saved and consequently emissions prevented by replacing these engine-powered taxi operations by electrically-powered taxi operations. Adopting sustainable ET procedures not only contributes to lower environmental impact, but could also lead to cost reductions for airlines due to less fuel consumption. Furthermore, the European Commission published their vision on the future of aviation in 2011, which states that all taxi operations at airports need to be electrically powered by 2050[4]. This might sound like there is still plenty of time for airports and airlines to adapt, but considering the investments and procedural changes required to make ET a reality, airports and airlines need to determine their strategies today rather than tomorrow.

This research will specifically focus on ET at a hub airport, using Amsterdam Airport Schiphol (AAS) as a case study. Therefore, this literature study discusses general information regarding ET, but also gives an overview of the relevant information regarding AAS. Furthermore, a collaboration between relevant Dutch parties (AAS, airlines, universities, consultants, Ministry of Infrastructure and Water Management, etc.) have come up with the 'Draft agreement sustainable aviation' (Dutch: ontwerpakkoord duurzame luchtvaart). This agreement states the ambition for ET to be the standard taxi procedure by the year 2030 at all Dutch airports[5]. This ambition provides AAS with an extra incentive to start pushing for developments in ET and aim to adopt

[1] https://www.iata.org/en/pressroom/pr/2018-10-24-02/, published: 24th of October 2018
[2] 'Airbus Global Market Forecast - Cities, Airports & Aircraft', published: 12th of September 2019
[3] The estimates in this section have been made before the COVID-19 pandemic, which will inevitably slow down growth
[4] European Commission, Flightpath 2050 Europe's Vision for Aviation, published: 2011
[5] Ontwerpakkoord Duurzame Luchtvaart, published: 12th of February 2019

this new taxi procedure within a short time span.

This literature study first gives an overview of conventional taxi procedures in chapter 2. After that, the same chapter explains the concept of ET, its (dis)advantages and the state-of-the-art products currently being developed. Chapter 3 discusses the business opportunities and possible pitfalls of ET. Then, the practical information regarding AAS required for the implementation of ET and the data required for setting up the optimisation model at AAS are given in chapter 4. After that, possible optimisation techniques are discussed and summarised in chapter 5. Furthermore, this literature study is part of a larger thesis project that aims to answer one main research question; this research question is divided into sub-questions and translated into a research objective, which is divided into two sub-goals, in chapter 6. This chapters also defines the scope of this research. The information gathered in the aforementioned chapters and the research objective are combined into a practical use case that will be the basis of the optimisation model; this use case and its related design choices are given in chapter 7. Finally, an overview of the planned work for the next stages of this research is given in chapter 8.

2

Taxi operations

This chapter discusses the general taxi procedures and rules at an airport. This is important information in order to understand the implications ET might have on airport operations. A description of the concept of ET is given to get a good impression of the advantages and disadvantages of ET. Finally, the electric taxiing systems (ETS) currently being developed and used are introduced and elaborated upon.

2.1. Procedures

In general terms, taxiing is the process of an aircraft moving across an airport's surface. This seems to be quite a clear definition; however, the limits of what is part of the taxi procedure and what is not, often differ slightly within different contexts. Therefore, the EUROCONTROL definition from their Collaborative Decision Making (CDM) manual is given as a benchmark. This definition states which ground operations are part of the taxi procedure by giving a definition of the taxi time. The taxi time can be split into two parts: the taxi-in time and the taxi-out time. The taxi-in time starts at the moment the aircraft lands and ends when the aircraft reaches its first parking position. The taxi-out time starts at the moment the aircraft starts push-back or vacates its parking position and ends when the aircraft takes off from the runway.[1] Similar definitions are often used in literature as well: in [17], an extensive analysis of conventional and electric taxi operations is performed using the same descriptions to divide the taxi operations in phases.

During push-back the aircraft is moved backwards and turned in the right direction by a towing vehicle. Depending on the way an aircraft is parked, it can also leave its parking position on its own. While being pushed back, the auxiliary power unit (APU) of the aircraft is running to power a few relevant aircraft systems (e.g. cabin air conditioning). After push-back, the main engines are started using bleed air produced by the APU. Then the APU is turned off in order to save fuel and the main engines are used to taxi to the start of the runway. The engines are generally used in idle mode, which comes down to a thrust level of about 7% [22]. When the aircraft reaches the runway threshold, it asks for permissions to take-off and starts the take-off procedure. [38]
The taxi-in procedure starts with the aircraft landing. The aircraft brakes in order to reach taxi velocity and at the same time uses part of its built-up velocity to reach the runway exit. After that, the engines are set to idle mode and are used to taxi to the assigned parking location. If there is no ground power supply available at the parking location, the APU is switched on during taxiing. Once the aircraft reaches the parking location, the engines are turned off. [38]
From an aircraft perspective, push-back is just one of the movements in its taxi procedure. However, from the perspective of the towing vehicle, a lot of pre-push-back and post-push-back operations need to be performed. These operations can be interesting in terms of towing vehicle scheduling. Figure 2.1 gives an overview of all operations concerned with aircraft push-back.

[1] EUROCONTROL, The Manual -Airport CDM Implementation, published: 31st of March 2017

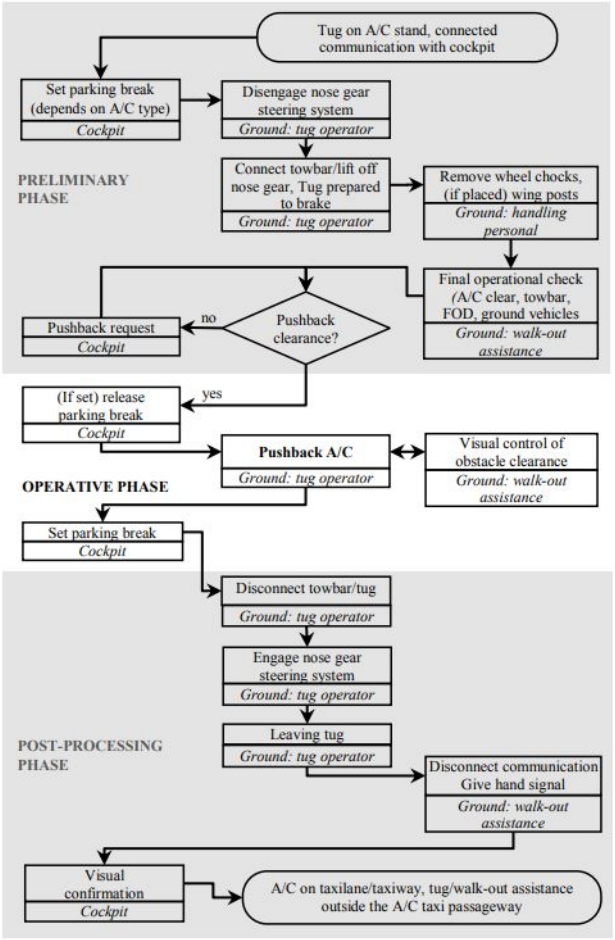

Figure 2.1: The full push-back process for conventional taxiing [6]

The procedures described above focus on the use of both engines to taxi. An alternative strategy to this procedure, is one-engine taxiing. This taxi strategy is more efficient in terms of fuel consumption and produces less noise than taxiing with both engines turned on. Furthermore, it is an easy strategy to implement as the aircraft does not require any modifications to enable one-engine taxiing. Drawbacks are the increased chance of jet blast, due to the higher engine thrust levels needed, and the limited applicability on sloped or slippery runways. [22]

The most important factor in taxiing, like everything aviation-related, is ensuring safe operations. Compared to airborne safety, taxiing is a relatively easy operation in terms of guaranteeing safety. However, it is still of utmost importance to avoid any conflicts between aircraft on taxiways. In [44], three main conflict types are defined (figure 2.2 gives a visual representation of these conflicts):

- **Intersection conflict:** two aircraft arrive at the same intersection at the same moment in time. In practice, the controller has to make sure this situation does not occur or one of the aircraft needs to wait for the other one to pass.
- **Rear-end conflict:** two aircraft are taxiing on the same taxiway and the trailing aircraft has a higher velocity than the leading aircraft. The trailing aircraft bumps its nose into the leading aircraft's tail.
- **Head-on conflict:** two aircraft are taxiing on the same taxiway in the opposite direction and bump into each other.

Figure 2.2: Possible taxi conflicts: intersection conflict (left), rear-end conflict (middle) and head-on conflict (right) [44]

2.2. Rules

During taxiing, aircraft need to adhere to certain rules. These rules mainly focus on a minimum separation distance between aircraft and a maximum allowed speed at certain parts of the taxiway network. Furthermore, airport service roads have a different set of rules than the taxiway network.

2.2.1. Separation

The main reasons to uphold separation minima during taxiing are to avoid conflicts between aircraft and to avoid another aircraft's jet blast. The minimum separation distance between taxiing aircraft differs per airport. In [41], 200 meters is used as minimum separation distance in their numerical example and this is enforced by creating 'links' in their network that satisfy this minimum separation distance and allowing a maximum of one aircraft per link. In [2], temporal separation is used as a way of ensuring separation minima are met: aircraft are not allowed to arrive at a node in the network within a certain time after another aircraft has been there. In [24], a model with temporal separation limits based on a minimum separation distance of 200 meters is used. A table of minimum separation distances based on the size of the leading aircraft, assuming another aircraft is following it, is used in [23]. These distances vary from 100 to 200 to 300 meters for small, medium and large leading aircraft. In [14], the smallest minimum separation distance is used, which is equal to 60 meters. Last but not least, a separation distance of 200 meters for their AAS case study is used in [44]. These distances give an idea of the minimum separation distance that can be used for this research.

One important factor to consider, is that one of the reasons for separating taxiing aircraft, jet blast, is caused by the engines. However, the engines are turned off during ET, which makes a separation minimum to prevent adverse affects of jet blast redundant. On the other hand, a minimum taxi separation distance is also enforced to aid in the process of ensuring enough time between consecutive departures in order to avoid wake turbulence negatively affecting trailing aircraft [18]. A smaller separation distance might therefore lead to queues at the runway threshold. However, if this does not influence on-time performance, this might not necessarily be an issue.

2.2.2. Velocity

Another rule, closely related to the separation distance, is the taxi velocity of the aircraft. The aircraft are not allowed to surpass a certain maximum velocity, but are also not expected to drop their velocity far below the maximum, in order to prevent slowing down other aircraft. The rules regarding velocity differ per airport as well and therefore it is interesting to see which aircraft velocities have been used by other researchers in similar situations. In [41], two categories of aircraft are used: slow aircraft travelling at 8 m/s and fast aircraft travelling at 16 m/s. In [2] and [24], different taxi velocities per aircraft type are used; the latter, however, uses a constant taxi velocity of 10 m/s in their numerical example. In [23], all aircraft are assumed to taxi at the same maximum velocity, but the aircraft are allowed to decrease their speed to avoid conflicts. In this paper's numerical example, an average taxi velocity of 10 m/s is used. In [14], the maximum taxi velocity is based on the turning rate of the aircraft. Furthermore, this paper applies an uncertainty factor to the aircraft velocity (10% in the numerical example) to account for deviations from the aircraft's taxi velocity.

2.2.3. Service roads

Lastly, the rules regarding operations on service roads is discussed. Airport service roads are the roads used by service vehicles (e.g towing vehicles, refuelling vehicles etc.) and cannot be used by aircraft. Separation rules like the ones applicable to taxiways, do not apply to service roads. Airports do define speed limits for their service roads, but these have not necessarily been published. AAS does not give a specific maximum speed for its service roads, but it does state that the maximum driving speed at the apron and perimeter

roads, which are the roads alongside the apron, is equal to 30 km/h (≈ 8.33 m/s)[2]. This values is also agreed upon by nearby airports like Munich Airport[3], Brussels Airport[4] and Ostend-Bruges International Airport[5]. Therefore, a good benchmark value for the speed limit at service roads is 8.33 m/s.

2.3. Electric Taxiing

This section discusses the concept of ET. It gives an overview of its practical consequences and the advantages and disadvantages that come with it. Furthermore, an overview of the currently available ETS is given. These ETS are compared and their main characteristics are summarised in table 2.1.

2.3.1. Concept

The difference between conventional and electric taxiing is quite clear: the former uses the main engines to move an aircraft around the airport's surface and the latter does exactly the same thing but using an electrically powered system to propel the aircraft. The two main categories of ETS are the ones that are installed on-board the aircraft and the external ones. Examples of both of these systems will be given in section 2.3.2. In [38], three basic tasks the ETS must be able to fulfil are identified: perform push-back, move the aircraft from standstill with sufficient acceleration and drive the aircraft along the taxi route. Furthermore, this paper points out that the ETS must be able to go into fail-safe mode in case of a malfunction and allow the pilot to perform conventional taxiing by using the main engines.

Advantages

Apart from the economic aspects, which will be discussed in chapter 3, ET also has some more technical advantages. First of all, in [30], the increased lifetime of the carbon brakes of the aircraft is mentioned. During conventional taxiing, the thrust level of the engines is often set to idle, which is generally too high for the maximum velocity the aircraft is allowed to taxi with or too high to perform certain (turning) manoeuvres. Therefore, a lot of braking needs to be applied by the pilot to adhere to these regulatory and physical limits. This wears down the carbon brakes, resulting in higher costs associated with replacing and maintaining them compared to the ET procedure which uses the carbon brakes less excessively [31]. In [31], it is pointed out that the chance of Foreign Object Damage (FOD) is decreased, since the engines will not be able to suck in any objects if they are turned off. This paper also mentions more efficiently using gate stands due to the possibility of parking parallel to the gate. The engines do not need to be warmed up or used near the gate, so the safety issues concerning jet blast or heat generation from the engines are non-existent.

Disadvantages

With these advantages, unfortunately, also come disadvantages. The main disadvantage related to all ETS, is the logistical issue of engine warm-up, which is required before take-off. During conventional taxiing, this automatically happens since taxiing with the engines in idle mode warms them up. The exact number of minutes required for warm-up, the engine spool-up time (ESUT), differs per aircraft. In [30], [31], [11] (for twin-engine aircraft) and [46], an ESUT of five minutes is assumed, whereas two to five minutes are assumed in [22], up to five minutes in [38] and three minutes in [45]. This means that ET does not make sense for a total taxi time of less than the ESUT, otherwise the total taxi time would be increased dramatically for small taxi routes without decreasing fuel consumption and emissions. Furthermore, it means that airports require holding bays near the runway thresholds to facilitate the engine warm-up required after ET. Another strategy would be to turn on the engines when the taxi time left is equal to the ESUT. However, no literature on ET is found that describes a procedure to accommodate turning on engines while taxiing electrically and the related safety considerations. In [39], it is mentioned that turning on the main engines during ET leads to safety issues due to the absence of ground staff and fire protection. If engine failure occurs, the aircraft will be stuck at the taxiway away from the apron. This blocks the taxiway for other aircraft and makes evacuation in case of a serious failure much more dangerous. Apart from that, operational and technical constraints related to the combination of using on-board or external ETS with turned-on engines might make it impossible to use them at the same time.

[2] Schiphol regulations, published: April 2017
[3] Traffic and Safety Rules for the nonpublic area at Munich Airport, published: August 2016
[4] Brussels Airport handbook - Traffic Rules, published: 18th of March 2019
[5] Airside Traffic Regulations, published: 2nd of April 2014

Apart from engine warm-up, the engine also needs to cool down after landing. This takes less time than engine warm-up, but also requires a few minutes of engine idle mode: the engine cool-down time (ECDT). In [11] and [45], three minutes are used to cool down the engines of twin-engine aircraft. In [22], two to five minutes are used and [46] assumes two and a half minutes of ECDT.
Another possible disadvantage is the limited taxi velocity of ET. It depends on the electric capacity of the ETS whether or not ET will be slower than conventional taxiing, but ideally electrically taxiing aircraft are able to reach the prevailing maximum allowed velocities at airports. In this way, ET does not have a negative influence on the traffic flow at airports.

Another logistical challenge that needs to be addressed is the responsibility for ET control. Air Traffic Control (ATC) needs to ensure efficient and safe operations of electrically taxiing aircraft and the required external ETS (section 2.3.2). ET with external ETS will add extra surface movements to the aerodrome network and these vehicles will need to be scheduled in order to perform their tasks. Furthermore, ET leads to different performance characteristics of aircraft (e.g. velocity), which need to be taken into account by the ET controller. Aerodrome controllers, part of Air Traffic Control (ATC), are currently responsible for aircraft movements within the taxiway network and on the runway.[6] Workload and complexity of tasks of air traffic controllers has been a major area of research since it is seen as a main issue related to aviation safety [8] [33]. These controllers will get extra responsibilities to accommodate ET, which might require extra training, and an increased workload might lead to a need for additional man power in the control tower.

2.3.2. State of the art

Currently, a few companies have taken up the challenge of designing and manufacturing a working ETS. These companies have different design philosophies, which can be categorised as external and on-board ETS. The following sections will discuss the most relevant products that are currently on the market or being developed.

External Electric Taxiing Systems

External ETS are characterised by the fact that they are separate vehicles. The main principle of both options being discussed in this section, is that they directly substitute present towing vehicles. They do not require any alterations to the aircraft and consequently do not require a lengthy certification process. Furthermore, no extra weight is added on-board, not increasing the in-flight fuel consumption [31]. The following list discusses the two most relevant external ETS.

- **Electric push-back (EP) vehicles:** the concept of these vehicles is the same as for present towing vehicles. EP are used to push back the aircraft, using an electric towing vehicle; once in position, the aircraft starts taxiing conventionally. This method decreases emissions during push-back, but does not pose a solution to the environmental impact of all stages of taxiing. A clear benefit of EP vehicles is that they can be readily implemented, as it does not change any of the procedures during the entire taxi process. Besides, there are EP vehicle designs that can be controlled remotely, which gives the remote pilot a very good overview of the aircraft's surroundings during push-back. Examples of such a system are the towbarless aircraft tug created by Mototok[7] and the towbarless tug by LEKTRO[8]. [31]

- **TaxiBot:** this system has been developed by Israeli Aerospace Industries (IAI) and is able to perform the entire taxi operation: taxi-in and taxi-out (including push-back). This procedure is called 'dispatch towing' [25]. It attaches to the nose landing gear (NLG) of the aircraft and it can be steered directly by the pilot by means of TaxiBot sensors transmitting the pilot's NLG inputs to the wheels of the tug. TaxiBot has been certified for the Boeing 737 family as well as for the A320 family and it can reach a taxi velocity of 23 knots (≈11.8 m/s) for a full Boeing 737. Furthermore, it is the only ETS currently used in commercial operations. [30]
  TaxiBot, however, also has a few disadvantages. First and foremost, the electric towing vehicles bring the aircraft to the runway threshold and subsequently have to drive back to the terminal. So for every taxi operation, an opposite-direction operation of more or less equal length needs to be performed. This puts a lot of pressure on the taxiway network and might lead to congestion. Secondly, taxi-in

[6] CAA Manual of Air Traffic Services - Part 1, 7th edition, published: 28th of December 2017)
[7] https://www.mototok.com/solutions/towbarless-tugs, accessed: March 2020
[8] https://www.lektro.com/, accessed: April 2020

operations might become more complicated due to the fact that arriving aircraft need to come to a standstill and have to attach TaxiBot to the NLG, which will induce some delay during taxi-in. Besides, the aircraft has residual velocity after it lands and needs to let the engines cool down for a few minutes, making the process of attaching TaxiBot even more complicated. Thirdly, TaxiBot is powered by two diesel engines that drive an electric generator; therefore, TaxiBot does not align with the desire for fully-electric taxiing. Also, TaxiBot can be steered by the pilot, but the system still requires a ground operator to be present in case of emergency and to drive back the towing vehicle after it has delivered the aircraft at the runway threshold [30]. Lastly, the price of TaxiBot is reported to be considerably higher than for normal towing vehicles [20].

On-board Electric Taxiing Systems

On-board ETS are characterised by the fact that they are an integral part of the aircraft design. Compared to external ETS, this has the clear advantage of not causing any extra taxiway network operations. Compared to conventional taxi operations, a possible advantage is a reduction in taxi time due to shorter push-back time, provided its taxi velocity is sufficient. Other advantages are an increase in aircraft autonomy (and consequently planning flexibility) and decrease in apron operations, since on-board ETS do not require towing vehicles. One of the main disadvantages is the fact that aircraft need to carry the ETS while flying, which adds to the total weight of aircraft and consequently to the in-flight fuel consumption. This might nullify the fuel gains accomplished during taxiing. Secondly, the on-board ETS induces extra complexity to the aircraft and requires extra certification efforts since it alters the aircraft design. [30]

- **WheelTug:** the on-board ETS developed by WheelTug is installed at the NLG of the aircraft. It is powered by the APU, which means that its capacity depends on the APU power of the specific aircraft on which the WheelTug ETS is installed. This also means that the WheelTug ETS does not fully comply with the guidelines on fully-electric taxi operations, as the APU consumes fuel. On the other hand, it uses only a fraction of the fuel used by the main engines. WheelTug was the first company to demonstrate a proof of concept for on-board ETS back in 2005 and have received 1000+ order from 20+ airlines in the meantime. The latest news on WheelTug's status says they are in the middle of the certification process for narrow-body aircraft, but no new information on this has come to light in the past 2 years. [30]

- **DLR:** the German Aerospace Centre (DLR) works on a similar design as WheelTug; the ETS is installed at the NLG. The main difference is that the DLR ETS is designed to be powered by on-board electric or hydrogen fuel cells; the latter is also suggested in [45]. This makes for a truly electric ETS, which is a big advantage. However, DLR is not nearly as far as WheelTug in the design and certification process and also has not received as many orders as WheelTug. [30]

- **Safran:** Safran has worked together with Honeywell Aerospace to develop the Electric Green Taxiing System (EGTS). Unfortunately, Safran and Honeywell Aerospace decided to terminate the project in 2016. However, Safran has stayed active in the ET business and has worked together with Airbus to create an on-board taxiing system for their A320 family. Unfortunately, Airbus has suspended their collaboration with Safran at the end of 2019 due to lack of technical maturity[9]. The main research Safran conducts, is research on ETS installed at the main landing gear (MLG) of the aircraft, powered by the APU[10]. The MLG carries about 90% of the weight of the aircraft and consequently creates more tractive forces. These tractive forces give the ETS more control over the aircraft, especially in rainy or snowy conditions which lead to a slippery taxiway. Furthermore, the MLG has more wheels (the exact number depends on the aircraft type) and therefore more motor installation locations than the NLG, increasing redundancy and reliability of the system. The main drawback of installing the ETS at the MLG is the lack of space available due to the presence of the brakes. [30]

Some general notes related to the options presented in the list above need to be made. First of all, in [30], heat management of the motors of the ETS and the brakes (in case of an MLG system) is seen as a major challenge. In [31], the MLG is described as a hostile environment for an ETS due to the proximity of the brakes, which function as an extra heat source. Furthermore, in both [30] and [31], it is concluded that the on-board

[9] https://www.reuters.com/article/us-safran-airbus-taxi/safran-suspends-electric-jet-taxiing-project-after\-airbus-ends-talks-idUSKBN1Y72MN, published: 3rd of December 2019

[10] Press kit 2019 Paris air show - Safran and aviation's electric future

ETS are unlikely to be useable for wide-body aircraft due to the lack of APU power to move the aircraft at a reasonable speed. These papers also suggest to look into the choice between using a geared or direct-drive system. The former is more practical in terms of generating torque but leads to a more complex design compared to the latter. Another consideration is the rotational speed of the wheels during aircraft landing. The ETS must be able to handle these wheel speeds without overheating. Therefore, a clutch might be a way to detach the ETS from the wheels when the aircraft is not taxiing.

Table 2.1 gives an overview of relevant parameters per ETS, partly distilled from the information given in this section and partly from [31]. The performance characteristics in the table can be used to decide which characteristics to use to model the ET network. It needs to be noted that the information given in table 2.1 is the most up-to-date information that could be found online, whereas the actual performance characteristics might have been improved in the meantime. The companies mentioned are all commercially active and are therefore likely to keep (part of) their design features undisclosed until the actual product is released or sold. In the last column of table 2.1, operations research papers that use (one of) the ETS in their model are given. It needs to be noted that some of these papers directly use characteristics one of the ETS in their model, whereas others use these ETS as an inspiration to define their own ETS characteristics.

Product/ company	**Type**	**Power supply**	**A/C weight (tons) [31]**	**Status**	**Vel. (kt) [31]**	**Paper**
EP vehicle [11]	External	Batteries	Up to 127	In service	3.5	-
TaxiBot [12]	External	Diesel engines and electric generator	68-85	In service	23	[16]
WheelTug	On-board	APU	85 [13]	Certification	9	-
DLR	On-board	Electric or hydrogen fuel cell	78	Unclear	13.5	-
Safran [14]	On-board	APU	78	Unclear	20	[42]

Table 2.1: Information on ETS

[10] LEKRO is used as benchmark for aircraft weight and velocity
[11] TaxiBot also has a more powerful version
[12] WheelTug is designed for the B737, so the MTOW of the B737-900ER (heaviest in the family) is assumed, since WheelTug does not specify the maximum aircraft weight it can tow
[13] Since two of Safran's collaborations have been terminated, some of these number might not be accurate anymore

3

Implications of electric taxiing

This chapters looks at the concept of ET from an economic and operational perspective. The aviation industry is notorious for its small financial margins and heavy competition between airlines [37]. Furthermore, airlines are in a continuous process of renegotiating terms and conditions with all the partners they work with, e.g. airport slots and pilot union salary negotiations. Therefore, new concepts that cut costs even slightly, could make a huge difference in terms of competitive position or bottom line profits. The next sections discuss the most important aspects of ET related to the executive decisions that need to be made in order to implement ET. Although this thesis research has its main focus on modelling of processes and optimisation instead of economics, this information gives the reader a good idea of the business context in which ET can be seen.

3.1. Cost reduction

The most direct way of cutting costs through ET, is the reduction in fuel consumption. Taxiing is generally performed with engines in idle mode, which is a highly inefficient engine setting as aircraft engines are designed for operation at thrust levels required to fly. This leads to a relatively large fuel consumption for such a low thrust level. Apart from the cost of kerosene, another inevitable consequence of burning fuel is the emission of greenhouse gasses. As mentioned in chapter 1, the aviation industry has the responsibility to minimise their impact on global warming; however, emissions also have a more direct effect on the airline's balance. Depending on the country the airline operates, a fee needs to be paid per tonne of CO2 emissions. Although multilateral organisations like the EU are planning to instate a carbon tax, it is not jet imposed by many countries in the world[1].

A number of studies have been performed to estimate the potential fuel savings of ET. In [10], three scenarios are defined, going from pessimistic to baseline to optimistic, based on APU fuel flow, ESUT, ECDT and ETS weight. Typical taxi and flight procedures are analysed to estimate the influence of on-board ETS on the total fuel consumption of domestic flight missions in the US, performed by aircraft from the A320 and B737 family. This results in potential fuel savings of 1.1%, 2.4% and 3.9% for the pessimistic, baseline and optimistic scenarios respectively.

In [22], a model has been developed to analyse the expected influence on fuel consumption and emissions at, among others, AAS; figure 3.1 gives these results. It is important to note that these calculations only apply to fuel consumption and emissions during taxiing, so the percentages do not say anything about reductions compared to fuel consumption and emissions of the entire flight. The fuel consumption and emission reductions are quite substantial but certainly not equal to a hundred percent, mainly due to the need for engine warm-up and cool down.

[1] https://www.carbonpricingleadership.org/news/2019/7/1/conference-on-carbon-pricing-and-aviation-taxes, published: 2nd of July 2019

Strategy	A	B	(A-B)%	C	(A-C)%	D	(A-D)%
Fuel consumption aircraft (ton)	1073	793	-26,1 %	682	-36,5 %	633	-41,0 %
Fuel consumption tug/ mass (ton)	N/A	N/A	-	115	-	140	-
CO_2 emission (ton x 1000)	3,39	2,51	-26,1 %	2,51	-26,0 %	2,00	-41,0 %
HC emission (ton)	2,59	1,91	-26,2 %	1,49	-42,6 %	1,34	-48,4 %
CO emission (ton)	23,25	17,15	-26.2 %	13,97	-39,9 %	11,91	-48,8 %
NO_x emission (ton)	4,69	3,47	-26,0 %	4,80	2,5 %	3,28	-29,9 %

Note:
A : Full-engine taxiing
B : Single-engine taxiing
C : Operational towing
D : Electrical nose gear

Figure 3.1: Fuel consumption and emission reductions during taxiing for different taxi strategies [22]

Another aspect to take into account is the fact that less fuel needs to be carried by the aircraft, since it does not need to perform the taxi-in procedure using the main engines. This decreases the weight of the aircraft and might partly make up for the addition of an on-board ETS. However, in [20] it also pointed out that, especially in the first years of ET, aircraft are likely to be obligated to carry the fuel anyway to account for possible ETS unavailability or failure.

Most of the maintenance related aspects of ET have already been mentioned in section 2.3.1. ET reduces wear of the carbon brakes located at the MLG wheels, since the aircraft velocity can be managed much more easily with an ETS. This reduces maintenance costs of the carbon brakes. Furthermore, taxiing with the engines turned off makes sure nothing will be sucked into the engines, reducing maintenance costs related to FOD. In [22], it is pointed out that that main engine maintenance costs might decrease due to the less use of the main engines at the idle thrust level for which the engines were not designed. On the other hand, in [20], it is mentioned that there will also be extra maintenance costs for the new ETS. These systems or vehicles will have to be maintained as well, especially the more complex on-board ETS.

A study on ET using hydrogen fuel cells for an on-board ETS is presented in [45]. This paper assesses the costs associated with using a hydrogen-powered ETS (e.g. impact of carrying the fuel cells during flight) and compares this to the benefits. He takes into account the reduction in maintenance costs for the main engines, APU, power plant and the carbon brakes. It also takes into account the abovementioned fuel and emissions cost reduction and also considers the cost reduction of not having to pay the ground handlers for push-back operations. For the year 2016, this results in a 5.97% net profit increase compared to Twin-Engine Taxiing (TET) and a 4.02% net profit increase compared to Single-Engine Taxiing (SET).

3.2. Operations and regulations

The phrase 'time is money' could not be more true for aviation. If ET structurally incurs delays, less departures can be scheduled in the same time window and less revenue will be generated. On the other hand, if ET improves operational efficiency and on-time performance, it will definitely have a positive effect on revenue. The difficulty in assessing the influence of ET on on-time performance stems from the uncertainty in performance of electrically taxiing aircraft. In [30], it is pointed out that a decrease in push-back time and aircraft autonomy could lead to a decrease in taxi time. However, in [20], it is stated that lower taxi velocities will eventually lead to longer taxi times. Furthermore, as previously mentioned, the engine warm-up and cool-down will probably add time to the taxi procedure; however, the possibility that engine warm-up during the last minutes of taxiing might increases taxi velocity is mentioned in [42].

Another interesting factor to look at, is the responsibility of the parties involved. The four main parties to take into account are the airports, airlines, ground handling companies and original equipment manufacturers (OEMs). As pointed out in [31], their might be a conflict of interest if these parties do not agree on a shared business model. Looking at the case of a fleet of electric towing vehicles performing dispatch towing for multiple airlines, there is a discrepancy between the party making the investment and the parties reaping the benefits. In many cases, ground handling companies own the push-back vehicles and are responsible for this part of airport operations. If they acquire the (expensive) electric towing vehicles, they will make the investment whereas the airlines are saving fuel. Thirdly, the airports are obliged to electrify all their taxi procedures due to new regulations, but they are partly dependent on the cooperation of ground handling companies and, especially in case of on-board ETS, airlines and OEMs. Therefore, clear agreements must be made with these four parties to fairly divide costs and benefits. A possible example of a model that might work, is the ground handling companies and airports acquiring new ET vehicles together and raising slot prices and ground handling fees for airlines based on their expected fuel savings.

Last but not least, the regulations that have been mentioned in chapter 1 are a leading factor in deciding to adopt ET. The fuel savings mentioned in section 3.1 can have a significant influence on the revenue of an airline, but the uncertainty related to on-time performance mentioned in this section might be a reason for executives to adopt a cautious attitude towards ET. However, all of these economic factors are of minor importance if governmental bodies compel airports and airlines to electrify their taxi operations. The Dutch ambition to use ET as standard taxi procedure by 2030[2] and the European Commission's ambition to achieve the same in 2050[3], ensure that research on ET performance is of very high significance, irrespective of the projected economic consequences.

[2] Ontwerpakkoord Duurzame Luchtvaart, published: 12th of February 2019
[3] European Commission, Flightpath 2050 Europe's Vision for Aviation, published: 2011

4

Airport

This chapter focuses on the influence the airport lay-out has on optimisation of (electric) taxi operations. The first two sections of this chapter give an overview of previous research that has been performed on taxi operations at airports; specifically focusing on the lay-out of airports and flight schedules that have been used in these papers. Table 4.1 summarises the findings regarding the airport lay-out and table 4.2 gives a summary of the flight schedules used in literature. Secondly, an overview of relevant aspects of the airport used in this study, AAS, is given.

4.1. Lay-out

Research on the optimisation of taxi operations requires a model of an airport that can be used as a location to perform these operations. The strategy employed by all papers on taxi optimisation, is to convert a physical airport lay-out into a node and edge network. This node and edge network is an abstract representation of the airport where nodes denote 'junctions' and edges denote the connections between these junctions. These edges can be directed or undirected, which means they can allow one-way or two-way traffic respectively. Furthermore, values that represent the real-life airport distances are assigned to each edge.

The first set of research papers discussed in this section focuses on AAS. AAS is a perfect example of a hub airport, since a very high percentage of flights going through AAS are connecting flights. AAS has six runways and uses the one-terminal concept. First of all, in [44] and [42], all the taxiways are converted into a network of nodes and edges. The latter added a maximum allowed velocity per edge to the airport model. These papers both incorporated all six runways available at AAS and all their runway entrances and exits. In [16], only one runway entrance or exit per runway end (i.e. a holding area) has been modelled in order to simplify the network. Furthermore, this paper only includes the runway ends relevant for the flight schedules used in its case study, so not all taxiways are included. On the other hand, this paper did include the service roads relevant to the case study. The last paper that used AAS as a case study, is [22]. This paper only uses the two main arrival and departure runway modes in its network, since they account for about 90% of operations, according to [22].

Multiple other airports have been modelled as well to accommodate taxi operations research. In [48], Guangzhou Baiyun International Airport has been modelled, which has two parallel runways with two airport terminals located in between. London Heathrow Airport has been used as a case study in [2], which has two parallel runways with four passenger terminals of which three are located in between the runways and one south of the southern most runway. In [14], two airports are discussed; however, the paper only uses one to present the results. This airport is Paris Charles de Gaulle Airport, which has four parallel runways with three terminals, two located near the two northern runways and one located near the southern runways.
In both [24] and [23], an unidentified hub airport in China has been chosen. The former models an airport with two parallel runways and one terminal building in between the runways. The latter only picks one of the runways of the airport and forms a taxiway network with the taxiways relevant for that runway. The number of terminals is equal to one as well. Lastly, a mock airport with three runways has been defined in [41]: two parallel and one perpendicular to the two parallel ones. Runway lengths are not given, so it is not clear if the

perpendicular runway intersects any of the parallel runways.

Table 4.1 gives an overview of the papers discussed and the basic characteristics of the airports used and the node and edge networks created. An interesting conclusion is that the only airport, not counting the mock airport from [41], which does not use parallel runways only is AAS. Furthermore, all of the analyses have been performed for hub airports. This is probably due to the higher urgency for efficient taxi operations at hub airports than at less complex regional airports.

Paper	Year	Airport	Type	#Runways	Orientation	#Terminals
[44]	2004	AAS	Hub	6	Parallel & intersecting	1
[42]	2008	AAS	Hub	6	Parallel & intersecting	1
[16]	2018	AAS	Hub	5 (not all modes)	Parallel & intersecting	1
[22]	2013	AAS	Hub	Unknown (2 modes)	Unknown	1
[48]	2017	Baiyun	Hub	2	Parallel	2
[2]	2011	Heathrow	Hub	2	Parallel	4
[14]	2001	Charles de Gaulle	Hub	4	Parallel	3
[24]	2015	Unknown	Hub	2	Parallel	1
[23]	2013	Unknown	Hub	1	-	1
[41]	2008	Mock airport	Unknown	3	Parallel & perpendicular	1

Table 4.1: Overview of airport models in literature

4.2. Flight schedule

In order to optimise a taxi schedule, boundary conditions for the aircraft in the network need to be set. This is done by the flight schedule. For arriving aircraft, these boundary conditions consists of a time of arrival, an arrival runway and a gate the aircraft needs to park. For departing aircraft, this consists of the scheduled departure time, a departure runway and a parking gate. Naturally, the more aircraft that need to be scheduled for a certain period of time, the more complicated the network becomes and the more difficult it becomes to minimise delays. Therefore, it is interesting to get a good overview of the flight data used in comparable research. Table 4.2 gives a summary of the papers discussed in this section.

First of all, like in section 4.1, the AAS papers are discussed. In [44], five and a half hours of AAS flight data are used (11:30 a.m. - 05:00 p.m.); the paper divides it into 12 time sets of on average just shy of half an hour, the reason for this division is explained in section 5.1. The total number of aircraft in this time window is equal to 406. In [42], a mock flight schedule of 10 aircraft divided over a time period of 15 minutes is used. These 10 aircraft are departing aircraft and the model only focuses on one runway at a time. In [16], two full-day AAS flight schedules are analysed separately. The first day is picked since it employs AAS' preferred runway configuration and is therefore the runway configuration responsible for most of the day-to-day operations. The second day is picked since it employs a runway configuration with long taxi times due to the larger distance between the active runways and the apron. In [22], an AAS daytime schedule of one day from 06:45 a.m. until 09:45 p.m is used.
In [48], a Baiyun Airport flight schedule of four hours, from 01:00 p.m. until 05:00 p.m., is used and one day of Heathrow Airport flight data from 09:00 a.m. until 12:00 noon, which holds 240 aircraft, is used in [2]. In [14], one full-day flight schedule at Charles de Gaulle Airport is used.
In [24], a mock flight schedule of 20 aircraft has been constructed; all aircraft have a scheduled departure time or arrival time set at time equal to zero. The model tries to schedule them all with as little delay as possible; the delay of the departing aircraft starts to count after 30 minutes from the starting time. In [23], a mock flight schedule of nine flights has been constructed, also with the same scheduled departure and arrival times starting from time equal to zero. Since there is only one runway, all aircraft depart from or arrive at the same runway; the gate assignments of the aircraft are different. Lastly, in [41], a mock flight schedule has been constructed as well, consisting of eight flights with scheduled departure and arrival times within a time frame of six minutes. The aircraft arrive at or depart from the three different runways in the airport model.

Paper	Year	Airport	Real/mock	Time window	#Aircraft	A/D[1]
[44]	2004	AAS	Real	11:30 a.m.- 05:00 p.m.	406	A & D
[42]	2015	AAS	Mock	15min	10	D
[16]	2018	AAS	Real	2x full-day	-	A & D
[22]	2013	AAS	Real	06:45 a.m. - 09:45 p.m.	-	A & D
[48]	2017	Baiyun	Real	01:00 p.m. - 05:00 p.m.	-	A & D
[2]	2011	Heathrow	Real	09:00 a.m. - 12:00 noon	240	A & D
[14]	2001	Charles de Gaulle	Real	full-day	-	A & D
[24]	2015	Unknown	Mock	-	20	A & D
[23]	2013	Unknown	Mock	-	9	A & D
[41]	2008	Mock airport	Mock	6min	8	A & D

Table 4.2: Overview of flight schedules used in literature

4.3. Case study: Amsterdam Airport Schiphol

This section discusses the lay-out of AAS in more detail, highlighting some of the airport models from the papers mentioned in tables 4.1 and 4.2. Furthermore, airport data regarding flight schedules is discussed. It is pointed out which flight data is required for further analysis and how this data can be acquired.

4.3.1. Layout

The relevant AAS layout consists of three parts: apron, taxiways and runways. The gates and runways form the begin or end points of the network and the taxiways are used to traverse the airport. Figure 4.1 gives an overview of the AAS Aerodrome. This figure gives a good overview of what the aerodrome actually looks like and can be used to distil the taxi network from the full aerodrome overview.

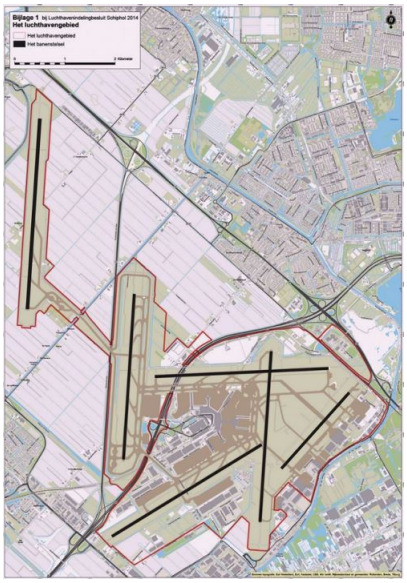

Figure 4.1: Overview of the AAS aerodrome[2]

As mentioned in section 4.1, in [44] a schematic overview of the AAS taxi network relative to the runways and apron/terminal has been created (see figure 4.2). This figure is an adaptation of the information presented in the aerodrome overview in order to make it easier to comprehend and translate into an optimisation model. This might be a useful strategy to create the airport model for this research as well.

[1] Arrival and/or departure aircraft incorporated in flight schedule
[2] Amsterdam Airport Schiphol Aerodrome Manual version 6.1, published: September 2019

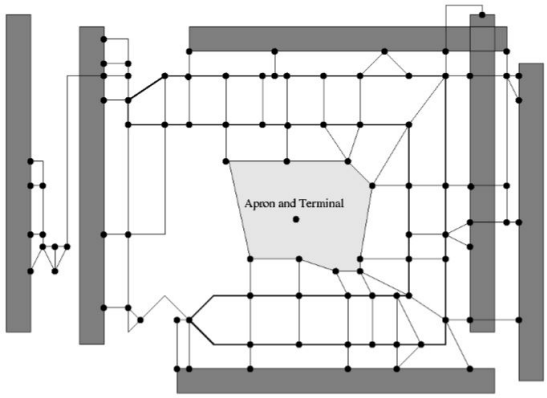

Figure 4.2: Schematic overview of AAS taxiways [44]

In [42], an AAS overview that preserves the actual AAS layout is provided (figure 4.3), which is a middle ground between the realistic figure 4.1 and the schematic view of figure 4.2. As mentioned in section 4.1, this node and edge network provides maximum narrow-body aircraft taxi speeds per taxiway segment that, according to [42], were obtained through analysis of data provided by AAS and LVNL. This figure also displays the runway names of the runways at AAS.

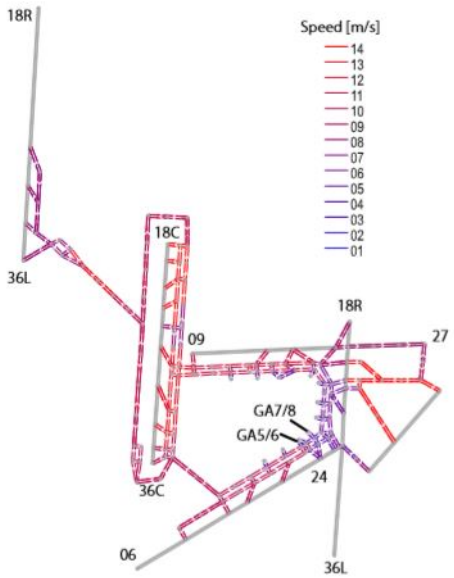

Figure 4.3: Overview of AAS taxiways with maximum taxi velocities [42]

The last representation of the AAS taxi network is shown in figure 4.4. As mentioned in section 4.1, it does not show all taxiways and service roads; however, it does give a very clear overview of the nodes and edges needed for its specific use case. A clear difference between figures 4.4 and 4.3, is that the former shows a network that brings the aircraft towards a dedicated holding area near the runway and does not distinguish between different runway entrances and exits. This is an interesting strategy that might be applicable to this thesis research as well.

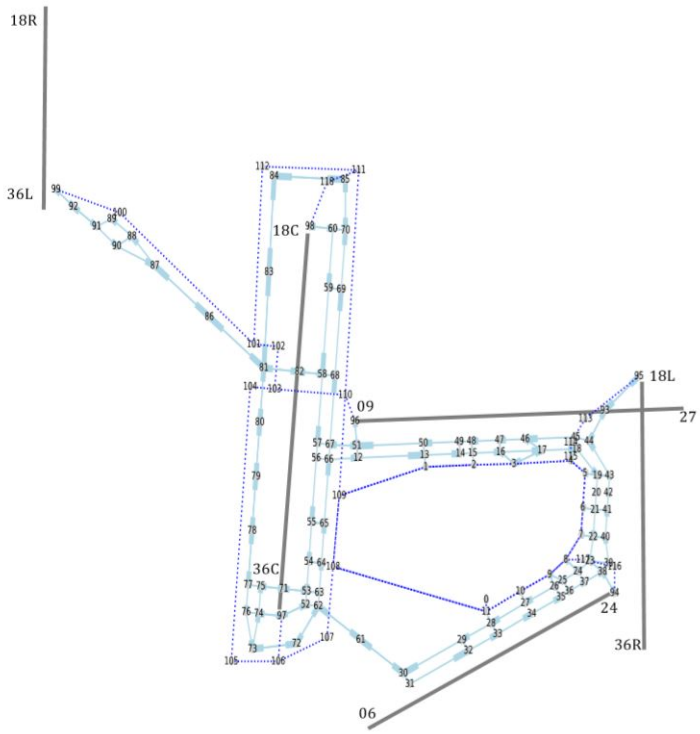

Figure 4.4: Node and edge network with limited access to runway entrances and exits [16]

An overview of the piers of AAS is given in figure 4.5. The AAS representations in figures 4.3 and 4.2 do not include a detailed overview of the apron and its piers, whereas figure 4.1 only gives a bird's-eye view of the aerodrome. The piers are an important part of the network, as the gates are located at the piers and the gates are the starting or ending points of each taxi operation.

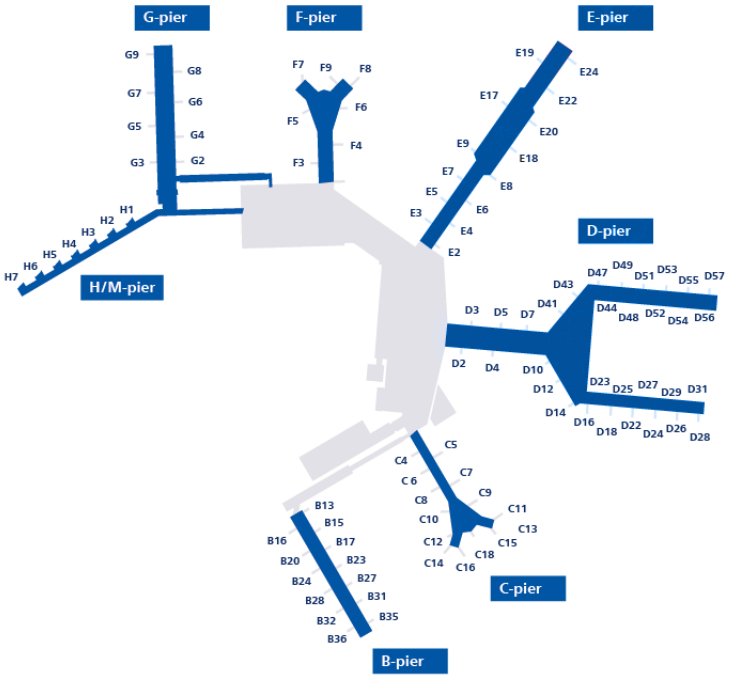

Figure 4.5: Overview of AAS piers[3]

4.3.2. Flight Schedule

The flight schedule data that is going to be used for this research depends on the data available and the data needed. AAS provides developers with a means of gathering AAS flight data programmatically through the Schiphol Application Programming Interface (API). However, the data set used for this research has been provided by AAS directly and will be discussed in this section.

The data set provided by AAS is a complete flight schedule spanning from the 1st of January 2019 until the 4th of April 2020. The data has 49 columns per flight, most of which is information irrelevant to this research. Therefore, an overview of the most relevant data provided for each flight is given in the following list. The names do not exactly match the names from the data set, but are modified to be easier to understand.

- **Aircraft type:** information which can be used to determine which type of ETS applies to which aircraft. As discussed in section 2.3.2, there are two main kinds of ETS: on-board and external. For some of the aircraft types the external option might be favourable, whereas for others the on-board option makes more sense.
- **Actual time:** the time the aircraft has actually arrived or departed. This might be needed to build a realistic flight schedule for one day of operations at AAS. For arriving flights, the actual time indicates the time the aircraft has actually arrived at the gate; for departing aircraft, the actual time is the time the aircraft has left the gate.
- **Flight number:** information to be able to identify flights if necessary. This flight number belongs to the main flight, so the individual airline flight numbers required for code sharing are not used.

[3] https://www.transport-online.nl/site/113578/alleen-d-e-en-f-pier-nog-in-gebruik-op-schiphol/, accessed: April 2020

- **Flight direction:** the flight direction has two option: A for arrival and D for departure. This is used to determine if the taxi procedure starts from the runway or from the gate.
- **Gate:** in order to simulate a taxi network, it is required to know where the aircraft starts taxiing in case of a departing aircraft or where it needs to park after landing.
- **Runway:** similar to the gate, the runway forms the start or end point of the taxi operation of each aircraft and is therefore essential information for the model.
- **Scheduled date:** can be used to check if all the flights are from the same day. This is not the most relevant piece of information in the table, but worth keeping in there if multiple days are being analysed.
- **Scheduled time:** the time the aircraft is expected to arrive or depart. This is similar to the 'Actual time', but then it shows the flight schedule the way it was planned. This might also be used to construct the one-day flight schedule.
- **Taxi time:** the time each aircraft has taxied from the runway to the gate or vice versa. This is relevant information since the flight schedule data gives the departure times from and arrival times at the gate, whereas the landing and take-off time also need to be known to create a complete schedule. Therefore, the taxi time can be used to get a good estimate of these times.

5

Optimisation methods for taxi operations

There are various optimisation methods that can be used to optimise the ET network at AAS. In this chapter, the optimisation models used in previous papers, mainly related to airport ground operations optimisation, are discussed. These models each use their own methods to optimise the problems faced in their research and this chapter gives a short description of the most important choices made. After that, a recommendation regarding the optimisation methods used in this research is made.

5.1. Mixed-integer linear programming

This section gives an overview of mixed-integer linear programming (MILP) optimisation models used for problems similar to the taxiing scheduling problem in this research.

In [44], a MILP model is described that optimises taxi procedures at AAS, by using decision variables that sequence aircraft at each node. The route of each individual aircraft is fixed beforehand, only the optimal times at which each node is reached are determined in the model. Each aircraft has a timing decision variable for each node in its route in order to ensure minimum separation and minimum/maximum velocity. The timing decision variable is also used to define the starting time of the taxi operations by setting it equal to the arrival time of an aircraft or forcing it to be equal or higher than the Off-Block Time (OBT) of an aircraft, in case of departures. Holding points are modelled by defining a series of successive nodes and edges with length equal to 0. The number of edges is equal to the capacity of that holding point. The objective function minimises the total taxi time and the difference between the time aircraft arrive at the runway and the time they are supposed to depart, which is basically the 'waiting time'.
A rolling window strategy is used in [44] to limit computational time. This makes sense from a practical point of view as well, since taxi schedules are usually made for every 15 to 30 minutes into the future. The paper uses three variants of the rolling horizon, listed below. These variants do not give the global optimum but are likely to give very reasonable schedules. This is due to the fact that taxiing aircraft at time X are unlikely to influence taxiing aircraft at e.g. time X + 2 hours. Also, the gains in computational time do justify a slightly suboptimal solution.

- **Variant 1** divides the total time into sets of size T. It assigns aircraft to one set based on their earliest starting time (OBT or arrival time). It solves the problem for a certain time period and fixes the schedules for the aircraft that are still taxiing in the next set. Then, in the next set, the problem is solved again for the aircraft with a starting time in that set, while taking into account the fixed schedules of the overlapping aircraft from the previous set.
- **Variant 2** does not fix the schedule of aircraft with starting times in previous sets. It sets the last node in the previous set as a constraint and allows the rest of its route to be rescheduled in the new optimisation set.
- **Variant 3** is called a sliding window and looks at a fixed number of aircraft per optimisation, size m. The schedule is optimised for the first 1,...,m aircraft, based on their arrival time or OBT. Then, aircraft 1's schedule is fixed and the optimisation is done for aircraft 2,...,m+1. This continues until the last aircraft is reached.

In [2], a MILP model with receding horizon (RH) is used to model a taxi network at Heathrow Airport, which is comparable to the rolling window in [44]. Virtual nodes are used for aircraft that are travelling in the network when the execution window of the RH is finished. The virtual node is the starting point for the aircraft at the beginning of the next execution window. The airport has been modelled by defining a matrix that holds a 1 if two nodes connect via a taxiway and a 0 if two nodes do not connect. A distance matrix holds the distances between all of the adjacent nodes and another matrix holds all of the shortest paths between all nodes in the network. The nodes in this model are assumed not to be connected to themselves, so holding at a node is not allowed except at the departure node. Doubling back is also disallowed by one of the constraints. Conflicts in the planning horizon are resolved by identifying them after the MILP model has been solved and adding them to a list of conflicts. These conflicts are then added as constraints and the model is solved again. This iterative process is repeated until there are no conflicts left. It is chosen to use this iterative process, instead of constraining the model to disallow conflicts from the start, to minimise computational time by not enforcing redundant constraints. Furthermore, the remainder of the taxi time for aircraft that did not reach the departure node at the end of the planning horizon is determined by using the shortest path matrix defined beforehand. The shortest path time between the last node of the aircraft and its departure node is added to the taxi time within the planning horizon to get an estimate of the total taxi time. A departure sequence is also enforced in the model if necessary. This could lead to problems for aircraft that have their earliest push-back time outside the planning horizon but need to depart before an aircraft in the previous planning horizon. Therefore, for the sake of departure sequence scheduling, the model is allowed to look 300 seconds into the future. This extra information is only used for this purpose and not to actually schedule the aircraft within these 300 seconds, in order to limit computational time.

Another paper that uses MILP to optimise taxi flows at an airport (AAS) is [40]. The paper does not specify the objective function, constraints etc. of the optimisation model, but it does give an interesting insight regarding route generation. Before solving the network, a set of possible routes for each aircraft is generated. These possible routes are a sequence of nodes; starting at the gate and ending at the runway for departing aircraft and vice versa for arriving aircraft. The route generator generates all possible routes for each aircraft, but only a subset of these routes is used in the MILP model in order to reduce problem size. The shortest possible route is always included in this subset and the route generator determines which additional routes are used for the optimisation process by calculating a factor that defines the difference between the shortest route possible and all of the other routes. This factor is calculated by dividing the number of nodes that are different between the two routes by the total number of nodes of both routes. In this way, a route that differs a lot from the shortest path gets a lower factor. Each route has its own difference factor for a specific aircraft; these factors are multiplied with the path length to get a new value. The routes with the lowest values are picked by the route generator as input to the MILP model. In this way, routes differing significantly from the shortest path are favoured over similar routes in order to give the model flexibility in picking substantially different routes for a specific aircraft. Furthermore, this model incorporates a simulator that can be used to visualise the location of all active aircraft in the network at any time in order to facilitate ATC.

In [15], new punctuality indicators that focus on sustainable management of airports are defined. The main conclusion regarding these new indicators, is to measure delay with respect to the planned take-off time of aircraft and not look at the push-back time. Sticking to a planned push-back time leads to large queues near the runway and in the taxiway network, at which point in time aircraft engines are turned on and produce emissions. Two optimisation strategies are used to solve the vehicle routing problem. The first is comparable to the one used in [44] and allows only one predefined route for each aircraft; the model optimises the times each node is reached. The second strategy is more similar to the one employed in [40] and defines a set of possible taxi routes beforehand. The model picks the optimal route for each aircraft and defines the time each node in this route is reached. Furthermore, the full-day schedule is divided into windows of 30 minutes to limit computation time.

In [41], a MILP model is created that updates every 10 seconds and uses the actual aircraft positions at that time as input. It also uses the part of the flight schedule that falls within the planning horizon as input and freezes part of the planning to avoid changing the entire schedule every 10 seconds. The algorithm is based on defining the shortest paths for all the aircraft within the planning horizon and resolving any conflicts by minimally changing the shortest paths. The user can give maximum delay per flight as an input to ensure individual flights are never penalised too heavily.

It can be observed that the abovementioned papers each apply their own strategies to minimise computational time. This indicates that for aircraft ground operations optimisation models, computational time is a very important factor to consider. In [44], different rolling window strategies are employed to minimise computational time and a maximum allowed computation time of 1000 seconds to solve each time window of approximately 30 minutes is used. In [2], one of the main focuses lies on efficient computations and decreasing solve time of the model. A comparison is made between the solve time when using the RH approach, iterative addition of constraints approach and a fully constrained non-RH approach. It is concluded that, the larger the set of aircraft considered, the more efficient the RH approach becomes compared to the other two approaches. Also, the iterative addition of constraints approach becomes more efficient compared to the fully constrained approach when the number of aircraft considered increases; however, the number of iterations required does also increase with problem size, as more aircraft conflicts need to be resolved iteratively. In [40], a key aspect of the optimisation model is also to minimise computational time. The strategy explained in this section, defining a subset of routes beforehand, leads to too high computational times and memory fragmentation [5] for a full-day schedule at AAS. Therefore, a few-hour schedule during the busiest time of day is used and solved in approximately 15 minutes. In [15], the first strategy only allows one taxi path, which drastically limits computation time compared to e.g. [2], where the paths can be defined freely by the model. This first strategy can solve the 30-minute time window problems within 2 seconds. The second strategy allows multiple predetermined paths to be chosen; however, the number of paths is fixed to two, in order to limit computation time and because the solutions barely improve if the number of paths is increased above that number. In [41], the problem size is much smaller and the purpose of the paper is to develop a decision support tool, which requires much shorter solve times. The problem discussed in this paper has a solve time for one update of less than one second.

5.2. Genetic algorithms

The other type of model often found in related literature, is the genetic algorithm (GA). This section gives an overview of some of the GAs found and the characteristics that could be useful for this research.

In [50], a GA is used, the NSGA-II algorithm [4], to perform multi-objective optimisation. This optimisation model does not optimise the taxi routes of multiple aircraft, but focuses on optimising the speed profile of an aircraft taxiing along a fixed set of taxiway segments. They have divided each taxiway segment in four different stages: acceleration, constant velocity, braking and fast braking. This creates a speed profile, which depends on certain parameters (e.g. the constant velocity distance, acceleration value etc.). These parameters have been linked using a set of equations, resulting in four independent variables whose optimal values need to be found to solve the optimisation problem. These values are the acceleration in the first stage, the distance of the acceleration stage, the distance of the constant velocity stage and the distance of the fast braking stage. The first step in the algorithm is to initialise the population; this is done by defining chromosomes of four genes, which are the four independent variables. The values of these variables for each chromosome are chosen randomly. Each of these chromosomes can be used to calculate the objective function value and each chromosome is ranked based on this value. After that, the congestion distance is calculated per Pareto front and based on the non-dominant rank and the congestion distance of each chromosome, the best chromosomes are used for the next parent population [26]. This parent population is generated by crossing and varying the best chromosomes from the last iteration and after that, the children are created again. This process repeats until a certain fixed number of iterations is reached.

In [14], two algorithms are used to solve an aircraft ground traffic problem. One of the two is a GA, hence the coverage of this paper in this section. The first algorithm discussed is the A* algorithm, a path search algorithm (PSA). This algorithm simply looks at all of the aircraft individually and determines the best (e.g. fastest, shortest etc.) route for that individual aircraft from the starting node to the end node. It takes into account the paths defined for earlier aircraft, so a node already in use at a certain point in time is not available for the aircraft under investigation. The algorithm looks at all flights one by one and comes up with a complete schedule in the end. Clearly, the order of optimisation is of high importance for this method, as the last aircraft considered will be constrained by all aircraft paths optimised earlier. Therefore, the order is determined based on whether it is an arriving or departing aircraft and the time the aircraft still has left to reach its last node.

Secondly, the paper discusses two GA strategies. Both strategies need all possible paths per aircraft (including the number of the path) and the time the aircraft arrives at the runway or gate if that path is used. The first one requires three numbers per aircraft: the number of the path chosen for that aircraft, the holding point of the aircraft and the time until which the aircraft has to hold. These last two numbers give the aircraft the option to build in a holding point within the path. The second strategy only needs two numbers: one specifying the path chosen and one giving the aircraft a priority number. Afterwards, chromosomes that consist of one path per aircraft in the network are constructed, leading to chromosomes of a length equal to the total number of aircraft that need to be scheduled. The fitness function of this chromosome is determined based on the delay and time spent in lengthened trajectory of all aircraft in the chromosome and/or the number of conflicts in the chromosome. Children are created by picking the best paths from their parents' chromosomes and mutations are applied to a chromosome by changing the paths with the worst local fitness. Furthermore, sharing is applied to avoid getting stuck at a local optimum. Sharing is the process of scaling the fitness function of chromosomes based on their proximity to other solutions. In this way, a solution far away from other solutions is favoured over solutions in a very dense solution space [49].

In [23], a GA with chromosomes that hold a string of node numbers that define the paths of the aircraft is used. Each node in the network has a number and each path belonging to a specific aircraft is separated from the other paths defined in the chromosome by a 0. The chromosomes are initialised by defining a set of feasible routes from start point to end point for each aircraft and randomly picking one of these for each aircraft in the chromosome. Children are created by using multi-point crossover of the parents' chromosomes: the chromosomes of the parents are compared, all genes (nodes) in the chromosome that are the same are kept constant and the sets of different genes in between the identical genes are switched alternately. The fitness of the chromosomes is calculated by using the path length and the extended path lengths in order to avoid conflicts with other aircraft.

In [24], a similar approach to the one presented in [14] is used: a set of possible routes for each aircraft to get from the starting node to the end node is defined using a shortest path algorithm. The chromosomes consist of one number, pertaining to one of the predetermined routes, per aircraft. In this way, cross-over can only switch one feasible route for another, whereas switching nodes leads to a lot of infeasible paths. The chromosomes also hold a second row, which keeps track of the delay of the chosen route for each aircraft compared to their optimal route. The fitness function for the chromosome takes into account the total taxi time, total delay and total number of conflicts in the network; the latter is penalised heavily to ensure no conflicts in the optimal solution. Mutations are performed in two ways: randomly and with a bias towards decreasing delays. Furthermore, reinsertion is used; this is a technique that replaces the parents with the lowest fitness by the children with the highest fitness, instead of just using the children as parents to the next generation. This is especially efficient for this application, as children are very likely to have conflicts within their solution due to the complexity of the taxi network.

5.3. Simulation

Besides the optimisation techniques discussed in sections 5.1 and 5.2, simulation is another way to analyse taxi operations. Simulation is not a method that gives the user the optimal solution to a problem, but it is a way to find out what the practical implications of certain rules or decisions in a system are. This is especially useful if one wants to test the behaviour of a system under different circumstances, e.g. by changing the initial conditions or introducing randomness. The papers discussed in this section use simulation as an aid in the process of optimising taxi operations, but the optimisation itself is performed using different techniques.

In both [29] and [34], the NASA Spot and Runway Departure Advisor (SARDA) tool is built upon. This tool is used to "assists airport ramp controllers to make gate push-back decisions and improve the overall efficiency of airport surface traffic" [29]. The goal in [29] is to improve the SARDA capabilities by using Linear Optimised Sequencing (LINOS) to predict taxi times of aircraft before push-back. This is an extra source of information for the controller who needs to decide on the push-back time of aircraft. LINOS makes these taxi time predictions by making use of fast-time simulations of the taxi route of the aircraft to the gate. LINOS runs these simulations multiple times to take into account uncertainties and records the total taxi time, possible conflicts and congestion at the airport. It aggregates the results and predicts a certain taxi time for a specific route that is proposed by SARDA. The LINOS model is tested with simulation data and compared to

four machine learning techniques in order to get an idea of the accuracy of LINOS.
Similarly, in [34], the aim is to integrate the DLR Taxi Routing for Aircraft: Creation and Controlling for push-back optimisation (TRACC_PB) and NASA SARDA tool in order to improve Target Movement Area entry Time (TMAT) compliance, which is the time the aircraft enters the taxiway to start taxiing to the gate. TRACC specifically focuses on apron operations, whereas SARDA looks at the entire taxi procedure and runway scheduling. The NASA simulation tool 'Surface Operations Simulator and Scheduler' (SOSS) is used as a link between SARDA and TRACC, which can best be visualised by figure 5.1. SOSS receives the TMAT from SARDA and sends it to TRACC_PB together with the Scheduled Off-Block Time (SOBT) and Target Movement area Exit Time (TMET). SOSS simulates all real-time aircraft movements and also sends this information to SARDA and TRACC_PB. TRACC_PB uses the information it receives from SOSS to define optimal push-back times, in figure 5.1 shown as Target Startup Approval Time (TSAT), and a speed profile (4D trajectory) of the route it needs to taxi in the apron. If changes in TMAT and TMET, the time arriving aircraft enter the apron, are necessary, this information is sent to SOSS as well.

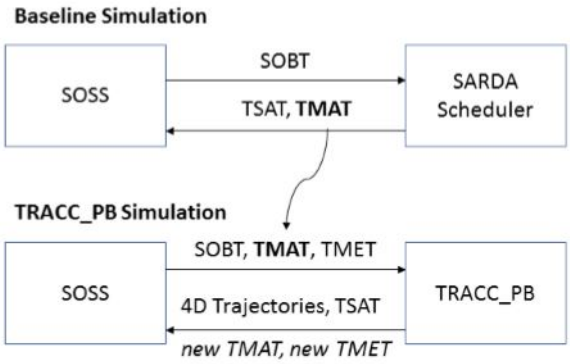

Figure 5.1: Relation between SARDA, SOSS and TRACC_PB [34]

Lastly, in [46], an analysis of the feasibility of ET at AAS and Rotterdam/The Hague Airport is presented. Simulation is used in the research stage in which preparations are made for the actual MILP optimisation of the vehicle routing problem. This paper first defines the performance characteristics of the aircraft and electric towing vehicles in terms of speed profiles (acceleration, constant velocity and deceleration), power demand and emissions. Three possible taxi situations are modelled: aircraft taxiing conventionally, ET vehicle towing aircraft and unloaded ET vehicle. Agent-based simulation is used to simulate the movements of the three situations between all nodes in the network. As a result, the travel duration, energy required and fuel consumption for each link between two nodes in the network is known for the three taxi situations. This is then used as a source of information for the vehicle routing problem solved later on in the paper.

5.4. Assignment problems

Unlike the topics discussed in the earlier sections of this chapter, an assignment problem is not an optimisation (or simulation) technique. It is merely one of the types of problems one can encounter in the world of optimisation problems. However, assignment problems are encountered very often in the context of airport ground operations and is thus interesting to cover separately in this chapter. Two papers solving an assignment problem and their approaches used are discussed in this section, as this might come in useful in the next stages of this research. It needs to be noted that the objective functions and constraints are formulated as MILP model.

In [36], a MILP model to assign electric aircraft to missions (return flights from a base airport to another airport) is designed. The optimisation is split into two parts: the first part assigns the electric aircraft to the missions taking into account constraints due to battery levels and turn-around time. It decides when to charge batteries and when to swap for a new one based on their related duration and cost. The second part of the optimisation has, given the choices made in the first optimisation, focused on distributing charged or spare batteries as efficiently as possible and consequently determining how many spare batteries are needed. In the first part of the optimisation, the author of [36] not only determines the optimal assignment of aircraft

to the missions, but also determines the number of aircraft required to fulfill all missions in the most economically beneficial way. The number of required vehicles is determined as follows: the model is run with a certain low starting number of aircraft available; this is set by the user. If this number is insufficient to cover all missions, the model assigns a high penalty for not fulfilling all missions. Therefore, if the objective function gives an answer in the order of magnitude of that penalty, the model must be run again with an extra aircraft. This can be repeated until the order of magnitude of the objective function drops well below the order of magnitude of the penalty. For the second optimisation, the number of batteries required for battery swaps and the number of available batteries (after recharging) is recorded for every time step. The difference between these numbers gives the number of spare batteries required at any point in time. The total required amount of spare batteries in the system equals the maximum required number of spare batteries reached within the model time horizon. Furthermore, the number of charging stations needs to be set by the user. The model gives an infeasible solution if the number of charging stations is too low, in which case the user needs to increase it and rerun the model.
This paper gives a new insight into the way part of this thesis' modelling can be approached. The above-mentioned papers focus on defining a route for each aircraft, whereas the paper discussed in this paragraph focuses on assigning an aircraft to a fixed mission. The information relevant for the aircraft assignment is available (departure time, arrival time and required energy level) and based on these factors, aircraft are assigned to missions. This might be a useful approach to assign external ET vehicles to aircraft.

In [7], the over-constrained Airport Gate Assignment Problem (AGAP) is solved, while trying to minimise the number of aircraft not assigned to a gate and the passenger walking distance. Two extra 'gates' are added to the total number of gates, one representing the airport entrance/exit for passengers leaving and coming to the airport and one 'apron gate' to assign aircraft to that cannot be assigned to a gate. The optimisation approach used is 'a hybrid simulated annealing with tabu search approach'. Firstly, a greedy method is used that sorts all flights from earliest departure time to latest departure time. Each gate has a variable that indicates the time it is available for a new flight, which is set to -1 for each gate at the beginning. Each flight is assigned to the gate of which this variable is closest to but lower than the flight's arrival time. If no gates are available at the flight's time of arrival, it is assigned to the apron gate. The greedy method is performed once at the beginning of the optimisation process and creates the starting set of gate assignments for the rest of the optimisation.
The optimisation alters the initial greedy solution in three different ways, called neighbourhood moves, which are an adaptation of the neighbourhood moves introduced in [47]. The first option is the 'insert move' which assigns an aircraft to a different gate than its current assignment. The second option is the 'interval exchange move' and exchanges two gate assignments between a certain start and end time. The number of flights assigned to the two gates does not have to be equal (e.g. two flights can be exchanged for three flights, as long as they fall within the same time interval), as long as the exchange move does not cut flights in half. The third option is the 'apron exchange move', which exchanges one flight assigned to a gate with one flight assigned to the apron gate. At the beginning, an annealing temperature T is set. Then, a random neighbourhood move is generated and the change in objective function, if this move would be performed, is calculated. Based on this value and the annealing temperature, a probability of performing this move is calculated, which is used to determine whether this move will be performed or not. The parameters 'unaccepted' and 'unimproved' are updated, based on whether the move is performed and whether the overall objective function is improved or not. Based on these parameters, the annealing temperature is updated and, if the termination condition has not been satisfied, the process is started again.

5.5. Concluding remarks

Sections 5.1, 5.2, 5.3 and 5.4 give an explanation of the optimisation models used in relevant literature. Tables 5.1 and 5.2 give a summary of each of the most interesting, relevant and unique aspects of each of these papers. These characteristics will be used to determine the most suitable optimisation model for his thesis' research.

As mentioned in the introduction of section 5.3, simulation is mainly used as a tool to accommodate optimisation or as a way to visualise real-time situations or optimisation results. In [29], simulation i used as a way to deal with the uncertainty related to aircraft taxiing. It takes into account the possible factors that could change after the decision to start push-back is made by the controller. However, this is mainly relevant for

making real-time decisions and less to make decisions on a strategic level, e.g. to look at the influence of ET on a larger scale. In [34], simulation is a way of providing information to the optimisation tools in real-time. It does not deal with uncertainty like in [29], but it is still unsuitable for strategic planning on a larger scale. Lastly, in [46], simulation is used in a comparable challenge to the one discussed in this thesis. Although it is used to generate information instead of performing optimisation, it is an interesting way of using agent-based modelling in a similar ET-related situation. However, in terms of optimisation methods, it can be concluded that simulation is not the most suitable approach for this thesis.

The MILP models and GAs discussed in this chapter are more fitting options to create an optimisation model. From a practical point of view, a RH type of optimisation seems to be suitable given the problem size of a one-day taxi schedule at a hub airport. These strategies are often used in the MILP models discussed in this chapter and therefore MILP seems like a logical candidate for further research.
However, in both [12] and [27], it is concluded that GAs are faster than MILP models, but MILP models give better solutions. Naturally, a more optimal solution is preferred in a complex problem like taxiway scheduling, but, as mentioned above, the execution time is also an important factor. Therefore, a combination between the more accurate MILP model and the faster RH technique seems to be a promising way to design the optimisation model.

Paper	Model type	Characteristics
[44]	MILP	• Each aircraft's route is fixed, only the timing of the route is optimised • Focus on sequencing aircraft at each node with sufficient separation time between them • Holding points are modelled by adding nodes with distance equal to zero • Three different rolling window strategies are used
[2]	MILP	• RH strategy with virtual nodes for aircraft that overlap multiple execution windows • Pre-defined matrices that define connections, distances and shortest paths between nodes • Iterative approach of adding conflict constraints once they occur • Departure sequence is enforced and planning window is extended for this purpose only
[40]	MILP	• The routes for all aircraft are generated before optimisation • A subset of routes is used in the optimisation model, based on path length and difference factor • Simulation tool has been developed for visualisation of network
[15]	MILP	• The first strategy used fixes aircraft routes and optimises the timing of this route • The second strategy allows the model to choose from a predefined set of routes and optimises the timing of the chosen route • Time windows of 30 minutes are used to limit computation time
[41]	MILP	• Model that updates every 10 seconds based on current aircraft positions • Freezing window is used to avoid changing the entire schedule every update • User can set maximum allowed delay for an individual aircraft
[50]	GA	• Focus on optimising speed profile of aircraft, not on optimising a schedule • Uses NSGA-II algorithm with chromosomes holding four genes which are the independent to-be-optimised variables • Children population is picked based on non-dominant rank and congestion distance of parents
[14]	PSA	• Determines shortest path for each aircraft with constraints imposed by previous aircraft's paths • Order of optimisation is determined based on whether an aircraft arrives or departs and on the time the aircraft has left to reach its last node
[14]	GA	• The routes for all aircraft are generated before optimisation • Chromosomes with one path per aircraft are randomly generated • Children inherit best path for each aircraft from their parents based on local fitness function • Fitness functions are scaled based on their proximity to other solutions in order to escape local optima
[23]	GA	• Each chromosome holds the entire path of each aircraft, separated by a 0 • The paths consist of a set of consecutive nodes and a set of feasible paths is created for each aircraft before optimisation • Children are created by multi-point crossover, the matching nodes between parents are kept constant
[24]	GA	• Similar chromosome to [14] but with second row that holds delay per path compared to their optimal route • During mutation, entire paths are switched instead of nodes within paths • Mutations are done in two ways: randomly and based on the delay of a certain path • Children with high fitness value replace parents with low fitness value

Table 5.1: Overview of literature optimisation models

Paper	Model type	Characteristics
[29]	Simulation	• Predicts taxi times of a single taxi event from gate to runway before push-back • Takes into account uncertainty of taxiing after push-back • Used as tool to assist controllers in making decisions on push-back time of aircraft
[34]	Simulation	• Simulation of real-time aircraft movements on the ground is used as information source for optimisation tool • Tool is used to improve TMAT compliance
[46]	Simulation	• Simulation is used as preparation for MILP optimisation • Simulation (agent-based modelling) is used to define travel duration, energy required and fuel consumption for each link in network • Performance characteristics of vehicles and distances between nodes are input to the simulation
[36]	Assignment Problem	• Assignment of aircraft to fixed missions, not optimisation of route/path of mission • Separate algorithms for assigning vehicles to task and battery management • Iterative process to determine number of aircraft and charging stations
[7]	Assignment Problem	• 'A hybrid simulated annealing with tabu search approach' is used to solve an over-constrained AGAP while minimising ungated flights and passenger walking time • A greedy method is used to get an initial flight-to-gate assignments solution • Alterations to the assignment are generated based on the neighbourhood search method • Alterations are accepted based on change in objective function, annealing temperature and randomness • Progress is recorded and process is stopped once termination condition is satisfied

Table 5.2: Overview of literature optimisation models

6

Research framework

This chapter gives an overview of the research that is going to be performed during this thesis. Firstly, a description of difficulties in the current situation of ET is given by using the knowledge gained in the previous chapters of this literature review. Secondly, the three papers with the closest links to this research are discussed with an eye on the research gap this paper wants to fill. Thirdly, the research questions for this thesis are determined based on the literature gap. After that, the the research objective and its sub-goals are defined based on the research questions and related literature. Lastly, the boundaries of this research are given.

6.1. Problem statement

As described in chapter 1, the collaboration of Dutch aviation parties[1] and the European Commission[2] have set their targets to electrify taxi operations for the years 2030 and 2050 respectively . A number of companies have taken up the challenge of designing systems to enable ET operations at airports; however, only one of the companies, TaxiBot, is currently operational on a (very limited) regular basis (see section 2.3). The seemingly slow adoption of ETS in commercial aviation can be explained from a combined economic and operational perspective.

First of all, the aviation industry is a difficult industry to bring about substantial change; safety standards are extremely high and every new product, procedure or design feature needs to be thoroughly tested and certified by the authorities. This leads to high development costs, which is a major issue in an industry with strong competition and low margins. Therefore, relevant aviation parties (airlines, ground operators, airports) want to know what to expect if they acquire an ETS. However, this is where the problem of limited (certified) suppliers comes in: limited information on ET operations is available. This leads to a difficult situation with, on the one hand, airports having to adapt to new sustainable ambitions and regulations and, on the other hand, airports being hesitant in making any decisions on acquiring and adopting ETS.

Current research regarding ET has mainly focused on analysing typical conventional taxi procedures and comparing them to ET procedures (section 3.1). Based on these analyses, conclusions on the potential fuel savings for certain types of flights have been drawn, often predicting savings in the order of magnitude of 1-4%. These numbers give a good impression of the economic benefits for airlines in terms of fuel, but forget to address the possible operational consequences of taxiing electrically. For example, 3% fuel savings are not much of a benefit if half of the flights are delayed due to subpar performance of the ETS.
On the other hand, extensive research has been done on optimising taxi operations; this has been analysed in chapter 5 and summarised in tables 5.1 and 5.2. However, these research papers do not look at the effects of ET on taxi operations (except for the papers discussed in section 6.2). Therefore, this thesis research will aim to fill the gap between research on ETS and airport ground operations by developing a model that optimises ET operations at AAS, focusing on minimal impact on current ground operations and flight schedules and taking into account performance characteristics and additional airport surface movements related to ET.

[1] Ontwerpakkoord Duurzame Luchtvaart, published: 12th of February 2019
[2] European Commission, Flightpath 2050 Europe's Vision for Aviation, published: 2011

6.2. Similar research

This section focuses on research that has most similarities with this thesis' topic. This section serves as a means to identify research questions and a research scope that truly add something new to the current research field. The three papers discussed here, each combine operations research with electric taxiing or a similar concept. The information presented in this chapter does not focus on optimisation techniques, but mainly on the situations modelled and the assumptions made by each of the papers.

First of all, in [42], the effects of ET on airport operations are analysed, using AAS as case study. This paper assumes all of the electric taxiing aircraft to use on-board ETS. The fleet mix used consists of 50% electrically and 50% conventionally taxiing aircraft. The goal of the paper is to find out what the minimum velocity of electrically taxiing aircraft needs to be to avoid delays caused by ET. In this paper, the only difference between electrically and conventionally taxiing aircraft is that the electrically taxiing aircraft have a lower maximum velocity. Since no ET vehicles are used, no additional airport surface movements need to be modelled.

Secondly, in [16], research on automated guided vehicles (AGVs) is presented, again with AAS used as case study. Taxibot is used as reference vehicle to model the AGVs. Operations-wise, looking at dispatch towing from an ET or AGV perspective is the same; the only difference is the fact that ET assumes the pilot to perform the taxiing and an operator to be on-board the towing vehicle for emergencies and driving back the towing vehicle. Furthermore, the AGVs in this paper only perform taxi-out procedures and charging of AGVs is not taken into account. The taxi network used consists of taxiways and service roads, which only lead to the runway ends relevant for the case study. Each runway entrance has one holding area to which aircraft are towed and one runway exit where aircraft enter the taxiway network after landing. This paper uses an objective function that minimises costs for airlines based on the costs of taxiing, holding while in the process of taxiing, delay and depreciation of AGVs. The goal of the research is not to perform all taxiing operations by means of AGVs, but to find an economically feasible way of incorporating them in ground operations.

Finally, in [46], the focus lies on feasibility of ET operations by consecutively designing a dedicated electric towing vehicle, determining fuel consumption, emissions and taxi duration for all links in the taxi network and then solving a vehicle routing problem to minimise fuel consumption. The optimisation does not force all flights to be towed, but aims to find an optimal assignment of towing vehicles to aircraft while fixing the maximum number of towing vehicles that can be used. An important factor to note, is that traffic is not taken into account in the model. The vehicle routing problem picks aircraft taxiing routes based on its individual fuel consumption and to be able to optimally use the electric towing vehicles. It does not take into account conflicts between taxiing aircraft or towing vehicles. Also, delay of aircraft due to ET is not taken into account in the model. This paper provides an analysis of the potential of ET for reductions in fuel consumption, emissions and energy consumption, but focuses less on the feasibility from an operational scheduling perspective.

6.3. Research questions

Based on the literature gap described in section 6.1 and the papers discussed in section 6.2, the following main research question has been formulated:

How can electric taxiing (ET) procedures be modelled at a hub airport and what operational implications would it have?

This question can be divided in four sub-questions. These sub-questions are divided into a set of their own sub-questions.

1. How can electrically taxiing aircraft be modelled at a hub airport?
    (a) What is the influence of ET on taxi performance of aircraft?
    (b) Which optimisation technique will be used to define the taxi routes?
    (c) How are conflicts between taxiing aircraft avoided?
    (d) How is ensured aircraft depart and arrive at the desired location in the taxi network?
    (e) How can the lay-out of a hub airport be modelled?

2. What is the influence of ET on aircraft departure and in-block times for one day of operations at a hub airport?
    (a) How will the original departure and in-block times be determined for one day of operations at a hub airport?
    (b) How will deviations from these original departure and in-block times be measured?
    (c) How will these deviations be minimised?
3. How can ET vehicle movements be modelled at a hub airport?
    (a) What are the performance characteristics of the ET vehicles used?
    (b) What are the operational constraints ET vehicles have to adhere to at a hub airport?
    (c) What kind of optimisation technique will be used to define ET vehicle routes?
    (d) At which locations can ET vehicles recharge their batteries?
4. How many ET vehicles are required to cover all taxi operations at a hub airport?
    (a) Which taxi operations need to be performed by the ET vehicles and when?
    (b) How will ET vehicles be assigned to these taxi operations?

6.4. Research objective

The research objective of this thesis is:

"To accurately model electric taxiing (ET) operations at a hub airport by optimising the airport ground surface movements of electrically taxiing aircraft and the ET vehicles involved, to determine the influence of ET on on-time performance of a hub airport by analysing the deviations from scheduled departure and in-block times of aircraft due to ET and to determine the ET vehicle fleet size required at a hub airport by optimally assigning ET vehicles to all scheduled towing tasks."

This thesis will be the first to fully incorporate ET in airport operations. As mentioned in section 6.1, research has always focused on either fuel savings due to ET or on conventional taxiing. The only papers found that do incorporate ET in ground operations optimisation are mentioned in section 6.2. However, this thesis research will explore the full range of ET operations at AAS. Firstly, a model will be developed that optimises the taxi operations at AAS, taking into account ET performance characteristics and taxi-in as well as taxi-out operations. The external ETS operations will be further investigated and an assignment model will be written that assigns the ET vehicles to their tasks in the most efficient way, assuming charging station locations where ET vehicles can charge their batteries. These two problems will be solved separately; however, the output of the first optimisation model will be used as an input to the second. Once these two sub-goals have been accomplished, the research objective will be fulfilled as well.

6.5. Research scope

The previous sections of this chapter clearly outline that the focus of this research will be on the operational side of ET. Like any research, limitations in resources (time, man power, information etc.) require clear boundaries to be defined beforehand. The following list points out these boundaries.

- This research does not focus on the technical (e.g. mechanical, electrical) aspects of ETS. Part of the literature study outlines the ETS that are currently out there and describes their characteristics; however, afterwards only the relevant practical information related to ETS is used for operations research at AAS. In later stages of the research, more in-depth analysis of a technical aspects of ETS might be needed, but this will only be done to obtain the practical information needed to model the operations properly.
- In this research, apron movements (push-back and taxiing to the start of the taxiway) are not modelled. It is assumed that a standard push-back and tow-to-taxiway manoeuvre using an electric towing vehicle takes as much time as with a conventional push-back vehicle. A standard period of time is added to the

moment in time an aircraft gets clearance for push-back to determine the time the aircraft arrives at the first node of the network. This first node will be fixed for each pier and its gates based on the apron lay-out.

- The flight schedule is deterministic: aircraft landing and departure times do not deviate from their scheduled time or their actual landing time given in the flight data set. This can be assumed since the research assesses performance of ET on AAS at a strategic level and not on developing a tool that deals with sudden changes in the schedule.
- Velocity of aircraft and towing vehicles is assumed to be constant and acceleration is not modelled. Therefore, no speed profiles of aircraft on taxiway segments are researched or defined.
- Departure sequencing is not part of this optimisation model. Departure sequencing is the process of forcing the departing aircraft to depart in a certain order. This does not mean, however, that excessive delay of individual aircraft will not be prevented or discouraged in some way or another.
- The slope of the taxiways is not taken into account in the analysis of energy requirements.

7

Use case

This chapters gives an overview of the real-life situation that is going to be modelled and the assumptions that are made to facilitate this. The research objective and questions described in chapter 6 are used as guidance to determine which information is relevant and which is not. The first section focuses on ETS and the second section defines a list of additional assumptions required for further research. After that, a basic analysis of battery performance and required energy for taxiing is provided. Then, the taxi-in and taxi-out operations for ET are defined. Lastly, the flight schedule and airport model specific to AAS are discussed.

7.1. Electric taxiing

In this section, a choice regarding the performance characteristics of ET is made. Table 2.1 and the accompanying information from section 2.3 is used to make an informed decision. General remarks regarding the use of an external or on-board system are made and a choice regarding this trade-off is presented.

7.1.1. External vs. on-board

ET is not a frequently used procedure in aviation nowadays. The number of relevant state-of-the-art ETS is limited and their performance characteristics are often worse than for standard taxi procedures. However, an important aspect of the context of this thesis is the draft agreement of Dutch aviation parties, defining the ambition to use ET as a standard procedure from 2030 onwards. The focus of this research is on the operational impact ET would have on AAS. Therefore, assumptions on the performance characteristics of ET aircraft will be made in this section in order to facilitate the operational research in this thesis.
These assumption will be as realistic as possible, but are also going to be quite optimistic. These optimistic estimates are justifiable because of the following three reasons. First of all, ET procedures need to be in place in the Netherlands in roughly 10 years time from now and in roughly 30 years from now by European Commission standards. Considering the limited ETS currently in operations and the fact that this paper is (one of) the first to research the operational aspects of ET, the ETS companies are likely to have quite a few years left until airports start implementing ET. Therefore, ETS performance is going to improve significantly before implementation and this research's results are expected to stay accurate for longer with more optimistic performance estimates.
Secondly, the information on ETS is quite limited and press releases regarding new developments in ETS have been very scarce in the last couple of years. The companies from table 2.1 do not provide much information on their websites and the figures found are often a few years old. Therefore, on top of the abovementioned development years still to come, the ETS are likely to have matured in the last 2-5 years outside the public eye.
Finally, this research focuses on developing an optimisation model. The performance characteristics are inputs to that model and can be changed easily. If the estimates turn out to be slightly over-optimistic, the input parameters can be changed and the model can still be used. Although the performance characteristics should not be chosen carelessly, this notion does put the choice of performance characteristics into perspective.
The next two sections separately analyse the external and on-board ETS options and draw conclusions on their performance and applicability within their category. After that, the conclusion regarding usage of external and/or on-board ETS in this research is drawn.

External ETS

The analysis of external ETS consists of two options: EP vehicles and TaxiBot. The big advantage of EP vehicles in the context of this research, is the fact that they are fully electric. However, EP vehicles only perform push-back and are therefore not a viable alternative to conventional taxiing. TaxiBot is already in service and does perform the full taxi operation from gate to runway (and vice versa). The reported velocity TaxiBot can reach for narrow-body aircraft is 23 knots (≈ 11.8 m/s). Furthermore, although there are no reported cases of airports or airlines using this version, the most powerful TaxiBot can reach a taxi velocity of 20 knots (≈ 10.3 m/s) while towing a fully loaded Airbus A380 [20]. According to the information from [42], a taxi velocity of 10 m/s is required to make sure ET aircraft do not cause delay for other aircraft. However, this paper assumes a mix of conventionally taxiing and ET aircraft; therefore, these velocity differences will play a different role for a model with 100% ET aircraft.

On-board ETS

Table 2.1 holds three on-board ETS systems. None of them are in operation and it is difficult to assess when they will be. A few years ago WheelTug expected to be in operation by now, DLR has not published any information on their expected time to market and the information Safran published dates from before Airbus suspended their collaboration. Furthermore, it can be seen that the taxi velocities vary greatly between the three on-board ETS, 9 to 20 knots. In the light of the abovementioned choice to go with a realistic but optimistic estimate of the performance characteristics, the 20 knots taxi velocity is adopted for the on-board ETS. Furthermore, DLR and Safran set 78 tonnes as the maximum towing weight of the ETS, whereas WheelTug is designed for the B737 family with a highest Maximum Takeoff Weight (MTOW) of about 85 tonnes for the B737-900ER. Due to the proximity of these two maximum towing weight values and the assumption regarding positively estimating performance characteristics, the maximum towing weight of 85 tonnes is used. This MTOW practically limits the on-board ETS to ET for narrow-body aircraft only.

Conclusion

The three available options for this research in terms of ETS are an external ETS (TaxiBot) for narrow-body aircraft with a maximum velocity of 23 knots, an external ETS (TaxiBot) for wide-body aircraft with a maximum velocity of 20 knots and the generic on-board ETS for narrow-body aircraft with a velocity of 20 knots. Clearly, TaxiBot is the best (and only) option for wide-body aircraft. Theoretically, it could also be decided to perform conventional taxiing for wide-body aircraft, but this would defeat the purpose of electrifying all taxi procedures in the near future. Therefore, wide-body aircraft are going to be towed by an external ETS with a maximum velocity of 20 knots.
Secondly, it needs to be decided which system is used for narrow-body aircraft. TaxiBot for narrow-body aircraft is currently operational and is therefore the safer choice in terms of practical feasibility and correctness of performance characteristics. Besides, airlines are unlikely to unanimously decide to install and certify the required ETS equipment on-board their aircraft due to high costs and limited gains. Airports will have a hard time compelling airlines to do so, whereas providing ET vehicles for all aircraft is a responsibility that can be taken on by airports themselves. On the other hand, using external ETS for narrow- and wide-body aircraft puts a large burden on the taxiway network due to the extra airport surface movements. Taking these two factors into account, it is determined that it is more realistic to use external ETS for narrow-body aircraft. Electric towing vehicles are a more realistic alternative in the foreseeable future. Currently, the progress of on-board ETS is limited and leads to too much uncertainty to base results on.

7.2. Assumptions

Based on the decisions made in 7.1.1 and the information gathered in previous chapters, assumptions regarding the situation that is going to be modelled need to be made. This section provides these assumptions, including an explanation of the implications these assumptions have.

First of all, as a result of the conclusion drawn in section 7.1.1, the following remark needs to be made. The characteristics of the electric towing vehicles, velocity per aircraft size, are based on TaxiBot. However, TaxiBot is not a fully-electric taxi system and does not satisfy the requirement to electrify all taxi operations at AAS. Therefore, it assumed that the electric towing vehicles in this research do have a battery on-board that provides enough power to deliver the same performance as TaxiBot. It needs to be determined what the charging time and capacity of these batteries are in order to be able to incorporate these two parameters in

the model.

The next challenge that needs to be addressed is related to engine warm-up and cool-down, an issue already pointed out in section 2.3.1. The ESUTs assumed by literature mentioned in section 2.3.1 vary from two to five minutes, but the consensus seems to be to allow five minutes for engine warm-up. The consensus for engine cool-down is to allow three minutes. The question that arises from the situation regarding engine warm-up and cool-down is: how to incorporate it into ET operations? There are two main ways to address this issue.
The first is to simply perform taxi-out and park the aircraft for five minutes in a designated holding area near the runway threshold before take-off. Similarly, each aircraft has to wait for three minutes after landing until the engines have cooled down. This seems to be quite a straight-forward solution, but unfortunately it has a few negative consequences. First of all, taxi time will increase dramatically. To put this into context, major airlines in the US are reported to have an average taxi-out time of 16.7 minutes and an average taxi-in time of 6.9 minutes [13]. An increase in taxi-out time of five minutes and an increase in taxi-in time of three minutes would lead to respectively a 30% and 43% increase in taxi time. Furthermore, large queues are bound to form near the runway thresholds. This requires a lot of space that might not be available right now and would incur extra airport development costs.
The other option, as mentioned in section 2.3.1, is to turn on the engines when five minutes from the runway entry and turn off the engines after three minutes of taxi-in. The towing vehicle and engines could be providing thrust at the same time and higher taxi velocities could be reached. However, the towing vehicle must be able to handle these speeds and, looking at figure 4.3, it is clear that the velocity will be limited by taxiway speed limits. Engines warming up in idle mode might be able to reach these maximum velocities by themselves, rendering the electric towing vehicle redundant. However, disconnecting towing vehicles in the middle of the taxiway, instead of at a holding area, might not be practical and cause delays. Furthermore, thorough research on the safety implications of turning on engines during ET needs to be performed before implementation.
As mentioned in section 2.3.1, ET for taxi-out procedures of less than five minutes and taxi-in procedures of less than three minutes would be pointless from an emissions point of view, since engine warm-up would produce the same emissions as main engine taxiing would. However, it is interesting to know how the organisations that defined the ambitions for fully electric taxi operations[1] [2] want to deal with these situations. Their aims to perform zero-emission taxiing should not extend to taxi-out below five minutes, since that would only incur delays due to pointless ET and consecutive engine warm-up at a holding area.

Therefore, the engine warm-up and cool-down situation will be modelled as follows. The electric towing vehicle performs push-back for all aircraft. If the optimisation model assigns a route with a taxi time of less than the ESUT (five minutes), the electric towing vehicle detaches at the taxiway, which is the starting node of the route of the aircraft. If the taxi time exceeds the ESUT, the electric towing vehicle performs the entire taxi procedure and detaches at the holding area near the runway end. Similarly, when the aircraft lands and reaches the runway exit, which is the starting node of its taxi route, the electric towing vehicle picks up the aircraft if the planned taxi time is longer than the ECDT (three minutes). If the taxi time is shorter, the aircraft performs its taxi operations using its main engines.
Secondly, the moments in time when engine warm-up and cool-down are performed need to be chosen. As mentioned in section 2.3.1, no literature supports the idea of engine warm-up or cool-down during taxiing with ET vehicles. Therefore, it is assumed that engine warm-up and cool-down takes place at a dedicated holding area near each runway entrance/exit.

Section 2.2 gives an overview of the separation distances used in other papers. It is pointed out that one of the main reasons for separating the aircraft is the influence of jet blast on trailing aircraft. However, since the engines are turned-off while taxiing, this factor does not have to be considered. Furthermore, aircraft using the same taxiway do not necessarily taxi to the same runway. Therefore, the argument that time gains due to shorter separation distances are nullified by minimum time separations between departing aircraft, is not true for all taxiing aircraft. Therefore, the shortest minimum separation distance found in literature, 60 meters, is used for this model.

[1] Ontwerpakkoord Duurzame Luchtvaart, published: 12th of February 2019
[2] European Commission, Flightpath 2050 Europe's Vision for Aviation, published: 2011

A considerable part of the electric vehicle movements will be performed while not towing an aircraft. Logically, the electric towing vehicles are able to drive faster without this extra load. However, this is not a specification provided by the manufacturer of the reference vehicle (TaxiBot). Section 2.2 discusses the prevailing service roads speed limits at AAS and nearby airports and concludes that 8.33 m/s is a realistic speed limit for service roads at AAS. This value is lower than the velocities the loaded ET vehicles can reach, so it is assumed that the ET vehicles will always be travelling at 8.33 m/s on service roads.

7.3. Battery performance

The choices made and assumptions stated in sections 7.1.1 and 7.2 require a basic design of the battery performance of the ET vehicles. As mentioned in the research scope in section 6.5, the focus of this research does not lie on the technical aspects of ET. Therefore, the performance of the batteries and their subsequent charging characteristics are mainly based on previous literature.

First of all, in [46], three conceptual ET vehicles have been designed. Each of the three ET vehicles tows aircraft from a certain weight class. Furthermore, a sensitivity analysis has been performed with a set of vehicles lighter and a set of vehicles heavier than the first set. Since the author concludes that the battery capacity of the first set of ET vehicles is over-dimensioned, it is chosen to use the lightest version of the ET vehicles presented in [46] in this research. The ET vehicles specifications are shown in figure 7.1. Since three different ET vehicles classes are used, instead of the two classes (NB and WB) mentioned in section 7.1.1, the WB aircraft class will be split into WB standard aircraft and WB heavy aircraft, based on the same criteria as used in [46]. Maximum taxi velocity for the NB and WB categories as defined in section 7.1.1 does not change.

	Medium	Heavy	Super Heavy
Total mass $[kg]$	15,000	35,000	50,000
Battery mass $[kg]$	3,250	10,500	16,000
Battery volume $[m^3]$	1.77	5.73	8.73
Battery capacity $[kWh]$	390	1,260	1,920
Max. power $[kW]$	650	2,100	3,200
Drive train $[-]$	4x4	6x6	6x6

Figure 7.1: Conceptual ET vehicles for different aircraft weight classes [46]

Secondly, the energy required to tow an aircraft from A to B needs to be determined. In [46], it is indicated that equation 7.1 can be used to calculate the energy consumption for the constant velocity taxi phase, which, according to the scope presented in section 6.5, is applicable to the taxi procedure in this research. This equation calculates the rolling resistance of an aircraft. According to the information found in [46], the aerodynamic drag can be ignored for the low velocities at which aircraft taxi.

$$P_{req} = \mu_g \cdot (N_{ac} + N_t) \cdot V \tag{7.1}$$

Furthermore, the research scope also states that taxiway slope is not taken into account, which simplifies equation 7.1 to equation 7.2, since the slope is assumed to be 0. This means that the weights per aircraft type need to be determined and used to calculate the required power for a certain taxi route. To determine the required power for an unloaded ET vehicle, the weight of the aircraft simply needs to be set to zero.

$$P_{req} = \mu_g \cdot (W_{ac} + W_t) \cdot V \tag{7.2}$$

According to information from [3], the Coefficient of Rolling Resistance (CRR) of taxiing aircraft can be estimated by using equation 7.3. The CRR depends on the velocity of the taxiing aircraft and will therefore differ per taxiway segment and aircraft type. v_0 and μ_0 are defined in [3] and equal 80 knots and 0.01 respectively. Therefore, a taxiing velocity of for example 20 knots leads to a CRR of 0.0125. Although equation 7.3 is meant for aircraft, it will also be used to determine μ_g for unloaded ET vehicles.

$$\mu_g(v) = \mu_0 \left(1 + \frac{v}{v_0}\right) \tag{7.3}$$

The next step is to define the charging time required to charge the batteries of the ET vehicles from a certain state of charge (SOC) to a new one. The charging time can be determined by defining the charging power and dividing the energy to-be-charged by it, shown in equation 7.4, which is an adapted version of the charging time equation from [9]. Subscripts 1 and 2 denote the situation before and after charging the battery.

$$t_{charge} = \frac{E_2 - E_1}{P_C} \tag{7.4}$$

In [36], the charging power is determined using equation 7.4. P_{max} can be found in the 'Max. power [kW]' row of the table in figure 7.1. The C-rates C_{MAX} and C_{NOM} are assumed to be 1 and 6 respectively in [36], which are "a measure of the rate at which a battery charges/discharges relative to its maximum capacity" [36]. Since the batteries used for the conceptual vehicles from 7.1 are Lithium-based as well, these C-rates are also used in this research. Lastly, in [36], a minimum SOC of 20% is used as safety margin for emergencies; so the minimum SOC during nominal operations is set to 20% of the maximum capacity of each ET vehicle.

$$P_C = \frac{P_D^{MAX}}{\frac{C_{MAX}}{C_{NOM}}} \tag{7.5}$$

7.4. Operations

This section gives an overview of the operations performed by the aircraft and the towing vehicles. It gives a schematic overview of the actions that need to be performed and the duration of each standard action. In this way, all actions that require time are taken into account in scheduling the aircraft and towing vehicles using the optimisation model. This makes sure the results are realistic and practically feasible. The figures also show when the engines are turned on and off. The light-blue parts of the tables denote active aircraft, electric towing vehicle or engines and the grey parts indicate inactivity.

7.4.1. Taxi-in

Figure 7.2 shows the actions that need to be performed during a taxi-in procedure of longer than three minutes. This means that the ET vehicle is used to pick-up the aircraft and the ECDT is reached before the end of the taxi procedure. It is assumed that the time between touchdown and the aircraft reaching the runway exit is 30 seconds; during this time, the engines are not cooling down yet. At the time, the aircraft reaches the runway exit, the pilot puts the engines in idle mode and performs cool-down for three minutes. After engine cool-down, the electric towing vehicle needs to be ready to connect to the aircraft. This is assumed to take 60 seconds, as the post processing part (which includes detaching the electric towing vehicle) takes 60 seconds as well [6]. After that, the aircraft is towed to its assigned gate and post-processing is performed. After post-processing, the electric towing vehicle is available for a new assignment or charging action again.

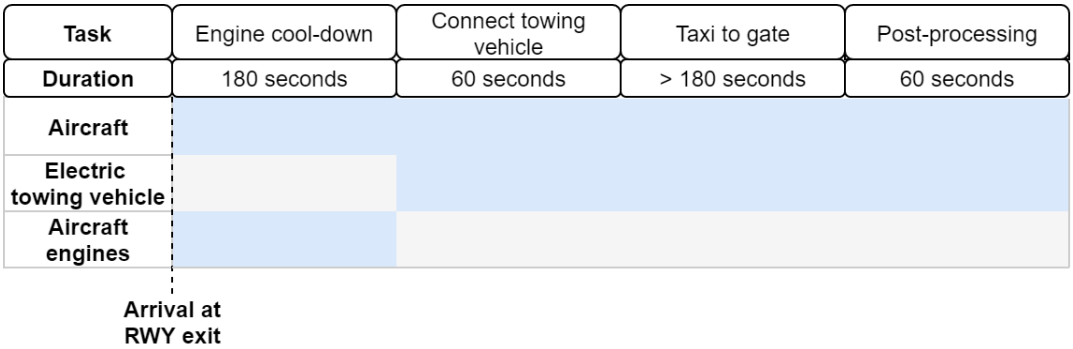

Figure 7.2: Overview of taxi-in procedure with taxi time longer than three minutes

Figure 7.3 shows the overview of the actions for a taxi-in operation of less than three minutes. In this situation, conventional taxiing is performed since the ECDT is longer than the taxi time.

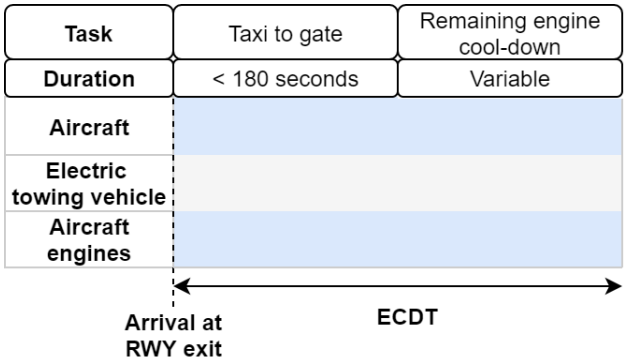

Figure 7.3: Overview of taxi-in procedure with taxi time shorter than three minutes

7.4.2. Taxi-out

The taxi-out procedure for taxi operations longer than the ESUT is given in figure 7.4. The connect towing vehicle block only highlights the electric towing vehicle as active even though the aircraft is also required to be able to attach the electric towing vehicle. This operation is modelled like this since the connection of the towing vehicle to the aircraft can happen before the Earliest Off-Block Time (EOBT) defined in the flight schedule and therefore does not 'cost' the aircraft any time. However, the electric towing vehicle does have to arrive 60 seconds before the OBT, which is why it needs to be incorporated in its schedule. Push-back of the aircraft takes 118 seconds [6] and the post-processing again takes 60 seconds. Once the electric towing vehicle detaches from the aircraft, it is free to be scheduled again; it can drive back to the apron for a new taxi-out procedure, drive directly to a runway exit for taxi-in or go to a charging station to replace its batteries. The aircraft still needs to perform engine warm-up before it is ready for take-off.

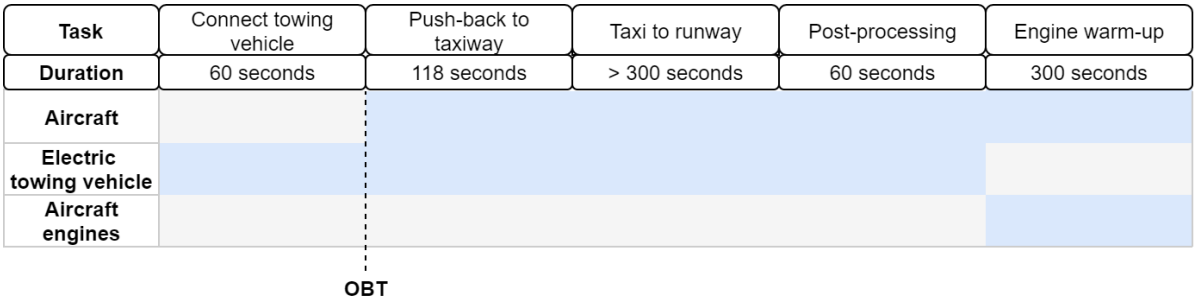

Figure 7.4: Overview of taxi-out procedure with taxi time longer than five minutes

Figure 7.5 shows the taxi procedure for operations shorter than the ESUT. This means that the electric towing vehicle will simply act like an EP vehicle: it connects to the aircraft, performs push-back and disconnects. After that, the aircraft taxis to the gate conventionally, while at the same time warming up its engines.

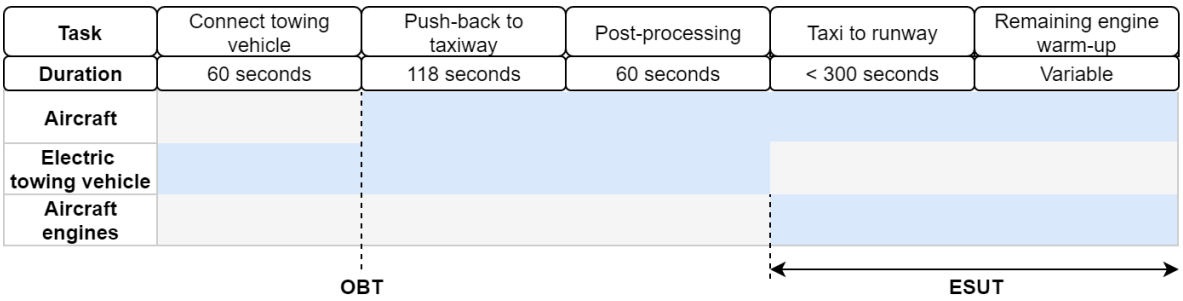

Figure 7.5: Overview of taxi-out procedure with taxi time shorter than five minutes

7.5. Flight schedule

This section gives an overview of the data used in this research, based on the information given in section 4.3.2. The assumption, made in section 7.2, to add the ESUT and ECDT to the total taxiing time instead of performing engine warm-up and cool-down during taxiing, makes for a more complicated taxi schedule. As pointed out, the ESUT and ECDT are expected to cause serious delays compared to the original (conventional) taxi schedules. Therefore, it is decided to use two data sets for analysis of the influence of ET: one relatively quiet and one relatively busy day at AAS. The reason for this choice, is that the engine warm-up and cool-down are likely to have less of an effect on quiet days than on busy days. Therefore, it is interesting to see what the difference in terms of ET performance is for both schedules. Besides, airports are unlikely to start implementing ET on the busiest day of the year right away. This makes the analysis of a relatively quiet day more interesting from an implementation perspective, whereas a busy day might be more interesting in the long run. The flight data that is likely to be used for the analysis is the same as explained in section 4.3.2. Table 7.1 shows a sample of what the flight data looks like. The quiet day chosen is the 14th of December 2019 (day 348) and the busy day chosen is the 2nd of October 2019 (day 275). They are both randomly picked from a list of the ten quietest and busiest days at AAS in the year 2019 in terms of number of flights departing and arriving. These might not necessarily be the quietest and busiest days in terms of passengers.

date_SCH	A/D	Taxi_time	datetime_BLK	datetime_SCH	gate_POS	rwy_NR	AC_type	FltNR
275	A	4.0	2019-10-02 15:14:00	2019-10-02 15:35:00	A04	27	E190	KL1334
275	A	5.0	2019-10-02 08:28:00	2019-10-02 08:45:00	A04	27	E75L	KL1322
275	A	7.0	2019-10-02 18:59:00	2019-10-02 18:55:00	A04	36C	E190	KL1326
275	A	5.0	2019-10-02 14:01:00	2019-10-02 13:40:00	A04	27	B738	HV6116
275	A	5.0	2019-10-02 08:56:00	2019-10-02 08:50:00	A04	27	B738	KL1662
275	A	6.0	2019-10-02 12:32:00	2019-10-02 12:30:00	A04	27	E190	KL1186
275	A	8.0	2019-10-02 15:57:00	2019-10-02 16:00:00	A04	36C	E195	KL1188
275	A	5.0	2019-10-02 15:53:00	2019-10-02 15:55:00	A04	27	E75L	KL1584
275	A	5.0	2019-10-02 11:14:00	2019-10-02 11:20:00	A04	27	E190	KL1586
275	A	6.0	2019-10-02 19:13:00	2019-10-02 19:35:00	A04	27	E190	KL1592

Table 7.1: Sample of flight schedule. (NB: cancelled flights have already been deleted)

Table 7.2 gives an overview of the difference between the quiet and busy day at AAS. It can be seen that there is a clear difference in number of flights and passengers carried. The ratio NB and WB flights is similar for both days, but there is a clear difference in average taxi time. This can be explained by either the busier flight schedule on the 2nd of October or the use of runways further from the terminal. However, as can be seen in the last column in table 7.2, one of the runways furthest away from the terminal (18R and 36L) is being used on each of the two days. Therefore, the likely main cause for the difference in average taxi time is the busier flight schedule.

	#Flights	NB flights	WB flights	Average taxi time (min)	#Pax	Runways used
2nd of October	2730	2269	461	11.6	384360	27, 36C, 6, 24, 36L
14th of December	949	757	192	9.5	135294	18R, 22, 27, 18C, 24, 18L

Table 7.2: Key figures busy (2nd of October) and quiet (14th of December) day

Table 7.3 shows the types of aircraft present on the 2nd of October 2019, the busy day, and their number of operations on that day. The only aircraft type that is not present on the 2nd of October, but is present on the 14th of December, is the Airbus A300-600. This aircraft is a standard WB aircraft. It needs to be noted that aircraft have been grouped based on general aircraft type, e.g. the A350-900 and A350-1000 have been combined in the A350 aircraft type group. The column 'size' indicates which aircraft is considered to be NB and which aircraft is considered WB; as discussed in section 7.3, the WB aircraft are divided into the standard and heavy category. This information is added since the ET vehicle and the taxi velocity differs for different aircraft categories. The definition of a NB aircraft is an aircraft with one isle; a WB aircraft has two isles. The weights in the table are based on the heaviest version of the aircraft type in the family.

Aircraft type	Frequency	Size	MTOW (t)	MLW (t)
A220	8	NB	69.9[3]	58.7[3]
A318	8	NB	68.0 [4]	57.5[4]
A319	162	NB	75.5[3]	63.9[3]
A320	316	NB	79.0[3]	67.4[3]
A321	105	NB	97.0[3]	79.2[3]
A330	105	WB standard	251.0[3]	191.0[3]
A340	2	WB standard	380[5]	265[5]
A350	14	WB standard	319[3]	236[3]
A380	8	WB heavy	575[3]	394[3]
B737	907	NB	79.0[4]	66.3[4]
B747	68	WB heavy	396.9[6]	295.7[6]
B757	12	NB	123.8[7]	101.6[7]
B767	56	WB standard	204.1[8]	158.8[8]
B777	132	WB standard	351.5[4]	251.3[4]
B787	76	WB standard	254.0[4]	202.0[4]
Bombardier CRJ	6	NB	41.6[9]	37.0[9]
Bombardier DHC-8	34	NB	29.2[4]	28.0[4]
Embraer 120	4	NB	12.0[10]	11.7[10]
Embraer 170/175	253	NB	44.6[11]	40.0[11]
Embraer 190/195	441	NB	61.5[11]	54.0[11]
Embraer RJ145	13	NB	24.1[11]	20.0[11]

Table 7.3: Aircraft types, frequencies, size and weights at AAS on the 2nd of October 2019

[3] Airbus Family Figures, published: December 2019
[4] https://modernairliners.com/, accessed: April 2020
[5] https://www.airbus.com/aircraft/previous-generation-aircraft/a340-family/a340-600.html accessed: April 2020
[6] https://www.boeing.com/resources/boeingdotcom/company/about_bca/startup/pdf/historical/747-400-passenger.pdf, accessed: April 2020
[7] http://www.b757.info/boeing-757-300-specifications/ accessed: April 2020
[8] https://www.boeing.com/commercial/aeromagazine/aero_03/textonly/ps01txt.html accessed: April 2020
[9] Bombardier CRJ Series Brochure, accessed: April 2020
[10] http://aviationsvcs.com/emb120specs.htm, accessed: April 2020
[11] https://www.embraercommercialaviation.com/ accessed: April 2020

7.6. Airport model

The model of AAS is the backbone of the optimisation models that will be developed in this research. AAS needs to be translated into a network representation that can be used as node-edge model for aircraft movements. The lengths of the edges determine the distances that need to be taxied and taxi velocity restrictions per taxiway segment need to be defined. Furthermore, the possible charging station locations for ET vehicles need to be determined. Finally, the taxiway and service road networks will be shown.

7.6.1. Design choices

Before the actual networks can be defined, a couple of choices regarding the different aspects of the networks need to be made.

Nodes and edges

The network of nodes and edges can be defined based on information on the aerodrome AAS. The information that needs to be present in the networks is: taxiway nodes/edges including specific starting and final nodes, service road nodes/edges, holding points and charging station nodes. As mentioned in section 6.5, the network does not involve the apron, but starts at the taxiways.

First of all, each runway has multiple entrances and exits. The data presented in table 7.1 does not give the actual runway entrance or exit that has been used by the aircraft. Besides, the aircraft engines need to be warmed up after taxi-out and cooled down before taxi-in. Therefore, it is logical to have a dedicated holding area per runway end that covers each of the runway entrances or exits at that end in order to facilitate engine warm-up and cool-down. This means, that one final node per runway end will be defined. This node will be located at the very end of each runway, since this entrance/exit would give any aircraft assigned to that runway sufficient runway length to take off or land. For taxi-out, this means that all aircraft taxiing to a specific runway detach from the ET vehicle once they arrive at the holding area. For taxi-in, this means that it is assumed that each aircraft will use its main engines or remaining velocity after landing to get to the holding area; after that, engine cool-down takes place.

Distance and velocity

The next step to set up the network is to define the length of the edges and the maximum taxi velocity allowed for each edge. The latter will be determined by using the velocity data defined in [16]. This paper provides information on taxiway velocities at AAS for the network used in its use case. This information can be used to determine the velocities applicable to the taxiway network in this research. These values will be used as upper limits for the NB as well as the WB aircraft.
The distances between nodes (i.e. the edges) are determined by measuring chart distances (figures 9.1 and 9.2) using Rhinoceros, version Rhino 6[12]. This method is not completely accurate, but it gives very reasonable estimates and is used due to a lack of available distance data.

Apron

As mentioned in section 6.5, the apron is not modelled. However, the starting or ending points of taxiing aircraft provided in the data set are the gates. Therefore, each gate needs to be assigned to a certain taxiway node. These starting nodes will be defined by looking at the piers and taxiways shown in figure 9.1. This results in the allocation of gates to nodes in the network as shown in figure 7.6.

[12] http://www.rhino3d.nl/

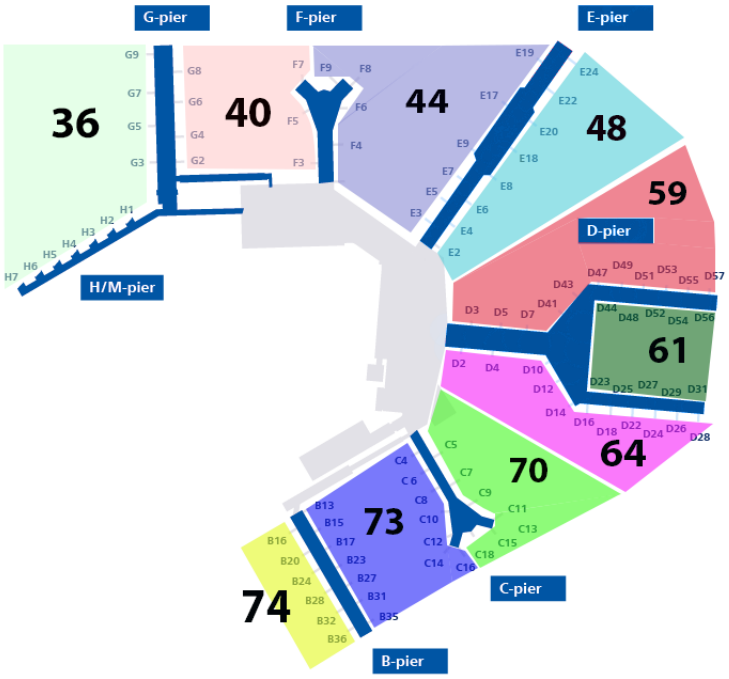

Figure 7.6: Gates assigned to nodes in taxiway network

Charging stations

The locations of charging stations are an important factor in the optimisation of ET vehicle movements. However, these charging stations are currently non-existent due to the absence of ET vehicles at AAS. Therefore, a set of charging station locations needs to be determined. Choosing these locations can be rather arbitrary due to the lack of available information on preferred or planned locations. The most important criterion kept in mind while determining the locations, is the fact that they have to be located next to a service road, since unloaded towing vehicles are forced to use the service roads. Furthermore, the charging stations must be within reasonable distance from each gate and runway. Lastly, charging stations need to take into account buildings that are currently in place at AAS. In the long term, this last requirement might be lifted to some extent, but for the sake of applicability at this point in time, charging stations will only use relatively open areas. The charging station locations are depicted as grey rectangles in figure 7.8.

7.6.2. Model of AAS

The main information sources used to set up the AAS network are shown in figures 9.1 and 9.2. A schematic overview of the taxiways, service roads, runways and apron has been made by distilling the relevant information from the charts and projecting them onto the AAS lay-out. In section 6.4, it is explained that the goal of this research is to create two models that will be used separately to solve two optimisation problems. The ET vehicle assignment problem is solved after the taxi optimisation problem, which means that unloaded ET vehicles (i.e. ET vehicles not towing an aircraft) cannot use the same tarmac as the aircraft, since these operations have not been accounted for in the first optimisation and would inevitably lead to conflicts. Therefore, unloaded ET vehicles can only use service roads. For this reason, the AAS model has been divided into two parts.

The first model contains the runways and taxiways and is shown in figure 7.7. The arrows in the figure indicate one-way taxiways; all other taxiways allow two-way traffic. Tables 9.1 and 9.2 give an overview of the distances between all nodes and indicates which nodes are apron or runway nodes. The maximum number

of nodes connected to one individual node is five and nodes one to five are defined clockwise starting at 12 o'clock from the center node's perspective. The table also shows the allowed maximum velocity per taxiway edge, based on the information from 4.3. The complete taxiway network consists of a total of 98 nodes and 234 edges, counting two-way edges as two edges and one-way edges as one edge.

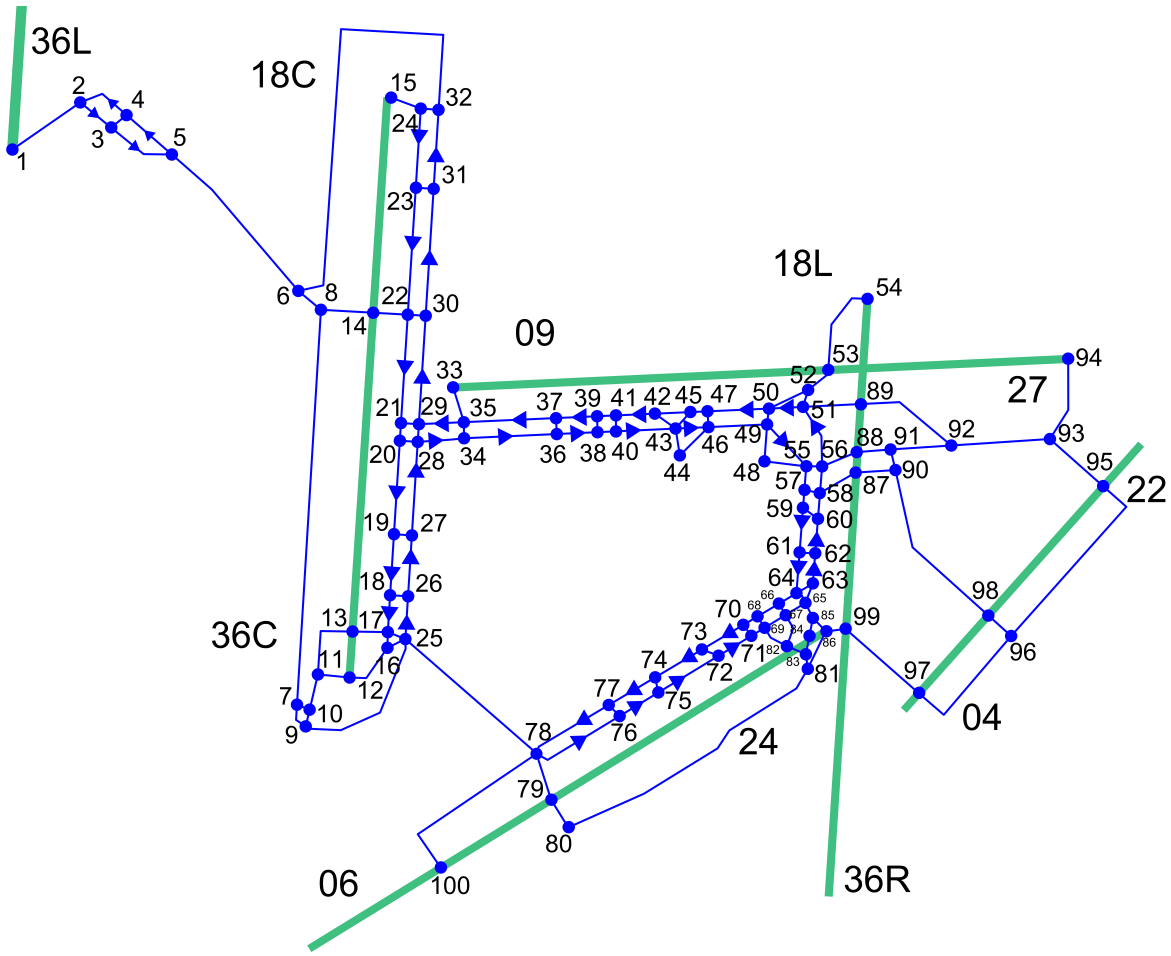

Figure 7.7: Taxiway node-and-edge network

The second model contains the runways, service roads and charging stations and is shown in figure 7.8. All service roads allow two-way traffic. Table 9.3 gives an overview of the distances between all nodes and indicates which nodes are apron, runway or charging station nodes. The maximum number of nodes connected to one individual node in the service road network is four and they are defined in the same way as for the taxiway network. The velocity of the ET vehicles is constant for each service road edge: 8.33 m/s. The complete service road network consists of a total of 48 nodes and 112 edges, counting each edge as two edges since they are all two-way edges.

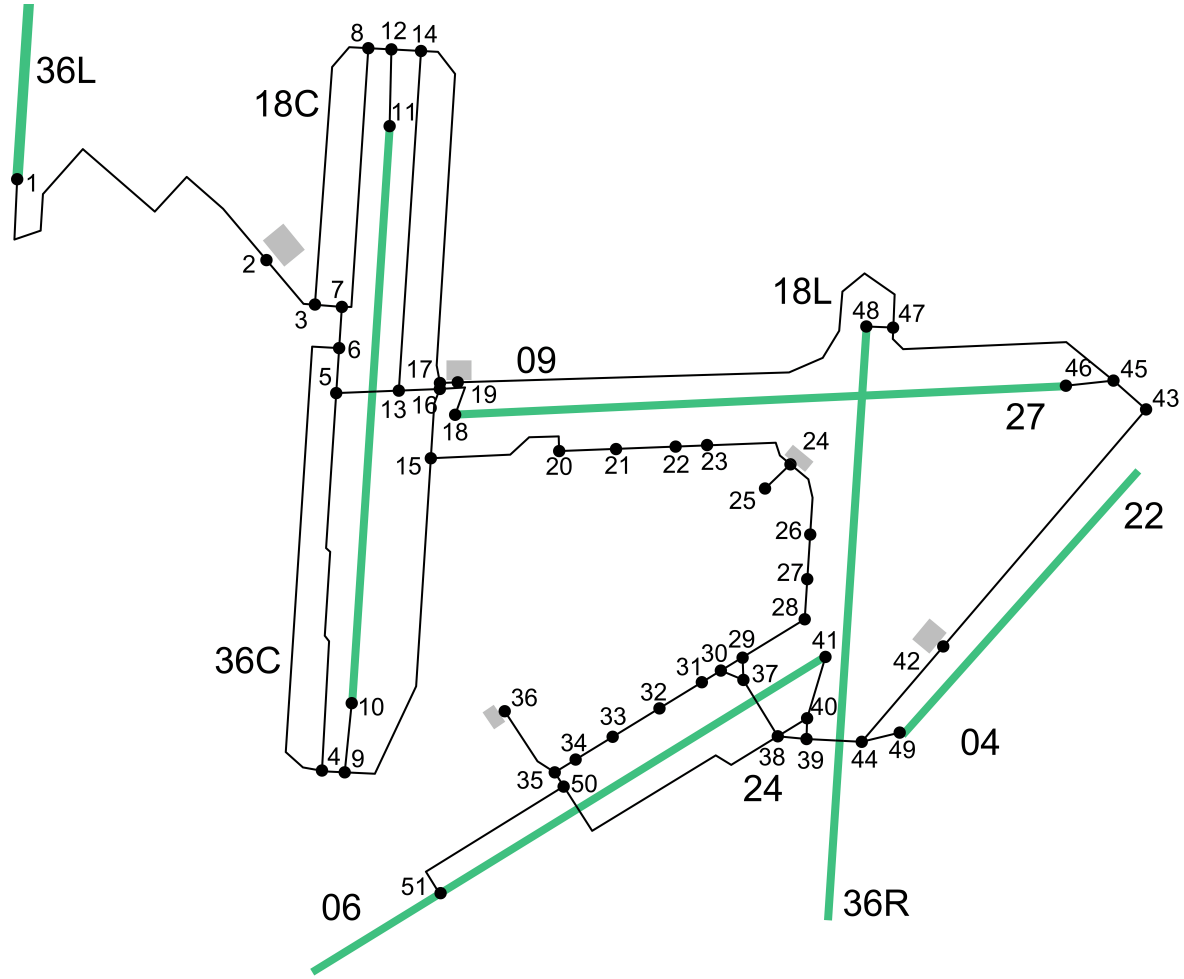

Figure 7.8: Service road node-and-edge network

These two networks will be used for two separate optimisation problems; however, they do need to be connected properly. The input to the second model, is a set of tasks that needs to be performed by the ET vehicles. These tasks have a certain starting and ending point, which are either runway or apron nodes. For example, if a taxi-out task operations from the first optimisation model ends at runway node number 14 (runway end of 36L), the ET vehicle in the second optimisation model will have to start driving from node 9, which corresponds to the same location in the service road network. Therefore, table 7.4 is defined, which connects the runway and apron nodes of the two networks.

Runway nodes		**Gate nodes**	
Taxiway	**Service road**	**Taxiway**	**Service road**
1	1	36	20
12	10	40	21
15	11	44	22
33	18	48	23
54	48	59	25
86	41	61	26
94	46	64	27
97	44	70	28
		73	29
		74	31

Table 7.4: Node connections between taxiway and service road network

8

Project Planning

This chapters gives an overview of future work that is going to be performed in this thesis. The first section discusses the functional flow of the to-be-created models. After that, a Gantt chart that gives an overview of the tasks that will be performed in order to create the models is presented. This Gantt chart gives an estimate of the timeline of these tasks.

8.1. Functional flow diagram

Figure 8.1 gives an overview of the functions and data that is going to be used for this research. It shows how each function is connected to other functions and shows the order in which the functions are performed. The functions can be recognized by the straight rectangular blocks and the data is presented in tilted rectangular blocks. The following list gives a short description of each of the function blocks.

- **Create flight schedule:** the AAS flight data is used to generate a flight schedule that can be used as input to the vehicle routing problem. The arrival times, departure times and taxi times given in the flight data need to be processed to get a representative flight schedule to define the aircraft taxiing routes and compare the performance of the electrically towed aircraft to conventionally taxiing aircraft in a fair way.

- **Create taxiway network:** the aerodrome chart of AAS is used as main source to set up the taxiway network that can be used by the taxiing aircraft. Distances, velocities and directions between nodes are defined in order to get a taxiway network that represents AAS as realistically as possible.

- **Create service road network:** similarly to the taxiway network, the service road network is defined using the AAS aerodrome chart and realistically represents AAS. Velocities are the same for each service road and all service roads are two-way roads.

- **Formulate vehicle routing problem:** the flight schedule, taxiway network and performance characteristics of the aircraft are used to formulate a MILP model that solves the vehicle routing problem. The constraints and objective function are defined in Python in a way that the CPLEX optimisation software can solve the problem.

- **Optimise for minimum delay:** CPLEX solves the vehicle routing problem. The aircraft routes and times are determined in order to minimise delay. This delay will be determined by comparing the moment in time aircraft are ready for take-off or arrive at the gate while taxiing electrically to the situation while taxiing conventionally. The influence of ET on delay is the most important performance metric of this model.

- **Define ET vehicle tasks:** once all aircraft routes have been determined, these routes are used to define the tasks the ET vehicles need to perform. The relevant information for the ET vehicle assignment problem consists of the start and end node of each task, the duration of the task, the energy required to perform the task and the ET vehicle type required to perform the task.

- **Perform shortest path for ET vehicle routes:** the ET vehicles tasks are aircraft towing tasks. However, the ET vehicles also need to drive from the end node of a previous task to the start node of a new task. Furthermore, ET vehicles do not have unlimited power storage and might have to recharge after finishing a task. Therefore, a set of possible routes an ET vehicle can take from a certain end node to a new start node or charging station is determined before the ET vehicle assignment problem is solved. The information defined for each route consists of the time it takes to drive along that route, the energy required to perform this drive operation and the start and end point of the route. An ET vehicle which, for example, ends its task at a certain runway node can choose between a fixed set of operations, each starting at the runway node the last task has ended and ending either at a runway, gate or charging station node. Note that ET vehicle tasks can only end at runway or gate nodes; therefore, the shortest path only needs to be performed for the connections between runway, gate and charging station nodes.
- **Pick number of ET vehicles and starting locations:** the goal of the vehicle assignment problem, is to perform all tasks with as few ET vehicles as possible. Therefore, the number of ET vehicles is picked as an input to the model. A high penalty will be given if tasks are not performed. If the outcome of the ET vehicle assignment problem is in the order of magnitude of the penalty, the number of available ET vehicles will be increased and the model will be run again. This process repeats itself until all tasks are performed, with the minimal required number of ET vehicles. Another factor that can be varied is the starting position of the ET vehicles. Each ET vehicle has to start somewhere in the network, which is most likely going to be at one of the charging stations. This factor can have influence on the performance of the ET vehicles, but is not expected to play as big a role as the number of ET vehicles available.
- **Solve ET vehicle assignment problem:** the ET vehicle assignment problem is solved. The most important outcome of the model will be the number of ET vehicles required to perform all tasks.

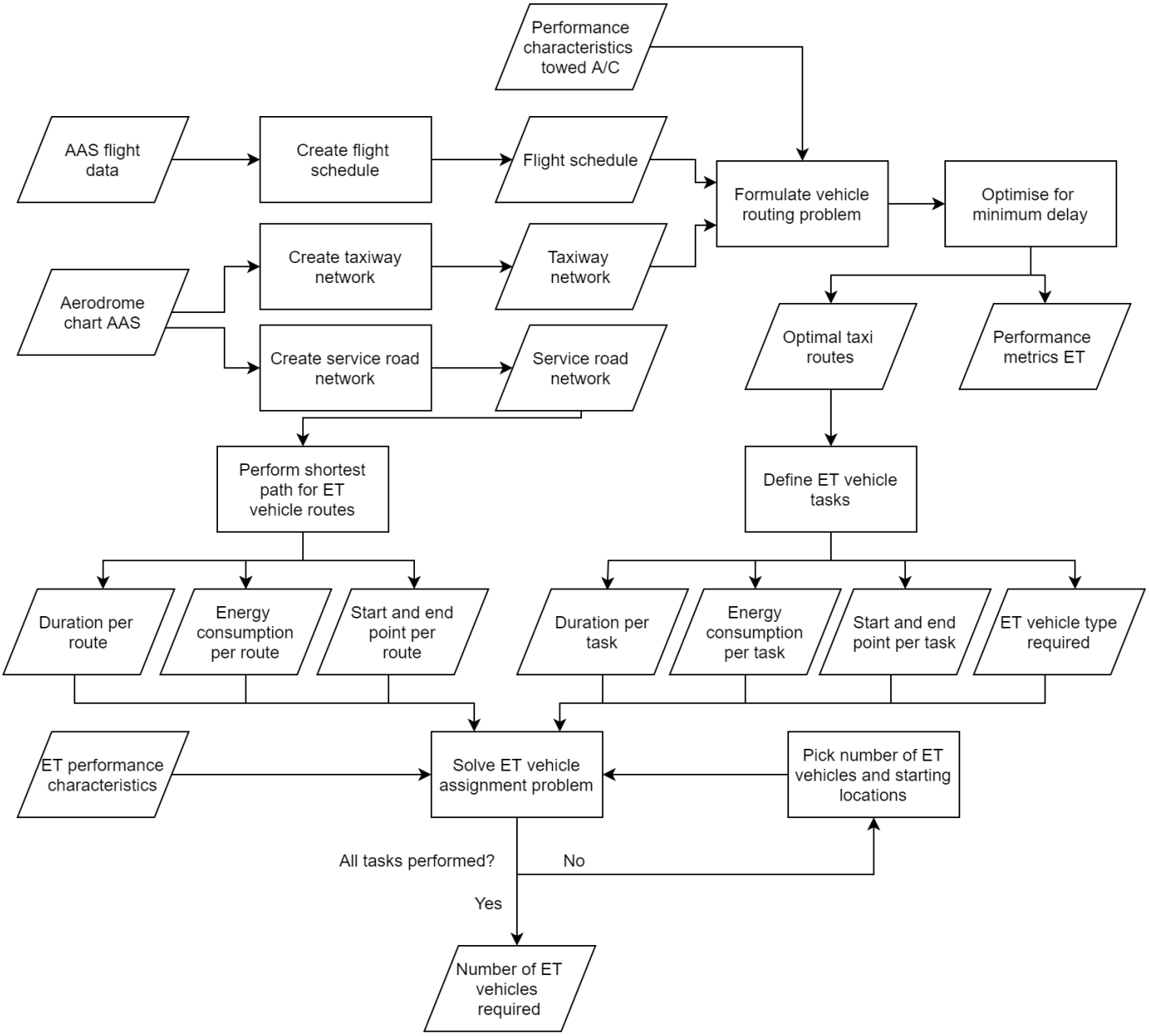

Figure 8.1: Functional flow diagram

8.2. Gantt chart

Figure 8.2 shows the Gantt chart of this thesis. The tasks shown in the list on the left side of the figure are aligned with their time span in the chart.

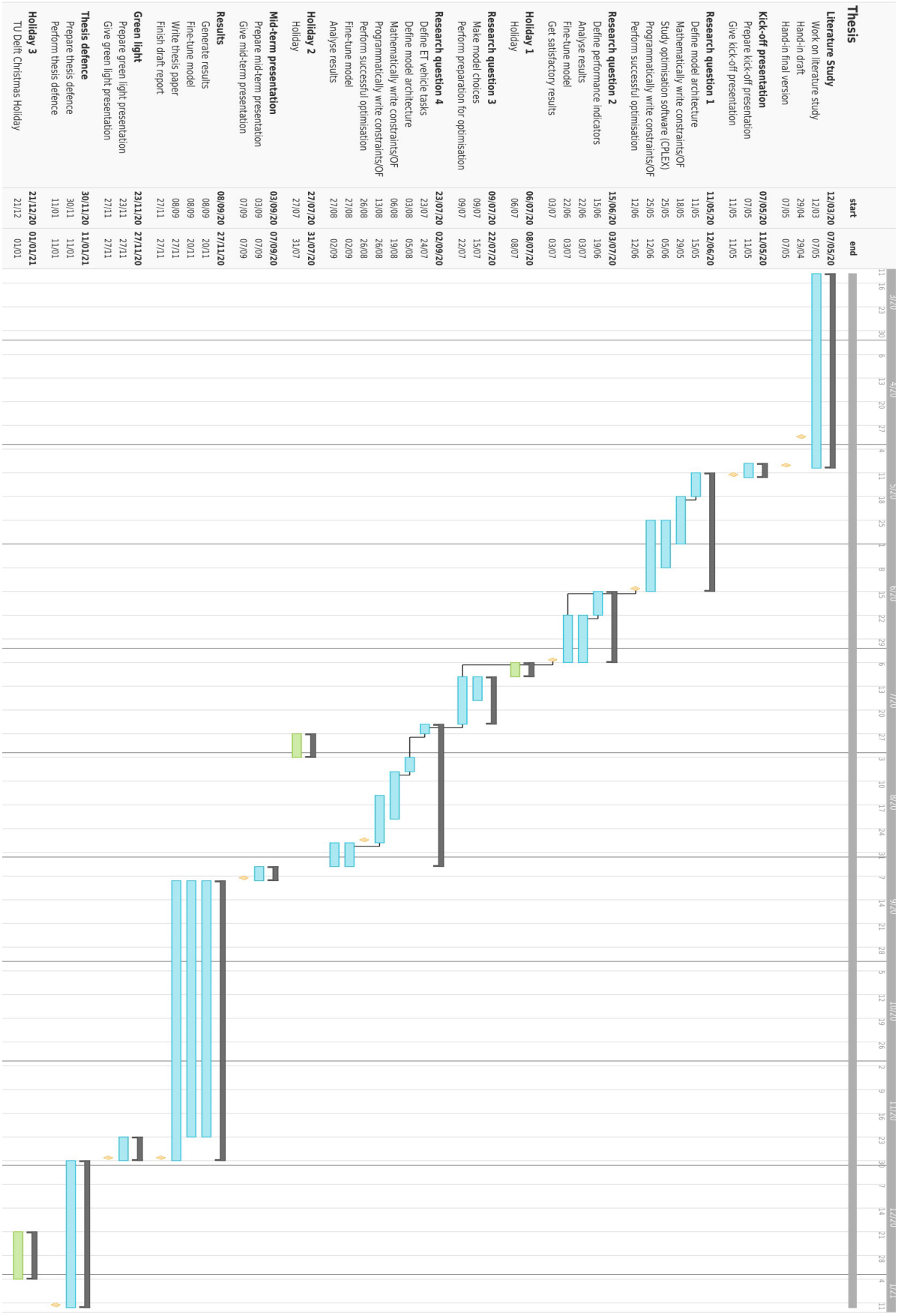

Figure 8.2: Thesis Gantt chart

9

Appendix

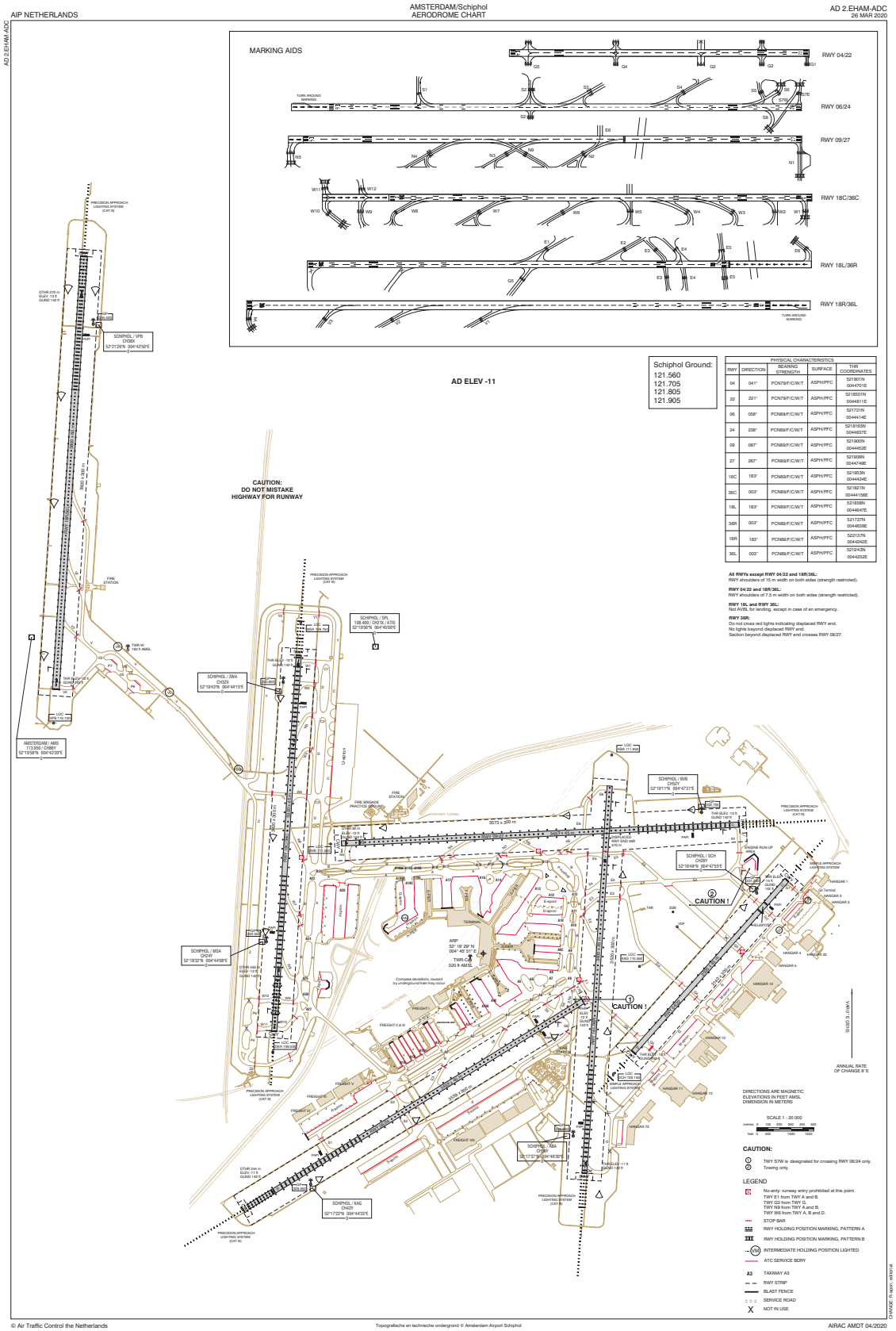

Figure 9.1: Aerodrome Chart AAS [32]

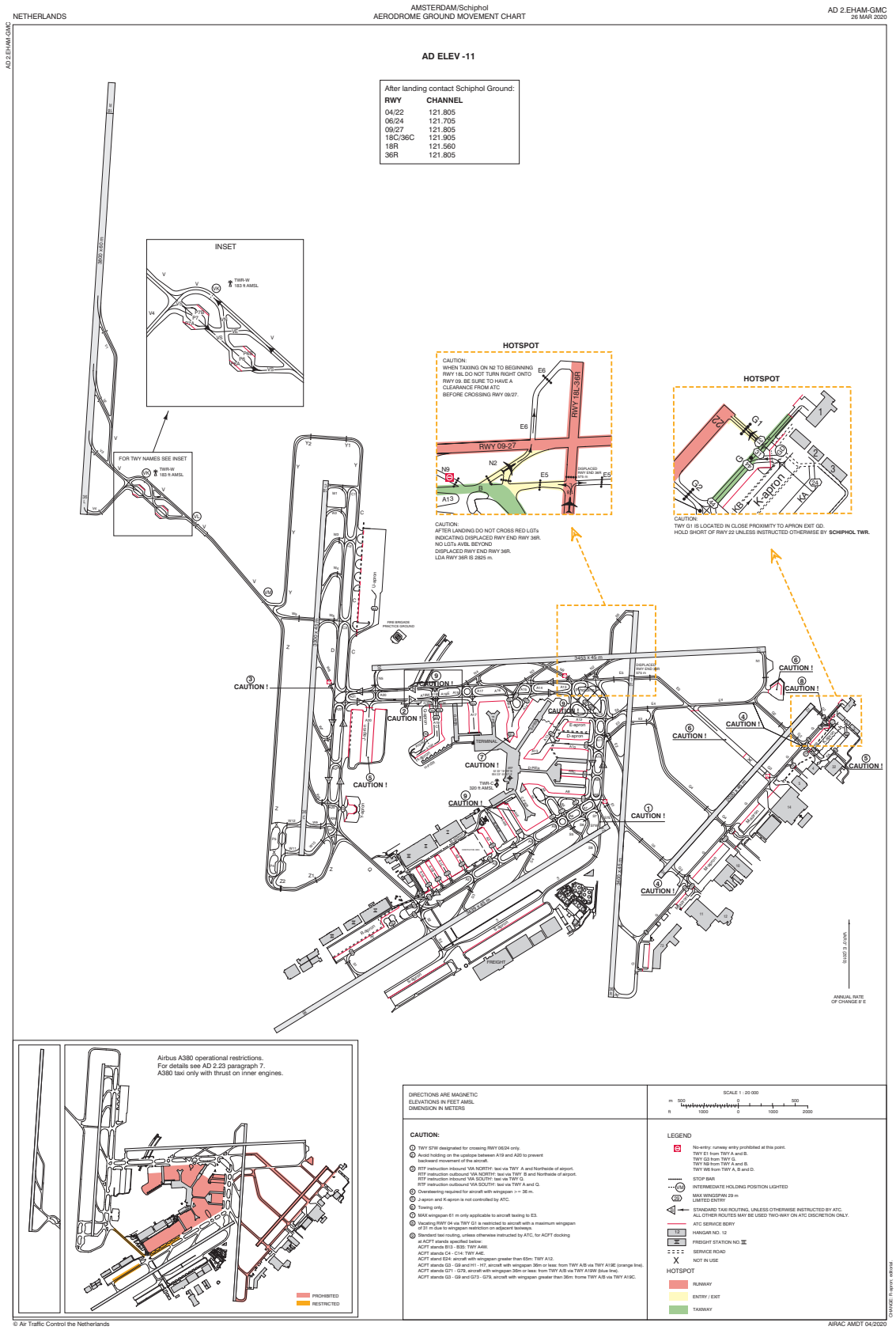

Figure 9.2: Aerodrome ground movement chart AAS [32]

Node	Distance nodes					Runway?	Gate?	Holding?	Velocity nodes				
	1	2	3	4	5				1	2	3	4	5
1	468	-	-	-	-	1	0	0	10	-	-	-	-
2	226	468	-	-	-	0	0	0	10	10	-	-	-
3	111	398	-	-	-	0	0	0	10	10	-	-	-
4	111	317	-	-	-	0	0	0	10	10	-	-	-
5	1056	340	-	-	-	0	0	0	12	10	-	-	-
6	2607	167	1056	-	-	0	0	0	12	12	12	-	-
7	2243	77	152	-	-	0	0	0	14	10	10	-	-
8	297	2243	167	-	-	0	0	0	10	14	12	-	-
9	97	891	152	-	-	0	0	0	10	10	10	-	-
10	205	97	77	-	-	0	0	0	10	10	10	-	-
11	425	181	205	-	-	0	0	0	10	10	10	-	-
12	303	181	-	-	-	1	0	0	10	10	-	-	-
13	200	425	-	-	-	0	0	1	10	10	-	-	-
14	195	297	-	-	-	0	0	1	10	10	-	-	-
15	178	-	-	-	-	1	0	0	11		-	-	-
16	89	113	303	-	-	0	0	0	10	10	10	-	-
17	107	89	200	-	-	0	0	0	10	10	10	-	-
18	102	210	-	-	-	0	0	0	11	11	-	-	-
19	102	347	-	-	-	0	0	0	11	11	-	-	-
20	100	101	531	-	-	0	0	0	11	11	11	-	-
21	616	102	100	-	-	0	0	0	11	11	11	-	-
22	721	102	616	196	-	0	0	0	11	11	11	10	-
23	450	100	721	-	-	0	0	0	11	11	11	-	-
24	101	450	179	-	-	0	0	0	12	11	11	-	-
25	242	988	891	113	107	0	0	0	10	10	10	10	10
26	346	102	-	-	-	0	0	0	11	11	-	-	-
27	531	102	-	-	-	0	0	0	11	11	-	-	-
28	100	263	101	-	-	0	0	0	11	11	11	-	-
29	617	100	263	-	-	0	0	0	11	11	11	-	-
30	721	617	102	-	-	0	0	0	11	11	11	-	-
31	449	721	100	-	-	0	0	0	11	11	11	-	-
32	449	2607	101	-	-	0	0	0	11	12	12	-	-
33	207	-	-	-	-	1	0	0	10	-	-	-	-
34	91	526	-	-	-	0	0	0	10	10	-	-	-
35	91	255	207	-	-	0	0	0	10	11	10	-	-
36	89	231	-	-	-	0	1	0	10	10	-	-	-
37	89	523	-	-	-	0	0	0	10	10	-	-	-
38	91	105	-	-	-	0	0	0	10	10	-	-	-
39	91	233	-	-	-	0	0	0	10	10	-	-	-
40	91	338	-	-	-	0	1	0	10	10	-	-	-
41	91	107	-	-	-	0	0	0	10	10	-	-	-
42	221	-	-	-	-	0	0	0	10	-	-	-	-
43	187	154	145	-	-	0	0	0	10	4	10	-	-
44	228	154	-	-	-	0	1	0	4	4	-	-	-
45	126	202	-	-	-	0	0	0	10	10	-	-	-
46	333	228	90	-	-	0	0	0	10	4	10	-	-
47	90	97	-	-	-	0	0	0	10	10	-	-	-
48	209	239	-	-	-	0	1	0	4	4	-	-	-
49	91	325	209	-	-	0	0	0	10	9	4	-	-
50	246	91	349	-	-	0	0	0	9	10	10	-	-

Table 9.1: Overview of taxiway network

Node	Distance nodes					Runway?	Gate?	Holding?	Velocity nodes				
	1	2	3	4	5				1	2	3	4	5
51	100	325	193	-	-	0	0	0	9	9	-	-	-
52	144	100	246	-	-	0	0	0	9	9	9	-	-
53	560	144	-	-	-	0	0	1	9	9	-	-	-
54	560	-	-	-	-	1	0	0	9		-	-	-
55	89	135	239	-	-	0	0	0	7	7	4	-	-
56	212	89	367	-	-	0	0	0	7	7	-	-	-
57	88	102	-	-	-	0	0	0	7	7	-	-	-
58	152	234	88	-	-	0	0	0	7	7	-	-	-
59	105	255	-	-	-	0	1	0	7	7	-	-	-
60	146	105	-	-	-	0	0	0	7	7	-	-	-
61	89	230	-	-	-	0	1	0	7	7	-	-	-
62	196	89	-	-	-	0	0	0	7	7	-	-	-
63	172	-	-	-	-	0	0	0	7		-	-	-
64	108	75	116	-	-	0	1	0	7	7	7	-	-
65	117	95	75	-	-	0	0	0	7	7	7	-	-
66	76	141	-	-	-	0	0	0	7	7	-	-	-
67	132	193	76	-	-	0	0	0	7	7	7	-	-
68	76	94	-	-	-	0	0	0	10	10	-	-	-
69	139	169	76	-	-	0	0	0	7	7	10	-	-
70	77	273	-	-	-	0	1	0	10	10	-	-	-
71	88	77	-	-	-	0	0	0	7	10	-	-	-
72	217	101	-	-	-	0	0	0	7	10	-	-	-
73	101	309	-	-	-	0	1	0	10	10	-	-	-
74	87	306	-	-	-	0	1	0	10	10	-	-	-
75	399	87	-	-	-	0	0	0	10	10	-	-	-
76	257	88	-	-	-	0	0	0	10	10	-	-	-
77	88	504	-	-	-	0	0	0	10	10	-	-	-
78	550	272	988	-	-	0	0	0	10	10	10	-	-
79	186	272	-	-	-	0	0	1	10	10	-	-	-
80	1658	186	-	-	-	0	0	0	10	10	-	-	-
81	238	1658	83	-	-	0	0	0	7	10	7	-	-
82	193	117	169	-	-	0	0	1	7	7	7	-	-
83	107	83	117	-	-	0	0	1	7	7	7	-	-
84	103	107	-	-	-	0	0	1	7	7	-	-	-
85	107	103	95	-	-	0	0	0	7	7	7	-	-
86	238	107	-	-	-	1	0	0	7	7	-	-	-
87	226	234	-	-	-	0	0	1	7	7	-	-	-
88	193	212	-	-	-	0	0	1	11	7	-	-	-
89	601	325	-	-	-	0	0	1	11	9	-	-	-
90	1035	226	120	-	-	0	0	0	11	7	11	-	-
91	345	345	193	-	-	0	0	0	11	11	11	-	-
92	560	345	601	-	-	0	0	0	11	11	11	-	-
93	481	403	560	-	-	0	0	0	9	11	11	-	-
94	481	-	-	-	-	1	0	0	9	-	-	-	-
95	176	403	-	-	-	0	0	1	11	11	-	-	-
96	480	1155	176	-	-	0	0	0	11	11	11	-	-
97	480	-	-	-	-	1	0	0	11	-	-	-	-
98	1155	1035	-	-	-	0	0	1	11	11	-	-	-

Table 9.2: Overview of taxiway network

Nodes	Distance nodes				Runway?	Gate?	Charging station?
	1	2	3	4			
1	2520	-	-	-	1	0	0
2	392	2520	-	-	0	0	1
3	1617	154	392	-	0	0	0
4	2142	2715	531	-	0	0	0
5	257	359	2142	-	0	0	0
6	235	2715	257	-	0	0	0
7	1534	235	154	-	0	0	0
8	132	1534	1617	-	0	0	0
9	397	2028	130	-	0	0	0
10	397	-	-	-	1	0	0
11	438	-	-	-	1	0	0
12	169	438	132	-	0	0	0
13	1942	234	359	-	0	0	0
14	2025	1942	169	-	0	0	0
15	402	854	2028	-	0	0	0
16	34	310	402	234	0	0	0
17	102	34	2025	-	0	0	0
18	310	-	-	-	1	0	0
19	3067	102	-	-	0	0	1
20	325	854	-	-	0	1	0
21	341	325	-	-	0	1	0
22	180	341	-	-	0	1	0
23	549	180	-	-	0	1	0
24	454	201	549	-	0	0	1
25	201	-	-	-	0	1	0
26	256	454	-	-	0	1	0
27	256	229	-	-	0	1	0
28	229	418	-	-	0	1	0
29	418	129	145	-	0	1	0
30	145	139	127	-	0	0	0
31	127	284	-	-	0	1	0
32	284	312	-	-	0	1	0
33	312	248	-	-	0	1	0
34	248	140	-	-	0	1	0
35	140	1635	459	-	0	0	0
36	459	-	-	-	0	0	1
37	378	139	129	-	0	0	0
38	197	165	1635	378	0	0	0
39	118	1029	165	-	0	0	0
40	367	118	197	-	0	0	0
41	367	-	-	-	1	0	0
42	1780	1029	-	-	0	0	1
43	749	1780	248	-	0	0	0
44	749	-	-	-	1	0	0
45	248	273	1427	-	0	0	0
46	273	-	-	-	1	0	0
47	1427	3067	154	-	0	0	0
48	154	-	-	-	1	0	0

Table 9.3: Overview of service roads network

III

Supporting work

1

Amsterdam Airport Schiphol

Tables 9.1 and 9.2 show the aerodrome chart and aerodrome ground movement chart of AAS. These charts have been used to develop the taxiway and service road node-edge networks used in this research.

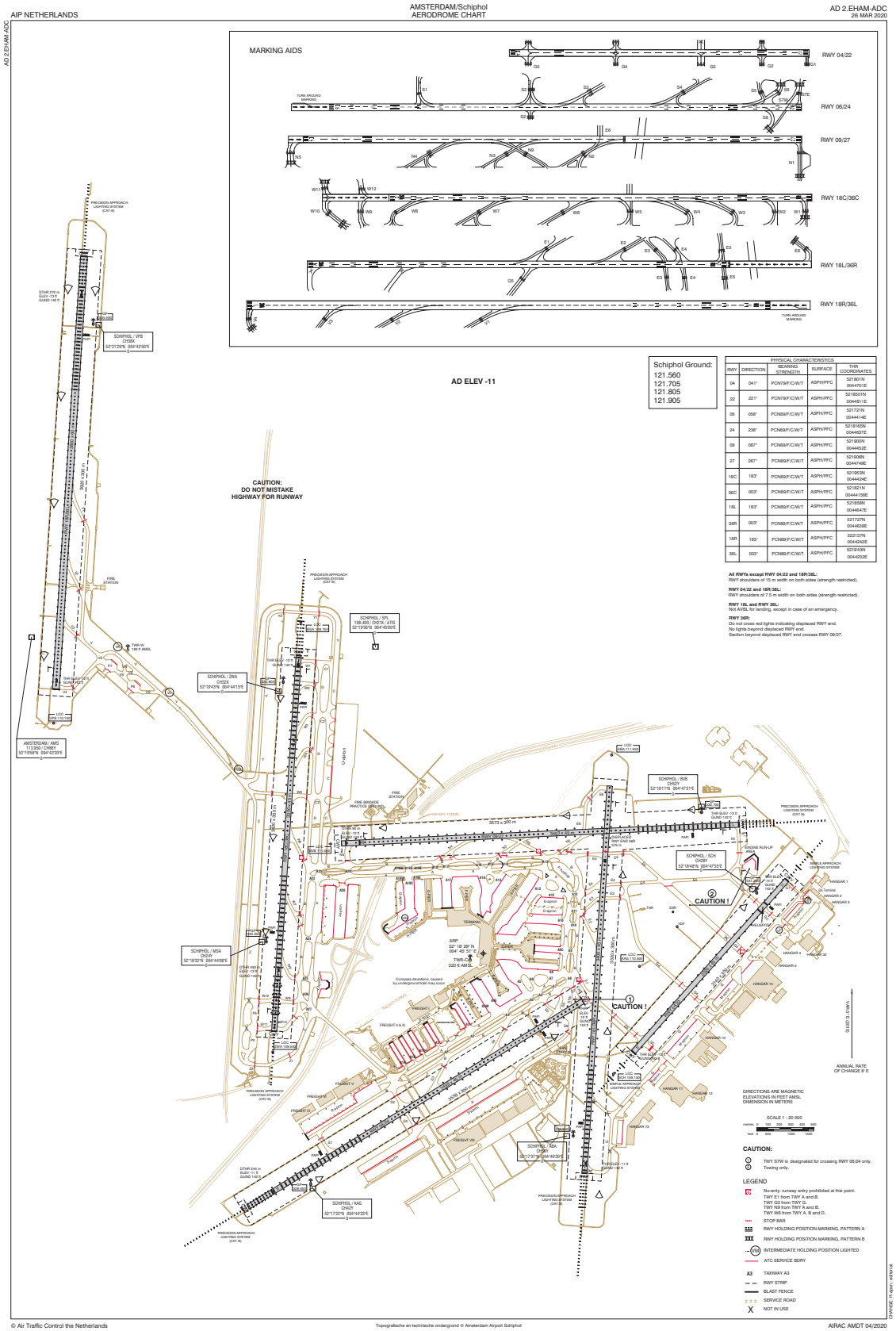

Figure 1.1: Aerodrome chart of AAS [32]

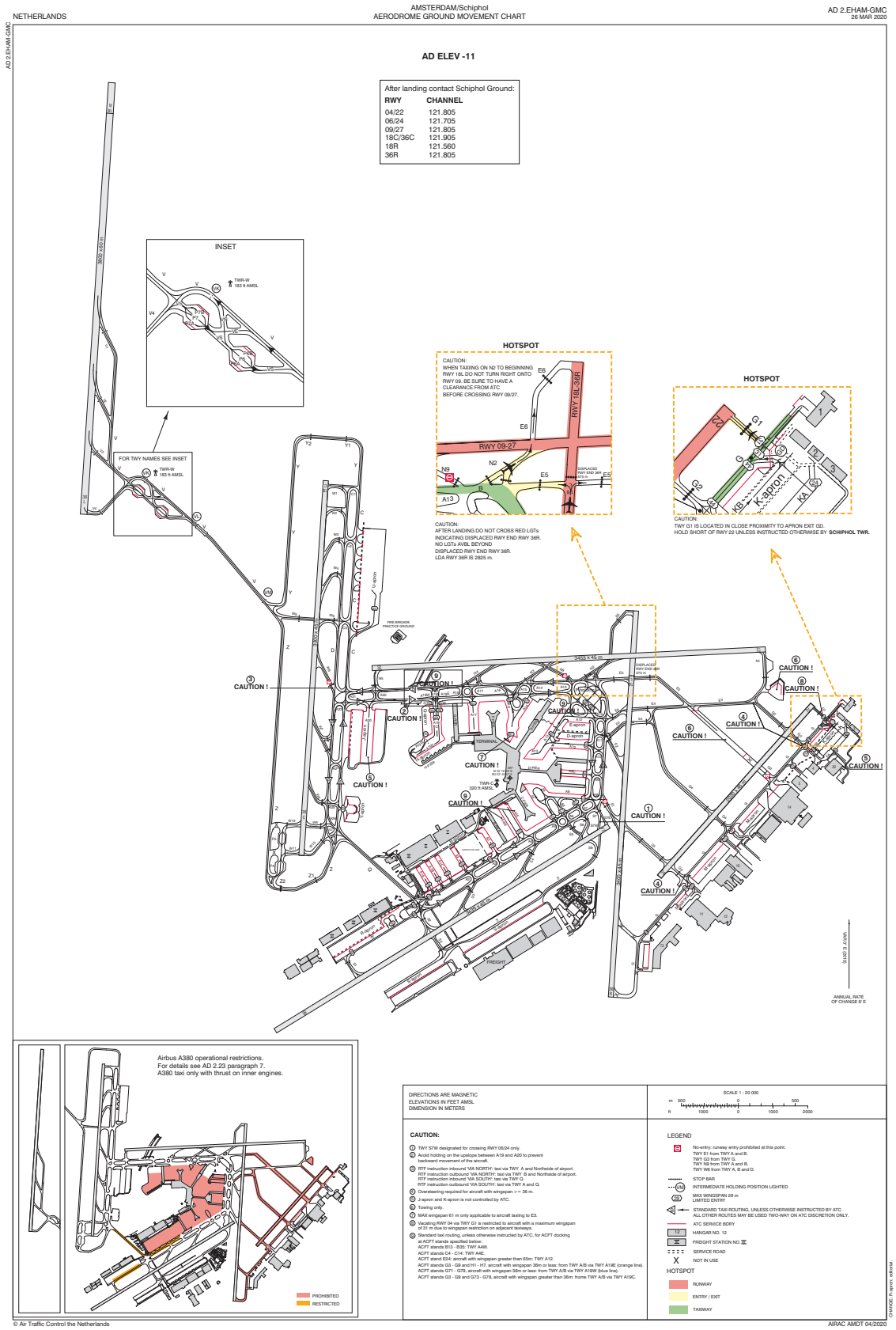

Figure 1.2: Aerodrome ground movement chart of AAS [32]

Tables 9.1 and 9.2 give an overview of the connections between each node in the taxiway network. It shows the distance and maximum velocity between all adjacent nodes. Nodes 1-5 have been defined in a clockwise manner from the perspective of the node in the left-most column.

Node	Distance nodes					Runway?	Gate?	Holding?	Velocity nodes				
	1	2	3	4	5				1	2	3	4	5
1	468	-	-	-	-	1	0	0	10	-	-	-	-
2	226	468	-	-	-	0	0	0	10	10	-	-	-
3	111	398	-	-	-	0	0	0	10	10	-	-	-
4	111	317	-	-	-	0	0	0	10	10	-	-	-
5	1056	340	-	-	-	0	0	0	12	10	-	-	-
6	2607	167	1056	-	-	0	0	0	12	12	12	-	-
7	2243	77	152	-	-	0	0	0	14	10	10	-	-
8	297	2243	167	-	-	0	0	0	10	14	12	-	-
9	97	891	152	-	-	0	0	0	10	10	10	-	-
10	205	97	77	-	-	0	0	0	10	10	10	-	-
11	425	181	205	-	-	0	0	0	10	10	10	-	-
12	303	181	-	-	-	1	0	0	10	10	-	-	-
13	200	425	-	-	-	0	0	1	10	10	-	-	-
14	195	297	-	-	-	0	0	1	10	10	-	-	-
15	178	-	-	-	-	1	0	0	11		-	-	-
16	89	113	303	-	-	0	0	0	10	10	10	-	-
17	107	89	200	-	-	0	0	0	10	10	10	-	-
18	102	210	-	-	-	0	0	0	11	11	-	-	-
19	102	347	-	-	-	0	0	0	11	11	-	-	-
20	101	531	-	-	-	0	0	0	11	11	-	-	-
21	102	100	-	-	-	0	0	0	11	11	-	-	-
22	721	102	196	-	-	0	0	0	11	11	10	-	-
23	450	100	-	-	-	0	0	0	11	11	-	-	-
24	101	450	179	-	-	0	0	0	12	11	11	-	-
25	242	988	891	113	107	0	0	0	10	10	10	10	10
26	346	102	-	-	-	0	0	0	11	11	-	-	-
27	531	102	-	-	-	0	0	0	11	11	-	-	-
28	100	263	101	-	-	0	0	0	11	11	11	-	-
29	617	263	-	-	-	0	0	0	11	11	-	-	-
30	721	102	-	-	-	0	0	0	11	11	-	-	-
31	449	100	-	-	-	0	0	0	11	11	-	-	-
32	2607	101	-	-	-	0	0	0	12	12	-	-	-
33	207	-	-	-	-	1	0	0	10	-	-	-	-
34	91	526	-	-	-	0	0	0	10	10	-	-	-
35	91	255	207	-	-	0	0	0	10	11	10	-	-
36	89	231	-	-	-	0	1	0	10	10	-	-	-
37	89	523	-	-	-	0	0	0	10	10	-	-	-
38	91	105	-	-	-	0	0	0	10	10	-	-	-
39	91	233	-	-	-	0	0	0	10	10	-	-	-
40	91	338	-	-	-	0	1	0	10	10	-	-	-
41	91	107	-	-	-	0	0	0	10	10	-	-	-
42	221	-	-	-	-	0	0	0	10	-	-	-	-
43	187	154	145	-	-	0	0	0	10	4	10	-	-
44	228	154	-	-	-	0	1	0	4	4	-	-	-
45	126	202	-	-	-	0	0	0	10	10	-	-	-
46	333	228	90	-	-	0	0	0	10	4	10	-	-
47	90	97	-	-	-	0	0	0	10	10	-	-	-
48	209	239	-	-	-	0	1	0	4	4	-	-	-
49	91	325	209	-	-	0	0	0	10	9	4	-	-
50	246	91	349	-	-	0	0	0	9	10	10	-	-

Table 1.1: Overview of taxiway network 1

Node	Distance nodes					Runway?	Gate?	Holding?	Velocity nodes				
	1	2	3	4	5				1	2	3	4	5
50	246	91	349	-	-	0	0	0	9	10	10	-	-
51	100	325	193	-	-	0	0	0	9	9	9	-	-
52	144	100	246	-	-	0	0	0	9	9	9	-	-
53	560	144	-	-	-	0	0	1	9	9	-	-	-
54	560	-	-	-	-	1	0	0	9		-	-	-
55	89	135	239	-	-	0	0	0	7	7	4	-	-
56	212	89	367	-	-	0	0	0	7	7	7	-	-
57	88	102	-	-	-	0	0	0	7	7	-	-	-
58	152	234	88	-	-	0	0	0	7	7	7	-	-
59	105	255	-	-	-	0	1	0	7	7	-	-	-
60	146	105	-	-	-	0	0	0	7	7	-	-	-
61	89	230	-	-	-	0	1	0	7	7	-	-	-
62	196	89	-	-	-	0	0	0	7	7	-	-	-
63	172	-	-	-	-	0	0	0	7		-	-	-
64	108	75	116	-	-	0	1	0	7	7	7	-	-
65	117	95	75	-	-	0	0	0	7	7	7	-	-
66	76	141	-	-	-	0	0	0	7	7	-	-	-
67	132	193	76	-	-	0	0	0	7	7	7	-	-
68	76	94	-	-	-	0	0	0	10	10	-	-	-
69	139	169	76	-	-	0	0	0	7	7	10	-	-
70	77	273	-	-	-	0	1	0	10	10	-	-	-
71	88	77	-	-	-	0	0	0	7	10	-	-	-
72	217	101	-	-	-	0	0	0	7	10	-	-	-
73	101	309	-	-	-	0	1	0	10	10	-	-	-
74	87	306	-	-	-	0	1	0	10	10	-	-	-
75	399	87	-	-	-	0	0	0	10	10	-	-	-
76	257	88	-	-	-	0	0	0	10	10	-	-	-
77	88	504	-	-	-	0	0	0	10	10	-	-	-
78	550	272	988	-	-	0	0	0	10	10	10	10	-
79	186	272	-	-	-	0	0	1	10	10	-	-	-
80	1658	186	-	-	-	0	0	0	10	10	-	-	-
81	238	1658	83	-	-	0	0	0	7	10	7	-	-
82	193	117	169	-	-	0	0	1	7	7	7	-	-
83	107	83	117	-	-	0	0	1	7	7	7	-	-
84	103	107	-	-	-	0	0	1	7	7	-	-	-
85	107	103	95	-	-	0	0	0	7	7	7	-	-
86	114	238	107	-	-	1	0	0	7	7	7	-	-
87	226	234	-	-	-	0	0	1	7	7	-	-	-
88	193	212	-	-	-	0	0	1	11	7	-	-	-
89	601	325	-	-	-	0	0	1	11	9	-	-	-
90	1035	226	120	-	-	0	0	0	11	7	11	-	-
91	345	345	193	-	-	0	0	0	11	11	11	-	-
92	560	345	601	-	-	0	0	0	11	11	11	-	-
93	481	403	560	-	-	0	0	0	9	11	11	-	-
94	481	-	-	-	-	1	0	0	9	-	-	-	-
95	1154	403	-	-	-	0	0	1	11	11	-	-	-
96	1154	773	174	-	-	0	0	0	11	11	11	-	-
97	773	554	-	-	-	1	0	0	11	7	-	-	-
98	1155	1035	-	-	-	0	0	1	11	11	-	-	-
99	554	114	-	-	-	0	0	1	7	7	-	-	-
100	1046	-	-	-	-	1	0	0	10	-	-	-	-

Table 1.2: Overview of taxiway network 2

Table 9.3 gives an overview of the connections between the nodes in the service road network. It only shows the distances between all adjacent nodes, since the velocity on the service road network (8.33 m/s) is constant for all service road network segments.

Nodes	**Distance nodes**				**Runway?**	**Gate?**	**Charging station?**
	1	**2**	**3**	**4**			
1	2520	-	-	-	1	0	0
2	392	2520	-	-	0	0	1
3	1617	154	392	-	0	0	0
4	2142	2715	531	-	0	0	0
5	257	359	2142	-	0	0	0
6	235	2715	257	-	0	0	0
7	1534	235	154	-	0	0	0
8	132	1534	1617	-	0	0	0
9	397	2028	130	-	0	0	0
10	397	-	-	-	1	0	0
11	438	-	-	-	1	0	0
12	169	438	132	-	0	0	0
13	1942	234	359	-	0	0	0
14	2025	1942	169	-	0	0	0
15	402	854	2028	-	0	0	0
16	34	310	402	234	0	0	0
17	102	34	2025	-	0	0	0
18	310	-	-	-	1	0	0
19	3067	102	-	-	0	0	1
20	325	854	-	-	0	1	0
21	341	325	-	-	0	1	0
22	180	341	-	-	0	1	0
23	549	180	-	-	0	1	0
24	454	201	549	-	0	0	1
25	201	-	-	-	0	1	0
26	256	454	-	-	0	1	0
27	256	229	-	-	0	1	0
28	229	418	-	-	0	1	0
29	418	129	145	-	0	1	0
30	145	139	127	-	0	0	0
31	127	284	-	-	0	1	0
32	284	312	-	-	0	1	0
33	312	248	-	-	0	1	0
34	248	140	-	-	0	1	0
35	140	1635	459	-	0	0	0
36	459	-	-	-	0	0	1
37	378	139	129	-	0	0	0
38	197	165	1635	378	0	0	0
39	118	1029	165	-	0	0	0
40	367	118	197	-	0	0	0
41	367	-	-	-	1	0	0
42	1780	1029	-	-	0	0	1
43	749	1780	248	-	0	0	0
44	749	-	-	-	1	0	0
45	248	273	1427	-	0	0	0
46	273	-	-	-	1	0	0
47	1427	3067	154	-	0	0	0
48	154	-	-	-	1	0	0

Table 1.3: Overview of service roads network

Table 1.4 gives an overview of which actual AAS gates are allocated to each gate node in the taxiway network.

Node	Gates
36	G03, G05, G07, G09, G11, G12, G13, G14, G15, G16, H01, H02, H03, H04, H05, H06, H07, M01, M02, M03, M04, M05, M06, M07
40	F03, F05, F07, G02, G04, G06, G08
44	A14, A15, F04, F06, F08, F09, E03, E05, E07, E09, E10, E11, E12, E13, E14, E15, E17, E19
48	E02, E04, E06, E08, E18, E20, E22, E24
59	D03, D05, D07, D41, D43, D45, D47, D49, D51, D53, D55, D57, D59, D61, D63, D71, D73, D77, D79, D81, D83, D85, D87
61	D19, D21, D23, D25, D27, D29, D31, D42, D44, D46, D48, D50, D52, D54, D56, D72, D74, D76, D78, D82, D86, A09, D84, Z07, Z10, Z02
64	A08, D02, D04, D06, D08, D10, D12, D14, D16, D18, D20, D22, D24, D26, D28, D60, D62, D64, D66, D68
70	C05, C07, C09, C11, C13, C15, C18
73	A04, B13, B15, B17, B23, B27, B31, B35, C04, C06, C08, C10, C12, C14, C16, C21, C22, C23, C24, C25, C26
74	B01, B02, B03, B04, B05, B06, B07, B08, B16, B18, B20, B22, B24, B26, B28, B30, B32, B34, B36

Table 1.4: Gate numbers mapping to taxiway network nodes

Table 1.5 gives an overview of the runways that are activate during each part of the busy and quiet day. This data has been obtained from the runway activity tool at the LVNL website [1].

14th of December 2019				13th of September 2019			
Start time	**End time**	**Active runways**	**Equivalent nodes**	**Start time**	**End time**	**Active runways**	**Equivalent nodes**
00:00	03:10	18CA, 24D	12, 86	00:00	02:30	18RA, 18LD	1, 54
03:10	07:50	18RA, 24D	1, 86	02:30	05:00	18RA, 18CD	1, 15
07:50	08:00	18RA, 24D, 18LD	1, 54, 86	05:00	06:30	36LD, 36CA	1, 15
08:00	08:45	18RA, 24D, 18LD, 27A	1, 33, 54, 86	06:30	07:40	36LD, 36CD, 36RA	1, 12, 54
08:45	10:40	18RA, 24D, 27A	1, 86, 33	07:40	09:35	36LD, 36CA, 36RA	1, 15, 54
10:40	11:25	27A, 24D, 18LD	33, 54, 86	09:35	11:15	36LD, 36CD, 36RA	1, 12, 54
11:25	12:20	24D, 27D, 22A	86, 94, 97	11:15	11:50	36LD, 36CA, 36RA	1, 15, 54
12:20	13:00	24D, 27A	33, 86	11:50	13:10	36LD, 36CD, 36RA	1, 12, 54
13:00	14:15	24D, 27D, 22A	86, 94, 97	13:10	13:50	36LD, 36CA, 36RA	1, 15, 54
14:15	15:00	24D, 27A, 18RA	1, 33, 86	13:50	15:10	36LD, 36CD, 36RA	1, 12, 54
15:00	16:20	24D, 27D, 22A	86, 94, 97	15:10	16:20	36LD, 36CA, 36RA	1, 15, 54
16:20	16:55	18RA, 24D, 27A	1, 33, 86	16:20	18:20	36LD, 36CD, 36RA	1, 12, 54
16:55	17:40	24D, 27A	33, 86	18:20	20:30	36LD, 36CA, 36RA	1, 15, 54
17:40	18:15	24D, 27D, 22A	86, 94, 97	20:30	22:40	36LD, 36CD, 36RA	1, 12, 54
18:15	21:30	24D, 27A	33, 86	22:40	23:55	36LD, 36CA	1, 15
21:30	22:55	24D, 18RA, 18LD	1, 54, 86				
22:55	23:55	24D, 18RA	1, 86				

Table 1.5: Active runways and nodes during the quiet (left) day and busy (right) day

[1] https://en.lvnl.nl/environment/runway-use

2

Results Vehicle Routing Model

This section gives the additional results of the vehicle routing model. First we show the preliminary data analysis performed on the flight data. Secondly, we give an overview of the taxi routes followed by the aircraft. Then we compare the moving averages of ET and conventional taxiing and show the average taxi times per hour for each runway mode. Lastly, we present three screenshots of the animation used to test the vehicle routing model results.

2.1. Preliminary data analysis

Figure 2.1 gives an overview of preliminary data analysis performed on the flight schedule data. It shows the number of arrivals and departures within every 15 minutes during the quiet day at AAS. It can be seen that arrival peaks are followed by departure peaks and vice versa.

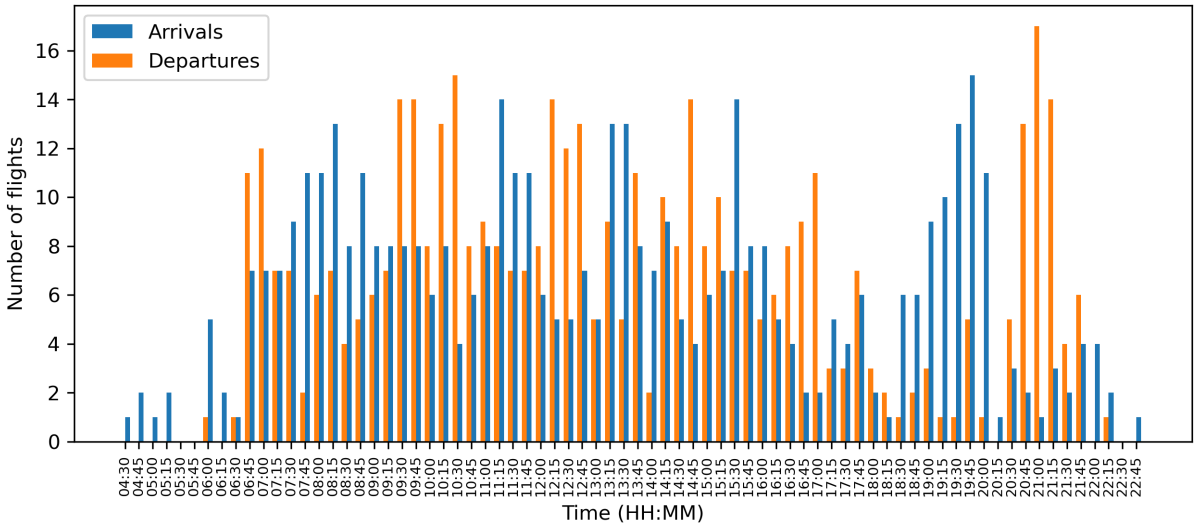

Figure 2.1: Arrivals and departures per 15 minutes on the 14th of December 2019, excluding very quiet time periods before 04:30 AM and after 22:45 PM

Figure 2.2 gives an overview of the arrivals and departures within every 15 minutes during the busy day at AAS. It can be seen that arrival peaks are again followed by departure peaks and vice versa.

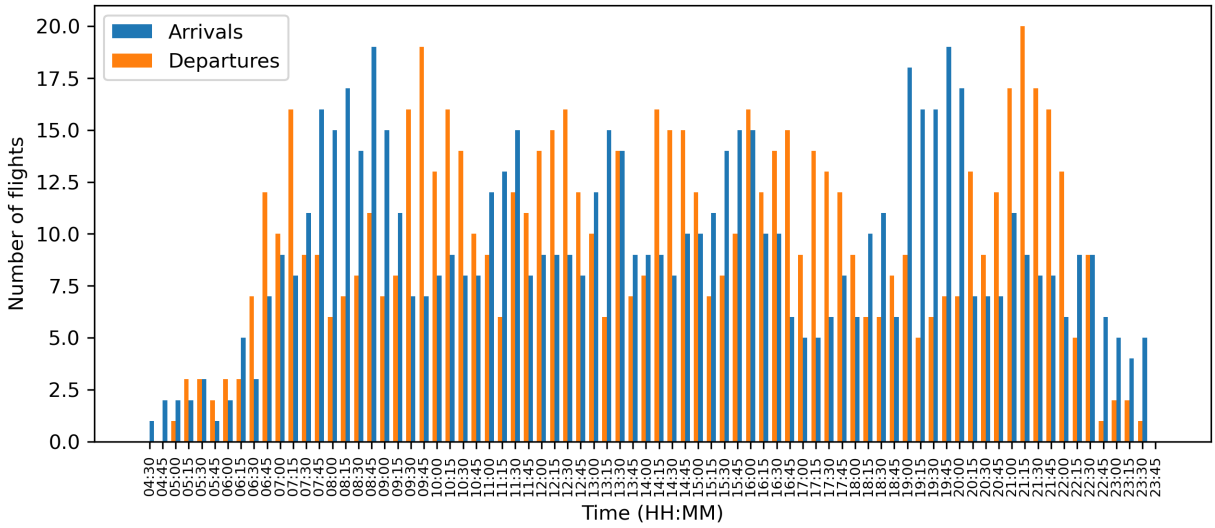

Figure 2.2: Arrivals and departures per 15 minutes on the 13th of September 2019, excluding very quiet time periods before 04:30 AM and after 23:45 PM

2.2. Routes

For each runway mode, two figures are shown: the left one showing the routes belonging to the electrically taxiing aircraft and the right one showing the routes belonging to the conventionally taxiing aircraft. These pairs of figures are compared in order to show the difference between the model outcome for electrically and conventionally taxiing aircraft. Only the relevant gate and runway node numbers are shown; the other node numbers are left out for the sake of readability and can be found in the figures displaying $T(N_T, E_T, d_T(e), v_T(e))$ and $S(N_S, E_S, G_S, d_S(e), v_S)$ in the paper.

2.2.1. 14th of December 2019

Figure 2.3 and 2.4 show the routes chosen for the aircraft taxiing from node 1 to the relevant gate nodes. Gate nodes 36 to 64 are covered by the clockwise taxi route and the others by the anti-clockwise taxi route. The main difference between the taxi routes chosen by the two types of taxiing is the use of the anti-clockwise taxi route going around the Zwanenburg runway. This route is used once, by an N aircraft arriving during peak hours (around 08:00 AM). Furthermore, the electrically as well as the conventionally taxiing aircraft include node 16 in one of the their optimal routes. This is due to departing aircraft leaving nodes 72 and 73 at the time the taxiing aircraft coming from node 1 would have arrived there. For this reason, the aircraft makes a small detour from node 17 to node 16 to node 25 in order to arrive at the gate node at the right time to avoid conflicts with departing aircraft.

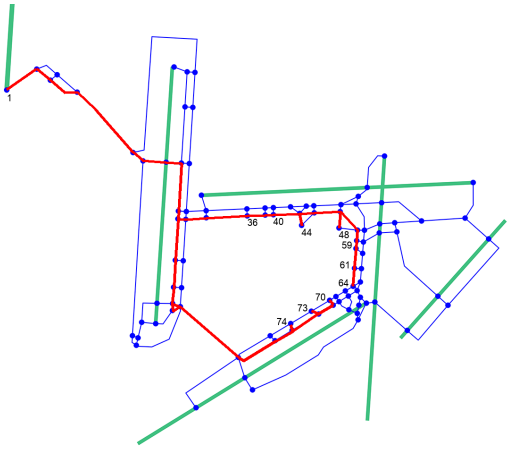

Figure 2.3: Routes used by ET aircraft arriving at runway 18R

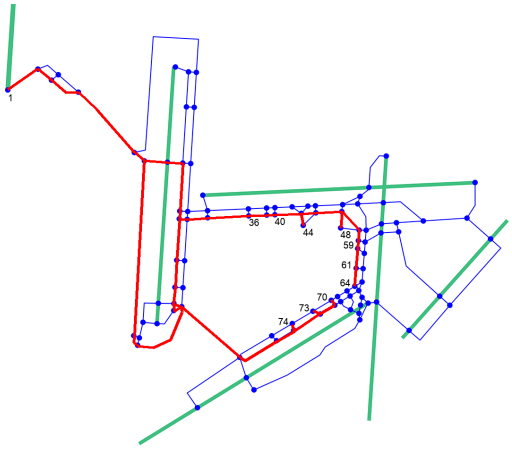

Figure 2.4: Routes used by conventional aircraft arriving at runway 18R

Figures 2.5 and 2.6 show the routes chosen for the aircraft taxiing from node 12 to the relevant gate nodes. No anomalies can be seen in these routes, since the aircraft only use the most optimal routes for each gate node and both the electrically and conventionally taxiing aircraft use the same routes.

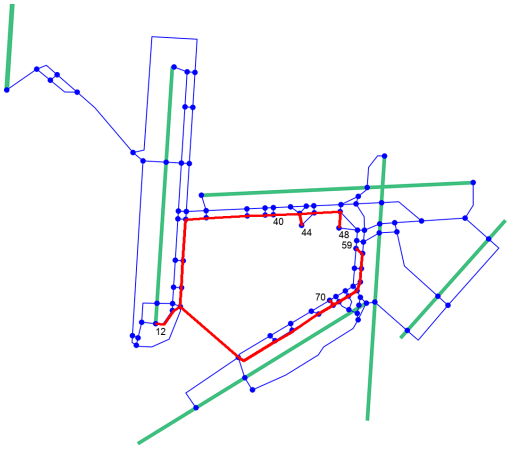

Figure 2.5: Routes used by ET aircraft arriving at runway 18C

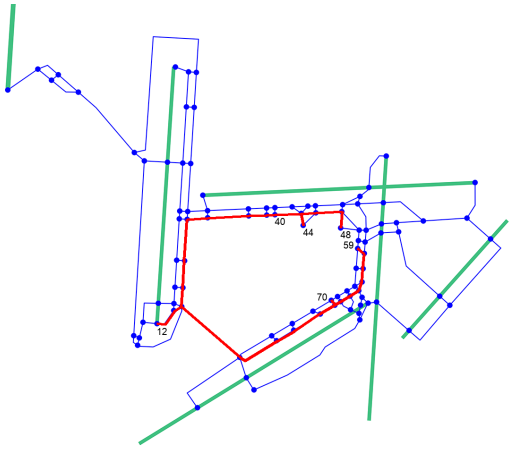

Figure 2.6: Routes used by conventional aircraft arriving at runway 18C

Figure 2.7 and 2.8 show the routes chosen for the aircraft taxiing from runway node 33 to the relevant gate nodes. Similar to figure 2.4, the conventional aircraft use node 16 in order to avoid conflicts with departing aircraft leaving nodes 73 and 74. This detour is made four times; this is probably due to the bigger separation distance required for conventional aircraft than for ET aircraft. Furthermore, the anti-clockwise route is used once to reach node 64. This is done to avoid conflicts with departing aircraft from gate nodes 36 to 61.

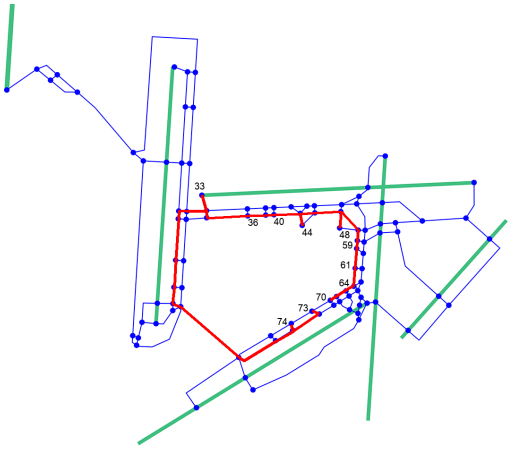

Figure 2.7: Routes used by ET aircraft arriving at runway 27

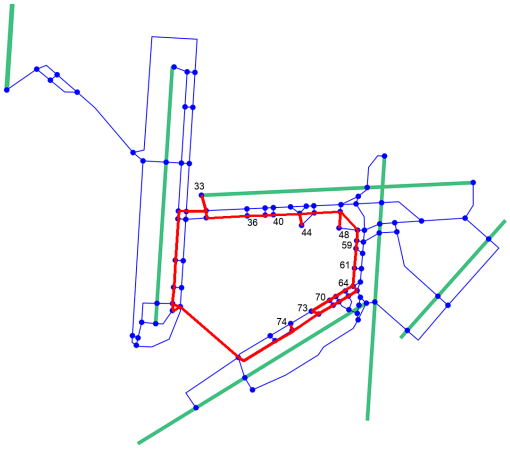

Figure 2.8: Routes used by conventional aircraft arriving at runway 27

Figures 2.9 and 2.10 show the routes chosen for the aircraft taxiing from runway node 97 to the relevant gate nodes. During the period of time runway 22 is active for arrivals, aircraft are also departing from runway 24 (see table 1.5). This creates a bottleneck around node 86. This is circumvented by the aircraft by using the northern route starting with node 96 in order to reach the northern gates. The aircraft also follow the route via node 81 to avoid traffic going to node 86. This does result in a situation in which the aircraft need to cross an active runway, but the time gained by using these detours is apparently worth the time penalties induced for crossing an active runway. One of the aircraft also chooses to taxi along the edge (43, 44) instead of 46-44, due to traffic coming from aircraft taxiing from gates 36, 40 and 44 to runways 27 and 24 for their departure. The only difference between electrically and conventionally taxiing aircraft is one electrically taxiing aircraft travelling the edges (85, 84) and (84, 83), which makes sure it avoids traffic around node 65. The same conventionally taxiing aircraft uses the route via nodes 81-83-82 due to its higher separation distance, which is slower but avoids any conflicts near nodes 85 and 86.

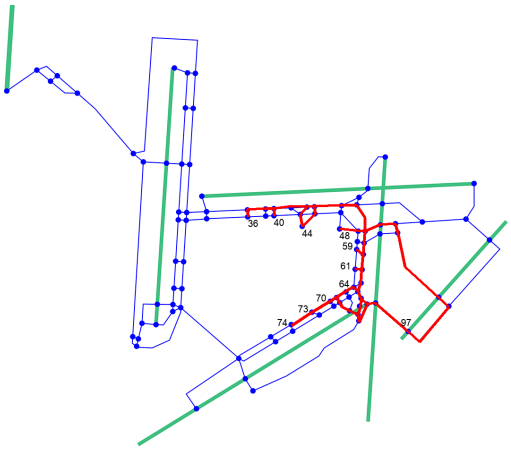

Figure 2.9: Routes used by ET aircraft arriving at runway 22

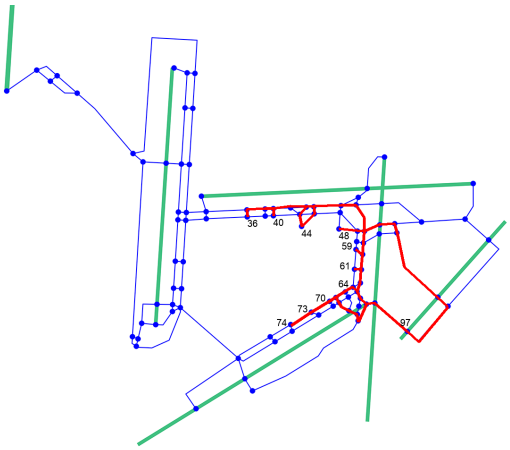

Figure 2.10: Routes used by conventional aircraft arriving at runway 22

Figures 2.11 and 2.12 show the routes chosen for the aircraft taxiing from runway node 100 to the relevant gate nodes. These routes are all routes one might expect since they cover the distance between runway and gate as quickly as possible. There are no differences between the ET and conventional taxi routes.

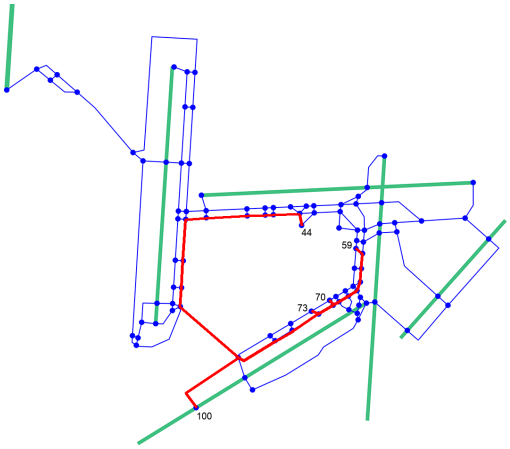

Figure 2.11: Routes used by ET aircraft arriving at runway 24

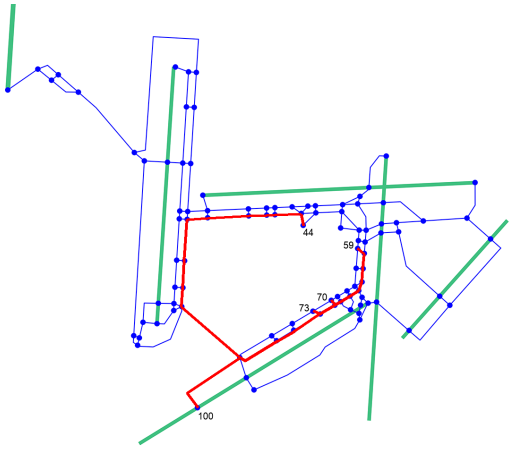

Figure 2.12: Routes used by conventional aircraft arriving at runway 24

Figures 2.13 and 2.14 show the routes chosen for the aircraft taxiing from the relevant gate nodes to runway node 54. The aircraft pick the optimal routes to node 54 and there are no differences between the ET and conventional taxi routes.

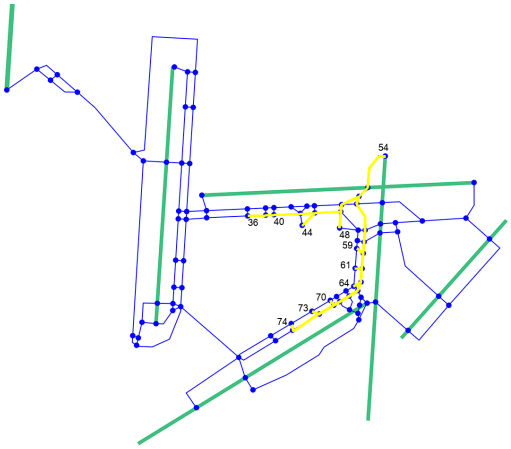

Figure 2.13: Routes used by ET aircraft departing from runway 18L

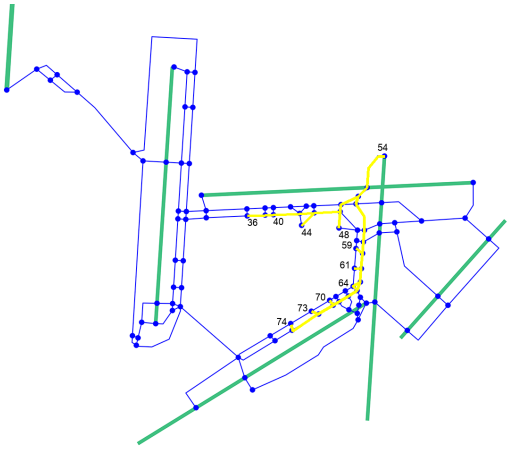

Figure 2.14: Routes used by conventional aircraft departing from runway 18L

Figures 2.15 and 2.16 show the routes chosen for the aircraft taxiing from the relevant gate nodes to runway node 86. It can be seen that, similar to figures 2.9 and 2.10, the bottleneck around node 86 leads to some sub-optimal routes to avoid any oncoming traffic travelling towards the gate section of the taxiway network. Furthermore, the aircraft leaving from node 44 very often choose to travel via node 43 instead of the slightly faster node 46 in order to avoid traffic. This is due to the fact that this part of the taxiway network is very busy during the entire day and runway 24 is used for departures during the entire day (see table 1.5). An interesting difference between the electrically and conventionally taxiing aircraft is that the former use node 66 in their optimal routes four times. This might be caused by the shift in flight schedule due to the addition of the ECDT and ET vehicle connection time to the electrically taxiing aircraft's earliest taxi time. It can also be caused by the smaller separation distance enabling the electrically taxiing aircraft to make a detour that eventually leads to an earlier arrival at runway node 86 compared to having to wait at the gate node.

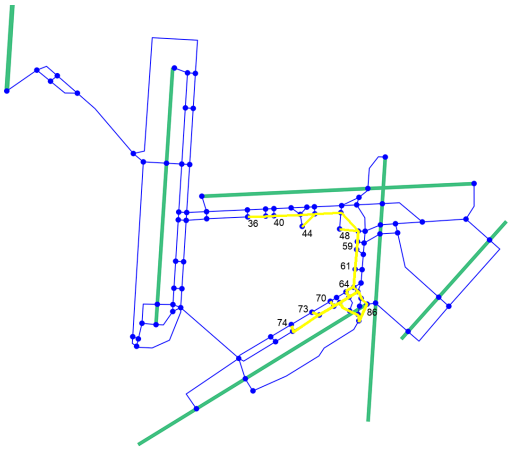

Figure 2.15: Routes used by ET aircraft departing from runway 24

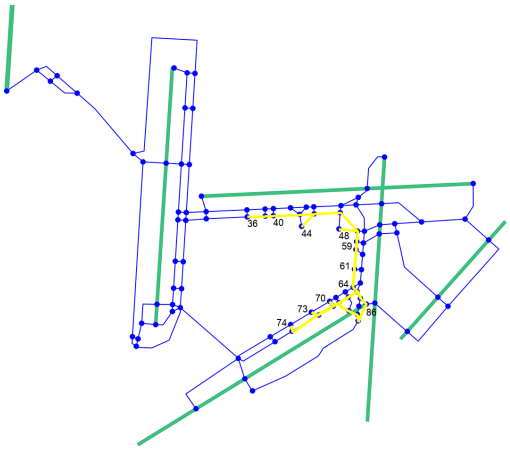

Figure 2.16: Routes used by conventional aircraft departing from runway 24

Figures 2.17 and 2.18 show the routes chosen for the aircraft taxiing from the relevant gate nodes to runway node 94. It can be seen that the 'Aalsmeerbaan' (i.e. runway 18L - 36R) is crossed at three different locations. The aircraft coming from gate nodes 36, 40 and 44 often use the taxi route via node 52 in order to get to node 94 as quickly as possible. These aircraft do have to avoid traffic coming from node 54, however. Edge (50, 51) is not used since this part of the taxiway network only allows traffic in the opposite direction. There are no differences between the ET and conventional taxi routes.

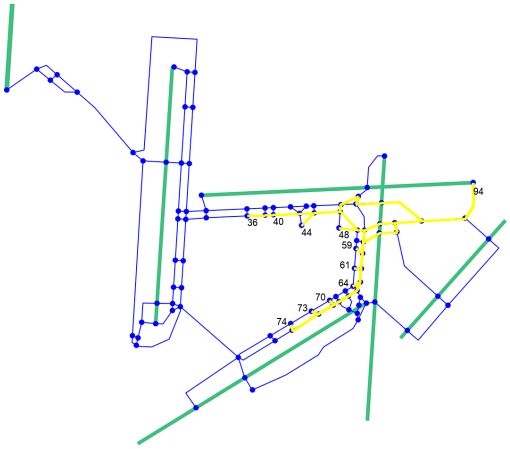

Figure 2.17: Routes used by ET aircraft departing from runway 27

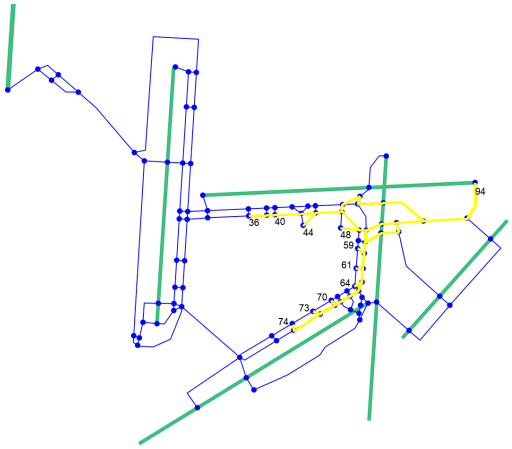

Figure 2.18: Routes used by conventional aircraft departing from runway 27

2.2.2. 13th of September 2019

Figures 2.19 and 2.20 show the routes chosen for the aircraft taxiing from runway node 1 to the relevant gate nodes. The routes chosen are the expected routes and there are no differences between the ET and conventional taxi routes.

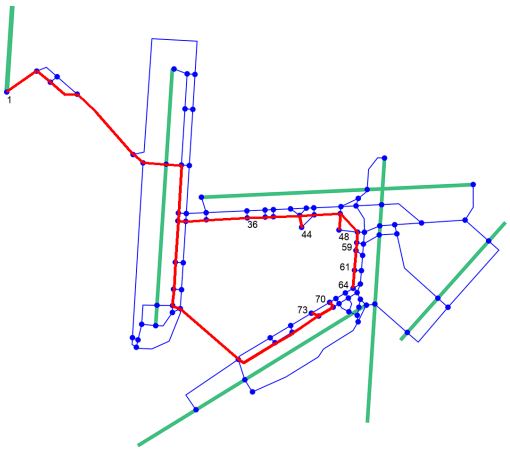

Figure 2.19: Routes used by ET aircraft arriving at runway 18R

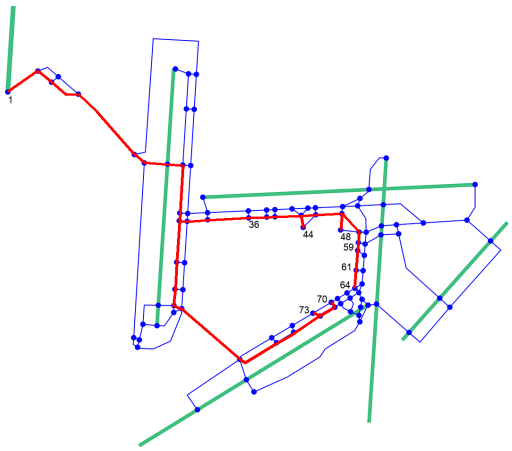

Figure 2.20: Routes used by conventional aircraft arriving at runway 18R

Figures 2.21 and 2.22 show the routes chosen for the aircraft taxiing from runway node 15 to the relevant gate nodes. The electrically taxiing aircraft use the expected routes, whereas the conventional taxiing aircraft use the anti-clockwise route to reach gate node 61 once and gate node 64 twice during the morning and early evening peak hours respectively. This is caused by the larger separation distance of conventionally taxiing aircraft, making it more difficult to fit each aircraft onto the busiest parts of the taxiway network.

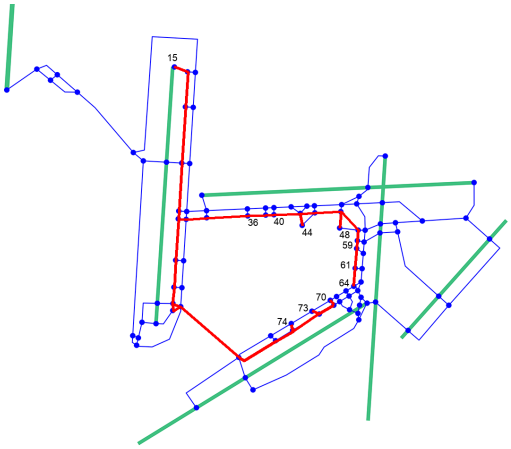

Figure 2.21: Routes used by ET aircraft arriving at runway 36C

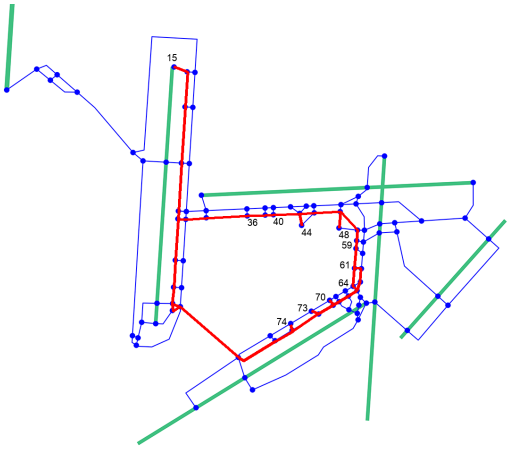

Figure 2.22: Routes used by conventional aircraft arriving at runway 36C

Figures 2.23 and 2.24 show the routes chosen for the aircraft taxiing from runway node 54 to the relevant gate nodes. Both the electrically and conventionally taxiing aircraft use two small detours, near gate node 44 and via node 51, to circumvent traffic at a moment during their routes.

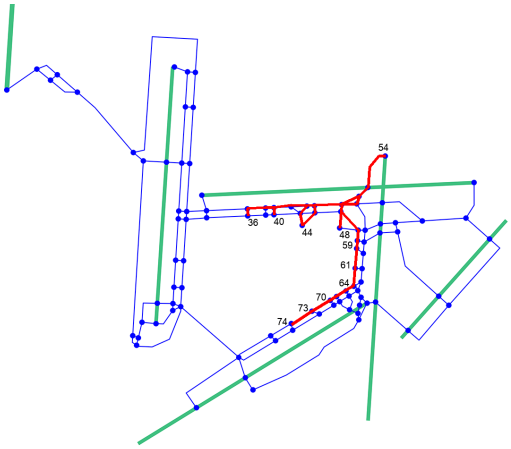

Figure 2.23: Routes used by ET aircraft arriving at runway 36R

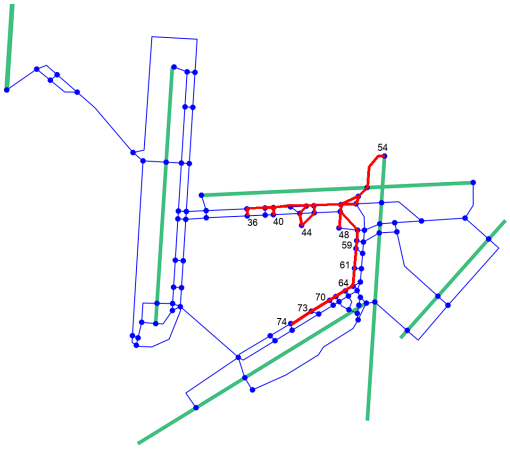

Figure 2.24: Routes used by conventional aircraft arriving at runway 36R

Figures 2.25 and 2.26 show the routes chosen for the aircraft taxiing from the relevant gate nodes to runway node 1. Both the electrically and conventionally taxiing aircraft use relatively straightforward routes. Conventional aircraft, however, do use more small detours, via nodes 46 and 52, to be able to adhere to their separation distance at all points during their taxi routes.

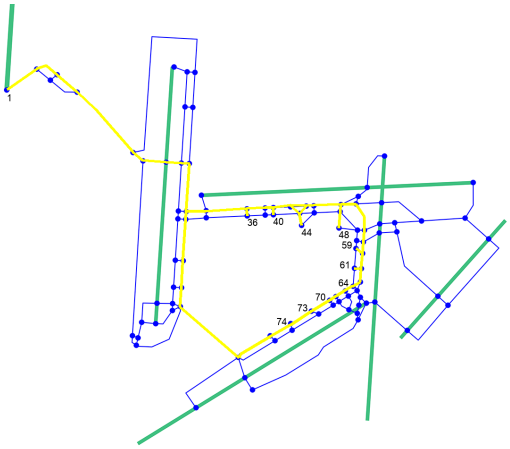

Figure 2.25: Routes used by ET aircraft departing from runway 36L

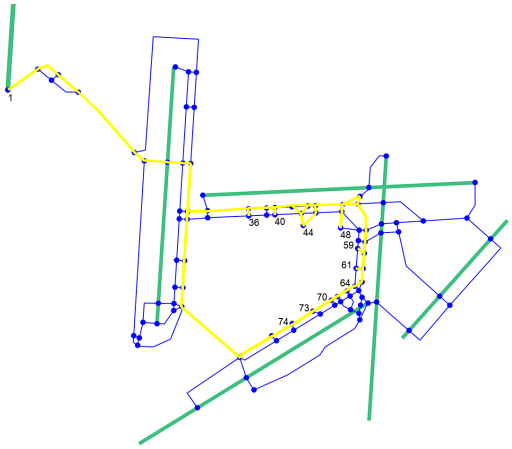

Figure 2.26: Routes used by conventional aircraft departing from runway 36L

Figures 2.27 and 2.28 show the routes chosen for the aircraft taxiing from the relevant gate nodes to runway node 12. The routes chosen are the shortest path, except for a small detour used by 2 conventionally taxiing aircraft via node 17. This detour is used to avoid conflicts with aircraft coming from the northern (anti-clockwise) route.

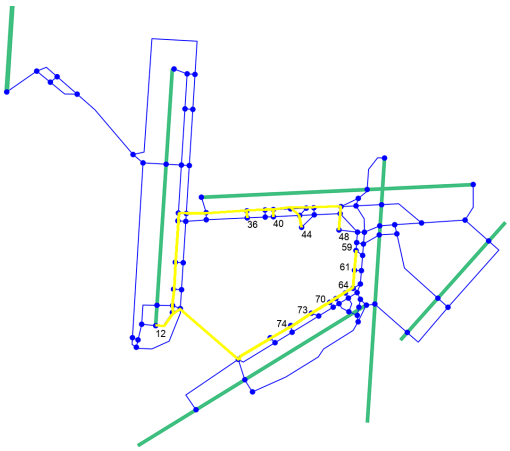

Figure 2.27: Routes used by ET aircraft departing from runway 36C

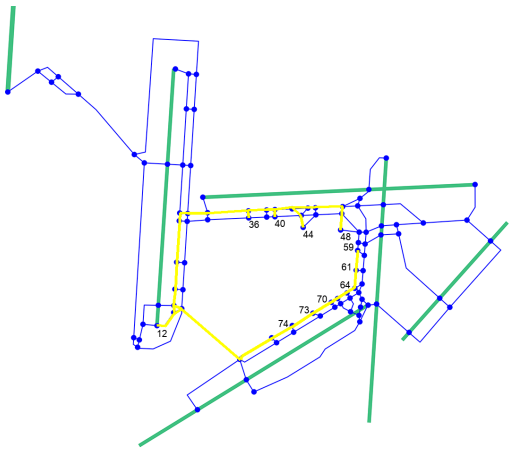

Figure 2.28: Routes used by conventional aircraft departing from runway 36C

Figures 2.29 and 2.30 show the routes chosen for the aircraft taxiing from the relevant gate nodes to runway node 15. These routes are very straightforward and only cover the two closest gate nodes.

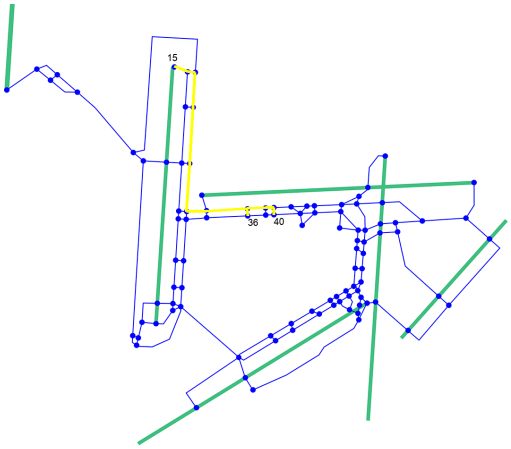

Figure 2.29: Routes used by ET aircraft departing from runway 18C

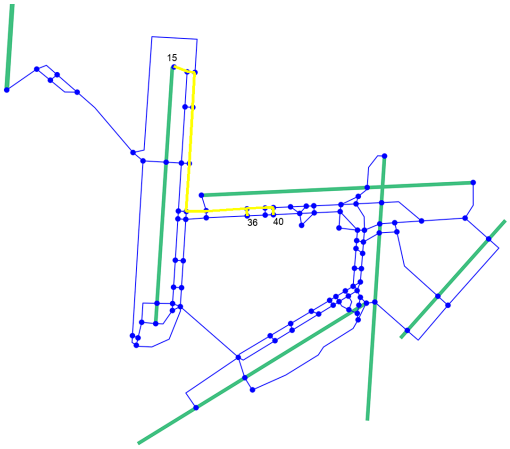

Figure 2.30: Routes used by conventional aircraft departing from runway 18C

Figures 2.31 and 2.32 show the routes chosen for the aircraft taxiing from the relevant gate nodes to runway node 15. The routes are as expected except for the anti-clockwise route used by the conventionally taxiing aircraft. The figure, however, gives a slightly exaggerated image of the actual situation, since only one aircraft taxis from gate node 61 to runway node 33. This aircraft uses the slightly longer detour via node 43 in order to avoid traffic near runway node 33.

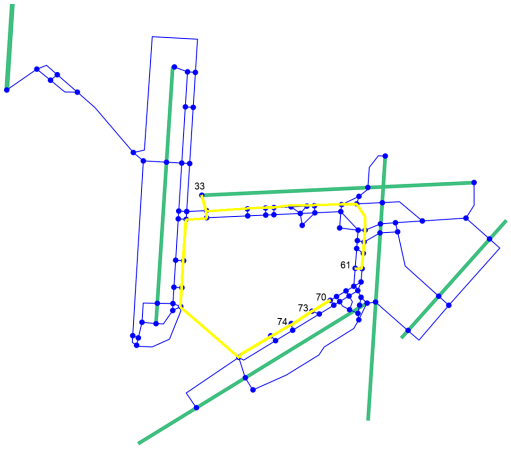

Figure 2.31: Routes used by ET aircraft departing from runway 9

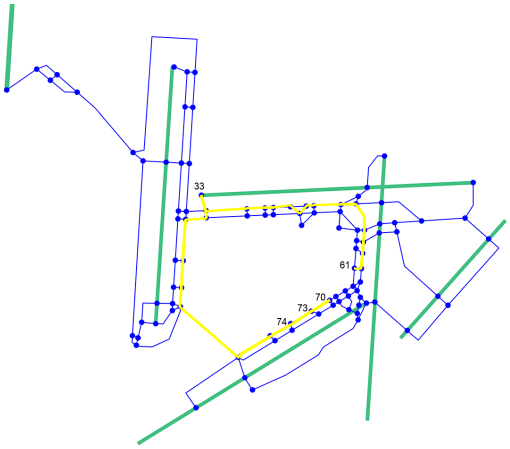

Figure 2.32: Routes used by conventional aircraft departing from runway 9

2.3. Moving average

This subsection presents the moving average figures for the quiet and the busy day.

2.3.1. 14th of December 2019

In order to get an idea of the taxi times during the day, the aircraft are split in departures and arrivals and ordered from earliest to latest start time. Then we calculate the moving average of the taxi time for the electrically and conventionally taxiing aircraft by using equation (2.1), with $\overline{taxi}^l$ being the moving average up to aircraft l.

$$\overline{taxi}^l = \frac{\overline{taxi}^{l-1} \cdot (l-1) + taxi^l}{l} \tag{2.1}$$

The moving averages of the taxi time per aircraft for the electrically taxiing arriving aircraft, electrically taxiing departing aircraft, conventionally taxiing arriving aircraft and conventionally taxiing departing aircraft

are plotted in figure 2.33. It can be seen that the electric and conventional arrivals and departures graphs have the same shape, indicating a relatively constant delay. This is also reflected when looking at the average delay of the arrivals and departures, which are equal to **159 seconds** and **296 seconds** respectively. These values are (just) below the ESUT of 300 seconds and the ECDT of 180 seconds, which is a result that can be expected. This is due to the higher taxi velocity and the lower separation distance of the electrically taxiing aircraft.

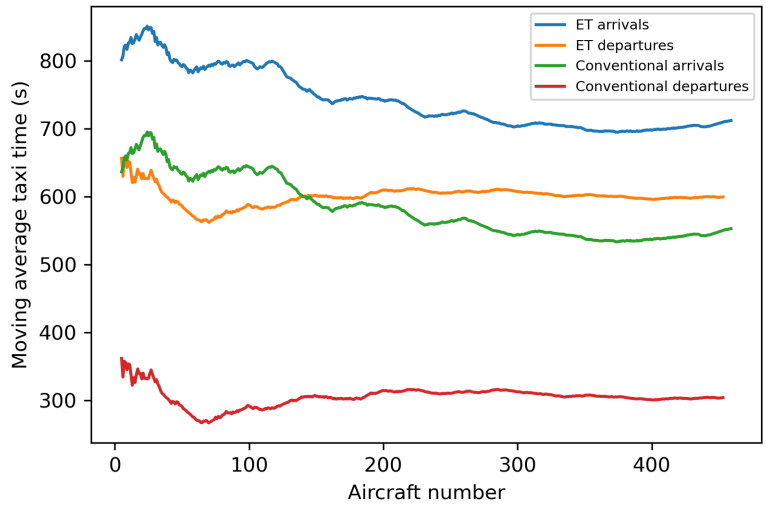

Figure 2.33: Moving average of taxi times for each aircraft while taxiing conventionally and electrically

2.3.2. 13th of September 2019

Similar to the results from section 2.3.1, the electric and conventional graphs of the moving average of the delay have the same shape. This indicates that the ESUT of 300 seconds and ECDT of 180 seconds are still the dominant factors. The average delay of the arriving and departing aircraft are equal to **162 seconds** and **268 seconds** respectively. This shows that the electrically taxiing aircraft are able to win back a limited part of their delay.

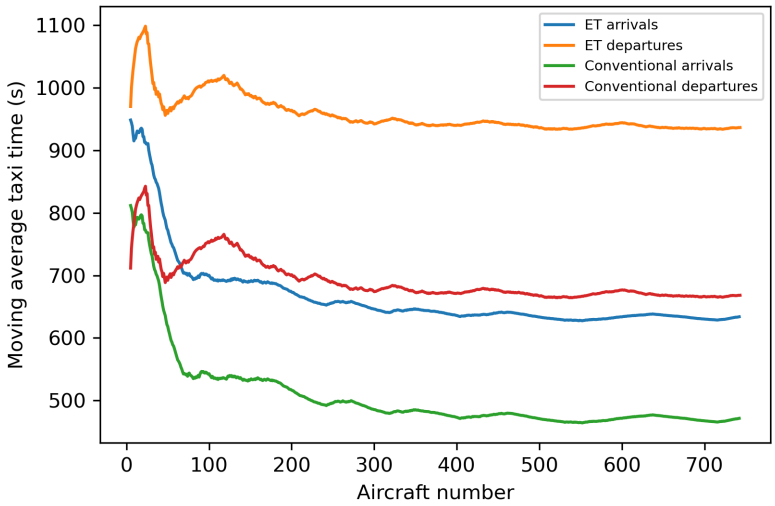

Figure 2.34: Moving average of taxi times for each aircraft while taxiing conventionally and electrically on the 13th of September 2019

2.4. Time windows

This section gives an overview of the taxi times per time window for each of the runway modes.

2.4.1. 14th of December 2019

Table 2.1 gives an overview of the average taxi time of electrically taxiing aircraft arriving at or departing from a certain runway spread over the entire day. Table 2.1 is generated to see if taxi times significantly change during the day due to increased traffic during peak hours or decreased traffic during quiet periods. An average for a certain time window is only shown if the time window holds at least three aircraft that make use of the same runway mode, in order to avoid outliers giving the wrong impressions of average taxi times during a certain time window. For this reason, runway modes 18CA and 24A did not have any entries and have been left out of the table. Furthermore, average taxi times in each column that are significantly higher than the other taxi times in that same column are highlighted.
From the table, it cannot be concluded that taxi times during certain hours are significantly higher than during other hours. The most important reason for this is the fact that aircraft taxi to and from different gates. The gate - runway combinations mainly determine how long the aircraft need to taxi; this is likely to obscure the influence of the peak hours. A fair comparison would be to only compare aircraft taxiing from a certain runway to one specific gate (or vice versa). However, the maximum number of aircraft on the 14th of December that use the same runway-gate combination is 62. This is not enough to draw any conclusions from, since divided over the entire day these aircraft do not provide enough taxi times per time window to produce meaningful averages.

Time window	Average taxi time 18RA [s]	Average taxi time 27A [s]	Average taxi time 18LD [s]	Average taxi time 24D [s]	Average taxi time 27D [s]	Average taxi time 22A [s]
00:00 - 01:00	-	-	-	-	-	-
01:00 - 02:00	-	-	-	-	-	-
02:00 - 03:00	-	-	-	-	-	-
03:00 - 04:00	-	-	-	-	-	-
04:00 - 05:00	885	-	-	-	-	-
05:00 - 06:00	840	-	-	-	-	-
06:00 - 07:00	865	-	**759**	500	-	-
07:00 - 08:00	913	612	724	508	-	-
08:00 - 09:00	947	632	-	508	-	-
09:00 - 10:00	927	580	724	519	-	-
10:00 - 11:00	-	537	-	553	742	555
11:00 - 12:00	951	637	723	565	-	505
12:00 - 13:00	858	579	-	543	769	533
13:00 - 14:00	945	617	-	534	725	463
14:00 - 15:00	-	-	-	546	750	524
15:00 - 16:00	936	640	-	547	-	573
16:00 - 17:00	-	639	-	525	743	-
17:00 - 18:00	-	535	-	544	**783**	**670**
18:00 - 19:00	-	639	-	**571**	-	-
19:00 - 20:00	**960**	572	-	540	-	-
20:00 - 21:00	**982**	615	713	503	-	-
21:00 - 22:00	903	-	714	529	-	-
22:00 - 23:00	938	-	-	**713**	-	-
23:00 - 23:59	907	-	-	-	-	-

Table 2.1: Average taxi times of arriving or departing aircraft for each runway mode

2.4.2. 13th of September 2019

Table 2.2 shows the same results as table 2.1 for the busy day. Similarly, it is not possible to draw any conclusions from the data, except that the difference in taxi time during peak hours does not outweigh the taxi time differences due to different gate allocations of aircraft. The maximum number of aircraft on the 13th of September that use the same runway-gate combination is 142, which is significantly larger than for the quiet

day. The runway-gate node pair in question consists of runway node 53 and gate node 72. However, further analysis shows that there is no difference between the average taxi times for the different time windows.

Time window	Average taxi time 18RA [s]	Average taxi time 36LD [s]	Average taxi time 36CD [s]	Average taxi time 36CA [s]	Average taxi time 9D [s]	Average taxi time 36RA [s]
00:00 - 01:00	929	-	-	-	-	-
01:00 - 02:00	953	-	-	-	-	-
02:00 - 03:00	-	-	-	-	-	-
03:00 - 04:00	-	-	-	-	-	-
04:00 - 05:00	848	-	-	-	-	-
05:00 - 06:00	-	**1124**	-	667	-	-
06:00 - 07:00	-	**1131**	667	694	-	518
07:00 - 08:00	-	1067	672	**825**	-	535
08:00 - 09:00	-	1075	-	787	-	568
09:00 - 10:00	-	1081	674	745	-	548
10:00 - 11:00	-	1051	713	-	-	542
11:00 - 12:00	-	1083	**727**	779	-	564
12:00 - 13:00	-	1066	704	-	-	531
13:00 - 14:00	-	1024	715	796	-	556
14:00 - 15:00	-	1080	**736**	-	788	561
15:00 - 16:00	-	1042	-	791	-	547
16:00 - 17:00	-	1108	701	808	-	553
17:00 - 18:00	-	1118	676	-	-	539
18:00 - 19:00	-	1036	-	711	-	526
19:00 - 20:00	-	1020	-	794	-	580
20:00 - 21:00	-	1075	703	799	-	558
21:00 - 22:00	-	1090	711	-	-	544
22:00 - 23:00	-	1044	694	770	-	559
23:00 - 23:59	-	1000	-	782	-	-

Table 2.2: Average taxi times of arriving or departing aircraft for each runway mode

2.5. Visualisations

This section presents screenshot of the visualisation tool built to visualise the aircraft taxi movements across the airport's surface. The screenshots shown in figures 2.35, 2.36 and 2.37 are taken from the visualisation of the aircraft taxiing electrically on the 13th of September. The number in the upper right corner shows the time of the day and the colour of the aircraft shows whether an aircraft arrives (red) or departs (green). The numbers printed next to each aircraft allow us to know which aircraft in the flight schedule we see.

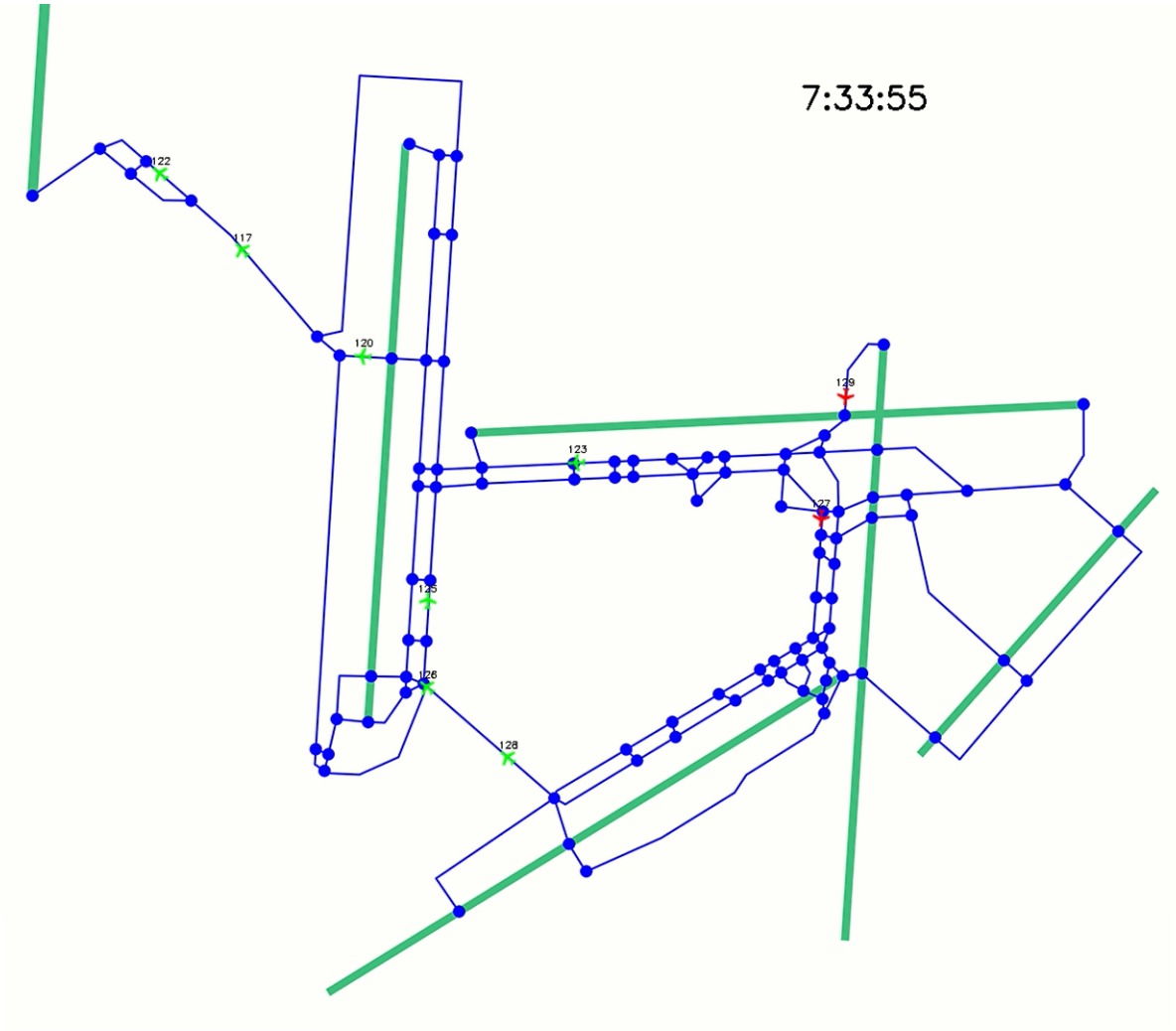

Figure 2.35: Screenshot visualisation tool 13th of September 07:33:55

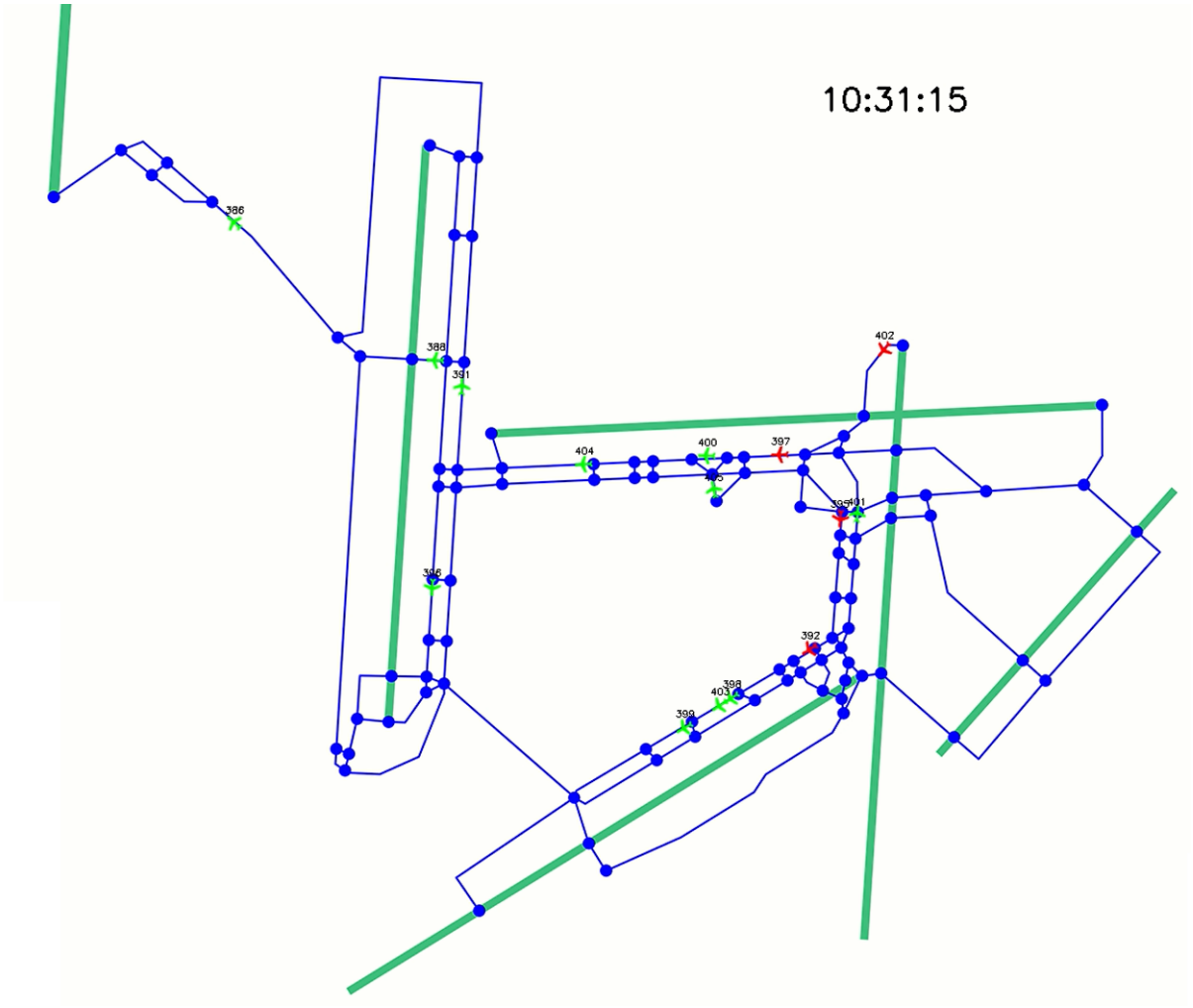

Figure 2.36: Screenshot visualisation tool 13th of September 10:31:15

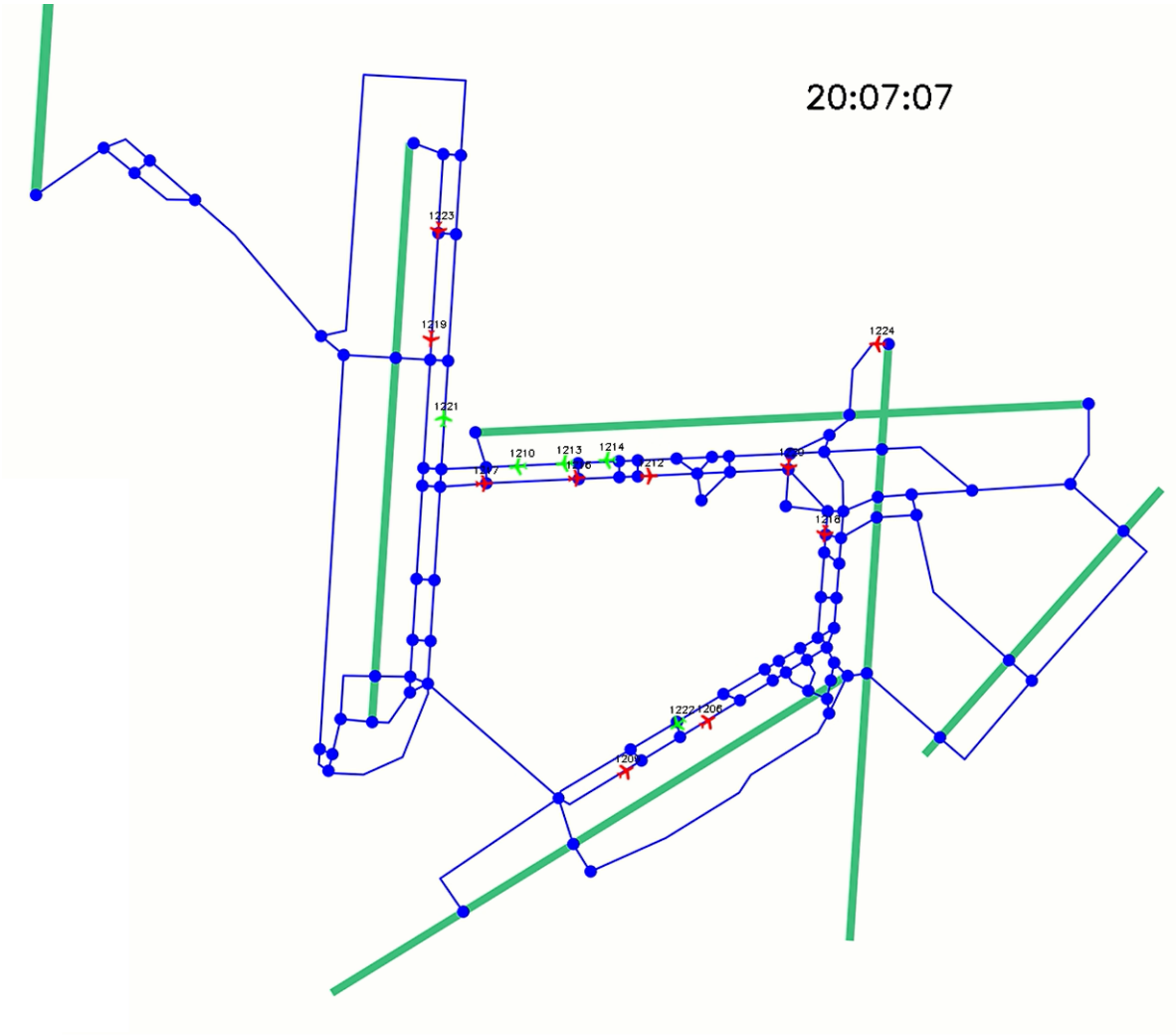

Figure 2.37: Screenshot visualisation tool 13th of September 20:07:07

3

Sensitivity Analysis

In this chapter, we show additional results of the sensitivity analysis for the slow and fast case in 3.1 and the low and high case in section 3.2. Then, section 3.3 explains an additional sensitivity analysis that investigates the effect of both increasing the maximum velocity at which aircraft can be towed by ET vehicles and the battery capacity and maximum power of these ET vehicles.

3.1. Taxi velocity

In this section, we present the additional results for the sensitivity analysis in which we decrease and increase taxi velocity.

3.1.1. Results 13th of September

This section presents the results for the slow and fast case for the busy day at AAS. Similar to the results of the quiet day, the results in table 3.1 are very logical. The fast case leads to shorter taxi times and smaller delays. The number of minutes decrease in delay mainly depends on the extent to which the electrically taxiing aircraft is allowed to drive at its higher maximum velocity.

	Runway	**Aalsmeer**	**Buitenveldert**		**Zwanenburg**			**Polder**		**Total**
	Mode	36A	27A	09D	36A	18D	36D	18A	36D	-
	#Flights	486	1	7	229	2	262	27	473	1487
Slow	$\overline{\textbf{taxi}}_{\textbf{E}}$ **[s]**	556	650	800	829	725	713	974	1137	820
	$\overline{\textbf{taxi}}_{\textbf{C}}$ **[s]**	376	470	506	639	425	407	768	817	570
D [s]		180	180	294	190	300	307	206	320	250	
Fast	$\overline{\textbf{taxi}}_{\textbf{E}}$ **[s]**	550	660	791	778	695	700	907	1065	783
	$\overline{\textbf{taxi}}_{\textbf{C}}$ **[s]**	376	470	506	639	425	407	768	817	570
D [s]		174	190	286	139	270	293	139	248	213	

Table 3.1: Overview of results for the slow and fast case per runway on the 13th of September 2019

We also use the routes generated for the two new cases to generate the towing tasks for the assignment model. The results of the assignment model for the busy day are shown in table 3.2. It can be seen that the new routes do not change the number of ET vehicles required for all three types of ET vehicles. This is due to the fact that the increase in velocity leads to a decrease in taxi time, but also to an increase in energy required. Apparently, these two factors outweigh each other and the results stay the same. Total solve times are 4938 and 5122 seconds for the low and high case respectively.

	Slow case			Base case			Fast case		
ET vehicle type	**1**	**2**	**3**	**1**	**2**	**3**	1	**2**	**3**
#ET Vehicles 13th of September	78	17	3	77	17	3	77	17	3

Table 3.2: Number of ET vehicles for all vehicle routing model cases

3.1.2. Moving average plots quiet and busy day

This section shows additional graphs for the slow and fast case of the sensitivity analysis. Figures 3.1, 3.2, 3.1 and 3.4 show the moving average graphs for the quiet and busy day for both the slow and fast case.

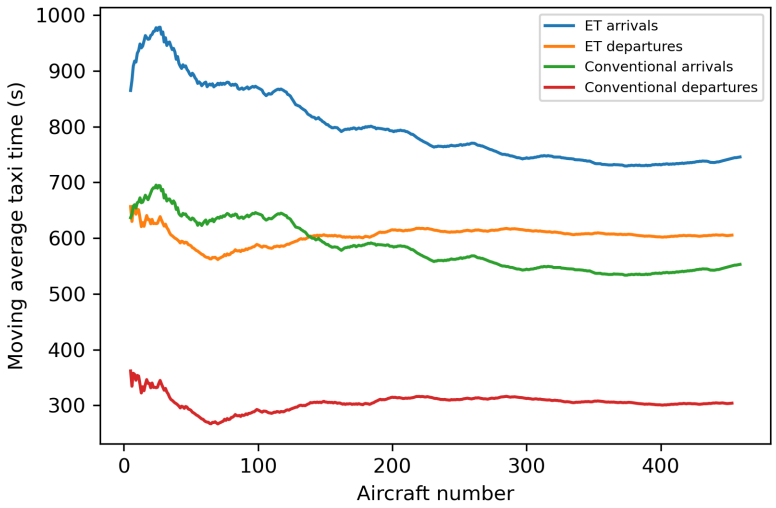

Figure 3.1: Moving average of taxi times on the 14th of December for the slow case

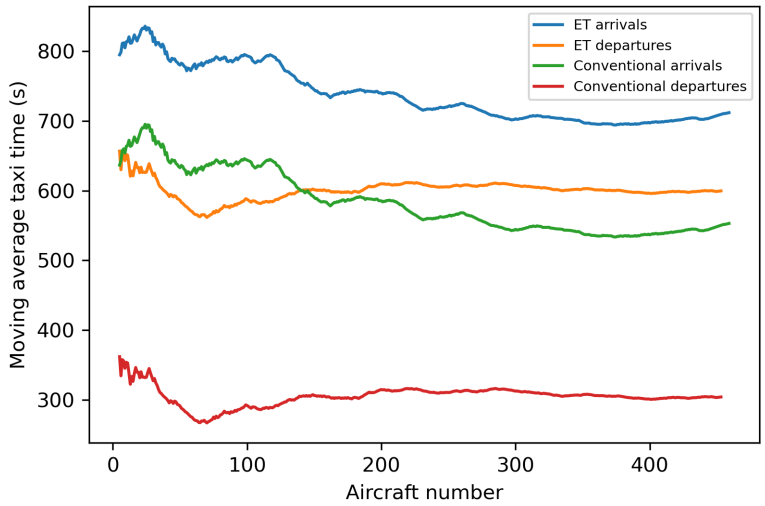

Figure 3.2: Moving average of taxi times on the 14th of December for the fast case

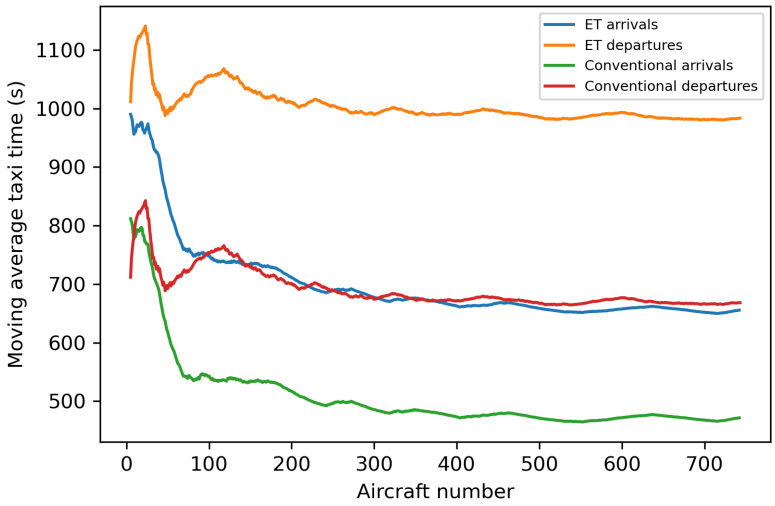

Figure 3.3: Moving average of taxi times on the 13th of September for the slow case

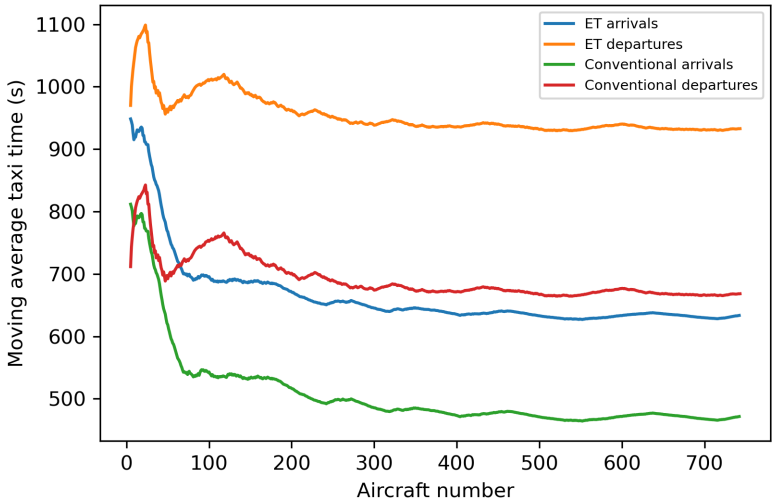

Figure 3.4: Moving average of taxi times on the 13th of September for the fast case

3.1.3. Assignment model

Figures 3.5, 3.6, 3.7 and 3.8 show the overviews of the tasks performed per ET vehicle for the busy and quiet day and both the slow and fast case.

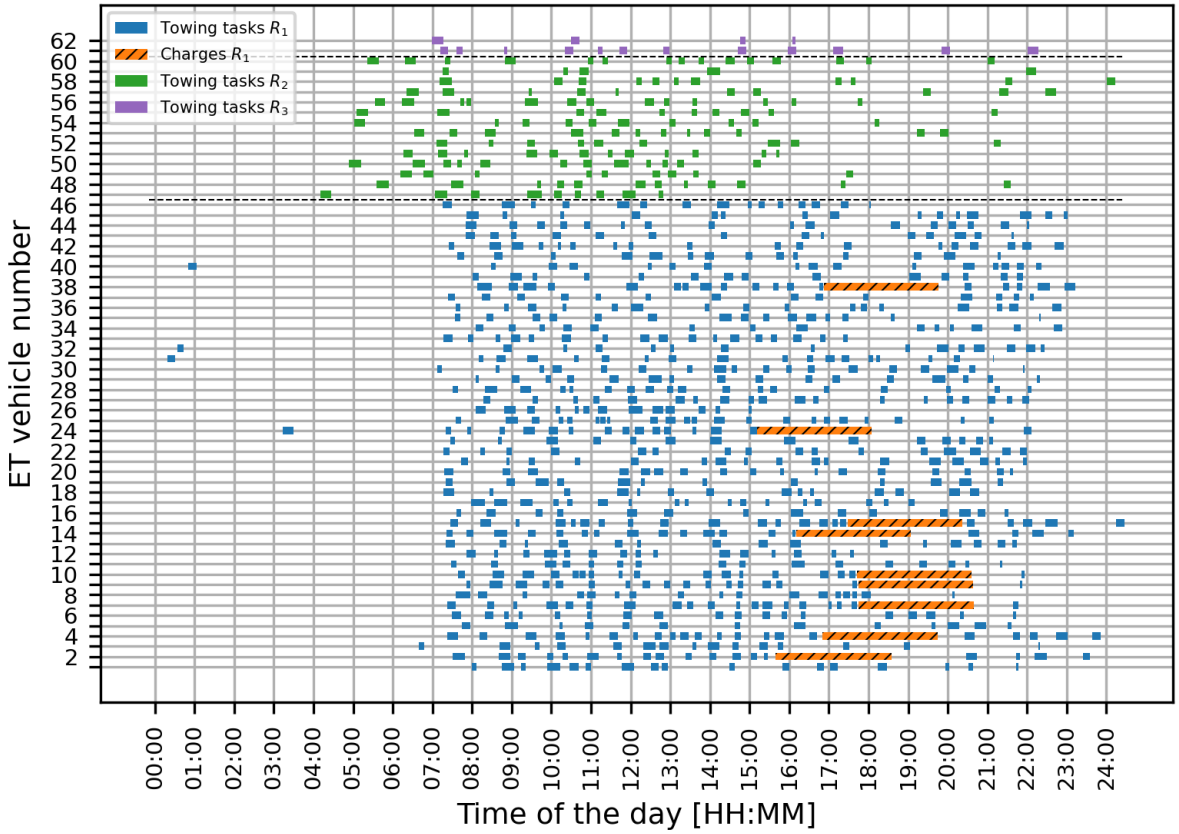

Figure 3.5: Results assignment model on the 14th of December for the slow case

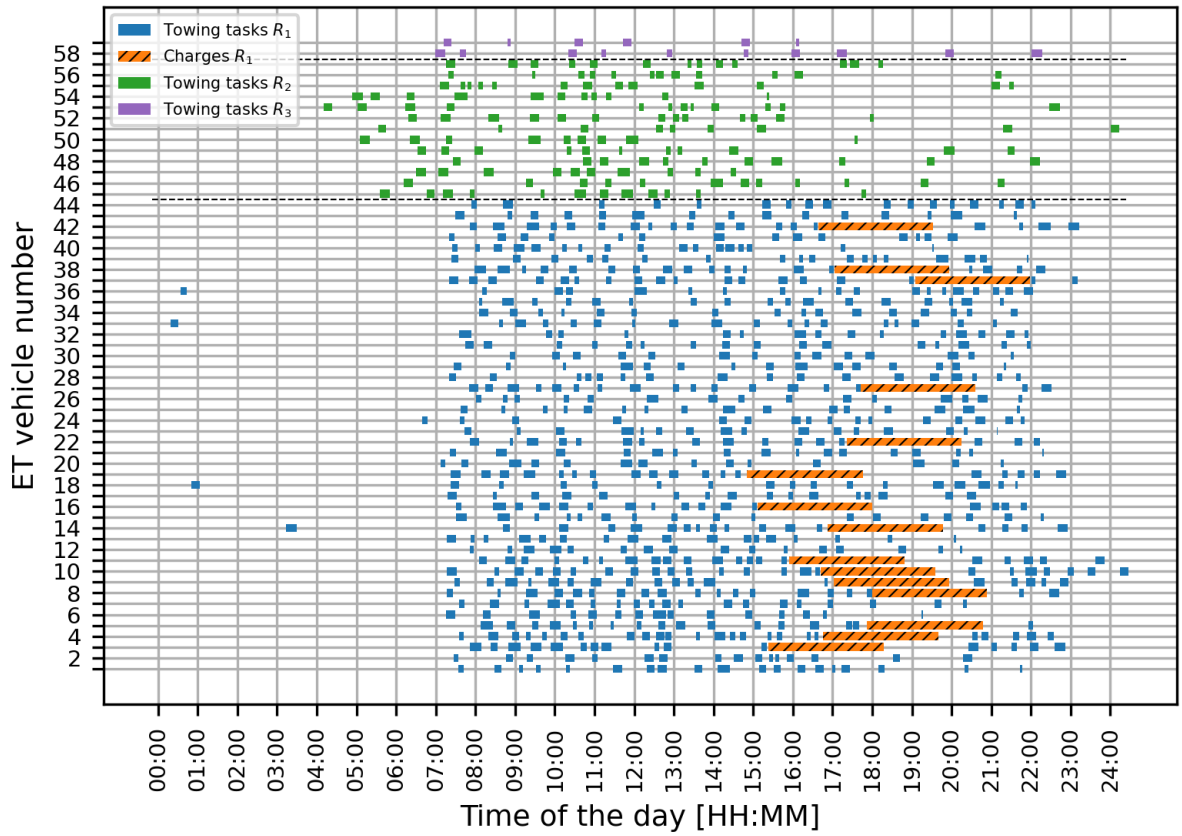

Figure 3.6: Results assignment model on the 14th of December for the fast case

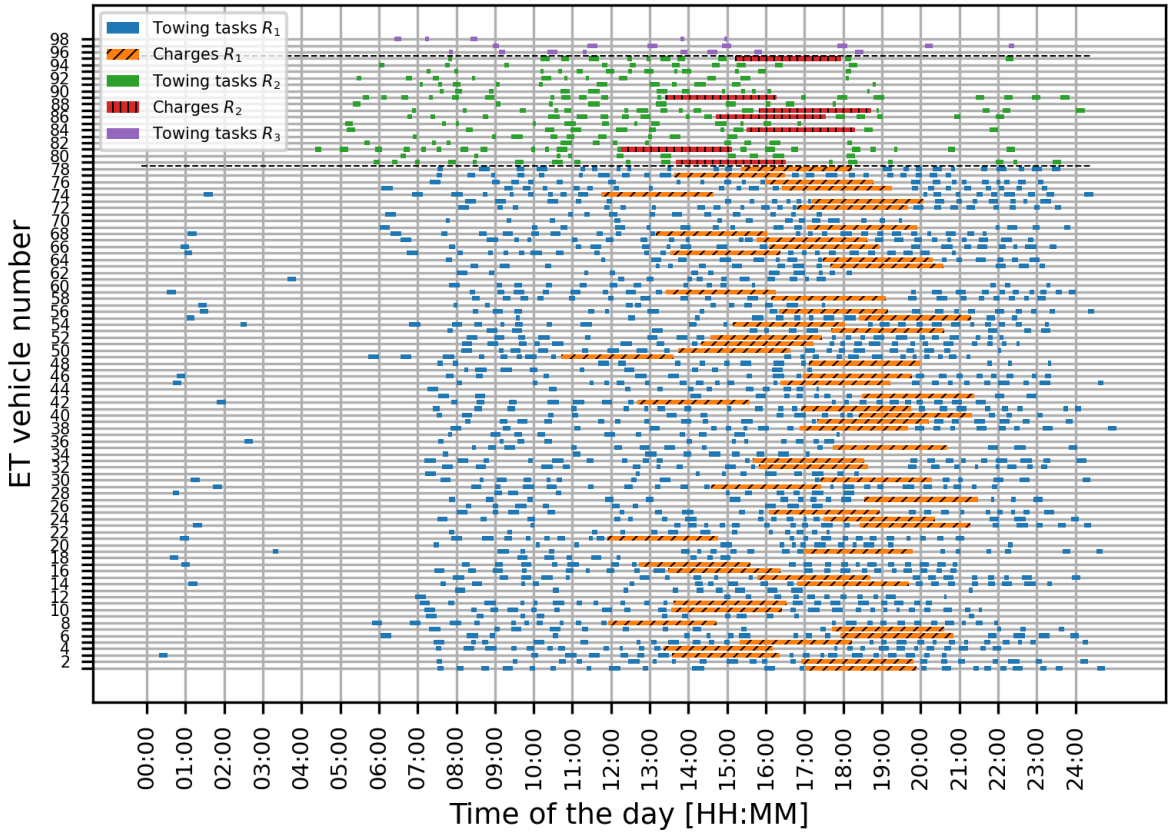

Figure 3.7: Results assignment model on the 13th of September for the slow case

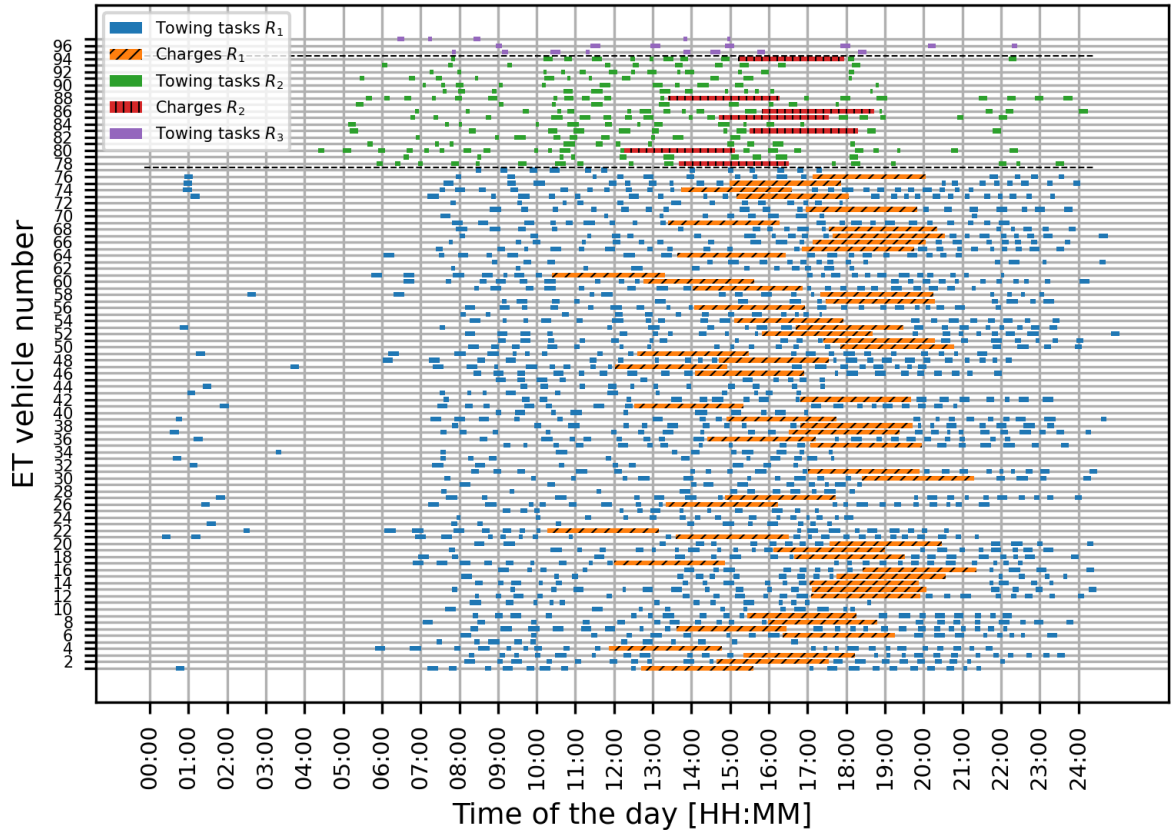

Figure 3.8: Results assignment model on the 13th of September for the fast case

3.2. Battery capacity

3.9, 3.11, 3.10 and 3.12 show the overviews of the tasks performed per ET vehicle for the busy and the quiet day and both the low and high battery capacity and maximum power cases.

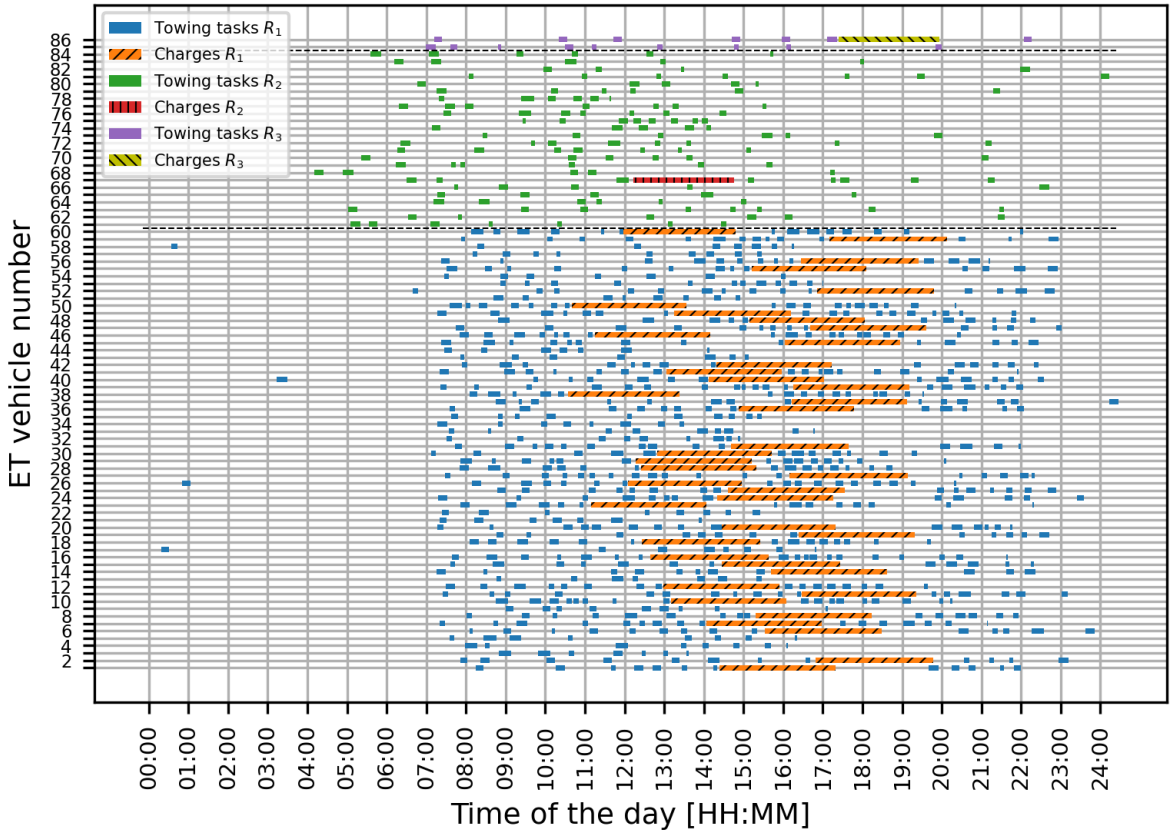

Figure 3.9: Results assignment model on the 14th of December for battery the low case

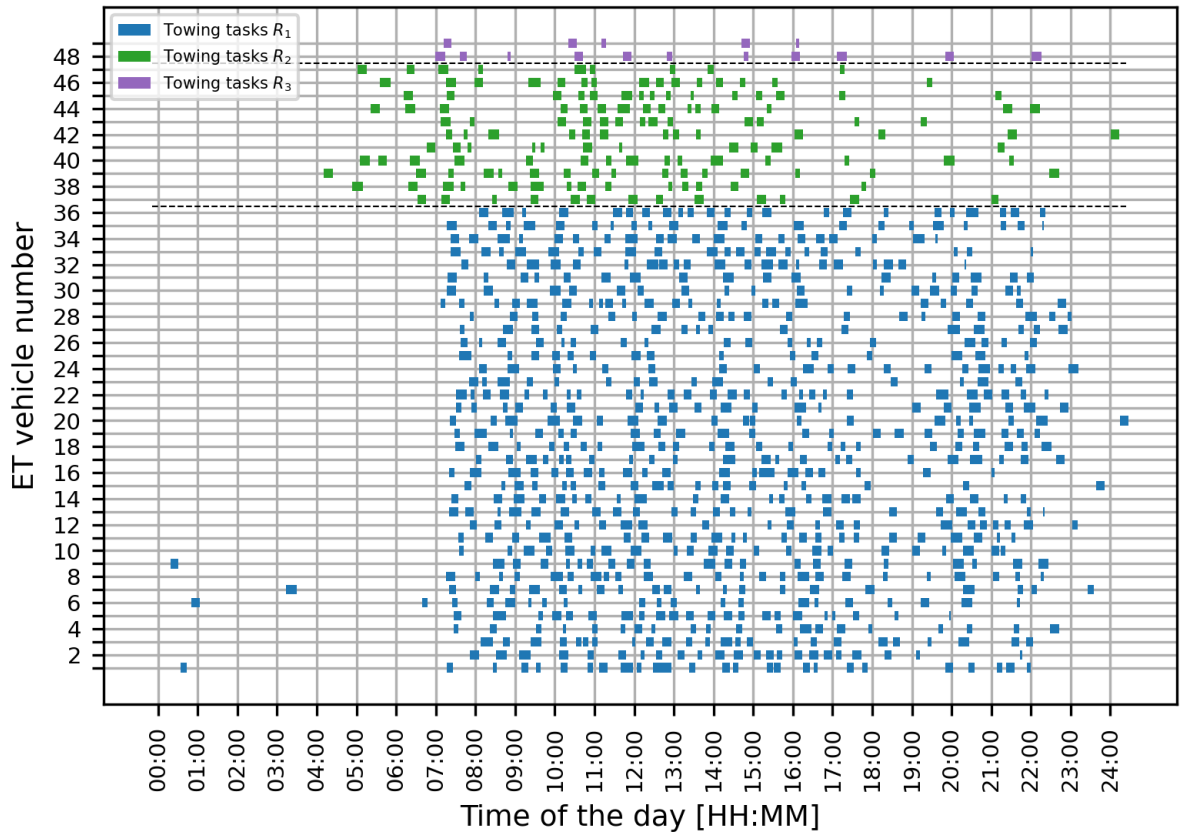

Figure 3.10: Results assignment model on the 14th of December for the high case

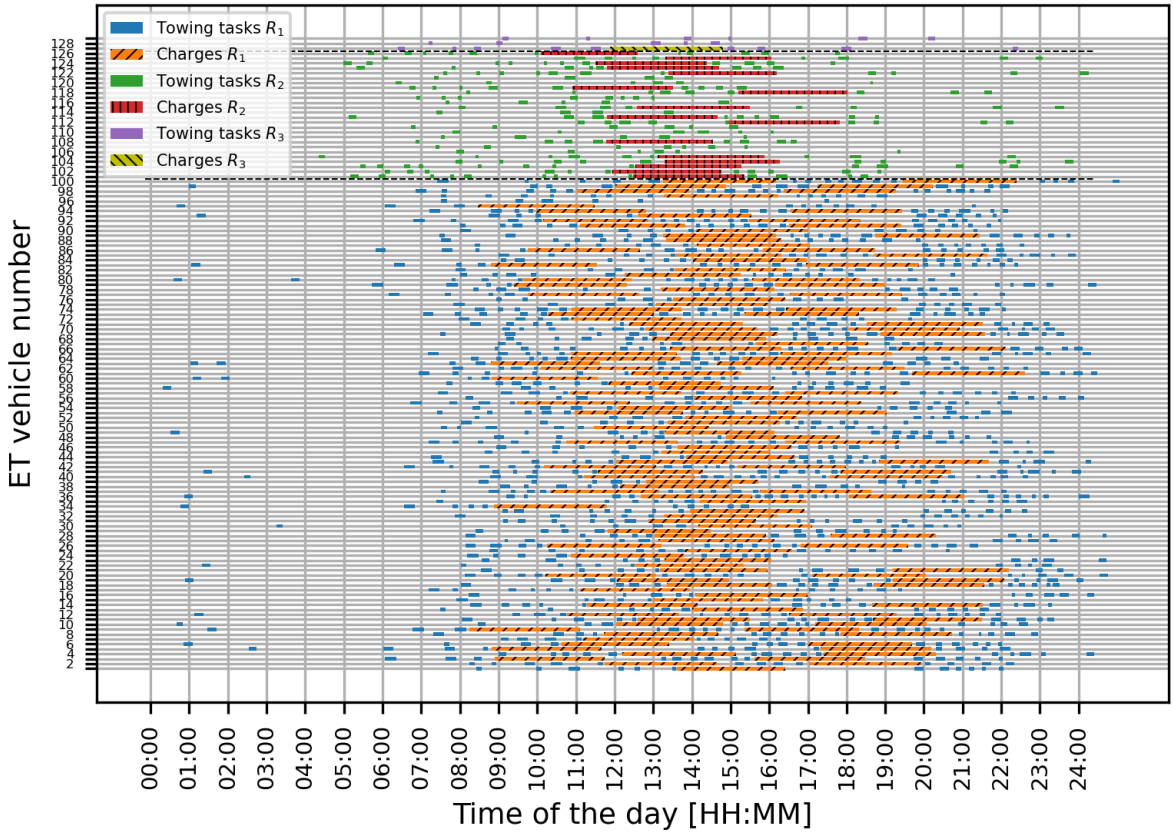

Figure 3.11: Results assignment model on the 13th of September for the low case

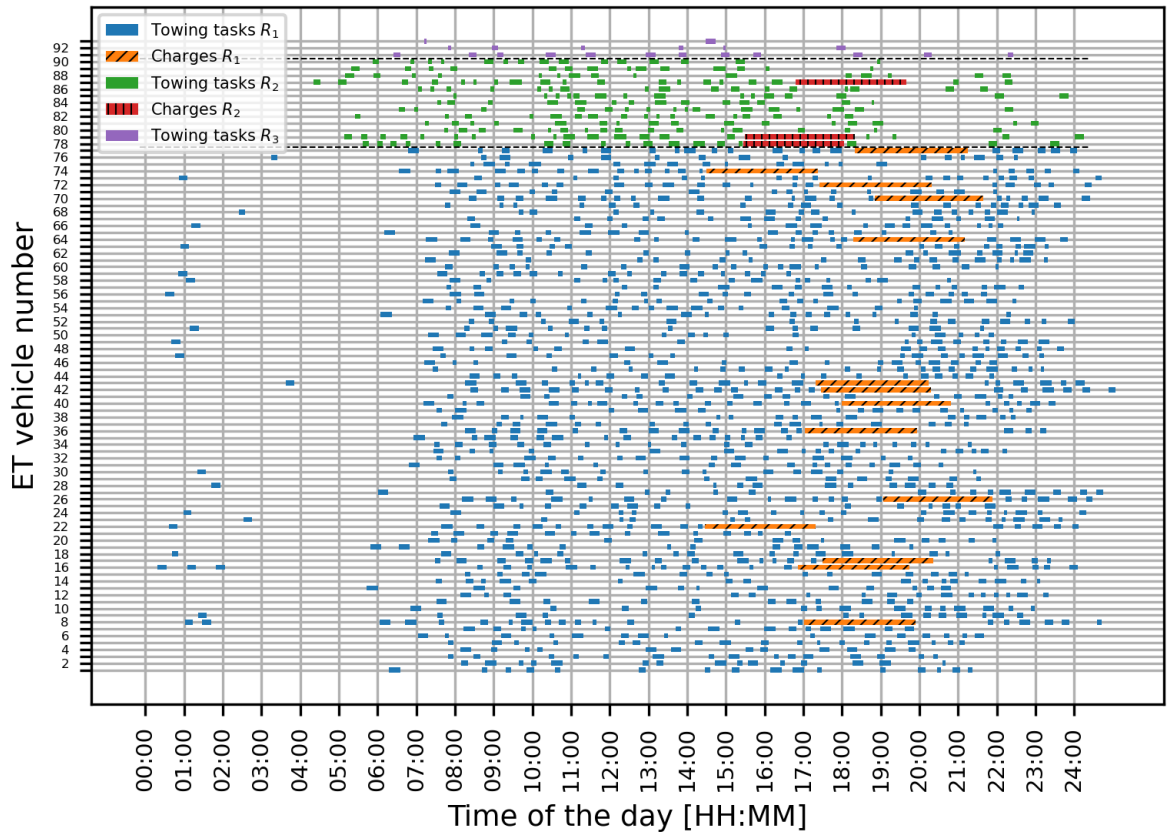

Figure 3.12: Results assignment model on the 13th of September for the high case

3.3. Taxi Velocity and Battery Capacity

The results from subsections 3.1 and 3.2 show that taxi velocity does not significantly affect the number of required ET vehicles, whereas battery capacity can significantly affect these numbers. This subsection combines both a higher taxi velocity and and a higher battery capacity to find out if the combined effect of both measures further decreases the number of required ET vehicles. Table 3.3 shows the results for both days. Total solve times for the quiet and busy day are **2060** and **4056** seconds respectively. It can be seen that the results are very similar to the results found for the high battery capacity and maximum power case. Therefore, we conclude that the most effective way to decrease the ET vehicle fleet size, is to only focus on increasing battery capacity.

	Quiet day			**Busy day**		
ET vehicle type	1	2	3	1	2	3
#ET vehicles	36	11	2	76	13	3

Table 3.3: Number of ET vehicles applying both the 'fast' and 'high' case

Figures 3.13 and 3.14 show the results related to the combined fast and high case discussed in this section.

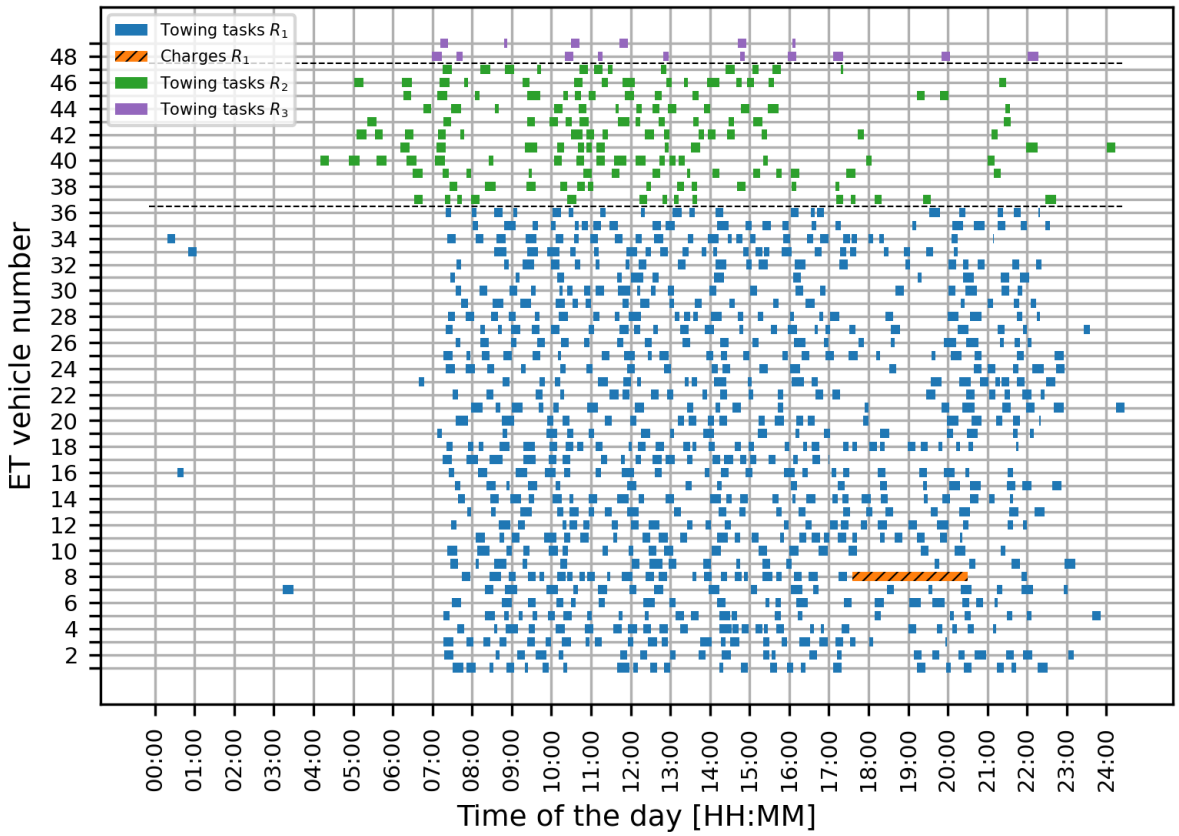

Figure 3.13: Results assignment model on the 14th of December for the higher velocity and battery case

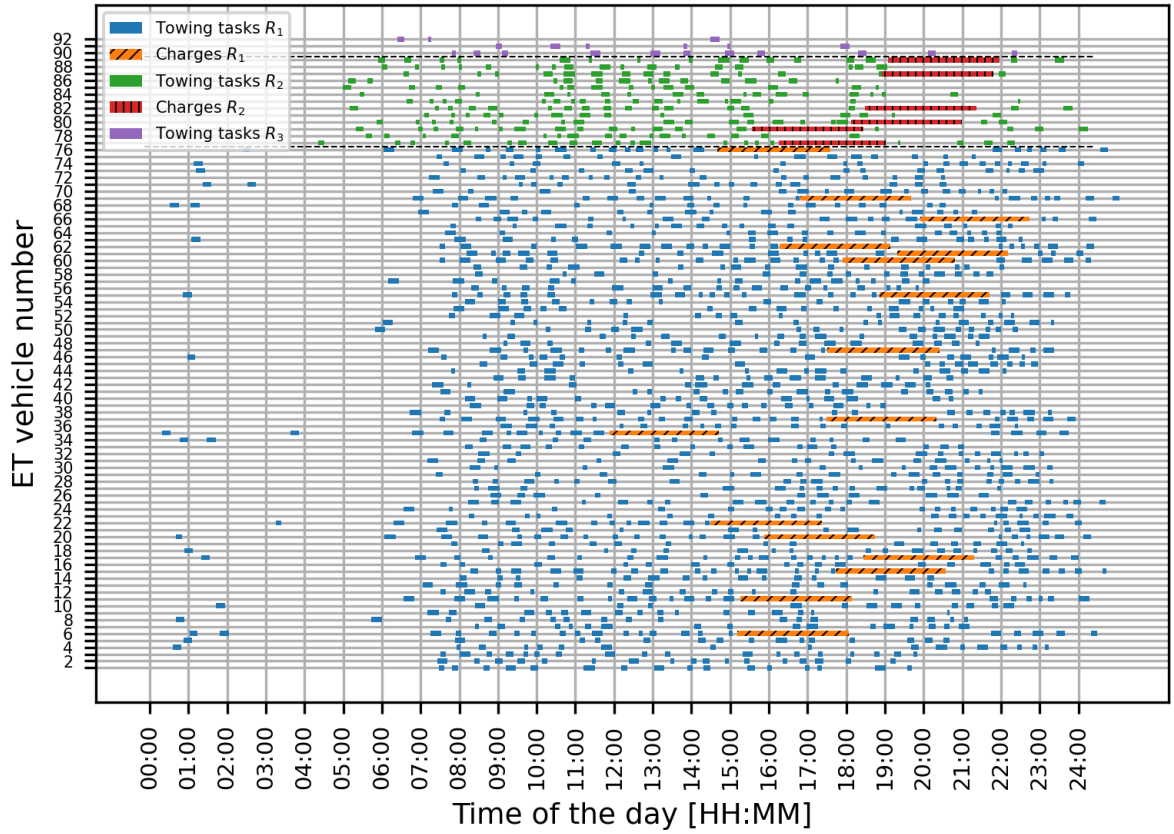

Figure 3.14: Results assignment model on the 13th of September for the higher velocity and battery case

4

Problem Size

The results in the paper are generated using a rolling window strategy, due to the large problem size. The rolling window strategy leads to a slightly suboptimal solution and requires an additional term in the objective function, which penalises charging. In this section, we want to show that the model is able to solve a similar smaller problem without the rolling window strategy and without the need to penalise charging in the objective function. The new objective function is given in equation equation (4.1); since we solve the problem in one window, the algorithm will determine which c-variables are set to 1 in order to minimise the total number of required ET vehicles and therefore c_{ij}^{k} is excluded from the objective function.

$$min\left(r - \sum_{l \in H} \sum_{i \in R} x_i^l\right) \tag{4.1}$$

We define the new set of towing tasks by ordering all tasks in R_1 on the 14$^{\text{th}}$ of December from earliest to latest t_i^S and picking 60 evenly distributed towing tasks from this list. The outcome of the assignment model for this set of tasks is displayed in figure 4.1 and shows that the model works the way we want it to. We require **3** type 1 ET vehicles to perform the defined set of towing tasks and the model assigns charging actions in a way that minimises the total number of ET vehicles. The total solve time amounts to **500** seconds.

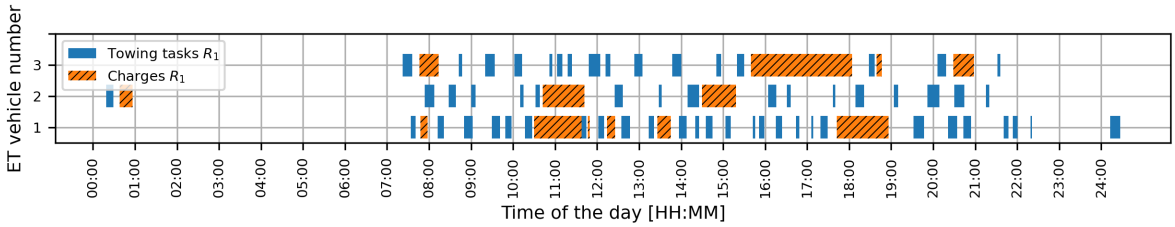

Figure 4.1: Results assignment model for 60 towing tasks on the 14$^{\text{th}}$ of December

Bibliography

[1] Airbus. Global market forecast - cities, airports & aircraft. 2019.

[2] Gillian Clare and Arthur G Richards. Optimization of taxiway routing and runway scheduling. IEEE Transactions on Intelligent Transportation Systems, 12(4):1000–1013, 2011.

[3] Nihad E Daidzic. Determination of taxiing resistances for transport category airplane tractive propulsion. Advances in aircraft and spacecraft science, 4(6):651, 2017.

[4] Kalyanmoy Deb, Amrit Pratap, Sameer Agarwal, and TAMT Meyarivan. A fast and elitist multiobjective genetic algorithm: Nsga-ii. IEEE transactions on evolutionary computation, 6(2):182–197, 2002.

[5] Christian Del Rosso. Reducing internal fragmentation in segregated free lists using genetic algorithms. In Proceedings of the 2006 international workshop on Workshop on interdisciplinary software engineering research, pages 57–60, 2006.

[6] Franziska Dieke-Meier and Hartmut Fricke. Expectations from a steering control transfer to cockpit crews for aircraft pushback. In Proceedings of the 2nd International Conference on Application and Theory of Automation in Command and Control Systems, pages 62–70, 2012.

[7] Huping Ding, Andrew Lim, Brian Rodrigues, and Yejun Zhu. The over-constrained airport gate assignment problem. Computers & Operations Research, 32(7):1867–1880, 2005.

[8] Jelena Djokic, Bernd Lorenz, and Hartmut Fricke. Air traffic control complexity as workload driver. Transportation research part C: emerging technologies, 18(6):930–936, 2010.

[9] JA Domínguez-Navarro, R Dufo-López, JM Yusta-Loyo, JS Artal-Sevil, and JL Bernal-Agustín. Design of an electric vehicle fast-charging station with integration of renewable energy and storage systems. International Journal of Electrical Power & Energy Systems, 105:46–58, 2019.

[10] Niclas Dzikus, Jörg Fuchte, Alexander Lau, and Volker Gollnick. Potential for fuel reduction through electric taxiing. In 11th AIAA Aviation Technology, Integration, and Operations (ATIO) Conference, including the AIAA Balloon Systems Conference and 19th AIAA Lighter-Than, page 6931, 2011.

[11] Niclas M Dzikus, Richard Wollenheit, Martin Schaefer, and Volker Gollnick. The benefit of innovative taxi concepts: the impact of airport size, fleet mix and traffic growth. In 2013 Aviation Technology, Integration, and Operations Conference, page 4212, 2013.

[12] James D Foster, Adam M Berry, Natashia Boland, and Hamish Waterer. Comparison of mixed-integer programming and genetic algorithm methods for distributed generation planning. IEEE transactions on power systems, 29(2):833–843, 2013.

[13] Bruce Goldberg, David Chesser, et al. Sitting on the runway: Current aircraft taxi times now exceed pre-9/11 experience. Technical report, United States. Dept. of Transportation. Research and Innovative Technology . . . , 2008.

[14] Jean-Baptiste Gotteland, Nicolas Durand, Jean-Marc Alliot, and Erwan Page. Aircraft ground traffic optimization, 2001.

[15] Julien Guépet, Olivier Briant, Jean-Philippe Gayon, and Rodrigo Acuna-Agost. The aircraft ground routing problem: Analysis of industry punctuality indicators in a sustainable perspective. European Journal of Operational Research, 248(3):827–839, 2016.

[16] N.J.F.P. Guillaume. Finding the viability of using an automated guided vehicle taxiing system for aircraft. Master's thesis, Delft University of Technology, 2018.

[17] Rui Guo, Yu Zhang, and Qing Wang. Comparison of emerging ground propulsion systems for electrified aircraft taxi operations. Transportation Research Part C: Emerging Technologies, 44:98–109, 2014.

[18] Gautam Gupta, Waqar Malik, and Yoon Jung. A mixed integer linear program for airport departure scheduling. In 9th AIAA Aviation Technology, Integration, and Operations Conference (ATIO) and Aircraft Noise and Emissions Reduction Symposium (ANERS), page 6933, 2009.

[19] Thushara Kandaramath Hari, Zahira Yaakob, and Narayanan N Binitha. Aviation biofuel from renewable resources: Routes, opportunities and challenges. Renewable and Sustainable Energy Reviews, 42:1234–1244, 2015.

[20] Jakub Hospodka. Electric taxiing–taxibot system. MAD-Magazine of Aviation Development, 2(10):17–20, 2014.

[21] IATA. IATA Forecast Predicts 8.2 billion Air Travelers in 2037, published: 24-10-2018. URL https://www.iata.org/en/pressroom/pr/2018-10-24-02/.

[22] MI Ithnan, T Selderbeek, WWA Beelaerts van Blokland, and G Lodewijks. Aircraft taxiing strategy optimization, 2013.

[23] Yu Jiang, Zhihua Liao, and Honghai Zhang. A collaborative optimization model for ground taxi based on aircraft priority. Mathematical Problems in Engineering, 2013, 2013.

[24] Yu Jiang, Xinxing Xu, Honghai Zhang, and Yuxiao Luo. Taxiing route scheduling between taxiway and runway in hub airport. Mathematical Problems in Engineering, 2015, 2015.

[25] Laura Khammash, Luca Mantecchini, and Vasco Reis. Micro-simulation of airport taxiing procedures to improve operation sustainability: Application of semi-robotic towing tractor. In 2017 5th IEEE International Conference on Models and Technologies for Intelligent Transportation Systems (MT-ITS), pages 616–621. IEEE, 2017.

[26] Il Yong Kim and Oliver L de Weck. Adaptive weighted-sum method for bi-objective optimization: Pareto front generation. Structural and multidisciplinary optimization, 29(2):149–158, 2005.

[27] Punyisa Kuendee and Udom Janjarassuk. A comparative study of mixed-integer linear programming and genetic algorithms for solving binary problems. In 2018 5th International Conference on Industrial Engineering and Applications (ICIEA), pages 284–288. IEEE, 2018.

[28] David S Lee, Giovanni Pitari, Volker Grewe, K Gierens, Joyce E Penner, Andreas Petzold, MJ Prather, Ulrich Schumann, A Bais, T Berntsen, et al. Transport impacts on atmosphere and climate: Aviation. Atmospheric environment, 44(37):4678–4734, 2010.

[29] Hanbong Lee, Waqar Malik, Bo Zhang, Balaji Nagarajan, and Yoon C Jung. Taxi time prediction at charlotte airport using fast-time simulation and machine learning techniques. In 15th AIAA Aviation Technology, Integration, and Operations Conference, page 2272, 2015.

[30] M Lukic, A Hebala, P Giangrande, C Klumpner, S Nuzzo, G Chen, C Gerada, C Eastwick, and M Galea. State of the art of electric taxiing systems. In 2018 IEEE International Conference on Electrical Systems for Aircraft, Railway, Ship Propulsion and Road Vehicles & International Transportation Electrification Conference (ESARS-ITEC), pages 1–6. IEEE, 2018.

[31] Milos Lukic, Paolo Giangrande, Ahmed Hebala, Stefano Nuzzo, and Michael Galea. Review, challenges and future developments of electric taxiing systems. IEEE Transactions on Transportation Electrification, 2019.

[32] LVNL. EHAM — AMSTERDAM/SCHIPHOL, accessed: April 2020. URL https://www.lvnl.nl/eaip/2019-08-01-AIRAC/html/eAIP/EH-AD-2.EHAM-en-GB.html.

[33] Arnab Majumdar and Washington Y Ochieng. Factors affecting air traffic controller workload: Multivariate analysis based on simulation modeling of controller workload. Transportation Research Record, 1788(1):58–69, 2002.

[34] Nikolai Okuniek, Zhifan Zhu, Yoon C Jung, Sergei Gridnev, Ingrid Gerdes, and Hanbong Lee. Performance evaluation of conflict-free trajectory taxiing in airport ramp area using fast-time simulations. In 2018 IEEE/AIAA 37th Digital Avionics Systems Conference (DASC), pages 1–10. IEEE, 2018.

[35] European Commission High Level Group on Aviation Research. Flightpath 2050 europe's vision for aviation. 2011.

[36] Madalena Pereira. Short-range route scheduling for e-ac with battery-charging and battery-swapping constraints. Delft University of Technology, 2019.

[37] Peter Belobaba, Amedeo Odoni and Cynthia Barnhart. The Global Airline Industry. Wiley, 2009.

[38] Fabrizio Re. Viability and state of the art of environmentally friendly aircraft taxiing systems. In 2012 Electrical Systems for Aircraft, Railway and Ship Propulsion, pages 1–6. IEEE, 2012.

[39] Fabrizio Re. Model-based Optimization, Control and Assessment of Electric Aircraft Taxi Systems. PhD thesis, Technical University of Darmstadt, 2017.

[40] Paul Roling. Airport surface traffic planning optimization: a case study of amsterdam airport schiphol. In 9th AIAA Aviation Technology, Integration, and Operations Conference (ATIO) and Aircraft Noise and Emissions Reduction Symposium (ANERS), page 7079, 2009.

[41] Paul C Roling and Hendrikus G Visser. Optimal airport surface traffic planning using mixed-integer linear programming. International Journal of Aerospace Engineering, 2008, 2008.

[42] Paul C Roling, Pjotr Sillekens, Richard Curran, and Wido D Wilder. The effects of electric taxi systems on airport surface congestion. In 15th AIAA Aviation Technology, Integration, and Operations Conference, page 2592, 2015.

[43] JA Rosero, JA Ortega, E Aldabas, and LARL Romeral. Moving towards a more electric aircraft. IEEE Aerospace and Electronic Systems Magazine, 22(3):3–9, 2007.

[44] JW Smeltink and MJ Soomer. An optimisation model for airport taxi scheduling*, 2004.

[45] JA Stockford, C Lawson, and Z Liu. Benefit and performance impact analysis of using hydrogen fuel cell powered e-taxi system on a320 class airliner. The Aeronautical Journal, 123(1261):378–397, 2019.

[46] E.V.M. van Baaren. The feasibility of a fully electric aircraft towing system. Master's thesis, Delft University of Technology, 2019.

[47] Jiefeng Xu and Glenn Bailey. The airport gate assignment problem: mathematical model and a tabu search algorithm. In Proceedings of the 34th annual Hawaii international conference on system sciences, pages 10–pp. IEEE, 2001.

[48] Lei Yang, Suwan Yin, Ke Han, Jack Haddad, and Minghua Hu. Fundamental diagrams of airport surface traffic: Models and applications. Transportation research part B: Methodological, 106:29–51, 2017.

[49] Xiaodong Yin and Noel Germay. A fast genetic algorithm with sharing scheme using cluster analysis methods in multimodal function optimization. In Artificial neural nets and genetic algorithms, pages 450–457. Springer, 1993.

[50] Ming Zhang, Qianwen Huang, Sihan Liu, and Huiying Li. Multi-objective optimization of aircraft taxiing on the airport surface with consideration to taxiing conflicts and the airport environment. Sustainability, 11(23):6728, 2019.